Emerging challenges in the management of community-acquired pneumonia: host-pathogen interaction

Desafíos emergentes en el manejo de la neumonía adquirida en la comunidad: interacción del huésped y patógeno

Alexander Rombauts

Emerging challenges in the management of community-acquired pneumonia: host-pathogen interaction.

Desafíos emergentes en el manejo de la neumonía adquirida en la comunidad: interacción del huésped y patógeno.

Memòria de tesi doctoral presentada per **Alexander Rombauts** per optar al grau de doctor per la Universitat de Barcelona.

Dirigida per: **Jordi Carratalà**
Servei de Malalties Infeccioses, Hospital Universitari de Bellvitge-IDIBELL Universitat de Barcelona, Departament de Medicina

Carlota Gudiol
Servei de Malalties Infeccioses, Hospital Universitari de Bellvitge-IDIBELL Universitat de Barcelona, Departament de Medicina

Programa de Doctorat Medicina i Recerca Translacional.

Facultat de Medicina i Ciències de la Salut. Universitat de Barcelona.

Abril 2024

Kinderen imiteren hun ouders, studenten
hun docenten en de meeste wetenschappers
andere wetenschappers
Samuel Ijsseling
(Wijsgeer, 1932 – 2015)

Het is de grootste dwaasheid dingen te leren
die men later weer moet vergeten
Lof der Zotheid,
Desiderius Erasmus
(Humanist en wijsgeer, 1466 – 1536)

Aan Sandra, Norah en Eira,
jullie zijn mijn alles

Acknowledgements

Agradezco en primer lugar a mis directores de tesis, Jordi Carratalà y Carlota Gudiol, por haberme dado la opurtunidad de seguir formándome en la patología infecciosa y de desarrollar este proyecto de investigación. Gracias por vuestra orientación constante, paciencia y dedicación a lo largo de este proceso. Vuestra sabiduría y apoyo han sido fundamentales para alcanzar este logro.

Expreso mi reconocimiento a la unidad de apoyo a la investigación, específicamente a Sebastián, por brindar de manera desinteresada, los recursos y ambiente para poder a llevar a cabos algunas de las investigaciones de esta tesis.

Agradezco sinceramente a mis compañeros de trabajo, que más que compañeros, son amigos. En concreto a Gabriela, por compartir sufrimientos (analísis estadísticos imposibles, realización de PK/PD nocturnos, exposición a patógenos fúngicos tras abrir historias archivadas hace >20 años, etc.). Agradezo a todos los demás compañeros y amigos, Sofia, Alba, Laura, Lluisa, Mar, Sara, su apoyo moral, sus palabras de aliento en los momentos más desafiantes. Quiero reconocer los invaluables consejos y el lujo que es poder contar con mentores como Inma, Nuria, Miguel y Miquel, así como Juan y Carmen y tantos otros. Agradecer a Guillermo los primeros artículos publicados como residente, y en parte, mi trabajo actual.

Agradezo a mis residentes grandes, sobre todo del pool de guardias, Boro, Adri, Nestor, Carmen, la paciencia que tuvieron conmigo y el tiempo que dedicaron a ese R1 un tanto peculiar. Sé que en momentos no fue (fui) fácil. Al pool, que hizo del hospital un hogar.

Mis gracias más profundas y significativas están dirigidas a las mujeres más importante de mi vida. A Sandra, que me hizo descubrir el amor, mi compañera de vida. Como alguien sabiamente dijo, eres una "mujer de diez", y cada día lo confirmas con tu constante apoyo, tus sacrificios incontables y tus muestras infinitas de cariño. A tu lado este viaje llamado vida vale la pena. Gracias por ser la persona exepcional que eres. Sin ti, esta tesis no existiría. A ti, Sandra, debo también el regalo más precioso: Norah y Eira, dos seres llenos de luz y alegría que han transformado nuestra existencia. Prometo seguir preparándote cada mañana esa cafetera que tanto te reconforta. Gracias Bellvitge, por hacer que hombres como yo puedan aspirar a estar con mujeres como Sandra.

Ook een dankwoord aan mijn dierbare familie. Walter en Marleen, dank u voor de moed om jullie kinderen naar een leefschool te sturen, de vergaarde levenservaring en drang om te blijven leren zijn van onschatbare waarde. Dank u voor jullie onvoorwaardelijke steun en aanmoedigingen. Dank u aan mijn broers voor de ontelbare blije ogenblikken die we samen hebben gedeeld. Bedankt voor de lachbuien, de avonturen, de fietstochten in San Juan, de gezelschapsspelen. Ook wil ik mijn dankbaarheid uiten aan Vava voor de ontelbare sprookjes en keren dat hij over de "troep" heft verteld. Aan Moemoe, waarbij we altijd een knuffel konden krijgen, en aan Moeke, die alles voor haar kleinkinderen over had, aan Bompa, om ons te leren een ongelovige Thomas te zijn.

Aan Norah en Eira, mijn lieve baby's, die mijn zwaarste nachten nog zwaarder maakten en mijn vermoeidheid naar nieuwe limieten dreven. Jullie stralende glimlachen en de onvoorwaardelijke liefde die ik voor jullie koester, zijn werkelijk onbeschrijfelijk. Jullie zijn mijn grootste zegeningen en de voortdurende bron van mijn vreugde. Moge jullie levens gevuld zijn met talloze kansen, succes en vooral liefde.

Finalmente, agradezco a todas las personas que de una forma u otra, y que no hayan sido nombrado antes, contribuyeron a la realización de esta tesis, su contribución ha sido fundamental en este proceso.

Funding

This doctoral thesis was supported by a predoctoral research grant from the Instituto de Salud Carlos III, the Spanish Ministry of Science, Innovation, and Universities, (PFIS grant FI18/00183), and by CIBERINFEC, Instituto de Salud Carlos III, Madrid, Spain.

Table of contents

Table of contents

Figures titles:

Figure 1. Aetiology of CAP among 2320 adults with radiographic confirmed pneumonia.
Figure 2. Structural elements of SARS-CoV-2.
Figure 3. The “omics revolution”, the interconnectedness of various 'omics studies.
Figure 4. Conceptual model of the different inflammatory factors involved in CAP and SARS-CoV-2 pneumonia and interventions tested.

Abbreviations and acronyms

Abbreviations and acronyms

ACE2	Human angiotensin-converting enzyme 2
ARDS	Acute respiratory distress syndrome
BCAA	Branched-chained amino acids
CAP	Community-acquired pneumonia
COVID-19	Coronavirus Disease 2019
HCoV	Human coronavirus
HDL	High-density lipoprotein
IDL	Intermediate-density lipoprotein
IFN	Interferon
LDL	Low-density lipoprotein
NAAT	Nucleic acid amplification test
PC	Phosphatidylcholine
PCV	Pneumococcal conjugate vaccine
RBD	Receptor-binding domain
RNA	ribonucleic acid
SARS-CoV-2	Severe acute respiratory syndrome coronavirus 2
sIgA	secretory IgA
TNF	Tumour necrosis factor
UPR	Unfolded protein response
VLDL	Very-low-density lipoprotein
WHO	World Health Organization

Scientific production

Thesis in compendium of publication. The thesis consists of 6 objectives and 6 articles.

1. Viasus, D. ✉, Simonetti, A. F., Nonell, L., Vidal, O., Meije, Y., Ortega, L., Arnal, M., Bódalo-Torruella, M., Sierra, M., **Rombauts, A**., Abelenda-Alonso, G., Blanchart, G., Gudiol, C., & Carratalà, J. (2023).

Whole-Blood Gene Expression Profiles Associated with Mortality in Community-Acquired Pneumonia.

Biomedicines, 11(2), 429. Impact factor: 4.7 (1st quartile)

2. **Rombauts, A.**, Abelenda-Alonso, G., Càmara, J., Lorenzo-Esteller, L., González-Díaz, A., Sastre-Escolà, E., Gudiol, C., Dorca, J., Tebé, C., Pallarès, N., Ardanuy, C., & Carratalà, J. ✉ (2020).

Host- and Pathogen-Related Factors for Acute Cardiac Events in Pneumococcal Pneumonia.

Open forum infectious diseases, 7(12), ofaa522. Impact factor (2022): 4.2 (2nd quartile)

3. **Rombauts, A**✉., Bódalo Torruella, M., Abelenda-Alonso, G., Perera-Bel, J., Ferrer-Salvador, A., Acedo-Terrades, A., Gabarrós-Subirà, M., Oriol, I., Gudiol, C., Nonell, L.✉, & Carratalà, J. (2023).

Dynamics of Gene Expression Profiling and Identification of High-Risk Patients for Severe COVID-19.

Biomedicines, 11(5), 1348. Impact factor: 4.7 (1st quartile)

4. Aydillo, T., **Rombauts, A**., Stadlbauer, D., Aslam, S., Abelenda-Alonso, G., Escalera, A., Amanat, F., Jiang, K., Krammer, F.✉, Carratala, J.✉, & García-Sastre, A.✉ (2021).

Immunological imprinting of the antibody response in COVID-19 patients. Nature communications, 12(1), 3781 Impact factor: 16.6 (1st decile)

5. Escalera, A., Rojo-Fernandez, A., **Rombauts, A.**, Abelenda-Alonso, G., Carratalà, J., García-Sastre, A., & Aydillo, T✉. (2024).

SARS-CoV-2 infection induces robust mucosal antibody responses in the upper respiratory tract. iScience, 27(3), 109210. Impact factor: 5.8 (1st quartile)

6. Mallol, R.*, **Alexander Rombauts, A**.*✉, Abelenda-Alonso, G., Gudiol, C., Balsalobre, M., Carratalà, J.
*Both authors contributed equally to the study.

Metabolomic profile associated with COVID-19 severity and a signature that predicts progression towards severe disease status, a prospective cohort study (METCOVID)

Submitted

Thesis summary (in Catalan)

Thesis summary (in Catalan)

Introducció:

La pneumònia adquirida a la comunitat constitueix la primera causa de mortalitat infecciosa tant a nivell mundial com Europeu, amb una taxa de mortalitat intrahospitalària d'aproximadament el 10%. Tot i que *Streptococcus pneumoniae* continua sent el principal agent etiològic, la pneumònia viral està guanyant protagonisme. Les complicacions de la pneumònia van més enllà de l'afectació local, involucrant altres òrgans. D'un interès especial són els esdeveniments cardíacs aguts, els quals empitjoren notablement el pronòstic. Alguns estudis suggereixen que el dany cardíac per *S. pneumoniae* està relacionat amb el tipus de soca.

Noves tecnologies han permès comprendre millor la patogènesi de la pneumònia. L'anàlisi metabolòmic –mitjançant l'espectroscòpia de RMN i l'espectrometria de masses–, transcriptòmic, genòmic, i proteomic, han donat peu a l'inici de l'anomenada "revolució òmica". Malgrat això, les investigacions sobre el perfil d'expressió gènica en la pneumònia continuen sent limitades.

L'aparició de la SARS-CoV-2 ha precipitat un augment en els estudis òmics que examinen la patogènesi de la COVID-19. Els estudis transcriptòmics i metabolòmics ofereixen oportunitats per estudiar l'heterogeneïtat clínica de la malaltia, identificant potencialment signatures de l'hoste associades amb el risc de progressió. La comprensió de la resposta immune humoral a la COVID-19, tant en sang com a nivell de mucoses, també és una àrea d'investigació clau.

Hipòtesi:

1. El transcriptoma de pacients hospitalitzats amb pneumonia adquirida a la comunitat presenta patrons distintius entre supervivents i no supervivents.

2. Els serotips i complexes clonals de *S. pneumoniae* són un determinant clau en el desenvolupament d'esdeveniments cardíacs aguts.

3. Els adults hospitalitzats amb COVID-19 que progressen cap a destret respiratori manifesten un perfil transcriptòmic característic comparat amb aquells amb símptomes moderats.

4. Les infeccions prèvies per altres coronavirus humans influeixen en la naturalesa de la resposta d'anticossos contra el SARS-CoV-2.

5. Les infeccions per SARS-CoV-2 indueixen una immunitat humoral mucosal local robusta, un procés influït per l'exposició prèvia a altres coronavirus humans.

6. Els pacients hospitalitzats amb COVID-19 moderada que posteriorment es deterioren presenten una signatura metabolòmica distintiva que prediu el risc de progressió de la malaltia.

Objectius:

1. Comparar el perfil transcriptòmic entre els pacients supervivents i no supervivents de pneumonia adquirida a la comunitat per identificar les vies fisiopatològiques i els biomarcadors pronòstics.

2. Determinar els factors de risc relacionats amb l'hoste i el patògen per al desenvolupament d'esdeveniments cardíacs aguts en la pneumònia pneumocòccica.

3. Determinar la diferència del perfil transcriptòmic entre els pacients hospitalitzats amb COVID-19 greu i moderada per ampliar la nostra comprensió de la heterogeneïtat del curs clínic de la malaltia.

4. Perfilar la resposta humoral dinàmica contra el SARS-CoV-2. Investigar el paper de l'emprempta immunològica de la infecció prèvia per coronavirus estacionals en la resposta d'anticossos dels pacients amb COVID-19.

5. Caracteritzar la resposta precoç d'anticossos a nivell de mucoses i el repertori d'immunoglobulines contra les proteïnes S del SARS-CoV-2 i HCoV-OC43 estacional en mostres d'aspirat nasofaringi de pacients amb COVID-19.

6. Caracteritzar l'alteració metabolòmica de la COVID-19 greu i desenvolupar un model predictiu basat en una signatura metabolòmica capaç de predir la progressió de la malaltia.

Mètodes:

La tesi consta de sis estudis realitzats en cinc cohorts diferents.

El primer estudi compara el perfil transcriptòmic, aplicant l'anàlisi d'enriquiment de conjunts de gens, de pacients hospitalitzats amb pneumònia adquirida a la comunitat entre supervivents i no supervivents. El segon estudi analitza els factors de risc de l'hoste i l'impacte del serotip i genotip de *S. pneumoniae* en el desenvolupament d'esdeveniments cardíacs aguts en la pneumònia pneumocòccica mitjançant una anàlisi tipus funnel plot. El tercer estudi compara el perfil transcriptòmic dinàmic, aplicant l'anàlisi d'enriquiment de conjunts de gens, de pacients hospitalitzats amb COVID-19 amb destret respiratori i aquells que no presenten aquesta condició. El quart i cinquè estudis determinen la resposta humoral en sang i en via respiratòria superior en la infecció per SARS-CoV-2, i analitzen el back-boost contra coronavirus estacionals previs per investigar l'emprempta immunològica. L'últim estudi investiga el perfil metabolòmic mitjançant espectroscòpia de RMN en pacients ingressats per COVID-19, creant un model multivariant incorporant les ràtios de metabòlits per predir el risc de progressió.

Principals resultats:

1. L'anàlisi d'enriquiment de conjunts de gens va indentificar quatre conjunts de gens positivament enriquits en els supervivents, principalment associats amb l'interferó-alfa,

l'apoptosi i les hormones sexuals. Contràriament, els set conjunts de gens enriquits en aquells que van ser èxitus estaven associats amb l'estrès oxidatiu, l'estrès del reticle endoplasmàtic i l'angiogènesi.

2. Els factors associats amb esdeveniments cardíacs van ser l'edat avançada, les condicions cardíaques preexistents, la presència de bacterièmia pneumocòccica i el xoc sèptic. Els anàlisis de funnel plot no van trobar associació entre els serotips o els complexes clonals amb esdeveniments cardíacs, tot i que es va observar una tendència per a CC230.

3. La COVID-19 greu es caracteritza per una resposta inflamatòria desregulada, amb un augment de l'expressió de gens relacionats amb molècules proinflamatòries i l'activació de neutròfils i macròfags, a més d'una pèrdua de regulació immune.

4. En la infecció per SARS-CoV-2 es va observar un fort efecte de reforç de la memòria a epítops conservats, però no variables, d'altres proteïnes d'espícula de betacoronavirus estacionals. Aquest reforç de la memòria d'anticossos es correlaciona negativament amb la inducció d'IgG i IgM contra la proteïna d'espícula i nucleocàpsida de SARS-CoV-2.

5. Les infeccions per SARS-CoV-2 promouen una resposta robusta d'anticossos a nivell de les mucoses. Es va detectar un recordatori de memòria immune a epítops conservats de beta-coronavirus al tracte respiratori superior.

6. El nostre model multivariant, basat en un perfil metabolòmic, va demostrar una AUC validada creuada de 0,82 amb una precisió del 72% per a la progressió cap a la gravetat en pacients ingressats amb COVID-19 moderada.

Conclusions:

1. Els perfils transcriptòmics dels supervivents i no supervivents a la pneumònia adquirida a la comunitat mostren diferències principalment relacionades amb la resposta a l'interferó-alfa, l'apoptosi, les hormones sexuals, l'estrès oxidatiu, la resposta de les proteïnes desplegades i les vies d'angiogènesi. Els gens diferencialment expressats podrien ser potencialment útils com a biomarcadors d'estratificació de risc.

2. Els factors de l'hoste semblen ser més importants que els factors relacionats amb el patogen per al desenvolupament d'esdeveniments cardíacs aguts en la pneumònia pneumocòccica. El complex clonal 230 sembla estar associat amb una incidència més alta d'esdeveniments cardíacs aguts, el que podria tenir implicacions clíniques rellevants ja que alguns serotips associats amb el CC230, com el 24F, no estan inclosos en les vacunes actualment disponibles.

3. La síndrome de destret respiratori agut a la COVID-19 és causada per una resposta inflamatòria desregulada i un augment de l'expressió de gens relacionats amb molècules proinflamatòries i l'activació de neutròfils i macròfags en el moment de l'ingrés, a més de la pèrdua de regulació immune.

4. L'empremta immunològica de les anteriors infeccions per coronavirus estacionals modula el perfil d'anticossos a la infecció per SARS-CoV-2, fet que pot influir en l'eficàcia de la resposta vacunal.

5. Els pacients amb COVID-19 generen una forta resposta d'anticossos a nivell de les mucoses contra la proteïna d'espícula de SARS-CoV-2 amb subtipus d'anticossos IgA secretores específiques (sIgA), IgA, IgG i IgM.

6. Els pacients que presenten malaltia per COVID-19 moderada però amb un alt risc de deteriorament exhibeixen una signatura metabolòmica característica, que es pot determinar utilitzant plataformes basades en RMN per predir la progressió de la malaltia.

1. Introduction

1. Introduction

1.1. General introduction

1.1.1. The burden of community-acquired pneumonia

Community-acquired pneumonia (CAP) is a public health problem worldwide and continues to be associated with high health costs, morbidity, and mortality.

According to the Lancet Global Burden of Disease, globally there were 488.9 million incident cases of lower respiratory infections in 2019 with the number of disability-adjusted life years of 97.2 million (1). Studies have shown that the incidence of CAP in Europe varies by country and age. The incidence is highest in the first 1-4 years of age and then increases again with age, being particularly high among older patients and those with comorbidities (2). In Western Europe alone, 163 million incident cases were registered with a 10-fold rise in certain subgroups, such as the elderly and patients with chronic obstructive pulmonary disease (3). In Spain, incidence of hospitalisation rates for CAP increased from 142.4 in 2004 to 163.87 cases per 100 000 inhabitants in 2013 (4).

Furthermore, the real burden of CAP is likely underestimated as most estimates of CAP incidence are obtained from national databases on hospitalised patients. It is estimated that between 50% and 80% of CAP patients are treated as outpatients (5). An illustrative example of this is a 3-year prospective, observational study of ambulatory CAP in adults, conducted in 24 Spanish primary care centres between 2016–2019. This study found an overall incidence rate of CAP of 652 per 100 000 inhabitants, with only 2.8% episodes requiring hospitalisation (6). Importantly, one-third of patients had not fully recovered after two weeks. Furthermore, over the coming years, the overall burden of CAP is likely to rise as its incidence and the number of elderly people increase (7).

Unsurprisingly, therefore, the economic burden of CAP is high, with an estimated yearly cost of €10.1 billion in Europe (8), and exceeding €14 billion in the United States alone (9). Although the majority of attributable CAP expenditures occurs during the acute phase and relates to inpatient care, the consequences of CAP are far reaching, as markers of healthcare utilization, and 50% of the cost of CAP, extend well beyond the typical symptom resolution of CAP (10).

1.1.2 Aetiology of community-acquired pneumonia.

The microbiological aetiology of CAP varies according to its clinical presentation and seasonal factors. Globally, it is estimated that in up to 50-60% of CAP cases, the exact cause remains unidentified (11). Figure 1 shows the most commonly identified CAP causes. This phenomenon can be attributed to various factors, including limited availability of adequate respiratory samples, heterogeneous diagnostic efforts, and ongoing debate regarding the clinical implications of etiological diagnosis in CAP (12).

Several bacteria and viruses are recognized as potential causative agents of CAP and are categorized as primary respiratory pathogens. *Streptococcus pneumoniae* remains the most common bacterial cause, although its incidence appears to be declining in the USA (13), apparently due to routine paediatric vaccination. However, the level of paediatric vaccination uptake required to produce herd immunity in other age groups is currently unknown, although data from the UK and US indicate substantial reductions in invasive pneumococcal disease associated with universal childhood pneumococcal conjugate vaccine (PCV) vaccination (14,15). Conversely, Europe continues to experience high pneumococcal pneumonia rates, with a notable proportion of infections caused by serotypes included in vaccine (16). Adult vaccination might change this picture as it offers moderate protection against pneumococcal CAP. A Dutch clinical trial evaluating the efficacy of the PCV-13 vaccine in 84 496 adults reported an efficacy of 45.5% (17). However, it has to be noted that replacement by non-vaccine serotypes has been observed following widespread vaccine uptake (18,19). Most notably increases of serotypes 8, 9N, 15A, 23B were noted in the United States, Australia and several European countries (18). In Spain, for instance, there has been an increase in serotype 19A of *S. pneumoniae* following the introduction of the pneumococcal conjugate vaccine comprising 7 serotypes (19). Despite increased vaccine coverage, the incidence of one of the most severe forms of pneumonia, characterized by invasive (bacteraemic) pneumococcal disease, remains high, with 8.3 cases per 100,000 inhabitants in Catalonia alone in 2022 (20).

Following *S. pneumoniae*, *Haemophilus influenzae* is the second most commonly identified bacterial cause of pneumonia in most series (7 – 16% of cases). The incidence of other notable bacteria such as *Staphylococcus aureus* (1- 10%) and *Pseudomonas aeruginosa* (0.8% - 4.5%) varies across studies conducted in the United States and Europe (11,21,22).

Less common pathogens should be considered in patients with specific risk factors, such as travel history or animal exposure. Among the so-called "atypical" bacteria, recent meta-analyses have identified *Mycoplasma pneumoniae* as the etiological agent in 4-11% of CAP cases, *Legionella pneumophila* in 3-8%, *Chlamydophila pneumoniae* in 2-7%, and *Coxiella burnetii* in <2% of cases (23,24).

Viruses are increasingly being recognized as causative agents in CAP, mostly due to improved diagnostic technique, mostly based on nucleic acid amplification tests (NAATs). Viral CAP aetiology accounted for 24.5% of cases, with rhinovirus responsible for approximately 4.1 – 11.5% and influenza for 6.2 – 13.7% of cases (11,25). Respiratory syncytial virus and human metapneumovirus were less common, followed by other viruses.

All prior studies investigating CAP aetiology, despite their best effort and NAATs, continue to fail to identify a causative organism in approximate 50% of cases. This is mostly due to the inability in obtaining a high-quality sputum. Furthermore, without a high-quality sputum, there might be no way to distinguish upper airway colonization from pulmonary infection, particularly with the use of NAATs. In this regard, microarray technology with metagenomics RNA sequencing or metabolomics studies offers the possibility to identify host transcriptional signatures, which can be used to differentiate viral, bacterial and non-infectious respiratory illness (26).

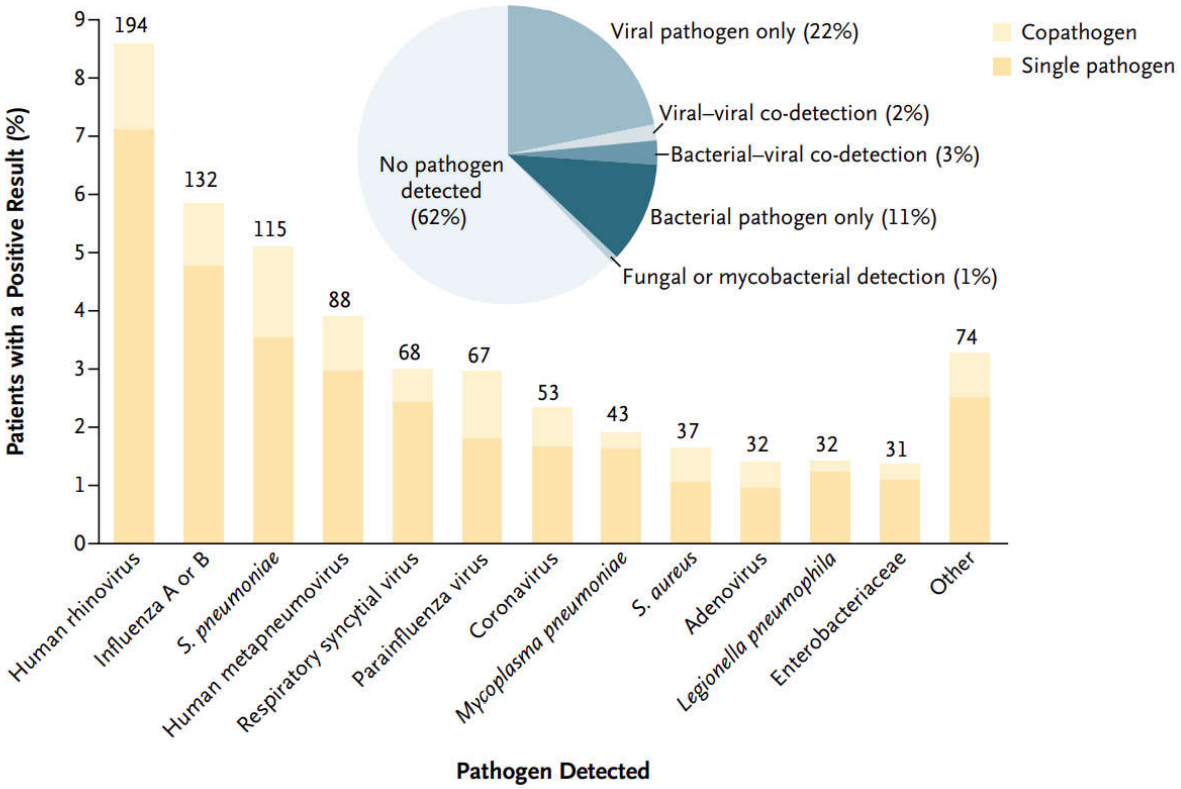

Figure 1. Aetiology of CAP among 2320 adults with radiographic confirmed pneumonia (11). From Jain, Seema et al. "Community-Acquired Pneumonia Requiring Hospitalization among U.S. Adults." The New England journal of medicine vol. 373,5 (2015): 415-27. doi:10.1056/NEJMoa1500245

1.1.3 Emergence of SARS-CoV-2.

In early December 2019 a surge of pneumonia cases of unknown origin were detected in Wuhan, China (27). A novel RNA betacoronavirus was rapidly identified as the causative microorganism (28). Coronaviruses are named as such because the S proteins resemble a halo or corona on scanning electron microscope imagery (29).

As this novel betacoronavirus bared a high genetic sequence similarity to severe acute respiratory syndrome coronavirus 1 (SARS-CoV-1), and produced a similar clinical syndrome, it was named as severe acute respiratory syndrome coronavirus 2 (SARS-CoV-2). The first two-thirds of the SARS-CoV-2 genome encode two large polypeptides, pp1a/pp1b, which undergo auto-proteolytic processing to yield 16 non-structural proteins (30). The remaining one-third of the SARS-CoV-2 genome codes for the structural proteins S (spike), E (envelope), M (membrane), and N (nucleocapsid), as well as several open reading frames

(ORFs), including 3a, 6, 7a, 7b, 8, 9b, and 10 (31). SARS-CoV, and SARS-CoV-2, infect cells through the direct interaction between the receptor-binding domain (RBD), present on the protein S1 subunit, and the angiotensin-converting enzyme 2 (ACE2) to infect cells (32). See figure 2 for an illustration of the structural elements of SARS-CoV-2 and its genome components.

SARS-CoV-2 belongs to a large family of viruses with the capacity to infect both mammals and birds. Humans are susceptible to at least six other viruses from the alpha and betacoronavirus genus (33). These viruses typically induce respiratory illness to varying degrees. While SARS-CoV-1 and Middle East Respiratory Syndrome Coronavirus are highly pathogenic betacoronaviruses responsible for zoonotic outbreaks in humans over the past two decades (34,35), the alphacoronaviruses 229E and NL63, as well as the betacoronaviruses OC43 and HKU1, often lead to mild upper respiratory tract diseases and have been circulating among humans as seasonal viruses (33,36). The syndrome caused by the infection of SARS-CoV-2 was named as coronavirus disease 2019 (COVID-19). SARS-CoV-2 can cause a different range of clinical manifestations, from asymptomatic to severe respiratory syndrome (37) with more than 86.2% of patients admitted with COVID-19 presenting new-onset radiological lung abnormalities (38).

SARS-CoV-2 quickly started to generate sustained transmission in other countries and caused the first documented pandemic of human coronavirus (HCoV) in history, although all circulating coronaviruses must have emerged and spread pandemically in the era prior to the recognition of viruses as human pathogens (39). The global spread of SARS-CoV-2 was so extensive that the WHO declared COVID-19 a pandemic on March 11, 2020 (40).

Although the World Health Organization has by now declared an end to the global Public Health Emergency for COVID-19 (41), it remains a public threat with tens of thousands newly diagnosed cases each week and hospitalised patients (42). The emergence of new variants of concerns and the antigenic evolution of SARS-COV-2, conferring immune escape and reinfections (43), have triggered surges in COVID-19 hospitalisation (44), even in populations with acquired immunity (45). The end of the Public Health Emergency does not mean COVID-19 is over as a global threat.

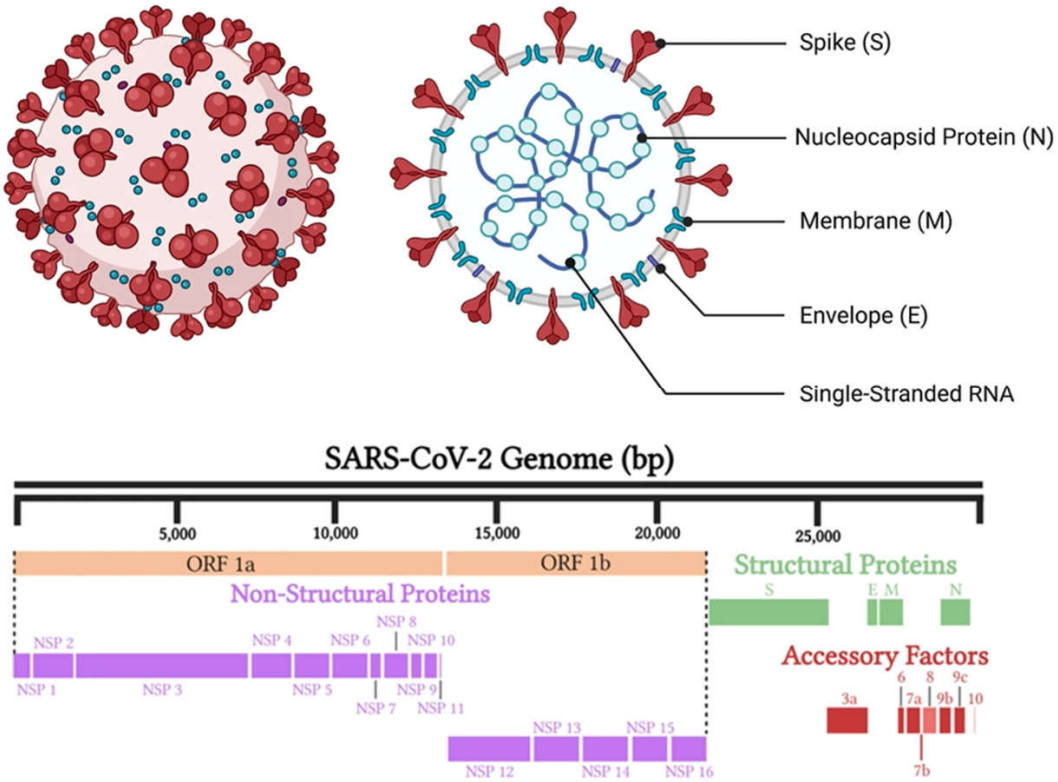

Figure 2. Structural elements of SARS-CoV-2. Including the spike protein, envelope, membrane, and internal components such as the viral single-stranded RNA and nucleocapsid proteins, above. SARS-CoV-2 genome components, below (30). From Jamison, David A Jr et al. "A comprehensive SARS-CoV-2 and COVID-19 review, Part 1: Intracellular overdrive for SARS-CoV-2 infection." European journal of human genetics: EJHG vol. 30,8 (2022): 889-898. doi:10.1038/s41431-022-01108-8.

1.1.4. Mortality due to community-acquired pneumonia and SARS-CoV-2 pneumonia

In 1918, Sir William Osler observed that pneumonia had replaced tuberculosis as the leading cause of death in Europe and described pneumonia as the "Captain of the men of death"(46).

More than one-century later, pneumonia remains one of the main causes of death. According to data provided by the World Health Organization (WHO), lower respiratory infections ranked as the fourth leading cause of death globally and stood out as the primary infectious cause, contributing to 4.7% of all recorded deaths. Notably, within the WHO European region, lower respiratory infections emerged as the sole infectious cause among

the top 20 leading causes of death, demonstrating a crude death rate of 28.6 per 100,000 inhabitants (47).

Despite a decrease in short-term mortality among adult patients hospitalised with CAP over recent years, about 10% of all patients continue to die (3,48,49), with this figure rising to 28% in patients admitted to intensive care units (ICU) even when antibiotic treatment is adequate (50). A rate that matches those of other known medical-emergency diseases, such as ST-elevation myocardial infarction (51). Of note, CAP has a significantly higher long-term mortality rate than many other conditions (52), occurring in nearly 1 in 4 adults one year after hospitalisation (3).

Mortality in CAP has been related to several factors with the host-pathogen interaction playing a crucial role. Mortality varies according to the causative microorganism, with higher fatality rates in pneumococcal CAP (53) –which remains the most frequent aetiology - and other less frequent pathogens such as *P. aeruginosa* or *S. aureus* (54). In this regard, inappropriate initial treatment has a negative impact on survival (55). Other important determining factors are age and underlying conditions (56) which have been related, even in viral CAP, to the development of severe sepsis (57).

The emergence of SARS-CoV-2 as a new respiratory pathogen in an immunologically naïve world population dramatically increased pneumonia mortality. In the year 2020 SARS-CoV-2 pneumonia was the third cause of death in the European Union, only behind circulatory diseases and cancer, accounting for 8% of all deaths with a standardized death rate of 89.3 per 100 000 inhabitants (58). Worldwide, the coronavirus disease 2019 pandemic has caused more than 760 million confirmed cases and closely to 7 million deaths (40). As staggering these numbers might be, the official statistics provide only a partial picture, underestimating the true burden of mortality. Studies evaluating COVID-19 excess mortality reveal a large gap between estimated excess mortality and reported COVID-19 deaths (59), particularly in Asia and Africa. In addition, despite increased vaccine coverage and natural immunity from previous infections, patients hospitalised with SARS-CoV-2 pneumonia remain at a high risk for mortality, ranging from 15% to 5% during delta and late omicron periods (60).

1.2. Complications in community-acquired pneumonia and COVID-19.

Emphasis should be placed on the fact that CAP and SARS-CoV-2 infection is not a disease confined to the lung parenchyma, but are highly dynamic systemic diseases. Relevant complications of CAP include local progression of the disease in the lungs or pleural space, with acute respiratory distress syndrome (ARDS) particularly frequent in COVID-19. Furthermore, CAP and COVID-19 exert both direct and indirect effect on other organs systems, such as the central nervous system, haematological, cardiac, renal, endocrine, hepatic systems and others (61–66) . Of particular concern are cardiac events in CAP and COVID-19. CAP and COVID-19 progression involves a complex host-pathogen interaction, which is detailed further in this thesis. Additionally, CAP and COVID-19 can lead to long-term consequences

1.2.1. Pulmonary and pleural complications

The majority of patients admitted to hospitals with CAP and COVID-19 experience a favourable clinical evolution. Nevertheless, it is important to recognize that complications are not uncommon. Up to 6% of patients with CAP present early failure, with progressive pneumonia, pleural effusion/empyema and uncontrolled sepsis being the main causes (67). Around 30% of hospitalised patients with CAP develop bilateral infiltrates (68), which increases the risk of treatment failure.

Furthermore, the incidence of pleural space infections, after an increase in the first decade of the 21th century (69,70), has remained stable in adults the last decade (71). The development of complicated pleural effusion remains one of the most common cause of treatment failure in CAP (67). The increased permeability of the mesothelial layer of the inflamed pleura can allow the invasion of bacteria into the otherwise sterile pleural space (70). While *S. pneumoniae* used to be the main cause of pleural space infection, this has shifted towards other microorganisms such as viridans streptococci group*, S. aureus*, with anaerobic microorganism present in up to 25% of cases (72). Notwithstanding the shift in microbiology, more than 50% and 8% of patients hospitalised with pneumococcal pneumonia, develop pleural effusion and empyema respectively (63). A minority of patients develops necrotizing pneumonia. Pulmonary gangrene is more commonly seen with *S. aureus* and gram-negative organisms like *Klebsiella pneumoniae* and *P. aeruginosa* (73,74). The

production of several staphylococcal toxins have been described in the pathogenesis of severe necrotizing pneumonia (75,76).

Local respiratory complications in hospitalised COVID-19 patients are almost always related with the development of ARDS, precipating rapid deterioration culminating in severe hypoxemic respiratory failure. COVID-19 ARDS is the most common complication in hospitalised COVDID-19 patients, with an incidence hovering around 15%. This surge of ARDS cases, due to the sheer number of infected individuals during the initial COVID-19 waves, overwhelmed ICU's. Notably, COVID-19 induced ARDS carries an increased mortality rate of approximately 28% (77). Traditionally, ARDS is characterised by lung oedema resulting in reduced ventilated lung volume, an increase in shunt fraction and diminished respiratory compliance (78). Early in the pandemic, distinction were drawn between COVID-19 induced ARDS and "classical" ARDS with reports highlighting particular high respiratory compliance, increased dead space fraction and specific vascular injuries (79–81). However, recent data suggest a substantial similarity in pathophysiology of COVID-19 induced ARDS to non-COVID-19 ARDS, although the increased endothelial damage and microthrombi might be associated with a slightly higher pulmonary vasoconstriction (82). A large metaanalysis involving 11 356 patients found no evidence supporting distinct respiratory compliance clinical phenotypes with COVID-19 induced ARDS (83). As such, specific ventilatory strategies in COVID-19 ARDS are not warranted and should mirror those employed in non COVID-19 patients (82). Lung autopsy of deceased COVID-19 patients also revealed severe endothelial injury and widespread thrombosis, accompanied by microangiopathy, with capillary microthrombi nine times as prevalent than in influenza (80). Pleural alterations are also observed in COVID-19 patients, commonly presenting as localized pleural thickening and rectraction, while pleural effusion is almost non-existent (84).

1.2.2. Systemic complications and cardiac events.

Sepsis is a life-threatening organ dysfunction caused by a dysregulated host response to infection (85) and is relatively frequent in CAP. Approximately 6% of hospitalised CAP patients present septic shock (68), this figure increases to 11% when the causative agent is *S. pneumonia* (53). A study analysing the host-pathogen related factors of septic shock in pneumococcal pneumonia found that active smoking, chronic corticosteroid and serotype 3

were independent risk factors (53). Additional extrapulmonary complications of CAP include delirium and increased risk of dementia in the years following hospitalisation (86).

Numerous extrapulmonary complications were quickly reported among COVID-19 patients. Neurological complications are commonly encountered, with encephalopathy being the most frequent, with an incidence ranging from 4.4% to 35%, followed by seizures, ischemic and haemorrhagic stroke (87,88). Encephalopathy often presents alongside headaches and appears unrelated to the severity of COVID-19 (87). Several comprehensive studies investigating the pathophysiology of neurological complications in COVID-19 refute the initial hypothesis of specific autoimmune neuronal injury. Instead they suggest the non-specific effects, with a disturbed brain homeostasis, impaired blood-brain barrier and vascular dysfunction, are the primary drivers of neurological complications (87,89). Acute kidney injury rates among hospitalised COVID-19 was 36.6% in a multicentric cohort study including 5449 patients. Acute kidney injury was primarily seen in those with COVID-19 related respiratory failure and is associated with a poor prognosis (90). Gastrointestinal complications were also observed, although less frequently. In a multicentric UK population based study, liver injury was detected in 7.4% of 73 197 hospitalised COVID-19 patients, with a higher prevalence among those with pre-existing liver disease, while gastrointestinal haemorrhage was recorded in only 1% (91). Another study examining abdominal CT imaging of 224 patients revealed bowel-wall abnormalities in 31% of images, with pathological findings in four patients indicating ischemic enteritis with patchy necrosis (92).

Of particular concern are cardiac events accompanying CAP (93–95) with an incidence ranging from 8% to 32% (96–99). It is increasingly evident that the development of acute cardiac events in patients with CAP is an independent predictor of adverse outcomes [5,7]. Additionally, hospitalised patients with CAP face a twofold elevation in the long-term risk for cardiovascular disease, new onset heart failure and mortality compared to the general population (52,61,100,101). Numerous cohort studies focusing on the overall population of all-cause CAP have identified certain host factors associated with the development of acute cardiac events (96–99,102,103). Importantly, the development of life-threatening acute cardiac events appears to be particularly frequent among patients with pneumococcal CAP (96,104). In addition pneumococcal bacteraemia has been found to increase the risk of new onset heart failure up to 10 years compared to controls (100). The invasive potential of *S. pneumoniae* into the myocardium, leading to cardiac injury through microlesion formation has

been demonstrated (105–107). A strong correlation between bacteraemia and elevated levels of cardiac troponin-L and cardiac damage has been observed (108,109). Pneumolysin, a key virulence factor of S. *pneumoniae*, mediates cardiac damage and impairs cardiomyocyte contractile function (108,110). Antimicrobial treatment has been associated with cardiac scarring as a result of collagen synthesis in damaged myocardium tissue, potentially explaining the increased risk of long-term cardiac complications such as arrhythmias and left ventricular dysfunction (105,106). A recent experimental study in mice suggested that cardiac damage might depend on certain pneumococcal strains' ability to induce severe bacteraemia, with lesion types potentially being strain-specific (109). Intriguingly, similar cardiac microlesions devoid of bacteria were observed in heart samples from three rhesus macaques infected with simian immunodeficiency virus who succumbed to pneumococcal pneumonia despite antibiotic treatment, as well as in two out of nine humans who died from invasive pneumococcal disease (106).

In addition, it was quickly noted that acute cardiac events frequently complicate SARS-CoV-2 pneumonia, significantly affecting patient outcomes. Approximately 11.4% of patients hospitalised with SARS-CoV-2 pneumonia experience acute cardiac events (111). Moreover, the increased risk for cardiac complications can persist up to 1 year following recovery from acute COVID-19 (112). Proposed mechanisms contributing to acute cardiac events in SARS-CoV-2 pneumonia include cytokine storms, microthrombi or macrothrombi, direct viral invasion, oxygen supply-demand imbalances, particularly among those with underlying ischemic heart disease (113) and pro-atherogenic metabolic alterations (114,115). Both SARS-CoV-2 infection and mRNA COVID-19 vaccination have been associated with increased risk of myocarditis, with COVID-19 posing a notably higher risk compared to the vaccine (116). Recent findings indicate that myocarditis associated with COVID-19 and mRNA vaccines manifests different clinical and imaging characteristics, with evidence suggesting the involvement of unique immunological mechanisms (117).

1.2.3 Long term complications of CAP and COVID-19.

Additionally, CAP can lead to long-term consequences. Although many patients typically regain normal lung function within weeks to months after pneumonia, some may not fully recover and face an elevated risk of developing lasting sequelae. The local inflammation may lead to bronchiectasis (118,119) and bronchiolitis obliterans (120). In addition, in children, bacterial pneumonia has been found to increase the risk of developing restrictive pulmonary

disease (121) and asthma (122). CAP patients also present an increased risk of dementia and cardiac events, such as new-onset arrhythmia and heart failure, in the years following hospitalisation (86,100).

Furthermore, the long-terms effect on the lung of SARS-CoV-2 pneumonia have been extensively studied. Functional and radiological pulmonary abnormalities in COVID-19 survivors are prevalent, with one-third of hospitalised patients still exhibiting ground-glass opacities and/or interstitial thickening, and fibrotic changes such as traction bronchiectasis and parenchymal bands on chest CT scans at six months (123). Most evidence indicate that these fibrotic-like changes result from severe COVID-19 and ARDS, with recent longitudinal studies demonstrating an improvement in radiological abnormalities in the months following the acute phase (124,125). Additionally, a small number continue to have a persistently elevated risk of venothromboembolic disease (126). To date, there have been no studies documenting progressive fibrosis due to SARS-CoV-2 (127). Moreover, many patients continue to experience a wide range of long-term symptoms following the acute phase of SARS-CoV-2 infection, now commonly referred to as "long-COVID". Studies indicate that up to 20% of patients are still symptomatic at 9 months, with fatigue (11%) and dyspnoea (8%) being the most commonly reported (128). Additionally, a high prevalence of neurologic and psychiatric symptoms has been observed, with depression, anxiety, and mood changes being widely reported (129). Some patients also report persisting cognitive impairment, including memory problems, attention deficit and sleep disorder (129,130). Female gender, age, preexisting hypertension, cardiovascular disease, diabetes, chronic obstructive pulmonary disease, smoking, obesity, chronic alcoholism, longer hospital stay, ICU admission and multiple symptoms at onset, all increase the likelihood of long-COVID (128,131). Furthermore, RNAemia at admission is associated with a poorer quality of life and the presence of more long-COVID symptoms at six months after hospital admission (132). It is noteworthy, that the presence of post-infective fatigue and most neurologic and psychiatric symptoms of long-COVID do not correlate with COVID-19 severity during the acute phase (133). Unfortunately, the pathogenesis of long COVID-19 is largely unknown and symptoms are usually resistant to treatment but may resolve over time (134).

1.3. Host-Pathogen Interaction in community-acquired pneumonia

The host–pathogen interaction in CAP is complex involving a myriad of factors including pathogen virulence, changes in microbiota composition, genetic predisposition, as well as transcriptomic, proteomic and metabolomic alterations all acting synergistically in modulating the inflammatory-immune response (135,136). Recent advancements in genomics, transcriptomics, proteomics and metabolomics have ushered in an era of integrated and comprehensive phenotype determination in living organisms, often referred to as "the Omics revolution". In Figure 3, the interconnectedness of various 'omics studies are illustrated.

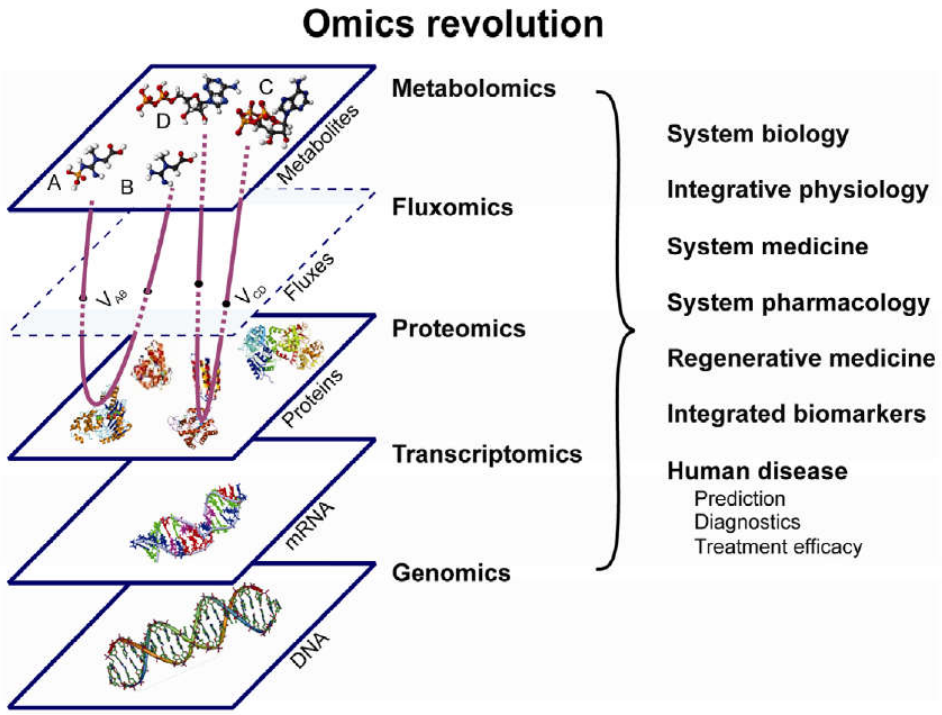

Figure 3. The "omics revolution", the interconnectedness of various 'omics studies. An integrated comprehensive "omics" approach combining genomics, transcriptomics, proteomics and metabolomics, for advancement of systemic sciences and for human disease diagnostics and treatment. Adapted from Nielsen, Jens, and Stephen Oliver. "The next wave in metabolome analysis." Trends in biotechnology vol. 23,11 (2005): 544-6. doi:10.1016/j.tibtech.2005.08.005.

1.3.1. Genetic predisposition

Genome-wide studies have been crucial in unravelling genetic predispositions for CAP, COVID-19, and the progression to more severe clinical courses.

One such study conducted a genome-wide association analysis of lifetime self-reported pneumonia diagnosis using participants obtained by 23andMe, Inc. revealing a significant signal in the major histocompatibility complex region on chromosome six (137). Furthermore, recently investigators uncovered additional association signals for lifetime pneumonia susceptibility outside of the major histocompatibility complex region, implicating genes such as TNFRSF1A, IL6R, and MUC5AC (138). MUC5AC is a Protein Coding Gene whose transcription results in a gel-forming glycoprotein of respiratory and gastric tract epithelia that protects the mucosa from infection and chemical damage by binding to inhaled microorganisms (139,140). Another study identified 18 genes across chromosomes 15, 16 and 9, including IL127, PBX3, ApoB receptor (APOBR) and smoking related genes CHRNA3/5, which were associated with pneumonia susceptibility (141).

Numerous genome-wide association studies have been conducted to elucidate COVID-19 susceptibility and severity (142). These studies identified certain regions, such as 3p21.31, and blood group A, related to SARS-CoV-2 pneumonia severity (143–145). Notably, the 3p21.31 locus, a complex genomic region rich in genes, stands out as the most significant. Within this loci, the SLC6A20 gene, responsible for encoding a sodium amino-acid transporter, has been proposed as a key determinant of infection susceptibility due to its functional interaction with the SARS-CoV-2 receptor ACE2 (146). Moreover, the leucine zipper transcription factor-like 1 (LZTFL1) gene located in this region influences the viral response pathway known as epithelial-mesenchymal transition in lung epithelial cells (147). Additionally, the 3p21.31 region also harbours a number of chemokine receptor genes. Several underlying mechanisms could explain the association of blood group A with SARS-CoV-2 infection susceptibility and severity. These include a hypothesized protective effect of ABO antibodies against viral infections (148), the potential role of ABO(H) antigens in facilitating viral entry into host cells, with antigen A maximizing the interaction of SARS-CoV-2 with the target cells (149), and the observed association between non-O blood types and an elevated risk of thromboembolic events (150). Furthermore, several ACE2 polymorphisms, which enhance RBD and ACE2 interaction, have been linked to predisposition to severity (145). Moreover, these genome-wide studies have also unveiled

rare genetic variant such as inborn errors of type 1 INF that correlated with increased severity and susceptibility to COVID-19 (151).

1.3.2. Microbiota, immunity and inflammation.

The lung should no longer be viewed as a sterile organ, as it harbours a diverse microbiota crucial for maintaining immunologic balance within the airways, thereby influencing pneumonia susceptibility (152–154). An imbalance in the lower airway microbiota, often termed "unhealthy" may favour inflammation and create a favourable environment for pathogen proliferation by increasing alveolar nutrients, leading to the dominance of harmful microorganisms (155).

However, the respiratory tract boasts a multitude of interconnected defence systems, categorized into innate and adaptive immunity, which serve to safeguard against microbial invasion. Neutrophils form the frontline of the innate immune response combating pathogens in the lower airways, with various adhesion molecules involved in their migration to the bronchial epithelium during CAP (156). Activated neutrophils unleash reactive oxygen species and granular enzymes, engage in phagocytosis, and deploy extracellular structures known as neutrophil extracellular traps to ensnare and kill microorganisms(157). Elevated markers of neutrophil extracellular traps have been correlated with higher mortality, prolonged time to clinical stability, and increased hospital stays in CAP (158). Furthermore, the host–pathogen interaction triggers remodelling of the pulmonary transcriptome, orchestrating the release of several cytokines, chemokines, growth factors, opsonins, enzymes, adhesion molecules, receptors, apoptotic, and anti-apoptotic factors (135). This complex response sets forth a proinflammatory cascade, culminating not only in local tissue damage, such as respiratory distress (159), but also systemic manifestations, including septic shock (160) and coagulation disorders. Elevated circulating levels of TNF-α, IL-1ra, and IL-6 in particular have been linked with higher mortality and worse outcomes (159,161). Additionally, IL-1 mediated inflammation triggers the endocrine–adrenal axis, precipitating relative adrenal insufficiency in severe CAP and sepsis patients (162). This hyperinflammatory state predisposes individuals to the development of acute cardiac events, a common complication of CAP (93–95). Furthermore, the procoagulant state observed in CAP, characterized by in vivo platelet activation and thromboxane B2 production, increases the risk of myocardial infarction (163). Platelet activation is further enhanced through lipopolysaccharide-mediated NOX2 activation (164), which has been associated with

arrhythmias development (165). Conversely, high concentrations of regulatory cytokines crucial for lymphocyte survival and homeostasis, such as IL-7, correlate with improved outcomes (166).

Regarding the immune and inflammatory response to SARS-CoV-2 infection, it was found that an early adaptive immune response with a rapid production of bystanders CD8 T cells and plasmablasts with almost no systemic inflammation appears to take place in asymptomatic patients or those with mild disease [4]. In contrast, progression to severe illness with acute respiratory distress is accompanied by a proinflammatory immune dysregulation featuring a robust type 2 response [5,6]. Additionally, activated monocytes and macrophages migrate to the lungs via chemotaxis, intensifying lung inflammation leading to pulmonary fibrosis (167). Severe COVID-19 is further distinguished by an inflammatory profile. This entails an initial evasion of the immune system through downregulation of Type I Interferon pathways along with significant upregulation of IL-6, IL-8 and TNF-α in the lungs that coincides with increased NF-ϰB activity (168,169).

Nonetheless, for many patients, a weakened inflammatory response, termed "sepsis-induced immunoparalysis", predominates as the primary immune dysfunction contributing to poor outcomes in CAP. Notably, lymphopenia stands out as an independent predictor of mortality among hospitalised CAP patients (170). Additionally, alterations in humoral response, such as decreased serum IgG2 concentrations, have been linked to increased ICU admission and mortality rates (170). In the context of influenza pneumonia, a state of sepsis induced immunosuppression often prevails. It has been found that low levels of the proinflammatory IL-17 correlated with a higher risk of death in severe influenza pneumonia (171). This sepsis induced immunosuppression elevates the risk of secondary infections like aspergillosis, particularly in patients requiring ICU admission and concurrent corticosteroid therapy (172). Similarly in SARS-CoV-2 pneumonia, approximately 18-19% of patients with critical COVID-19 develop COVID-19-associated aspergillosis (173,174).

The understanding of the inflammatory response in CAP and SARS-CoV-2 pneumonia has led to clinical trials evaluating immunomodulatory treatments, focused almost exclusively on anti-inflammatory therapies. Several studies have been performed with corticosteroids, tocilizumab, macrolides, statins, N-acetylcysteine, vitamin C, immunoglobulin, and other molecules, as well as targeting the coagulation pathways, as

adjuvant therapies in CAP and SARS-CoV-2. Figure 4 shows in a schematic the conceptual model of the different factors and interventions tested.

It is crucial to acknowledge that due to the compartmentalization of the immune response, inflammatory markers measured in the bloodstream may not fully represent the overall immune status. Local immune responses are expected to be induced in the respiratory tract upon infection (175). Within the mucosal compartment, humoral responses are primarily characterized by the production of secretory IgA (sIgA) antibodies (176,177). These antibodies undergo a complex multi-step process, beginning with dimeric IgA antibodies secreted by local plasma cells. Subsequently, this complex migrates to the mucosal lumen, where proteolytic cleavage occurs, resulting in the attachment of dimeric IgA to the secretory component. This secretory component, a hallmark of sIgA, shields the complex from proteolysis. Notably, mucosal sIgA and IgA antibodies act as the first line of defence (178,179) against respiratory pathogens like the influenza virus (180,181), effectively impeding infection. Similarly, studies have documented the presence of virus-specific IgG and IgA in the saliva and nasal secretions of individuals with COVID-19 (182,183).

However, our understanding of the specific local immune response in mucosal surfaces following *S. pneumonia*, *H. influenzae*, influenza and SARS-CoV-2 infection remains limited.

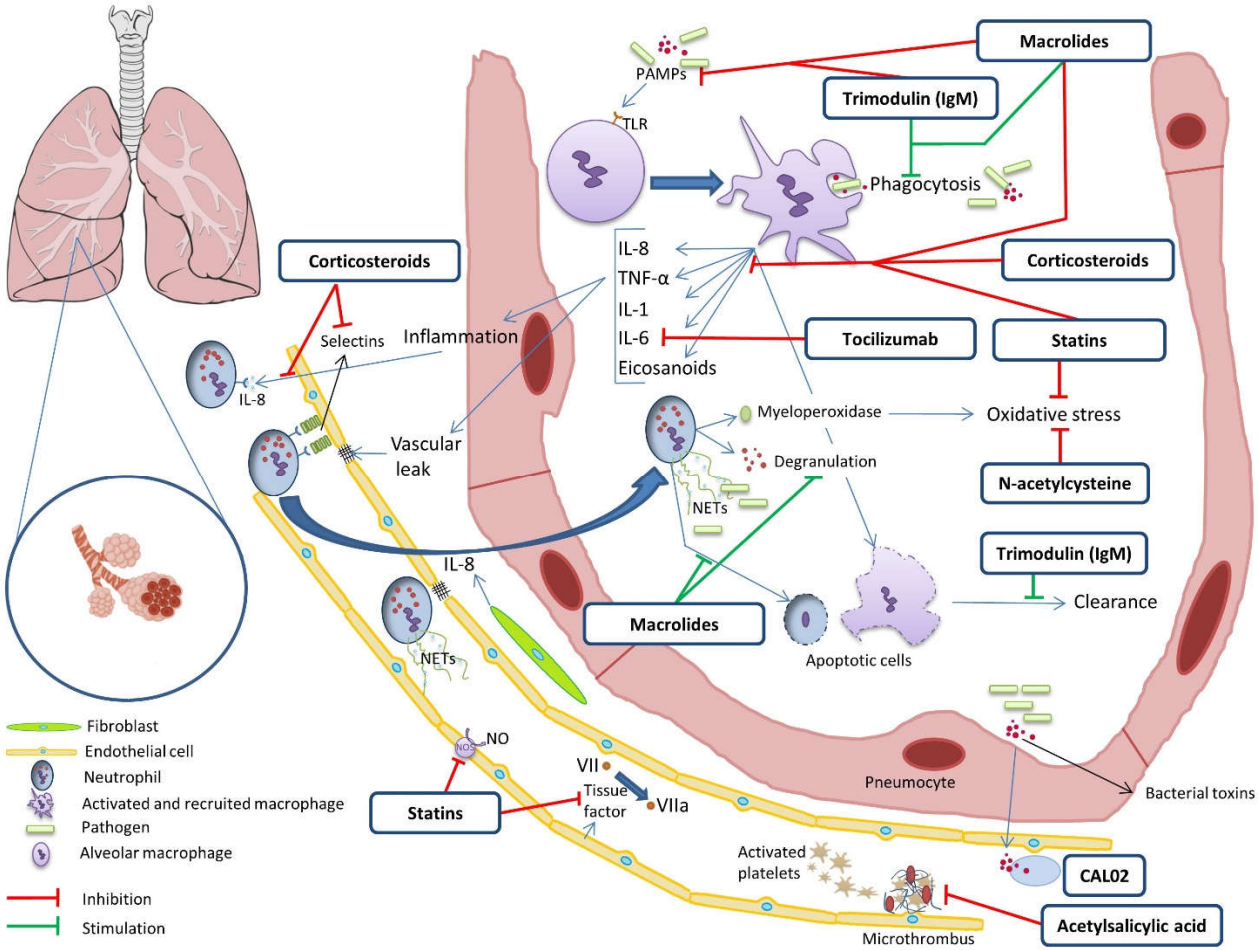

Figure 4. Conceptual model of the different inflammatory factors involved in CAP and SARS-CoV-2 pneumonia and interventions tested. From Rombauts, Alexander et al. "Role of the inflammatory response in community-acquired pneumonia: clinical implications." Expert review of anti-infective therapy vol. 20,10 (2022): 1261-1274. doi:10.1080/14787210.2021.1834848

1.3.3. Immune imprinting

The establishment of immunologic memory to viral pathogens is a fundamental feature of the adaptive immune system, enabling more robust and rapid immune responses upon subsequent re-infection (184,185). Viral pathogens continually undergo mutations in their surface antigens. Those mutations in epitopes, allowing evasion from antibodies generated in response to previous exposures to closely related epitopes, confer selective advantage to new viral strains. The concept of immune imprinting, also known as original antigenic sin, describes the tendency of the immune system to recall existing memory cells rather than eliciting de novo responses when encountering a novel but closely related antigen or epitope (186).

This phenomenon has been extensively observed, particularly in influenza virus, where subsequent infections with antigenically related strains trigger a recall response or 'back-boosting.' This leads to an increase in antibody titers toward epitopes shared between the current and previously encountered strains (187–189). Boost of cross-reactive antibody responses can also occur for viruses like dengue, where secondary infections with a different serotype result in higher titers specific to the original virus compared to the second infecting serotype (190,191).

Immune imprinting has lifelong effects, previous research has demonstrated that childhood immune imprinting to influenza A influences birth-specific risk during seasonal H1N1 and H3N2 epidemics (192). Although initially unclear, it has now been well established that immunological imprinting also occurs with SARS-CoV-2, with other related betacoronavirus and with different variants of concerns (193).

Understanding immunological imprinting holds crucial implications for influenza vaccine effectiveness (186,194). Additionally, this phenomenon can hinder the development and efficacy of vaccines against new variants of concern of SARS-CoV-2, such as the omicron variant (195).

1.3.4. Host transcriptomic response

Transcriptomics is the study of the 'transcriptome,' a concept widely recognized as the comprehensive ensemble of all ribonucleic acid (RNA) molecules, known as transcripts, expressed within a given entity, be it a cell, tissue, or organism(196).

Following transcription, human precursor RNAs undergo further processing and splicing to attain their mature forms. These mature messenger RNA transcripts encompass various elements, including 5' and 3' untranslated regions (UTRs), alongside the coding region that dictates protein translation. Among these transcripts are transfer RNA, ribosomal RNA, small nuclear RNA, small nucleolar RNA, short interfering RNA, micro RNA, long non-coding RNA and pseudogenes, all contributing to a diverse array of cellular functions (197). In contrast to the relatively stable DNA molecule, which primarily serves as a repository of genetic information across cell lineages, RNA exhibits a dual role as both a carrier of information and a catalyst. RNA displays dynamism, with its synthesis and degradation subject to regulation by various factors, thus contributing significantly to cellular dynamics. It is believed that an ancient RNA world preceded the contemporary genetic system, where DNA serves as the primary repository of hereditary information (198).

In this regard, the information derived from gene expression (transcriptomic) studies may help to a better understand of the complexity of immune response, identification of novel candidate pathways and targets for potential intervention, discovery of novel candidate diagnostic and stratification biomarkers, and the ability to stratify patients into clinically relevant, expression-based subclasses.

Recent transcriptomic studies in CAP patients found evidence of mitochondrial dysfunction, with a reduced expression of genes involved in oxidative phosphorylation in non-surviving CAP patients. (199,200). Furthermore, enrichment of aminoacyl-transfer RNA and genes related to hydrogen peroxide were downregulated in patients who died (200). In addition, Toll-like receptor and interferon cascades were down-regulated in septic CAP patients compared to controls (199).

Moreover, transcriptomic studies in severe CAP found more evidence of a subgroup of patients presenting “sepsis-induced immunoparalysis”. A gene expression profile (sepsis response signature, SRS1) associated with T-cell exhaustion, HLA class II downregulation

and endotoxin tolerance, thus reflecting an immunosuppressed state, was found in 41% (108 subjects) of patients with severe CAP. This specific transcriptomic signature predicted worse outcomes (201). Another transcriptomic study in CAP found that impaired expression of genes in the blood related with antigen presentation, B-cell development, T-helper cell differentiation, apoptosis, granzyme B signalling was associated with persistence of viral secretion and a more severe disease course (202).

Following the onset of COVID-19, there has been a surge in transcriptomic studies. While numerous studies have focused on analysing single-cell RNA extracted from peripheral mononuclear cells (203), only a handful have been performed on total RNA from whole blood. Among these, some studies identified transcriptomic signatures capable of distinguishing SARS-CoV-2 infection from influenza (204) and other viral respiratory pathogens (205). Concurrently, other studies pinpointed the transcriptomic signature of SARS-CoV-2 infection by comparing asymptomatic with symptomatic patients (206,207). In exploring whole blood transcriptomic profiles across varying clinical statuses, researchers have observed that more severe cases tend to exhibit upregulated expression of genes primarily associated with neutrophil activation (204,208–211), myeloid cells (210), Il2, Il6, IL8, protein autophagy, protein polyubiquitination (209), TNF-α, and glycolysis (208). Conversely, genes linked to T-cell activation were down-regulated in more severe SARS-CoV-2 pneumonia (204,209,210,212). Upon bulk analysis of whole blood cell transcriptomes of severe COVID-19 patients compared to non-critically ill COVID-19 patients, upregulation of interferon alpha emerged as a primary contributor to severe COVID-19 (167). However, the picture regarding interferon-γ (IFN- γ) gene expression is less straightforward. While two studies found an enrichment (208,210), another observed a down-regulation of IFN-γ related genes (209).

A significant limitation of many COVID-19 transcriptomic studies performed to date lies in their reliance on a single time point per patient (204,205,209,210,212), thereby overlooking the dynamic nature of the disease. Furthermore, several investigations observed heterogeneity in the transcriptomic profiles among the more severe groups of hospitalised COVID-19 patients (208,211,212).

1.3.5. Host metabolomics and proteomic response

Proteins and metabolites represent the end products of cellular regulatory processes, reflecting the ultimate response of biological systems to genetic or environmental changes (213). The collective set of metabolites synthesized by a biological system constitute its 'metabolome'. Metabolomics involves the comprehensive and simultaneous systematic profiling of multiple metabolite concentrations and their cellular and systemic fluctuations. This approach allows for the study of responses to various stimuli such as drugs, diet, lifestyle, environment, infections and genetic modulations, aiming to characterize both the beneficial and adverse effects of such interactions (214). Several metabolomics analytical platforms are available, with mass spectrometry (usually coupled with a chromatographic separation step) and nuclear magnetic resonance (NMR) spectroscopy being the most widely employed (215). Each technique has distinct advantages and drawbacks. NMR spectroscopy stands out due to its rapid, highly accurate, non-destructive, and quantitative features (216,217). However, it exhibits lower sensitivity, a larger peak can mask lower concentrations of potentially important compounds, which, thus cannot be identified (218).

Some proteomic and metabolomic studies recently have been conducted to provide a comprehensive understanding of the cellular physiology of CAP (219–223). These studies described the metabolites and molecules involved in inflammation, coagulation, oxidative stress, lipid metabolism, and complement activation. For instance, a cohort of 240 patients with CAP, proteome and metabolome signatures associated with severity and specific organ dysfunctions were identified, correlating with the Sequential Organ Failure Assessment (SOFA) score (219). Notably, low levels of circulating phosphatidylcholine (PC) and sphingolipid concentrations were found to correlate with severe CAP (219). Furthermore, alterations in lipoprotein profile characterized CAP patients, with reduced levels of high-density lipoprotein (HDL), phospholipids and apolipoproteins like A-II and D (223,224). Additionally, alterations in amino acids, including decreased tryptophan and elevated kynurenine, were observed in severe CAP, reflecting immune dysregulation (225–227).

Other studies have explored differences in lower airway lipid compositions based on the intensity of the inflammatory response (220), as well as the ability of metabolomics profiles to discriminate between severe and non-severe CAP (221).

In contrast to the relative paucity of proteomic and metabolomic studies in CAP, there has been a surge of such studies in SARS-CoV-2 pneumonia. Similar to transcriptomic

studies, the emergence of COVID-19 has led to an explosion in proteomic and metabolomic research.

Numerous studies have investigated the metabolic alterations associated with COVID-19 (115,225–239), with a focus on discriminating between SARS-CoV-2 infected patients and non-infected individuals. Among SARS-CoV-2 infected patients, significant alterations have been observed, including remodelling of glycerophospholipid metabolism (115,234,235), enriched purine metabolism (234,237), changes in lipoprotein distribution marked by elevated of very-low-density lipoprotein (VLDL) and triglycerides (228,238,239), and dysregulation in glycolysis (228). Moreover, increased COVID-19 severity has been associated with disruptions in mitochondrial activity (229,230,238), altered fatty acid oxidation (229), reduced amino-acids reflecting a catabolic state (230–232,238), impaired cholesterol homeostasis (115,233,234,238) and again, a decline in tryptophan reflecting immune dysregulation (225–227). Additionally, low levels of circulating lysoPCs and PCs have been directly associated with COVID-19 severity (226,229,232,234). Some studies have aimed to identify a metabolomic signature capable of predicting COVID-19 progression (225,226,235). However, most of the included patients in these studies had already progressed to critical states when their blood samples were collected, with the metabolomic profile correlating COVID-19 severity rather than disease progression risk. However, to date, only one NMR-based study involving a cohort of 36 patients has explored a prognostic metabolomic profile for mortality (240).

Proteomic and metabolomic studies provide invaluable insights into the pathophysiology of pneumonia, including CAP and SARS-CoV-2 pneumonia. These studies have identified key metabolic alterations associated with disease severity and progression, highlighting the potential for targeted therapeutic interventions and prognostic biomarker discovery.

1.3.6. Pathogen related factors

As mentioned before, the severity and clinical manifestations of CAP are influenced by the virulence factors possessed by the causative pathogens, which enable them to colonize, evade host defences, and cause tissue damage.

3.6.1. Bacterial pathogen virulence factors

As previously mentioned, *S. pneumoniae*, *H. influenzae*, *S. aureus* and atypical bacteria such as *M. pneumoniae* and *L. pneumonophila* are among the frequent bacterial microorganism causing CAP.

S. pneumoniae colonises the nasopharynx in asymptomatic carriers, spreading primarily through close contact (241), but also via fomites (242) to other individuals. Coinfection during viral infections can further facilitate increased host colonisation (243) with an elevated bacterial load (244). *S. pneumoniae* hosts an array of virulence factors crucial for pathogenesis (245). Notably, pneumolysin, a pore-forming cytolytic toxin binging to cholesterol-containing membranes stands as a key virulence determinant (246,247). Recent evidence highlights the strain dependent effect of pneumolysin on macrophage function, emphasizing the significance of other genetic background components (248). Moreover, pneumolysin has been implicated in mediating cardiac damage, impairing cardiomyocyte contractile function (108,110), and promoting biofilm formation (249). The pneumococcal surface protein A (PspA) interferes with the fixation of complement component C3, inhibiting complement mediated opsonisation (250), while pneumococcal surface protein C (PspC) hampers the function of secretory IgA (251). The pneumococcal polysaccharide capsule is crucial for pneumococcal virulence, possessing strong anti-phagocytic capabilities, and reducing snaring in neutrophil extracellular traps (252). The virulence of *S. pneumoniae* is closely linked to the capsule thickness in specific strains and serotypes (253). Distinct serotypes exhibit varying disease-causing capacities, with serotype 3, for instance, identified as an independent risk factor for septic shock in pneumococcal pneumonia (53). Serotype 3 and 9n have also been associated with cardiac events in invasive pneumococcal disease (254).

H. influenzae adheres to respiratory epithelial cells' extracellular matrix proteins via several adhesins, notably protein E, F, and outer membrane protein P4 (255,256). *H. influenza* strains strongly rely on the presence of their capsule for their survival in the presence of complement. During host colonisation, *H. influenzae* forms aggregates of hosts cells and live and dead bacteria on the mucosal surface, shielding itself from the host immune system (257). Extracellular DNA, such as DNABII, is critical for these aggregates integrity (258). Additionally, lipoprotein H, helps decreasing complement mediated killing (259).

S. aureus produces several toxins implicated in severe necrotizing pneumonia pathogenesis (75,76).

Atypical pathogens like *M. pneumoniae* encodes various virulence factors, including adhesins, glycolipids, toxic metabolites, community-acquired respiratory distress syndrome toxin, and capsular polysaccharides (260). Lacking a cell wall, *M. pneumoniae* adheres to the respiratory epithelial cells via a specific attachment organelle (protruding at one end of its cell) (261). The community-acquired respiratory distress syndrome toxin exhibits high binding affinity to surfactant protein A and annexin A2 (262) and is cytotoxic to mammalian cells (263). Furthermore, a nuclease encoded by MPN491, degrades neutrophil extracellular traps aiding the pathogen in evading host immune attack (264). *L. pneumophila* employs a Dot/Icm type IV secretion system to enable intracellular bacterial replication and subsequent disease (265).

3.6.2. Viral pathogen virulence factors

To initiate infection, viruses must first attach to the surface of host cell, binding to one or more cellular receptors. Subsequently, they need to gain access to the cytosol, very often requiring reaching a specific subcellular location to commence viral replication (266). Viral replication typically occurs within structures known as viroplasm (or viral factories) where nucleic acids and specific viral and cellular proteins accumulate. However, some viruses, such as influenza and coronaviruses rely on the endoplasmic reticulum, Golgi apparatus, and exocytic pathways for the maturation and folding of their proteins (267). Various viruses, including rhinoviruses, respiratory syncytial virus, adenovirus, influenza and coronaviruses such as SARS-CoV-2, can cause viral pneumonia. These viruses employ diverse strategies to infect respiratory epithelial cells and evade host immune responses.

For instance, hemagglutinin, found on the surface of influenza viruses, serves as both an attachment factor and membrane fusion protein, playing a key role in virulence (268). Mutations of hemagglutinin can expand tissue tropism, enhance host receptor biding and optimize membrane fusion (269,270). Similarly, mutations in influenza polymerase proteins can increase viral replication and the production of viral particles (271). The viral NS1 protein is crucial for overcoming host antiviral immunity (272).

Respiratory syncytial virus primarily enters cells through attachment of the G glycoprotein to various human surface proteins, including heparan sulphate proteoglycans,

CX3C chemokine receptor, EGFR, IGF1R, and ICAM-1 (273). Two non-structural proteins of respiratory syncytial virus NS1 and NS2 aide in immune evasion by antagonizing interferon (274).

SARS-CoV-2, akin to SARS-CoV-1, enters airway cells by binding its S protein to the ACE2 receptor. Mutations in the S-gene, such as the one that occurred with the alpha variant, that also led to the S gene dropout in the NAATs tests used for diagnosis, can increase infectivity (275). Variants of concerns such as, Alpha, Delta and Omicron all carry mutations that further enhance binding, with the mutation N501Y in the receptor binding domain being a notable example (276). Moreover, a furin cleavage site within the S protein essential for enabling membrane fusion, contributes significantly to the high transmission rates of SARS-CoV-2 (277). Further optimization of the furin cleavage site during the pandemic has led to enhanced furin cleavage of the Alpha and Delta spike proteins, associated with increased transmission effectiveness (278). Virulence of SARS-CoV-2 variants is also influenced by tissue or organ tropism. For example, the Omicron BA.1 variant shows a preference for efficient replication in the nasopharynx, unlike the ancestral virus, which primarily infected bronchial and lung cells, thus leading to increased transmissibility but milder infections (279).

2. Hypothesis

Hypothesis

1. The whole blood transcriptome of hospitalised CAP patients exhibits distinctive patterns between survivors and non-survivors, serving as a valuable prognostic biomarker.

2. *S. pneumoniae* serotypes and clonal complexes are a key determinant in the development of acute cardiac events in CAP.

3. Hospitalised adults with COVID-19 who progress to severe disease manifest a unique transcriptomic profile in whole blood compared to those with moderate symptoms.

4. Prior infections with other human coronaviruses influence the nature of the antibody response against severe acute respiratory syndrome coronavirus 2.

5. SARS-CoV-2 infection induces a robust local mucosal humoral immunity, a process influenced by previous exposure to other human coronaviruses.

6. A distinct metabolomic signature is present in hospitalised COVID-19 patients with initially moderate symptoms who subsequently deteriorate to severe disease. This signature is useful for assessing the risk of disease progression.

3. Objectives

Objectives

1. To analyse the difference in gene expression profile (transcriptomics) in whole blood between survivors and non-survivor CAP patients in order to identify pathophysiological pathways and prognostic biomarkers.

2. To delineate the host-pathogen related risk factors for the development of acute cardiac events in pneumococcal pneumonia.

3. To determine the dynamic difference in gene expression profile (transcriptomic) in whole blood between severe and moderate hospitalised COVID-19 patients in order to broaden our understanding of the heterogeneity in clinical outcome.

4. To identify the dynamic antibody responses characterizing de novo antibody responses against SARS-CoV-2. To characterize pre-existing immunity against selected endemic coronavirus being targeted by the humoral immune system to investigate the role of immunological imprinting on COVID-19 patients' antibody response.

5. To characterized the early mucosal antibody response and immunoglobulin repertoire against SARS-CoV-2 and seasonal HCoV-OC43 S proteins in nasopharyngeal swabs of COVID-19 patients.

6. To determine the metabolomic alteration of severe COVID-19 and to develop a predictive model based on a metabolomics signature able to predict disease progression.

4. Material, methods and results

Study 1

Whole-Blood Gene Expression Profiles Associated with Mortality in Community-Acquired Pneumonia.

Viasus, D. ✉, Simonetti, A. F., Nonell, L., Vidal, O., Meije, Y., Ortega, L., Arnal, M., Bódalo-Torruella, M., Sierra, M., **Rombauts, A**., Abelenda-Alonso, G., Blanchart, G., Gudiol, C., & Carratalà, J.

Biomedicines, 2023, 11(2), 429.

Impact factor: 4.7 (1st quartile)

biomedicines

MDPI

Article

Whole-Blood Gene Expression Profiles Associated with Mortality in Community-Acquired Pneumonia

Diego Viasus [1,*], Antonella F. Simonetti [2,3], Lara Nonell [4], Oscar Vidal [1], Yolanda Meije [5], Lucía Ortega [5], Magdalena Arnal [4], Marta Bódalo-Torruella [4], Montserrat Sierra [6], Alexander Rombauts [7], Gabriela Abelenda-Alonso [7], Gemma Blanchart [8], Carlota Gudiol [3,7,9] and Jordi Carratalà [3,7,9]

1 Department of Medicine, Division of Health Sciences, Universidad del Norte and Hospital Universidad del Norte, Barranquilla 081001, Colombia
2 Department of Internal Medicine, Consorci Sanitari Alt Penedès-Garraf, 08720 Sant Pere de Ribes, Spain
3 Centro de Investigación Biomédica en Red de Enfermedades Infecciosas (CIBERINFEC), Institulo de Salud Carlos III, 28029 Madrid, Spain
4 MARGenomics, Hospital del Mar Medical Research Institute (IMIM), 08003 Barcelona, Spain
5 Unit of Infectious Disease, Department of Internal Medicine, Hospital de Barcelona—Societat Cooperativa d'Instal·lacions Assistencials Sanitàries (SCIAS), 08029 Barcelona, Spain
6 Microbiology Unit, Department of Clinical Laboratory, Hospital de Barcelona—Societat Cooperativa d'Instal·lacions Assistencials Sanitàries (SCIAS), 08029 Barcelona, Spain
7 Department of Infectious Diseases, Bellvitge University Hospital—Bellvitge Biomedical Research Institute (IDIBELL), 08907 Barcelona, Spain
8 Cardiovascular Risk and Nutrition Research Group, Hospital del Mar Medical Research Institute (IMIM), 08003 Barcelona, Spain
9 Department of Clinical Sciences, University of Barcelona, 08907 Barcelona, Spain
* Correspondence: dviasus@uninorte.edu.co

Abstract: (1) Background: Information regarding gene expression profiles and the prognosis of community-acquired pneumonia (CAP) is scarce. We aimed to examine the differences in the gene expression profiles in peripheral blood at hospital admission between patients with CAP who died during hospitalization and those who survived. (2) Methods: This is a multicenter study of non-immunosuppressed adult patients who required hospitalization for CAP. Whole blood samples were obtained within 24 h of admission for genome-expression-profile analysis. Gene expression profiling identified both differentially expressed genes and enriched gene sets. (3) Results: A total of 198 samples from adult patients who required hospitalization for CAP were processed, of which 13 were from patients who died. Comparison of gene expression between patients who died and those who survived yielded 49 differentially expressed genes, 36 of which were upregulated and 13 downregulated. Gene set enrichment analysis (GSEA) identified four positively enriched gene sets in survivors, mainly associated with the interferon-alpha response, apoptosis, and sex hormone pathways. Similarly, GSEA identified seven positively enriched gene sets, associated with the oxidative stress, endoplasmic reticulum stress, oxidative phosphorylation, and angiogenesis pathways, in the patients who died. Protein–protein-interaction-network analysis identified *FOS*, *CDC42*, *SLC26A10*, *EIF4G2*, *CCND3*, *ASXL1*, *UBE2S*, and *AURKA* as the main gene hubs. (4) Conclusions: We found differences in gene expression profiles at hospital admission between CAP patients who died and those who survived. Our findings may help to identify novel candidate pathways and targets for potential intervention and biomarkers for risk stratification.

Keywords: community-acquired pneumonia; mortality; gene expression profile; gene set enrichment analysis

Citation: Viasus, D.; Simonetti, A.F.; Nonell, L.; Vidal, O.; Meije, Y.; Ortega, L.; Arnal, M.; Bódalo-Torruella, M.; Sierra, M.; Rombauts, A.; et al. Whole-Blood Gene Expression Profiles Associated with Mortality in Community-Acquired Pneumonia. *Biomedicines* **2023**, *11*, 429. https://doi.org/10.3390/biomedicines11020429

Academic Editor: Francesco B. Blasi

Received: 5 December 2022
Revised: 25 January 2023
Accepted: 27 January 2023
Published: 1 February 2023

1. Introduction

Community-acquired pneumonia (CAP) is a public health problem worldwide and continues to be associated with high health costs, morbidity, and mortality. Over the

coming years, the overall burden of CAP is likely to rise as its incidence and the number of elderly people increase [1]. Recent studies have found overall mortality rates of 5% to 15% among hospitalized patients with CAP, and mortality in the subset of patients who require intensive care unit (ICU) admission may be as high as 30%: a rate that matches those of other known medical-emergency diseases, such as ST-elevation myocardial infarction [2]. Most cases of CAP occur when its organisms translocate from the nasopharynx to the lungs. Infection takes place when there has been exposure to a large inoculum or a virulent microorganism and/or the host defenses are impaired.

Studies have stressed the importance of host features in the prognosis of CAP, including inflammatory response, susceptibility to specific pathogens, genome, and metabolic condition [3]. In this regard, the information derived from gene expression studies may broaden our understanding of the complexity of the immune response via identification of novel candidate pathways and targets for potential intervention, discovery of novel candidate diagnostic and stratification biomarkers, and our increased ability to categorize patients into clinically relevant expression-based subclasses. At present, however, information regarding the gene expression profile in CAP is scarce; most published studies have been performed in animal models or focused on patients with sepsis in ICU or patients with specific etiologies, such as pneumococcal pneumonia [4–6].

In the present study, we comprehensively examined differences in gene expression profiles in peripheral blood at hospital admission between CAP patients who subsequently died and those who survived in order to identify genes and related pathways that not only provide information about pathophysiology but may also serve as prognostic biomarkers.

2. Materials and Methods

This study was conducted at two university hospitals for adults in Barcelona, Spain. Nonimmunosuppressed adult patients who required hospital admission for CAP from May 2015 through January 2017 were prospectively recruited and followed up on. All patients included in this study were enrolled within 24 h of hospital admission. This study was approved by the Ethics Committee of the Bellvitge University Hospital (approval code: PR158/14; 6 November 2014). The relevant data and protocols comply with the minimum information about a microarray experiment (MIAME) guidelines [7].

Patients were classified as having CAP if they had an infiltrate on a chest radiograph plus acute illness associated with two or more of the following signs and symptoms: a new cough with or without sputum production, pleuritic chest pain, dyspnea, fever or hypothermia, altered breath sounds on auscultation, or leukocytosis or leukopenia. Patients were seen by the clinical investigators, who recorded data in a computer-assisted protocol, daily during their hospital stays. Demographic characteristics, comorbidities, causative organisms, antibiotic susceptibilities, biochemical analysis, empirical antibiotic therapy, and outcomes were recorded. Patients with neutropenia, solid organ transplantation, antineoplastic chemotherapy, acquired immunodeficiency syndrome (AIDS), current corticosteroid therapy ($\geq$20 mg prednisone/d or equivalent), and pregnancy at admission were excluded.

2.1. RNA Extraction

Whole blood samples (2.5 mL) were obtained within 24 h of hospital admission for genome expression profile analysis. Total RNA was isolated from these whole blood samples using the PaxGene™ blood RNA system (PreAnalytiX, Qiagen/Becton Dickson, Hombrechtikon, Switzerland) in accordance with the manufacturer's specifications. Extracted RNA was stored at minus 80 degrees Celsius until expression profiling. RNA quantification was performed using a spectrophotometer (NanoDrop Technologies, Wilmington, DE, USA) and RNA quality was assessed using an Agilent Bioanalyzer 2100 slide.

2.2. Gene Expression Profiles via Microarrays

Gene expression microarrays were performed at the MARGenomics facilities of the Hospital del Mar Medical Research Institute (IMIM). RNA samples were amplified and

labeled with a GeneChip WT PLUS Reagent kit and hybridized to a Clariom S Human array (Affymetrix, Santa Clara, CA, USA) in a GeneChip Hybridization Oven 640. The washing and scanning steps were performed using the Expression Wash, Stain and Scan Kit and the GeneChip System of Affymetrix (GeneChip Fluidics Station 450 and GeneChip Scanner 3000 7G). After quality control, the raw data were background-corrected, quantile-normalized, and summarized to a gene level using the robust multichip average (RMA) [8], obtaining a total of 20,893 transcripts, excluding controls. NetAffx 36 annotations that corresponded to the hg38 human genome version were used to summarize data into transcript clusters and annotate all of the transcripts analyzed. The microarray data from the present project were deposited in the Gene Expression Omnibus of the National Center for Biotechnology Information (NCBI) under accession number GSE188309.

2.3. Functional Analysis of Expression Data

Functional analysis was performed with gene set enrichment analysis (GSEA) [9,10]. To obtain a summary of the biological states and processes underlying our analysis, we used the Hallmark gene-set collection defined by the Molecular Signatures Database (mSigDB), UC San Diego and Broad Institute, USA (http://www.gsea-msigdb.org/gsea/msigdb). In addition, NetworkAnalyst 3.0, Canada, (https://www.networkanalyst.ca/) and IntAct Molecular Interaction Database, European Molecular Biology Laboratory, EMBL's European Bioinformatics Institute, UK, (https://wwwdev.ebi.ac.uk/intact) were used to construct the protein–protein interaction (PPI) network. These tools allow the generation of an enrichment network in which nodes that may be relevant in the analysis of gene expression can be visualized.

2.4. Statistical Analysis

To obtain the list of differentially expressed genes in the various analyses, a double strategy was followed. As a first approach, linear models for microarray (limma analysis) were used to detect differentially expressed genes between the conditions, including a variable batch to adjust for batch differences [11]. Next, using the same linear models, a subsampling strategy was applied. In brief, 1000 models were generated for each analysis, using a random and balanced subsample of the cases (representing between 55% and 77% of cases, depending on the model). To adjust the possible batch influence, a variable batch was also included in this model. The genes most frequently selected as being differentially expressed were defined as top differentially expressed. Genes with a p-value of less than 0.05 were selected as significant. GSEA results were considered statistically significant when a gene set had a p-value of less than 0.05 and the false discovery rate (FDR) was less than 0.25, following the Broad Institute FAQ guidance. Moreover, expression data for each gene and prognosis were recorded for each patient, and survival curves were generated using survminer R packages. Samples above the median expression were considered highly expressed whereas samples below the median were considered low-expressed. All data analyses were performed in R (version 3.4.2).

3. Results

3.1. Characteristics of the Cohort

During the study period, 228 consecutive nonimmunosuppressed CAP patients were admitted to the hospital, of whom 18 (7.9%) died during hospitalization. The main sociodemographic and clinical features and laboratory findings thereof are shown in Table 1. Most patients were older than 65 years (69.7%), and 154 (67.5%) presented comorbidities, mainly chronic pulmonary and cardiac diseases and diabetes mellitus. Nearly half of the patients had respiratory failure at admission. Regarding etiology, *Streptococcus pneumoniae* was the most frequent causative pathogen. Most patients (64%) were classified as high-risk (pneumonia severity index (PSI) IV–V). The causes of mortality were respiratory failure, multiorgan dysfunction, and septic shock.

Table 1. Characteristics of hospitalized patients with community-acquired pneumonia.

Characteristics	All Patients (N = 228)	Patients Who Died (N = 18)	Patients Who Survived (N = 210)	*p*-Value
Sociodemographic Data				
Age (years), Median (IQR)	75 (62.5–84)	84.5 (59–92)	74.5 (63–83)	0.04
Male Sex	136 (59.6)	12 (66.7)	124 (59)	0.52
Current Smoker	43 (18.9)	2 (11.1)	41 (19.5)	0.53
COPD	72 (31.6)	4 (22.2)	68 (32.4)	0.37
Chronic Heart Disease	82 (36)	9 (50)	73 (34.8)	0.19
Diabetes Mellitus	49 (21.5)	6 (33.3)	43 (20.5)	0.23
Clinical Features at Admission				
Time from Symptom Onset (Days), Median (IQR)	4 (2–7)	3.5 (1–5)	4 (2–7)	0.19
Fever (>38.0 °C)	84 (37)	3 (16.7)	81 (38.0)	0.06
Tachycardia ($\geq$100 Beats $\times$ min^{-1})	135 (59.2)	11 (61.1)	124 (59)	0.86
Tachypnea ($\geq$30 Breaths $\times$ min^{-1})	66 (34.4)	9 (60)	57 (32.2)	0.03
Impaired Consciousness	32 (14)	3 (16.7)	29 (13.8)	0.72
Septic Shock	17 (7.5)	5 (27.8)	12 (5.7)	0.001
Laboratory and Radiographic Findings				
Respiratory Failure ($PaO_2/FiO_2 < 300$ or $PaO_2 < 60$ mmHg)	130 (57)	15 (83.3)	115 (54.8)	0.019
Leukocytosis (Leukocytes $\geq 12 \times 10^9$/L)	136 (59.6)	12 (66.7)	124 (59)	0.52
Multilobar Pneumonia	71 (31.1)	6 (33.3)	65 (32.3)	0.93
Pleural Effusion	8 (3.5)	2 (11.1)	26 (12.4)	1
Bacteremia	19 (8.9)	3 (16.7)	16 (8.2)	0.20
Bacterial Pneumonia	82 (36)	6 (33.3)	76 (36.2)	0.80
Pneumococcal Pneumonia	48 (21.1)	3 (16.7)	45 (21.4)	0.77
Viral Pneumonia	12 (5.3)	1 (5.6)	11 (5.2)	1
CAP-Specific Scores				
PSI Score, Median (IQR)	100 (81.5–123.5)	142 (109–178)	99 (79–121)	<0.001
PSI High-Risk Classes (IV–V)	146 (64)	17 (94.4)	129 (61.4)	0.005

COPD, chronic obstructive pulmonary disease; ICU, intensive care unit; IQR, interquartile range; PSI, pneumonia severity index.

3.2. Differentially Expressed Genes between CAP Patients Who Died and Those Who Survived

A total of 198 samples were processed, 13 of them from patients who died. Missing samples were not processed due to quality or sample-quantity issues. Table 2 shows the list of genes that were differentially expressed in CAP patients who died in relation to in those who survived based on the lowest *p*-value. Analysis yielded 49 differentially expressed genes, 36 of which were upregulated and 13 downregulated in circulation of whole-blood cells. Figure 1 shows the heat map of the differentially expressed genes. In addition, the analyses of the expression data for each gene and prognosis indicated that low expression of the genes *SPRYD3*, *ESPLI*, and *HHIPL2* and high expression of the gene *PLXNA1* were significantly related to survival in CAP patients (Figure 2). Other genes whose expression tended to be related to survival were *COQ6*, *METTL20*, *PGAP2*, *DIXDC1*, *NRL*, and *ADCK4*. The curves of these analyses are shown in Supplementary Figure S1.

Table 2. List of genes differentially expressed in community-acquired pneumonia patients who died in relation to patients who survived based on the lowest *p*-value.

Symbol	Gene Name	*p*-Value	Fold Change	Resampling (N Times)
SCRG1	Stimulator of chondrogenesis 1	0.001	1.28	383
FAM72A	Family with sequence similarity 72, member A	0.001	1.45	363
KCNK16	Potassium channel, two-pore-domain subfamily K, member 16	0.001	1.20	270
SLC26A10	Solute carrier family 26, member 10	0.001	1.25	267
ZNF563	Zinc finger protein 563	0.001	1.18	448
OTUD7B	OTU deubiquitinase 7B	0.002	1.20	339
ADCK4	aarF domain containing kinase 4	0.004	1.16	533
F2RL2	Coagulation factor II (thrombin) receptor-like 2	0.004	1.18	337
GTPBP6	GTP binding protein 6 (putative)	0.004	−1.13	286
TBKBP1	TBK1 binding protein 1	0.004	1.35	365
HHIPL2	HHIP-like 2	0.005	1.14	346
PLXNA1	Plexin A1	0.005	−1.13	339
SPATA5	Transcript Identified with AceView, Entrez Gene ID(s) 166378	0.006	−1.18	418
NRL	Neural retina leucine zipper	0.006	1.17	317
UBE2S	Ubiquitin-conjugating enzyme E2S	0.006	1.18	268
MFSD9	Major facilitator superfamily domain containing 9	0.007	1.28	327
OXR1	Oxidation resistance 1	0.007	1.24	257
DIXDC1	DIX domain containing 1	0.007	1.23	344
SH3D21	SH3 domain containing 21	0.009	−1.16	337
PGAP2	Post-GPI attachment to proteins 2	0.009	1.18	265
FOS	FBJ murine osteosarcoma viral oncogene homolog	0.009	1.19	318
ZFYVE21	Zinc finger, FYVE domain containing 21	0.009	1.18	261
HS6ST1	Heparan sulfate 6-O-sulfotransferase 1	0.009	1.12	258
BTBD8	BTB (POZ) domain containing 8	0.012	1.22	315
RIMKLB	Ribosomal modification protein rimK-like family member B	0.012	1.19	312
EBF4	Early B-cell factor 4	0.012	−1.14	428
METTL20	Methyltransferase-like 20	0.013	1.16	293
EIF4G2	Eukaryotic translation initiation factor 4 gamma, 2	0.016	−1.15	279
CACNA1S	Calcium channel, voltage-dependent, L type, alpha 1S subunit	0.018	−1.14	304
TM4SF1	Transmembrane 4 L six family member 1	0.023	−1.19	357
ZNF311	Zinc finger protein 311	0.023	−1.12	268
HLA-DQA2	Major histocompatibility complex, class II, DQ alpha 2	0.026	−1.24	255
ESPL1	Extra spindle pole bodies like 1, separase	0.028	1.12	266
BUD31	Transcript Identified with AceView, Entrez Gene ID(s) 8896	0.030	1.17	283
CCND3	Memczak2013 ALT_ACCEPTOR, ALT_DONOR, coding, INTERNAL, intronic best transcript NM_001136017	0.031	1.34	318
GINS1	GINS complex subunit 1 (Psf1 homolog)	0.031	1.19	262
ASXL1	Additional sex combs like transcriptional regulator 1	0.031	1.21	404
C10orf54	Chromosome 10 open reading frame 54	0.033	1.18	403
AURKA	Aurora kinase A	0.034	1.18	332

Table 2. *Cont.*

Symbol	Gene Name	*p*-Value	Fold Change	Resampling (N Times)
ZNF506	Zinc finger protein 506	0.035	1.13	267
CASC5	Cancer susceptibility candidate 5	0.035	1.18	261
AIG1	Androgen-induced 1	0.039	−1.17	303
SPRYD3	SPRY domain containing 3	0.039	1.13	391
CDC42	Cell division cycle 42	0.039	−1.09	323
ZBTB37	Zinc finger and BTB domain containing 37	0.041	1.19	258
CAMP	Cathelicidin antimicrobial peptide	0.043	−1.46	304
CCDC183	Coiled-coil domain containing 183	0.044	1.10	343
COQ6	Coenzyme Q6 monooxygenase	0.046	1.13	252
CENPE	Centromere protein E	0.049	1.16	312

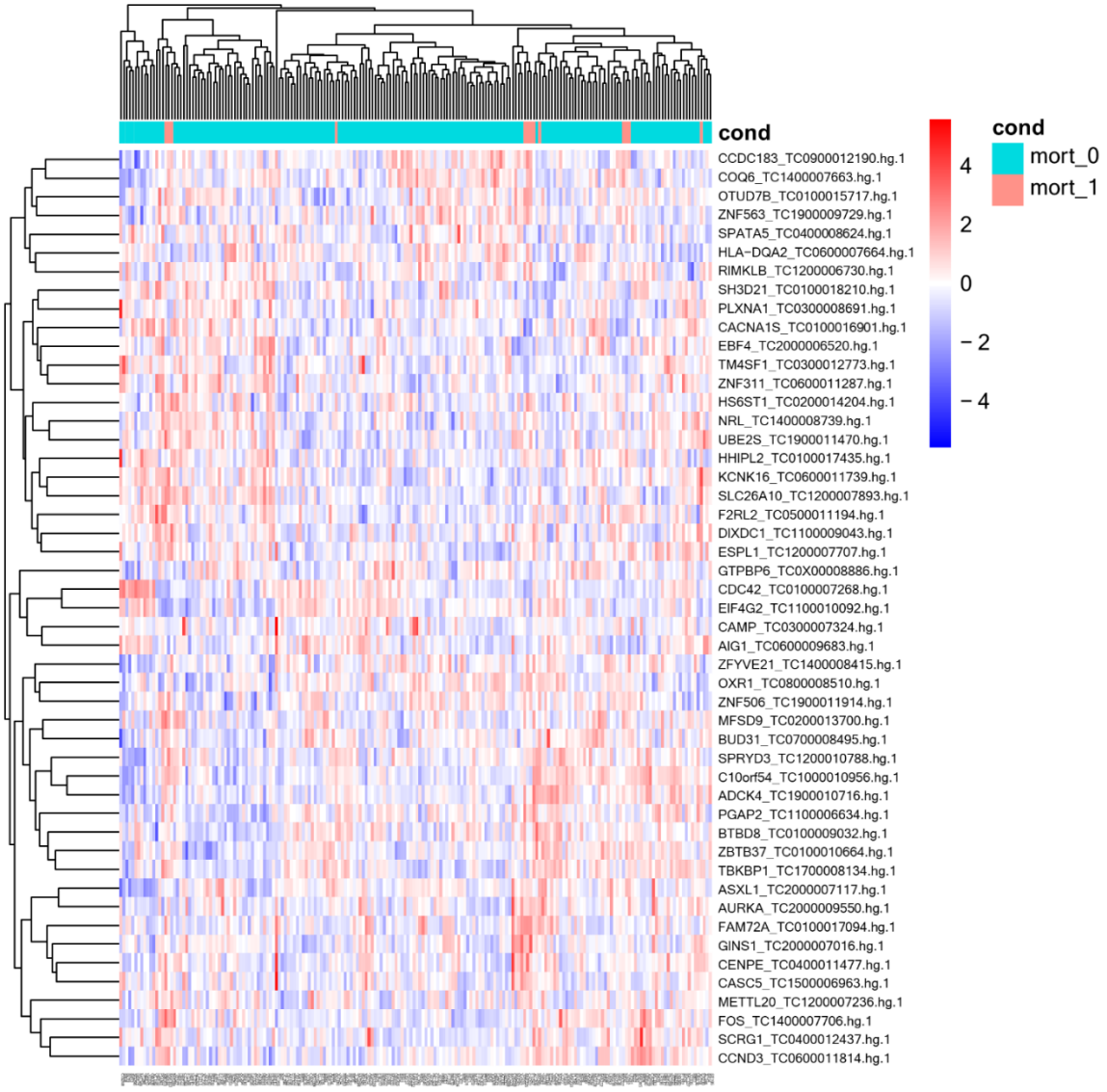

Figure 1. Heatmap of differentially expressed genes between community-acquired pneumonia patients who survived and died. mort_0, patients who survived; mort_1, patients who died.

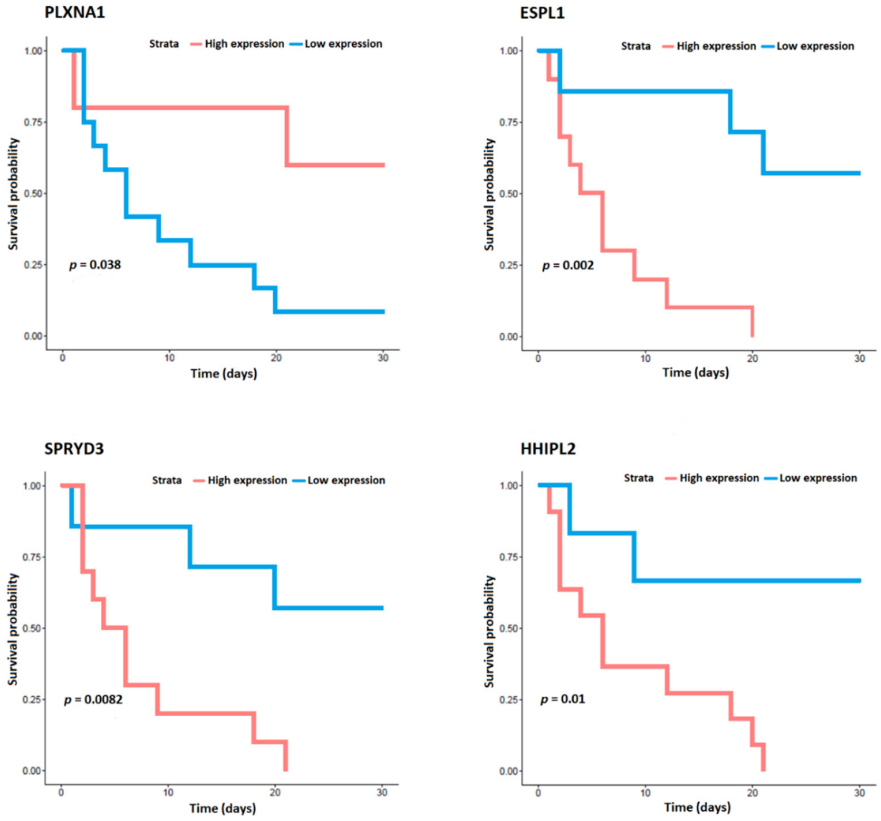

Figure 2. Analyses of the expression data for the genes *SPRYD3*, *ESPL1*, *HHIPL2*, and *PLXNA1* and for survival in community-acquired pneumonia patients.

3.3. Functional Analysis

GSEA was used to identify differentially expressed gene sets. A total of four out of fifty gene sets were positively enriched in the patients who died, and seven out of fifty gene sets were positively enriched in the patients who survived (NOM p-value < 0.05 and/or FDR < 25%) (Table 3 and Figure 3). Enrichment plots of the gene sets are shown in Supplementary Figure S2. Moreover, PPI analysis with NetworkAnalyst 3.0 and IntAct found FOS, CDC42, SLC26A10, EIF4G2, CCND3, ASXL1, UBE2S, and AURKA to be the main gene hubs (Figure 4). The names, abbreviations, and functions of these gene hubs are shown in Table 4.

Table 3. Gene set enrichment analysis of transcriptional differences in whole blood associated with mortality in community-acquired pneumonia.

Gene Set Name	NOM *p*-Value	FDR q-Value	NES	Brief Description
Positive Enrichment Score				
HALLMARK_SPERMATOGENESIS	0.000	0.034	1.66	Genes upregulated during production of male gametes (sperm), as in spermatogenesis.
HALLMARK_INTERFERON_ALPHA_RESPONSE	0.011	0.202	1.44	Genes upregulated in response to alpha interferon proteins.
HALLMARK_P53_PATHWAY	0.016	0.237	1.39	Genes involved in p53 pathways and networks.
HALLMARK_G2M_CHECKPOINT	0.020	0.199	1.37	Genes involved in the G2/M checkpoint, as in progression through the cell division cycle.

Table 3. *Cont.*

Gene Set Name	NOM *p*-Value	FDR q-Value	NES	Brief Description
Negative Enrichment Score				
HALLMARK_MYC_TARGETS_V1	0.000	0.000	−2.13	A subgroup of genes regulated with MYC—version 1 (v1).
HALLMARK_OXIDATIVE_PHOSPHORYLATION	0.000	0.005	−1.80	Genes encoding proteins involved in oxidative phosphorylation.
HALLMARK_MYC_TARGETS_V2	0.000	0.010	−1.67	A subgroup of genes regulated with MYC—version 2 (v2).
HALLMARK_UNFOLDED_PROTEIN_RESPONSE	0.000	0.010	−1.65	Genes upregulated during unfolded protein response, a cellular stress response related to the endoplasmic reticulum.
HALLMARK_ALLOGRAFT_REJECTION	0.000	0.051	−1.45	Genes upregulated during transplant rejection.
HALLMARK_ANGIOGENESIS	0.072	0.076	−1.39	Genes upregulated during formation of blood vessels (angiogenesis).
HALLMARK_REACTIVE_OXYGEN_SPECIES_PATHWAY	0.139	0.241	−1.24	Genes upregulated by reactive oxygen species (ROS).

FDR, false discovery rate; NOM, nominal *p*-value; NES, normalized enrichment score.

Table 4. Functional roles for hub genes of transcriptional differences in whole blood associated with mortality in community-acquired pneumonia.

Symbol	Gene Name	Function
FOS	FBJ murine osteosarcoma viral oncogene homolog	Cell proliferation, differentiation, and transformation. In some cases, also associated with apoptotic cell death. Among its related pathways are the IL-6 and Toll-like receptor signaling pathways.
CDC42	Cell division cycle 42	Controls diverse cellular functions, including cell morphology, migration, endocytosis, and cell-cycle progression. Also plays a role in phagocytosis, thymocyte development, T cell actin and tubulin cytoskeleton polarization, and T cell migration.
AURKA	Aurora kinase A	Mitotic serine/threonine kinase that contributes to regulation of cell-cycle progression.
UBE2S	Ubiquitin-conjugating enzyme E2S	An essential factor of the anaphase-promoting complex/cyclosome (APC/C), a cell-cycle-regulated ubiquitin ligase that controls progression through mitosis.
CCND3	Memczak2013 ALT_ACCEPTOR, ALT_DONOR, coding, INTERNAL, intronic best transcript NM_001136017	Regulatory component of the cyclin D3-CDK4 (DC) complex that phosphorylates and inhibits members of the retinoblastoma (RB) protein family, including RB1, and regulates the cell cycle during G(1)/S transition.
SLC26A10	Solute carrier family 26, member 10	Diseases associated with SLC26A10 include sialolithiasis and Pendred syndrome. Antiporter activity and sulfate transmembrane transporter activity.
EIF4G2	Eukaryotic translation initiation factor 4 gamma, 2	Appears to play a role in the switch from cap-dependent to IRES-mediated translation during mitosis, apoptosis, and viral infection. Cleaved with some caspases and viral proteases.
ASXL1	Additional sex combs-like transcriptional regulator 1	Determination of segment identity in the developing embryo. Necessary for the maintenance of stable repression of homeotic and other loci. Enhances transcription of certain genes while repressing transcription of others.

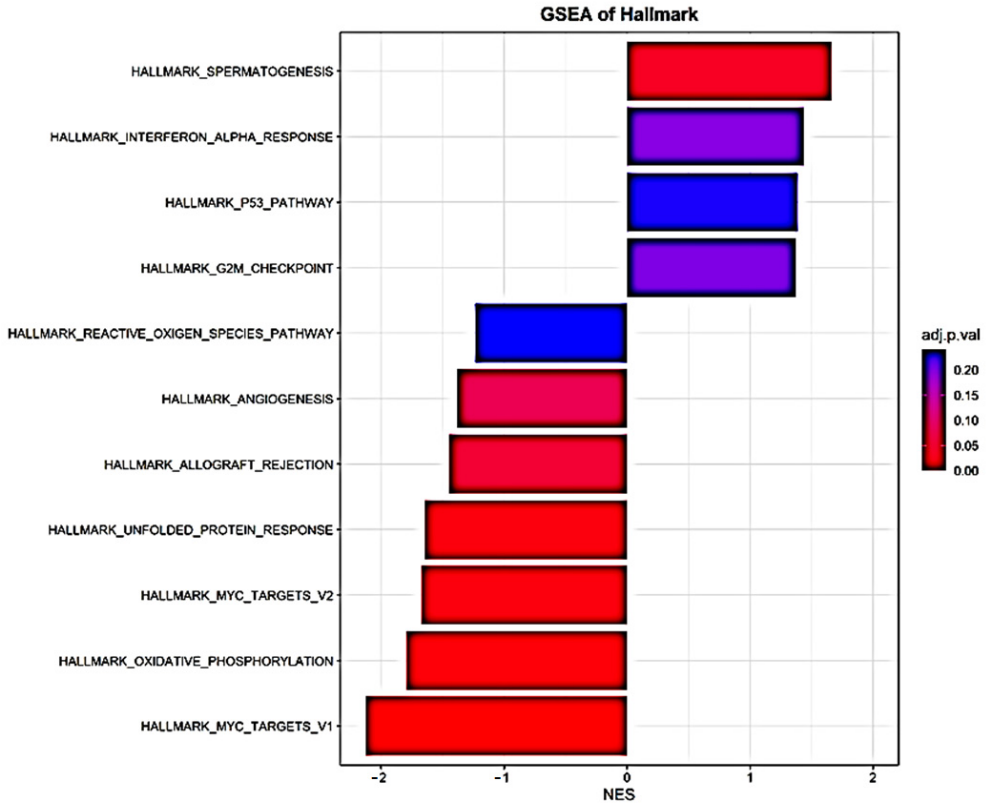

Figure 3. Histogram of Hallmark-gene-set enrichment analysis of transcriptional differences in whole blood associated with mortality in community-acquired pneumonia.

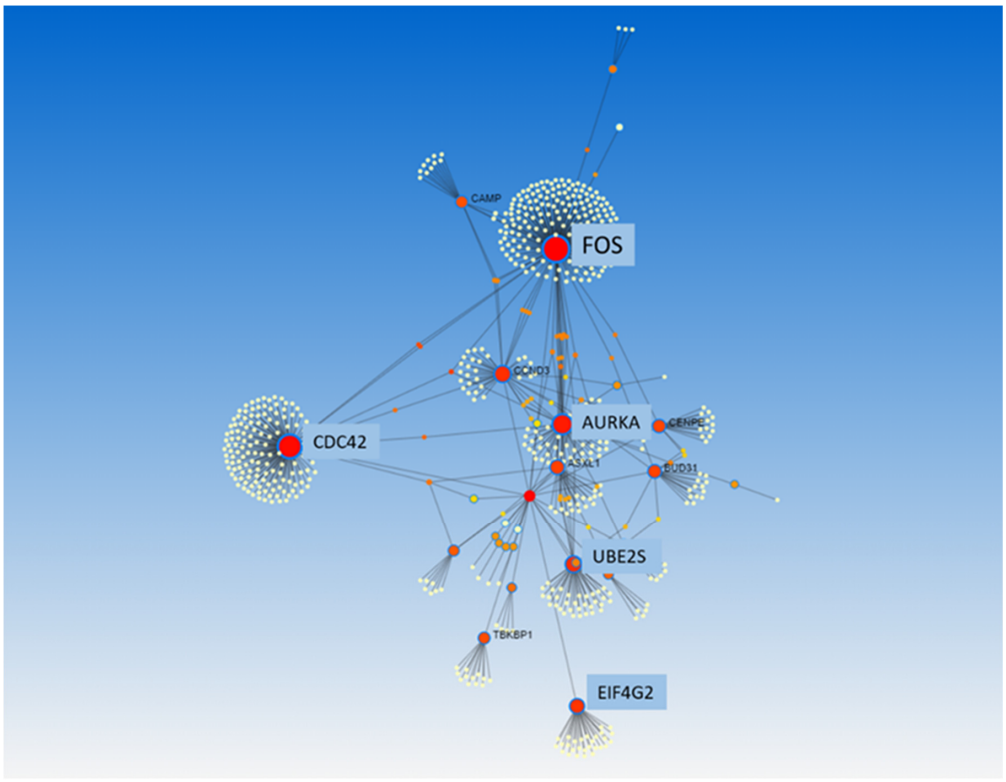

Figure 4. Protein–protein interaction analysis, from NetworkAnalyst 3.0, of transcriptional differences in whole blood associated with mortality in community-acquired pneumonia. All differentially expressed genes were used to perform this analysis.

4. Discussion

In this study, we identified the whole-blood gene expression profile associated with mortality in CAP patients. Functional enrichment analysis showed differences in gene expression profiles at hospital admission between CAP patients who died and those who survived, mainly regarding interferon alpha response, oxidative stress, apoptosis, endoplasmic reticulum stress, sex hormones, and angiogenesis pathways.

Studies that have evaluated gene expression profiles associated with severity or mortality in CAP are scarce. Hopp et al. [4] reported that in blood transcriptomes from septic patients in the ICU, CAP severity was associated mainly with immune dysregulation (T cell immune suppression, chemokine receptor deactivation, and macrophage polarization). Similarly, having evaluated patterns of gene expression in blood mononuclear cells from patients with sepsis secondary to CAP, Severino et al. [5] found that differences in oxidative phosphorylation seemed to be associated with prognosis at the time of patient enrollment. In addition, after comparing samples at admission and during follow-up, those authors found that gene expression profiles differed between survivors and nonsurvivors, with decreased expression of genes related to immune functions. Our study differs from these previously published papers with regard to objectives, inclusion criteria, and methods for assessing gene expression (mononuclear cells vs. whole blood). In fact, the differences between studies may provide insights into the distinct characteristics of the host response during CAP.

Furthermore, studies have also evaluated the performance of gene expression profiling in predicting prognosis in heterogeneous cohorts of sepsis patients. Hu et al. [12] performed a bioinformatic analysis of gene expression profiles for prognosis in patients with septic shock. Those researchers found that differentially expressed genes between septic shock patients and controls were primarily involved in the MAPK, tumor necrosis factor, HIF-1, and insulin signaling pathways. Six genes were identified to be positively correlated with prognosis in patients with septic shock. Another study found that sepsis response transcriptomic signatures (SRSs) can define subgroups of patients related to a sepsis outcome [13]. Cell death, apoptosis, necrosis, T cell activation, and endotoxin tolerance are enriched biological functions that pertain to SRSs in intra-abdominal and respiratory infection. SRSs is associated with higher early mortality in fecal peritonitis infection. Moreover, Baghela et al. [14] found gene expression signatures that predicted prognosis with 77–80% accuracy. Interestingly, those authors suggested that patients with early sepsis could be stratified into five distinct mechanistic endotypes, based on unique gene expression differences, with variable overall severity. Some of our results concur with those of previous studies; we also found that gene expression profiles from pathways such as apoptosis and oxidative stress were differentially expressed between groups.

In the present study, we found differences in the transcriptional profiles at hospital admission between CAP patients who died during hospitalization and those who survived. These findings are also supported by studies that have documented that the pathways that we found are related to prognoses in patients with sepsis or CAP. Some of these pathways can be regarded as "double-edged swords": on one hand, they are useful for fighting infectious pathogens, but on the other, they are harmful and produce organ damage. Functional analysis showed that gene sets positively enriched in CAP patients who died were associated with apoptosis, interferon alpha response, and sex hormones. Regarding apoptosis, p53 is a stress-induced transcription factor that can be activated via several stimuli, including hypoxia and reactive oxygen species [15]. It has been found that inappropriate regulation of apoptosis in immune, endothelial, and pulmonary epithelial cells may play a critical role in production of immune dysfunction, impaired perfusion, tissue hypoxia, and multiple organ failure in sepsis [16]. Evidence suggests that prevention of cell apoptosis can improve prognosis in animal models of sepsis. One study found that the lungs of naïve p53(−/−) mice displayed proinflammatory genes and clear pathogens more successfully than did controls after intrapulmonary infection [17].

Moreover, our data also identified a significant enrichment in genes associated with spermatogenesis. Sex hormone regulation is carried out via the hypothalamic–pituitary–gonadal axis. Sex hormones have been reported to have regulatory influences on immune responses; estradiol can stimulate production of proinflammatory cytokines and macrophage activation, and testosterone has a suppressive effect on immune responses and increases vulnerability to infection [18]. High levels of estrogens such as estradiol have been observed in male and female patients with sepsis and septic shock and have been associated with significantly higher risk of in-hospital mortality [18,19]. Moreover, in males with CAP, sex and mineralocorticoid hormone metabolites have been associated with inflammation, disease severity, and long-term survival [20].

Another key feature of the gene expression profiles in CAP nonsurvivors was upregulation of the interferon-alpha response pathway. Type 1 interferon-alpha is mainly an antiviral cytokine. However, it has proven useful for control of bacterial replication and lung inflammation and improved clinical outcomes in animal models of bacterial pneumonia via increased neutrophil and macrophage activation with release of reactive oxygen and nitrogen species and bacterial killing [21]. Nevertheless, interferon-alpha can also cause pathogenic damage and an uncontrolled inflammatory response [22]. Finally, interferon regulatory factor 5 (IRF5) and its related inflammatory cytokines, such as interferon-alpha, have been associated with severity and prognoses in CAP patients [23].

Functional analysis showed that gene sets related to the oxidative stress, angiogenesis, and endoplasmic reticulum stress pathways were positively enriched in patients who survived. Regarding oxidative stress, organisms that live under aerobic conditions are exposed to several oxidizing agents, including reactive oxygen species (ROSs) and reactive nitrogen species (RNSs). These species perform biological functions that are essential for normal cell development; however, an imbalance between reactive-species generation and antioxidant defense, known as oxidative stress, can result in impaired homeostasis and lead to various pathologies [24]. Oxidative stress is part of the pathogenic mechanism of CAP and is closely linked to inflammation [25].

Numerous biomarkers have been associated with angiogenesis, including angiopoietins, members of the vascular endothelial growth factor family, transforming growth factors, interleukins, platelet-derived growth factor, and the fibroblast growth factor family. During infection, factors related to angiogenesis and the endothelial barrier are essential for migration of immune-system cells into infected tissues but can also participate in the pathogenesis of septic shock and acute multiple organ dysfunction [26]. Moreover, under conditions that cause stress and inflammation, the endoplasmic reticulum loses homeostasis in a process termed endoplasmic reticulum stress. During endoplasmic reticulum stress, an unfolded protein response (UPR) is activated to restore the normal endoplasmic reticulum function. This UPR preserves a homeostatic environment and regulates a wide variety of cell processes, such as cell proliferation and differentiation, inflammation, apoptosis, and angiogenesis. However, the UPR becomes a threat when its activation is intense and prolonged, and may lead to cell dysfunction, death, and disease [27]. Finally, transcription factor MYC may be an important regulatory gene in the underlying dysfunction of sepsis-induced acute respiratory distress syndrome (ARDS) [28].

The present pilot study has several limitations that should be acknowledged. First, the number of nonsurvivors was small, and we were unable to complete subgroup analyses; therefore, our findings need to be validated in larger cohorts from different geographical areas. Second, we did not adjust the results for confounding variables such as age or underlying diseases. Third, we measured gene expression profiles at only one point in the disease and did not evaluate changes over the course of admission; therefore, we cannot rule out the possibility that gene expression may differ at other times during CAP. In this regard, it should be noted that the findings of our study show gene expression profiles specifically in the initial phases of CAP. Finally, we did not confirm the results with real-time quantitative polymerase chain reaction of the target genes.

5. Conclusions

The gene expression profiles of CAP survivors and nonsurvivors presented differences, mainly related to interferon-alpha response, apoptosis, sex hormones, oxidative stress, unfolded protein response, and angiogenesis pathways. These findings may expand our understanding of the immune response in CAP through identification of new candidate pathways and targets for potential intervention. In addition, the differentially expressed genes could potentially be useful as risk-stratification biomarkers that may facilitate healthcare utilization.

Supplementary Materials: The following are available online at https://www.mdpi.com/article/10.3390/biomedicines11020429/s1, Figure S1: Expression data for each gene and prognosis, Figure S2: Enrichment plot of gene sets.

Author Contributions: Conceptualization: D.V., A.F.S. and J.C.; data curation: D.V., L.N., O.V., Y.M. and J.C.; investigations: A.F.S., L.N., Y.M., L.O., M.A., M.B.-T., M.S., A.R., G.A.-A., G.B. and C.G.; formal analysis: D.V., O.V., L.N. and J.C.; funding acquisition: J.C.; project administration: D.V., A.F.S., L.N. and J.C.; supervision: D.V., A.F.S., L.N., Y.M. and J.C.; writing—original draft: D.V., L.N., O.V. and J.C.; writing—review and editing: Y.M., L.O., M.A., M.B.-T., M.S., A.R., G.A.-A., G.B. and C.G. All authors have read and agreed to the published version of the manuscript.

Funding: This study was supported by Instituto de Salud Carlos III (research grants 11/01106, 14/00580, and 17/01332) and CIBERINFECT (CB21/13/00009), Madrid, Spain. Gabriela Abelenda-Alonso is a recipient of a grant from Fundació La Marató-TV3 (201808-10), Barcelona, Spain. Alexander Rombauts is a recipient of a PFIS (FI18/00183) from Instituto de Salud Carlos III, Madrid, Spain. We thank the CERCA Programme/Generalitat de Catalunya for institutional support. The funders had no role in study design, data collection and analysis, decision to publish, or preparation of this manuscript.

Institutional Review Board Statement: This study was approved by the Ethics Committee of the Bellvitge University Hospital (approval code: PR158/14; 6 November 2014). The relevant data and protocols comply with the minimum information about a microarray experiment (MIAME) guidelines.

Informed Consent Statement: Informed consent was obtained from all subjects involved in this study.

Data Availability Statement: The original contributions presented in this study are included in the article/Supplementary Materials. The microarray data from the project have been deposited in NCBI's Gene Expression Omnibus under accession number GSE188309. Further inquiries can be directed to the corresponding authors.

Conflicts of Interest: The authors declare no conflict of interest.

References

1. Viasus, D.; Núñez-Ramos, J.A.; Viloria, S.A.; Carratalà, J. Pharmacotherapy for community-acquired pneumonia in the elderly. *Expert Opin. Pharmacother.* **2017**, *18*, 957–964. [CrossRef] [PubMed]
2. Ewig, S.; Torres, A. Community-acquired pneumonia as an emergency: Time for an aggressive intervention to lower mortality. *Eur. Respir. J.* **2011**, *38*, 253–260. [CrossRef]
3. Ferreira-Coimbra, J.; Sarda, C.; Rello, J. Burden of community-acquired pneumonia and unmet clinical needs. *Adv. Ther.* **2020**, *37*, 1302–1318. [CrossRef]
4. Hopp, L.; Loeffler-Wirth, H.; Nersisyan, L.; Arakelyan, A.; Binder, H. Footprints of Sepsis Framed Within Community Acquired Pneumonia in the Blood Transcriptome. *Front. Immunol.* **2018**, *9*, 1620. [CrossRef]
5. Severino, P.; Silva, E.; Baggio-Zappia, G.L.; Brunialti, M.K.; Nucci, L.A.; Rigato, O., Jr.; da Silva, I.D.; Machado, F.R.; Salomao, R. Patterns of gene expression in peripheral blood mononuclear cells and outcomes from patients with sepsis secondary to community acquired pneumonia. *PLoS ONE* **2014**, *9*, e91886. [CrossRef]
6. Scicluna, B.P.; van Lieshout, M.H.; Blok, D.C.; Florquin, S.; van der Poll, T. Modular Transcriptional Networks of the Host Pulmonary Response during Early and Late Pneumococcal Pneumonia. *Mol. Med.* **2015**, *21*, 430–441. [CrossRef] [PubMed]
7. Brazma, A.; Hingamp, P.; Quackenbush, J.; Sherlock, G.; Spellman, P.; Stoeckert, C.; Aach, J.; Ansorge, W.; Ball, C.A.; Causton, H.C.; et al. Minimum information about a microarray experiment (MIAME)-toward standards for microarray data. *Nat. Genet.* **2001**, *29*, 365–371. [CrossRef] [PubMed]
8. Irizarry, R.A.; Hobbs, B.; Collin, F.; Beazer-Barclay, Y.D.; Antonellis, K.J.; Scherf, U.; Speed, T.P. Exploration, normalization, and summaries of high density oligonucleotide array probe level data. *Biostatistics* **2003**, *4*, 249–264. [CrossRef]

9. Subramanian, A.; Tamayo, P.; Mootha, V.K.; Mukherjee, S.; Ebert, B.L.; Gillette, M.A.; Paulovich, A.; Pomeroy, S.L.; Golub, T.R.; Lander, E.S.; et al. Gene set enrichment analysis: A knowledge-based approach for interpreting genome-wide expression profiles. *Proc. Natl. Acad. Sci. USA* **2005**, *102*, 15545–15550. [CrossRef] [PubMed]
10. Mootha, V.K.; Lindgren, C.M.; Eriksson, K.F.; Subramanian, A.; Sihag, S.; Lehar, J.; Puigserver, P.; Carlsson, E.; Ridderstråle, M.; Laurila, E.; et al. PGC-1α-responsive genes involved in oxidative phosphorylation are coordinately downregulated in human diabetes. *Nat. Genet.* **2003**, *34*, 267–273. [CrossRef]
11. Ritchie, M.E.; Phipson, B.; Wu, D.; Hu, Y.; Law, C.W.; Shi, W.; Smyth, G.K. Limma powers differential expression analyses for RNA-sequencing and microarray studies. *Nucleic Acids Res.* **2015**, *43*, e47. [CrossRef] [PubMed]
12. Hu, Y.; Cheng, L.; Zhong, W.; Chen, M.; Zhang, Q. Bioinformatics Analysis of Gene Expression Profiles for Risk Prediction in Patients with Septic Shock. *Med. Sci. Monit.* **2019**, *25*, 9563–9571. [CrossRef]
13. Burnham, K.L.; Davenport, E.E.; Radhakrishnan, J.; Humburg, P.; Gordon, A.C.; Hutton, P.; Svoren-Jabalera, E.; Garrard, C.; Hill, A.V.S.; Hinds, C.J.; et al. Shared and Distinct Aspects of the Sepsis Transcriptomic Response to Fecal Peritonitis and Pneumonia. *Am. J. Respir. Crit. Care Med.* **2017**, *196*, 328–339. [CrossRef]
14. Baghela, A.; Pena, O.M.; Lee, A.H.; Baquir, B.; Falsafi, R.; An, A.; Farmer, S.W.; Hurlburt, A.; Mondragon-Cardona, A.; Rivera, J.D.; et al. Predicting sepsis severity at first clinical presentation: The role of endotypes and mechanistic signatures. *eBioMedicine* **2022**, *75*, 103776. [CrossRef] [PubMed]
15. Hotchkiss, R.S.; Tinsley, K.W.; Hui, J.J.; Chang, K.C.; Swanson, P.E.; Drewry, A.M.; Buchman, T.G.; Karl, I.E. p53-dependent and -independent pathways of apoptotic cell death in sepsis. *J. Immunol.* **2000**, *164*, 3675–3680. [CrossRef] [PubMed]
16. Harjai, M.; Bogra, J.; Kohli, M.; Pant, A.B. Is suppression of apoptosis a new therapeutic target in sepsis? *Anaesth. Intensive Care* **2013**, *41*, 175–183. [CrossRef]
17. Madenspacher, J.H.; Azzam, K.M.; Gowdy, K.M.; Malcolm, K.C.; Nick, J.A.; Dixon, D.; Aloor, J.J.; Draper, D.W.; Guardiola, J.J.; Shatz, M.; et al. p53 Integrates host defense and cell fate during bacterial pneumonia. *J. Exp. Med.* **2013**, *210*, 891–904. [CrossRef]
18. Feng, J.Y.; Liu, K.T.; Abraham, E.; Chen, C.Y.; Tsai, P.Y.; Chen, Y.C.; Lee, Y.C.; Yang, K.Y. Serum estradiol levels predict survival and acute kidney injury in patients with septic shock—A prospective study. *PLoS ONE* **2014**, *9*, e97967. [CrossRef]
19. Tsang, G.; Insel, M.B.; Weis, J.M.; Morgan, M.A.; Gough, M.S.; Frasier, L.M.; Mack, C.M.; Doolin, K.P.; Graves, B.T.; Apostolakos, M.J.; et al. Bioavailable estradiol concentrations are elevated and predict mortality in septic patients: A prospective cohort study. *Crit. Care* **2016**, *20*, 240. [CrossRef] [PubMed]
20. Zurfluh, S.; Nickler, M.; Ottiger, M.; Steuer, C.; Kutz, A.; Christ-Crain, M.; Zimmerli, W.; Thomann, R.; Hoess, C.; Henzen, C.; et al. Dihydrotestosterone is a predictor for mortality in males with community-acquired pneumonia: Results of a 6-year follow-up study. *Respir. Res.* **2018**, *19*, 335. [CrossRef]
21. Damjanovic, D.; Khera, A.; Medina, M.F.; Ennis, J.; Turner, J.D.; Gauldie, J.; Xing, Z. Type 1 interferon gene transfer enhances host defense against pulmonary *Streptococcus pneumoniae* infection via activating innate leukocytes. *Mol. Ther. Methods Clin. Dev.* **2014**, *1*, 5. [CrossRef]
22. Goritzka, M.; Makris, S.; Kausar, F.; Durant, L.R.; Pereira, C.; Kumagai, Y.; Culley, F.J.; Mack, M.; Akira, S.; Johansson, C. Alveolar macrophage-derived type I interferons orchestrate innate immunity to RSV through recruitment of antiviral monocytes. *J. Exp. Med.* **2015**, *212*, 699–714. [CrossRef] [PubMed]
23. Wang, X.; Guo, J.; Wang, Y.; Xiao, Y.; Wang, L.; Hua, S. Expression Levels of Interferon Regulatory Factor 5 (IRF5) and Related Inflammatory Cytokines Associated with Severity, Prognosis, and Causative Pathogen in Patients with Community-Acquired Pneumonia. *Med. Sci. Monit.* **2018**, *24*, 3620–3630. [CrossRef]
24. Carvajal-Carvajal, C. Especies reactivas del oxígeno: Formación, función y estrés oxidativo. *Med. Leg. Costa Rica* **2019**, *36*, 91–100.
25. Trefler, S.; Rodríguez, A.; Martín-Loeches, I.; Sanchez, V.; Marín, J.; Llauradó, M.; Romeu, M.; Díaz, E.; Nogués, R.; Giralt, M. Oxidative stress in immunocompetent patients with severe community-acquired pneumonia. A pilot study. *Med. Intensiva* **2014**, *38*, 73–82. [CrossRef]
26. Faiotto, V.B.; Franci, D.; Enz Hubert, R.M.; de Souza, G.R.; Fiusa, M.M.L.; Hounkpe, B.W.; Santos, T.M.; Carvalho-Filho, M.A.; De Paula, E.V. Circulating levels of the angiogenesis mediators endoglin, HB-EGF, BMP-9 and FGF-2 in patients with severe sepsis and septic shock. *J. Crit. Care* **2017**, *42*, 162–167. [CrossRef]
27. Khan, M.M.; Yang, W.L.; Wang, P. Endoplasmic reticulum in sepsis. *Shock* **2015**, *44*, 294–304. [CrossRef] [PubMed]
28. Zhang, J.; Luo, Y.; Wang, X.; Zhu, J.; Li, Q.; Feng, J.; He, D.; Zhong, Z.; Zheng, X.; Lu, J.; et al. Global transcriptional regulation of STAT3- and MYC-mediated sepsis-induced ARDS. *Ther. Adv. Respir. Dis.* **2019**, *13*, 1753466619879840. [CrossRef]

Study 2

Host- and Pathogen-Related Factors for Acute Cardiac Events in Pneumococcal Pneumonia.

Rombauts, A., Abelenda-Alonso, G., Càmara, J., Lorenzo-Esteller, L., González-Díaz, A., Sastre-Escolà, E., Gudiol, C., Dorca, J., Tebé, C., Pallarès, N., Ardanuy, C., & Carratalà, J. ✉ (2020).

Open forum infectious diseases, 7(12), ofaa522.

Impact factor (2022): 4.2 (2nd quartile)

Open Forum Infectious Diseases

MAJOR ARTICLE

Host- and Pathogen-Related Factors for Acute Cardiac Events in Pneumococcal Pneumonia

Alexander Rombauts,[1,2] Gabriela Abelenda-Alonso,[1,2] Jordi Càmara,[2,3,4] Laia Lorenzo-Esteller,[1] Aida González-Díaz,[2,3,4] Enric Sastre-Escolà,[1] Carlota Gudiol,[1,2,5,6] Jordi Dorca,[2,6,7] Cristian Tebé,[8] Natàlia Pallarès,[8] Carmen Ardanuy,[2,3,4,6] and Jordi Carratalà[1,2,5,6]

[1]Department of Infectious Diseases, Bellvitge University Hospital, Hospitalet de Llobregat, Barcelona, Spain, [2]Bellvitge Biomedical Research Institute (IDIBELL), Hospitalet de Llobregat, Barcelona, Spain, [3]Department of Microbiology, Bellvitge Universtiy Hospital, Hospitalet de Llobregat, Barcelona, Spain, [4]Research Network for Respiratory Diseases (CIBERES), Instituto de Salud Carlos III, Madrid, Spain, [5]Spanish Network for Research in Infectious Diseases (REIPI), Instituto de Salud Carlos III, Madrid, Spain, [6]University of Barcelona, Barcelona, Spain, [7]Department of Pneumology, Bellvitge University Hospital, Hospitalet de Llobregat, Barcelona, Spain, and [8]Biostatistics Unit at Bellvitge Biomedical Research Institute (IDIBELL), Hospitalet de Llobregat, Barcelona, Spain

Background. Acute cardiac events (ACEs) are increasingly being recognized as a major complication in pneumococcal community-acquired pneumonia (CAP). Information regarding host- and pathogen-related factors for ACEs, including pneumococcal serotypes and clonal complexes, is scarce.

Methods. A retrospective study was conducted of a prospective cohort of patients hospitalized for CAP between 1996 and 2019. Logistic regression and funnel plot analyses were performed to determine host- and pathogen-related factors for ACEs.

Results. Of 1739 episodes of pneumococcal CAP, 1 or more ACEs occurred in 304 (17.5%) patients, the most frequent being arrhythmia (n = 207), heart failure (n = 135), and myocardial infarction (n = 23). The majority of ACEs (73.4%) occurred within 48 hours of admission. Factors independently associated with ACEs were older age, preexisting heart conditions, pneumococcal bacteremia, septic shock at admission, and high-risk pneumonia. Among 983 pneumococcal isolates, 872 (88.7%) were serotyped and 742 (75.5%) genotyped. The funnel plot analyses did not find any statistically significant association between serotypes or clonal complexes with ACEs. Nevertheless, there was a trend toward an association between CC230 and these complications. ACEs were independently associated with 30-day mortality (adjusted odds ratio, 1.88; 95% CI, 1.11–3.13).

Conclusions. ACEs are frequent in pneumococcal pneumonia and are associated with increased mortality. The risk factors defined in this study may help identify patients who must undergo close follow-up, including heart rhythm monitoring, and special care to avoid fluid overload, particularly during the first 48 hours of admission. These high-risk patients should be the target for preventive intervention strategies.

Keywords. acute cardiac events; community-acquired pneumonia; genotype; pneumococcal pneumonia; serotype.

Acute cardiac events pose a significant challenge in the management of community-acquired pneumonia (CAP) [1–3]. The incidence of acute cardiac events during the course of hospitalization for CAP ranges from 8% to 32% [4–7]. It is increasingly being recognized that the development of acute cardiac events in patients with CAP is an independent predictor of poor outcomes [5, 7]. Moreover, hospitalized patients with CAP have a 2-fold increase in the long-term risk for cardiovascular disease, new-onset heart failure, and mortality compared with the general population [8–11].

Several cohort studies focusing on the overall population of all-cause CAP have identified certain host factors associated with the development of acute cardiac events [4–7, 12, 13]. Importantly, the development of life-threatening acute cardiac events appears to be particularly frequent among patients with pneumococcal CAP [4, 14]. The first study linking acute cardiac events and pneumococcal pneumonia was carried out by Musher and colleagues in 2007 [15]. However, that seminal study reported only 33 cardiac events occurring in 170 patients, precluding an analysis of risk factors. Other researchers have found that pneumococcal bacteremia significantly increased the risk of new-onset heart failure up to 10 years after CAP compared with controls [9].

Interestingly, recent animal experimental models have shown that *Streptococcus pneumoniae* is capable of invading the myocardium and inducing cardiac injury by promoting the formation of microlesions [16–18]. In these studies, bacteremia strongly correlated with increasing levels of cardiac troponin-L and cardiac damage [19, 20]. Pneumolysin, a major virulence factor of *S. pneumoniae*, mediates cardiac damage and depresses cardiomyocyte contractile function [19, 21]. Antimicrobial

Received 3 August 2020; editorial decision 19 October 2020; accepted 21 October 2020.

Correspondence: J. Carratalà, MD, PhD, Department of Infectious Diseases, Bellvitge University Hospital, Feixa Llarga s/n, 08907, Hospitalet de Llobregat, Barcelona, Spain (jcarratala@bellvitgehospital.cat).

Open Forum Infectious Diseases®2020

DOI: 10.1093/ofid/ofaa522

treatment has been associated with cardiac scarring as a result of collagen synthesis in damaged myocardium, which may explain the increased risk for long-term cardiac complications in humans due to the promotion of arrhythmias and/or impairment of left ventricular function [16, 17]. A recent experimental study in a small sample of mice found that cardiac damage is probably dependent on the ability of certain pneumococci to cause high-grade bacteremia and that the type of lesions might be strain-specific [20]. Interestingly, similar cardiac microlesions largely devoid of bacteria were observed in heart sections from 3 rhesus macaques infected with simian immunodeficiency virus that died of pneumococcal pneumonia despite antibiotic therapy, and in 2 out of 9 humans who succumbed to invasive pneumococcal disease [17].

To date, however, no clinical studies have specifically assessed host risk factors for acute cardiac events in pneumococcal pneumonia. Moreover, the potential link between pneumococcal genotypes (clonal complexes) and cardiac complications in humans with pneumococcal CAP has not been explored. Nevertheless, a recent study has found an association between the development of acute cardiac events and pneumococcal serotypes 3 and 9N in 310 patients with invasive pneumococcal disease (of whom 60% had CAP) [22]. An association between any pneumococcal serotype or clonal complex and cardiac events could have important public health implications with regard to the composition of further pneumococcal vaccines.

Here, we aim to assess the host- and pathogen-related factors, more specifically serotypes and genotypes (clonal complexes), related to a high risk of developing acute cardiac events in a large prospective cohort of hospitalized patients with pneumococcal CAP.

METHODS

Setting, Patients, and Study Design

This retrospective cohort study was performed at the Bellvitge University Hospital, a 750-bed tertiary academic hospital for adults in Barcelona, Spain. All nonimmunocompromised patients aged ≥18 years with pneumococcal CAP who were hospitalized through the emergency room from January 1, 1996, to September 30, 2019, were included. Data on all patients were prospectively recorded using a computer-assisted protocol. Patients with neutropenia, HIV infection, or transplantation were not included.

To identify risk factors for acute cardiac events during hospitalization, patients with pneumococcal pneumonia were divided into 2 groups: those who developed acute cardiac events (new-onset or worsening cardiac arrhythmias, new-onset or worsening congestive heart failure and/or myocardial infarction) and those without acute cardiac events during hospital stay. A comparison of *S. pneumoniae* strains isolated from patients with pneumococcal pneumonia and with or without acute cardiac events was performed. Local clinical practices regarding initial microbiological testing and empirical antibiotic therapy are detailed in the Supplementary Data. Serotypes, genotypes (clonal complexes), and penicillin susceptibility of isolated strains were analyzed.

Patients were seen during their hospital stay by 1 or more of the investigators who recorded clinical data, including the occurrence of any acute cardiac event, and microbiological findings in a computer-assisted protocol (case report form, Supplementary Data). Patients were seen at the outpatient clinic 30 days after hospital discharge.

Patient Consent Statement

The study was approved by the Bellvitge University Hospital Ethics Committee. Informed consent was waived because of the observational nature of the study and because the analysis used anonymous clinical data. The STROBE guidelines were used to ensure the reporting of the study (Supplementary Table 1).

Definitions

New-onset or worsening cardiac arrhythmias were considered when they were documented by an electrocardiogram (ECG). New-onset or worsening congestive heart failure was considered when patients fulfilled Framingham criteria [23]. Myocardial infarction was defined as the detection of an increase in cardiac biomarkers (creatine kinase fraction MB and/or troponin) with at least 1 of the following manifestations: symptoms of ischemia, ECG changes (new ST-T changes or a new left bundle branch block), or development of pathological Q waves. Early and overall mortality were defined as death due to any cause ≤48 hours and ≤30 days after hospitalization, respectively. The definitions for pneumococcal CAP and other variables are detailed in the Supplementary Data.

Microbiological Studies

S. pneumoniae was identified using standard microbiological procedures. *S. pneumoniae* urinary antigen detection was performed with a rapid immunochromatographic assay (BinaxNOW *Streptococcus pneumoniae*, Abbott, Lake Bluff, Illinois, USA). Penicillin susceptibility was tested by the microdilution method, following the European Committee on Antimicrobial Susceptibility Testing methods and criteria (EUCAST).

Serotypes were identified using the Quellung reaction at the Spanish Reference Laboratory [24] and/or by conventional polymerase chain reaction following the methodology described by the Centers for Disease Control and Prevention [25]. For genotyping all available strains, pulsed-field gel electrophoresis with multilocus sequence typing (PFGE/MLST) scheme was performed following a previously described methodology [26]. PFGE patterns were visually compared. Representative strains of the main clusters (those accounting for >5 pneumococci) were studied by MLST. Allele numbers and sequence

types (STs) were assigned using the pneumococcal multilocus sequence typing website [27]. Unusual serotype–genotype combinations were retested.

Statistical Analysis

Categorical variables were presented by the number of cases and percentages, and continuous variables by means and SDs or medians and interquartile ranges (IQRs). Continuous variables were compared using the Student *t* test or Mann-Whitney *U* test where appropriate. The Fisher exact test or Pearson χ^2 test was applied to assess the relationship between categorical variables.

To estimate the magnitude of the associations between covariates and the development of acute cardiac events, multivariable adjusted ORs and their corresponding 95% confidence intervals were computed by logistic regression. A potential set of predictors was prespecified based on the literature. The cohort was sampled by bootstrapping with replacement 1000 times. A model was fitted in each sample using stepwise elimination and the Akaike information criterion. Predictors retained in more than 70% of the models were considered for inclusion in the selected model. Factors included in the model are detailed in the Supplementary Data. Comparison of acute cardiac event rates between serotypes and clonal complexes was carried out taking into account the volume of patients at risk and was represented graphically with funnel plots [28]. Using the overall acute cardiac event rate as a benchmark, serotypes or clonal complexes above or below the benchmark's confidence interval would indicate that the risk observed was significantly higher or lower than expected. If the serotypes or clonal complexes were within the benchmark's confidence interval, this would indicate that the risk observed was as expected. Only serotypes and genotypes (clonal complexes) isolated in 10 or more cases were analyzed. As a general strategy, variables with >25% of missing values were not considered. No imputation was performed for missing values, and no sensitivity analysis was carried out. Whenever possible, 95% confidence intervals accompanied point estimators. All analyses were performed with a 2-sided significance level of .05 and were conducted with R Statistical Software, version 3.6.3 [29].

RESULTS

Over the study period, 1739 consecutive adults with pneumococcal pneumonia were included, of whom 304 (17.5%) developed 1 or more acute cardiac events during hospitalization. The most frequent cardiac complications were arrhythmia (n = 207, of which 124 were new-onset atrial fibrillation/flutter), heart failure (n = 135, of which 85 were new-onset heart failure), and myocardial infarction (n = 23), with the majority of events occurring within 48 hours (73.4%) of admission. Details of the microbiological methods used to establish the diagnosis of pneumococcal pneumonia are shown in the Supplementary Table 2. In brief, *S. pneumoniae* was isolated in 1 or more clinical samples in 983 (56.5%) patients, with the remaining patients being diagnosed through antigen testing, and 495 (28.5%) had pneumococcal bacteremia.

Baseline characteristics of patients with pneumococcal pneumonia who developed acute cardiac events and those who did not are detailed in Table 1. Patients who developed acute cardiac events were significantly older, had more preexisting heart conditions, and had more comorbidities such as stroke, dyslipidemia, arterial hypertension, peripheral artery disease, chronic renal disease, and chronic obstructive pulmonary disease. They were more often receiving oral anticoagulants, antiplatelet therapy, statins, beta-blockers, angiotensin-converting enzyme inhibitors or angiotensin II receptor blockers, and diuretics. They also had more often pneumococcal bacteremia, a more severe presentation with a higher pneumonia severity index (PSI), and higher rates of septic shock at admission, hypoalbuminemia, and respiratory insufficiency. Patients without acute cardiac events were more likely to have received prehospitalization antibiotic treatment for the acute episode of pneumonia, which was associated with a lower frequency of bacteremia (13.3% vs 30.8%; $P < .001$), a lower proportion of septic shock at admission (7.3% vs 13.3%; $P < .01$), and a lower rate of high-risk pneumonia (PSI classes IV and V, 56% vs 65.6%; $P = .017$). In the adjusted multivariate logistic regression analysis, age, preexisting heart conditions, pneumococcal bacteremia, septic shock at admission, and high-risk pneumonia (PSI classes IV and V) were found to be independent risk factors for the development of acute cardiac complications in pneumococcal CAP (Table 2).

Regarding pathogen-related factors, among 983 pneumococcal isolates, 872 (88.7%) were serotyped and 742 (75.5%) genotyped. A complete distribution of identified serotypes and clonal complexes is detailed in Supplementary Tables 3 and 4. Serotype 3 was the most common, and it was mainly related to clonal complexes CC180 and CC260; the β-lactam-resistant CC156, which included serotypes 9V and 14, was third. A funnel plot analysis (Figure 1) showed a trend toward a higher incidence of acute cardiac complications than expected with serotype 4, whereas serotypes 6A, 5, and 1 had a lower incidence than expected. The clonal complex CC230 showed a trend toward a higher rate of acute cardiac events in the funnel plot analysis (Figure 2), whereas the serotype 5–associated clonal complex CC289 had a lower incidence than expected. No differences in penicillin minimum inhibitory concentration were observed between the 2 groups (Supplementary Table 5).

Initial empirical antibiotic treatment and outcomes are summarized in Table 3. According to our local guidelines for treatment of CAP, combination therapy with β-lactam and fluoroquinolone is recommended for severe pneumonia. Accordingly, it was associated with a higher rate of septic shock, respiratory failure, intensive care unit (ICU) admission, and a higher PSI score. A higher rate of acute cardiovascular events

Table 1. Baseline Characteristics of Patients With Pneumococcal Pneumonia who Developed Acute Cardiac Events and Those who Did Not

Patients (n = 1739)	Pneumococcal Pneumonia With Acute Cardiac Events (n = 304), No. (%)	Pneumococcal Pneumonia Without Acute Cardiac Events (n = 1435), No. (%)	*P* Value
Mean age (SD), y	73.4 (12.6)	65.8 (17.2)	<.001
Age ≥70 y	200/304 (65.8)	710/1435 (49.5)	<.001
Female sex	111/304 (36.5)	509/1435 (35.5)	.78
Vaccination status			
Influenza vaccine (season)	147/256 (48.4)	628/1328 (43.8)	.14
Pneumococcal vaccination (<5 y)	53/245 (21.6)	233/1296 (18)	.21
Current smoker	59/302 (19.5)	407/1431 (28.4)	.002
Heavy alcohol consumption	39/302 (12.9)	244/1429 (17.1)	.091
Underlying disease			
Chronic obstructive pulmonary disease	115/304 (37.8)	434/1435 (30.2)	.012
Cancer	31/304 (10.2)	120/1435 (8.4)	.36
Chronic renal disease	40/304 (13.2)	110/1435 (7.7)	.003
Chronic liver disease	25/304 (8.2)	122/1435 (8.5)	.96
Dementia	13/304 (4.3)	77/1435 (5.4)	.52
Stroke	36/304 (11.8)	112/1435 (7.8)	.029
Peripheral artery disease	23/284 (7.6)	52/1266 (3.6)	.004
Arterial hypertension	126/288 (43.8)	424/1352 (31.4)	<.001
Diabetes mellitus	80/304 (26.3)	303/1435 (21.1)	.056
Dyslipidemia	75/286 (26.2)	264/1342 (19.7)	.017
Preexisting heart conditions	173/304 (56.9)	344/1435 (24)	<.001
Arrhythmia	94/304 (30.9)	162/1435 (11.3)	<.001
Coronary disease	60/304 (19.7)	120/1435 (8.4)	<.001
Congestive heart failure	71/304 (23.4)	98/1435 (6.8)	<.001
Baseline treatment			
Oral anticoagulation	51/281 (18.1)	84/1253 (6.7)	<.001
Antiplatelet therapy	85/283 (30)	267/1266 (21.1)	.002
Statin treatment	61/282 (21.6)	171/1264 (13.5)	.001
Beta-blockers	37/282 (13.1)	101/1266 (7.98)	.009
ACE inhibitor and/or angiotensin II receptor blocker	88/283 (31.1)	286/1266 (22.6)	.003
Diuretic therapy	105/283 (37.1)	256/1266 (20.2)	<.001
Prehospitalization antibiotic treatment	24/287 (8.36)	202/1404 (14.4)	.004
Multilobar pneumonia	97/304 (31.9)	389/1435 (27.1)	.10
Respiratory insufficiency[a]	218/304 (71.7)	847/1435 (59)	<.001
Pleural effusion	38/304 (12.5)	200/1435 (13.9)	.57
Empyema	13/304 (4.28)	79 /1434 (5.5)	.47
Septic shock at admission	60/304 (19.7)	162/1432 (11.3)	<.001
Hypoalbuminemia (<30 g/L)	129/259 (49.8)	512/1225 (41.8)	.021
Pneumococcal bacteremia	121/304 (39.8)	374/1435 (26.1)	<0.001
High-risk pneumonia (PSI >90 points, classes IV and V)	259/304 (85.2)	866/1433 (60.3)	<.001

Abbreviations: ACE, acute cardiac event; PSI, pneumonia severity index.

[a]Respiratory insufficiency defined as PaO2 <60 mmHg or peripheral oxygen saturation <90%.

Table 2. Adjusted Multivariate Logistic Regression for Acute Cardiac Events in 1739 Episodes of Pneumococcal Pneumonia

Variable	Odds Ratio for Acute Cardiac Events (95% CI)	*P* Value
Age	1.02 (1–1.03)	.009
Preexisting heart disease	3.45 (2.54–4.71)	<.001
Pneumococcal bacteremia	2.52 (1.86–3.42)	<.001
Septic shock at admission	1.77 (1.21–2.59)	.003
High-risk pneumonia (PSI >90 points, classes IV and V)	2.33 (1.56–3.54)	<.001

Abbreviation: PSI, pneumonia severity index.

was observed in patients who were empirically treated with β-lactam and fluoroquinolone combination therapy in the univariate analysis; however, fluoroquionolone exposure (either as mono- or combination therapy) was not. Patients with pneumococcal pneumonia with acute cardiac events had a greater need for ICU admission, mechanical ventilation, and a longer hospital stay. Among the 304 patients with pneumococcal pneumonia with acute cardiac events, the 30-day mortality was 13.9%, compared with 4.7% among those patients without cardiac complications (P = .001). Acute cardiac events were

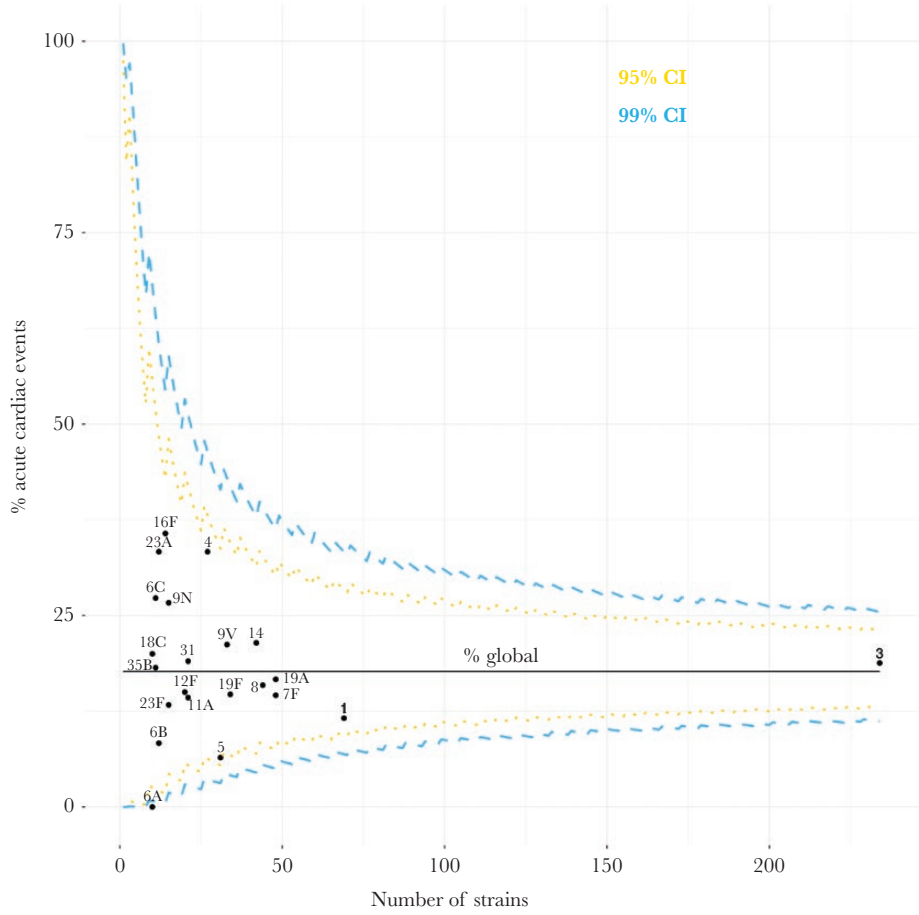

Figure 1. Funnel plot analysis of serotypes and acute cardiac events.

independently associated with 30-day mortality (adjusted odds ratio, 1.88; 95% CI, 1.11–3.13; $P = .017$).

DISCUSSION

This retrospective study of a large cohort of patients with pneumococcal pneumonia defined several host factors associated with the development of acute cardiac events. We also studied a possible link between both pneumococcal serotypes or clonal complexes and the risk of developing cardiac complications.

The host factors we found to be independently associated with acute cardiac events in pneumococcal pneumonia were older age, preexisting heart conditions, pneumococcal bacteremia, septic shock at admission, and high-risk pneumonia. A finding of interest in our study is the fact that prehospitalization antibiotic treatment for the acute episode of pneumococcal pneumonia tended to display a protective effect for acute cardiac events, although it did not reach statistical significance in the multivariate analysis. Interestingly, experimental animal studies have shown a significant positive correlation between pneumococcal blood load and cardiac damage [17, 20]. In addition, pneumococcal bacteremia has been shown to be an important trigger for the development of acute cardiac events in CAP patients [31]. We found a lower incidence of bacteremia and a less severe clinical presentation in patients with prehospitalization antibiotic treatment, which may, to some extent at least, explain the lower incidence of cardiac complications.

Previous information regarding characteristics of pneumococcal strains and cardiac complications is derived from 2 studies [20, 22]. An experimental study evaluating not more than 6 mice per strain showed that only serotypes able to cause high-grade bacteremia, such as serotypes 2, 3, 4, and 6A, produced cardiac damage [20]. Moreover, for the serotypes that could invade the heart, the type of cardiac damage was strain specific. In addition, a recent study of 310 patients with invasive pneumococcal disease, of whom 71 presented an acute cardiac event, found an association between serotypes 3 and 9N [22]. In that study, clonal complexes were not analyzed. In contrast, in our study, which included a large number of patients, we did not find any significant association of serotypes 3 and 9N with acute cardiac events. Our study, analyzing serotypes isolated from 872 patients and clonal complexes from 742, found a negative trend linking acute cardiac events with some highly clonal serotypes, such

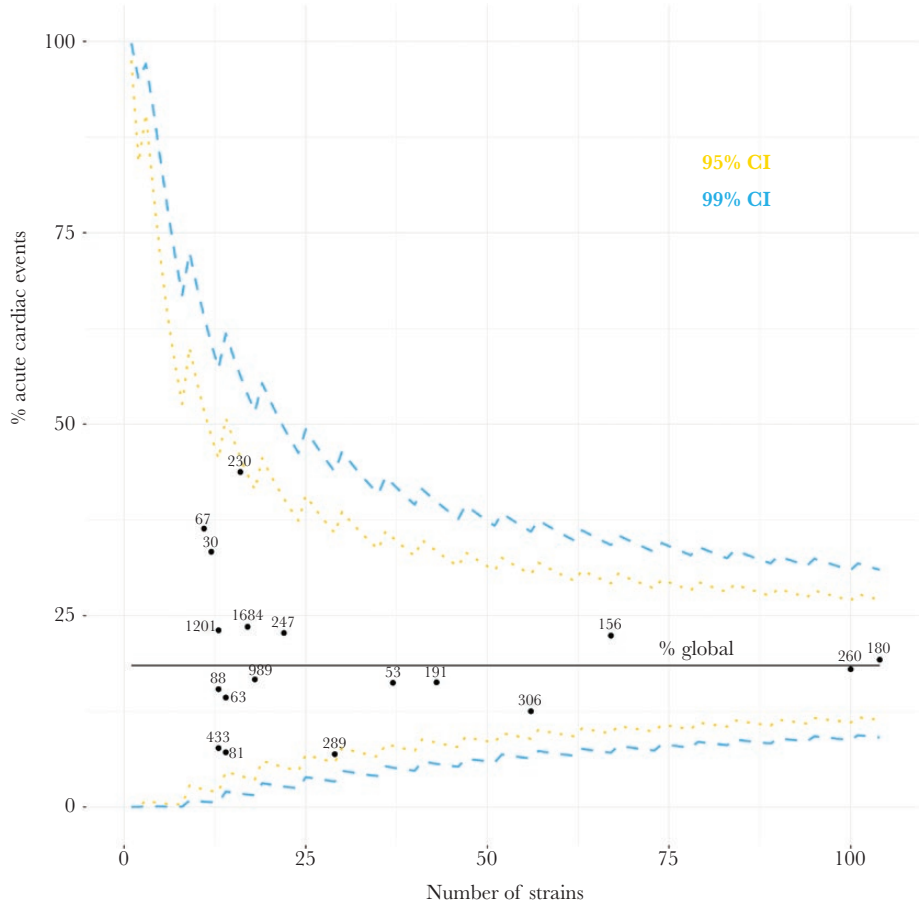

Figure 2. Funnel plot analysis of genotypes (clonal complexes) and acute cardiac events.

Table 3. Treatment and Outcomes of Pneumococcal Pneumonia in Patients who Developed Acute Cardiac Events and Those who Did Not

Patients (n = 1739)	Pneumococcal Pneumonia With Acute Cardiac Events (n = 304), No. (%)	Pneumococcal Pneumonia Without Acute Cardiac Events (n = 1435), No. (%)	*P* Value
Initial antibiotic treatment			
β-lactam monotherapy	131/304 (43.1)	700/1435 (48.8)	.082
β-lactam + macrolide	5/304 (1.6)	32/1435 (2.2)	.672
Fluoroquinolone monotherapy	24/304 (7.9)	140/1435 (9.8)	.37
β-lactam + fluoroquinolone	134/304 (44.1)	525/1435 (36.6)	.017
Fluoroquinolone (alone or any combination)	158/304 (52)	669/1435 (46.6)	.102
Macrolide (alone or any combination)	6/304 (2)	37/1435 (2.6)	.68
Other	10/304 (3.3)	37/1435 (2.6)	.62
Door-to-needle antibiotic time, median (IQR[a]), h	5 (3.00–8.00)	5 (3.00–7.00)	.72
Intensive care unit admission	79/304 (26)	147/1435 (10.2)	<.001
Need for mechanical ventilation[b]	74/304 (24.3)	111/1435 (7.7)	<.001
Length of hospital stay, median (IQR), d	10 (7.00–18.2)	8 (5.00–11.00)	<.001
Early mortality (≤48 h)	8/304 (2.6)	22/1435 (1.71)	.24
30-d mortality	42/304 (13.8)	68/1435 (4.7)	<.001

Abbreviation: IQR, interquartile range.

[a]Data missing in 482 patients.

[b]Includes invasive and noninvasive mechanical ventilation.

as 5 (CC289) or 1 (CC306). Moreover, clonal complex CC230 tended to be associated with a higher incidence of acute cardiac events. This finding, although not statistically significant in the funnel plot, may be clinically relevant. In our study, clonal complex CC230 was mainly related to serotypes 19A and 24F. Serotype 19A was not associated with acute cardiac events, suggesting that genetic background, and not serotype, could play a major role in these serious complications. Importantly, while serotype 19A is included in both conjugated and polysaccharide pneumococcal vaccines, serotype 24F is not covered by the current vaccines or by any of those under development. It is plausible that certain strains disproportionally impact individuals who have risk factors for ACEs—older age, preexisting heart disease. Multivariate analyses that include serotype-specific information should be performed in future investigations.

Our finding that CC230 tends to be associated with a higher incidence of acute cardiac events is hypothesis-generating and should be explored in further multicenter studies in other geographical areas and including a higher number of pneumococcal strains. Our study also opens up avenues for further research exploring the association of the pneumococcal serotypes and genotypes and long-term risk of serious cardiac events.

Despite a number of strengths, our study has some limitations that should be acknowledged. First, the study involved a cohort of adults with pneumococcal pneumonia recorded over more than 20 years at a single center. This may limit the extrapolation of our results to other geographical areas where other serotypes and clonal complexes may be more prevalent [30]. Second, serotyping and genotyping were not performed in all isolates; however, serotypes and genotypes were determined in the majority of the 983 isolates (89% and 76%, respectively). Third, the small number of some serotypes and clonal complexes limited the analysis of their potential relationship with acute cardiac complications. Lastly, worsening of preexisting heart conditions was included as an acute cardiac event and may have confounded the results; however, analyzing exclusively new-onset arrhythmia, new-onset heart failures, and myocardial infarction yielded similar results.

In summary, acute cardiac events are frequent and confer worse clinical outcomes in pneumococcal pneumonia. Although CC230 tends to be associated with a higher incidence of acute cardiac events, host factors appear to be more important than pathogen-related factors for developing these life-threatening complications. The host factors defined in this study may help identify the patients who require close follow-up including heart rhythm monitoring and special care to avoid fluid overload, particularly within the first 48 hours of admission. These high-risk patients should be the target for urgent preventive intervention strategies.

Supplementary Data

Supplementary materials are available at *Open Forum Infectious Diseases* online. Consisting of data provided by the authors to benefit the reader, the posted materials are not copyedited and are the sole responsibility of the authors, so questions or comments should be addressed to the corresponding author.

Acknowledgments

Financial support. A. Rombauts is a recipient of a research grant from the Instituto de Salud Carlos III, Spanish Ministry of Science, Innovation and Universities, through the 2018 call for predoctoral contracts for training in health research (PFIS contract FI18/00183), with additional help from the European Social Fund (programming period 2014–2020) "The European Social Funds invests in your future." G. Abelenda-Alonso is a recipient of a research grant from TV3-Fundació La Marató (201808-10). The study was supported by Instituto de Salud Carlos III (research grants 11/01106, 14/00580, and 17/01332). The project was also supported by Plan Nacional de I+D+i 2013–2016 and Instituto de Salud Carlos III, Subdirección General de Redes y Centros de Investigación Cooperativa, Ministerio de Economía, Industria y Competitividad, Spanish Network for Research in Infectious Diseases (REIPI RD16/0016/0005)—co-financed by European Development Regional Fund "A way to achieve Europe," Operative program Intelligent Growth 2014–2020, and by Centro de Investigación Biomédica en Red (CIBER) de Enfermedades Respiratorias (CIBERES) CB06/060037. We thank CERCA Programme/Generalitat de Catalunya for institutional support.

Potential conflicts of interest. We declare no competing interests. All authors: no reported conflicts of interest. All authors have submitted the ICMJE Form for Disclosure of Potential Conflicts of Interest. Conflicts that the editors consider relevant to the content of the manuscript have been disclosed.

Role of the funding source. The funders had no role in the design or conduct of the study; collection, management, analysis, or interpretation of the data; preparation, review, or approval of the manuscript; or the decision to submit the manuscript for publication. The corresponding author had full access to all study data and had final responsibility for the decision to submit the paper for publication.

References

1. Corrales-Medina VF, Musher DM, Shachkina S, Chirinos JA. Acute pneumonia and the cardiovascular system. Lancet **2013**; 381:496–505.
2. Feldman C, Anderson R. Prevalence, pathogenesis, therapy, and prevention of cardiovascular events in patients with community-acquired pneumonia. Pneumonia **2016**; 8:11.
3. Musher DM, Abers MS, Corrales-Medina VF. Acute infection and myocardial infarction. N Engl J Med **2019**; 380:171–6.
4. Viasus D, Garcia-Vidal C, Manresa F, et al. Risk stratification and prognosis of acute cardiac events in hospitalized adults with community-acquired pneumonia. J Infect **2013**; 66:27–33.
5. Violi F, Cangemi R, Falcone M, et al. Cardiovascular complications and short-term mortality risk in community-acquired pneumonia. Clin Infect Dis **2017**; 64:1486–93.
6. Griffin AT, Wiemken TL, Arnold FW. Risk factors for cardiovascular events in hospitalized patients with community-acquired pneumonia. Int J Infect Dis **2013**; 17:e1125–9.
7. Corrales-Medina VF, Musher DM, Wells GA, et al. Cardiac complications in patients with community-acquired pneumonia: incidence, timing, risk factors, and association with short-term mortality. Circulation **2012**; 125:773–81.
8. Corrales-Medina VF, Alvarez KN, Weissfeld LA, et al. Association between hospitalization for pneumonia and subsequent risk of cardiovascular disease. JAMA **2015**; 313:264–74.
9. Eurich DT, Marrie TJ, Minhas-Sandhu JK, Majumdar SR. Risk of heart failure after community acquired pneumonia: prospective controlled study with 10 years of follow-up. BMJ **2017**; 356:j413.
10. Corrales-Medina VF, Taljaard M, Yende S, et al. Intermediate and long-term risk of new-onset heart failure after hospitalization for pneumonia in elderly adults. Am Heart J **2015**; 170:306–12.
11. Eurich DT, Marrie TJ, Minhas-Sandhu JK, Majumdar SR. Ten-year mortality after community-acquired pneumonia. A prospective cohort. Am J Respir Crit Care Med **2015**; 192:597–604.

12. Perry TW, Pugh MJ, Waterer GW, et al. Incidence of cardiovascular events after hospital admission for pneumonia. Am J Med **2011**; 124:244–51.
13. Cangemi R, Calvieri C, Falcone M, et al; SIXTUS Study Group. Relation of cardiac complications in the early phase of community-acquired pneumonia to long-term mortality and cardiovascular events. Am J Cardiol **2015**; 116: 647–51.
14. Warren-Gash C, Blackburn R, Whitaker H, McMenamin J, Hayward AC. Laboratory-confirmed respiratory infections as triggers for acute myocardial infarction and stroke: a self-controlled case series analysis of national linked datasets from Scotland. Eur Respir J **2018**; 51:1701794.
15. Musher DM, Rueda AM, Kaka AS, Mapara SM. The association between pneumococcal pneumonia and acute cardiac events. Clin Infect Dis **2007**; 45:158–65.
16. Reyes LF, Restrepo MI, Hinojosa CA, et al. Severe pneumococcal pneumonia causes acute cardiac toxicity and subsequent cardiac remodeling. Am J Respir Crit Care Med **2017**; 196:609–20.
17. Brown AO, Mann B, Gao G, et al. *Streptococcus pneumoniae* translocates into the myocardium and forms unique microlesions that disrupt cardiac function. PLoS Pathog **2014**; 10:e1004383.
18. Brissac T, Shenoy AT, Patterson LA, Orihuela CJ. Cell invasion and pyruvate oxidase-derived H2O2 are critical for *Streptococcus pneumoniae*-mediated cardiomyocyte killing. Infect Immun **2017**; 86:e00569-17.
19. Alhamdi Y, Neill DR, Abrams ST, et al. Circulating pneumolysin is a potent inducer of cardiac injury during pneumococcal infection. PLoS Pathog **2015**; 11:e1004836.
20. Shenoy AT, Beno SM, Brissac T, Bell JW, Novak L, Orihuela CJ. Severity and properties of cardiac damage caused by *Streptococcus pneumoniae* are strain dependent. PLoS One **2018**; 13:e0204032.
21. Anderson R, Nel JG, Feldman C. Multifaceted role of pneumolysin in the pathogenesis of myocardial injury in community-acquired pneumonia. Int J Mol Sci **2018**; 19:1147.
22. Africano H, Serrano-Mayorga C, Ramirez-Valbuena P, et al. Major adverse cardiovascular events during invasive pneumococcal disease are serotype dependent. Clin Infect Dis. **In press**.
23. McKee PA, Castelli WP, McNamara PM, Kannel WB. The natural history of congestive heart failure: the Framingham Study. N Engl J Med **1971**; 285:1441–6.
24. Fenoll A, Granizo JJ, Aguilar L, et al. Temporal trends of invasive *Streptococcus pneumoniae* serotypes and antimicrobial resistance patterns in Spain from 1979 to 2007. J Clin Microbiol **2009**; 47:1012–20.
25. Center for Disease Control and Prevention (CDC). Streptococcus Laboratory. Available at: https://www.cdc.gov/streplab/pneumococcus/resources.html. Accessed 28 July 28 2020.
26. Garcia-Vidal C, Ardanuy C, Tubau F, et al. Pneumococcal pneumonia presenting with septic shock: host- and pathogen-related factors and outcomes. Thorax **2010**; 65:77–81.
27. Public databases for molecular typing and microbial genome diversity. *Streptococcus pneumoniae*. Available at: https://pubmlst.org/spneumoniae/. Accessed, July 28, 2020.
28. Spiegelhalter DJ. Funnel plots for comparing institutional performance. Stat Med **2005**; 24:1185–202.
29. R Core Team. R: A Language and Environment for Statistical Computing. Vienna, Austria: R Foundation for Statistical Computing; **2018**.
30. Lewnard JA, Hanage WP. Making sense of differences in pneumococcal serotype replacement. Lancet Infect Dis **2019**; 19:e213–20.
31. Borsa N, Iturriaga LAR, Fernandez LS, et al. Bacteremic pneumococcal pneumonia is associated with an increased rate of cardiovascular events. Eur Respir J **2019**; 54:OA3306.

Study 3

Dynamics of Gene Expression Profiling and Identification of High-Risk Patients for Severe COVID-19.

Rombauts, A✉., Bódalo Torruella, M., Abelenda-Alonso, G., Perera-Bel, J., Ferrer-Salvador, A., Acedo-Terrades, A., Gabarrós-Subirà, M., Oriol, I., Gudiol, C., Nonell, L.✉, & Carratalà, J.

Biomedicines, 2023, 11(5), 1348.

Impact factor: 4.7 (1st quartile)

biomedicines

MDPI

Article

Dynamics of Gene Expression Profiling and Identification of High-Risk Patients for Severe COVID-19

Alexander Rombauts [1,*], Marta Bódalo Torruella [2], Gabriela Abelenda-Alonso [1], Júlia Perera-Bel [2], Anna Ferrer-Salvador [3], Ariadna Acedo-Terrades [2], Maria Gabarrós-Subirà [2], Isabel Oriol [1], Carlota Gudiol [1,4,5], Lara Nonell [2,*] and Jordi Carratalà [1,4,5]

1 Department of Infectious Diseases, Hospital Universitari de Bellvitge-IDIBELL, 08908 Barcelona, Spain; isaoriolbermudez@gmail.com (I.O.); cgudiol_ext@iconcologia.net (C.G.)
2 MARGenomics, Hospital del Mar Medical Research Institute (IMIM), 08003 Barcelona, Spain; mbodalo@imim.es (M.B.T.)
3 Centre for Genomic Regulation (CRG), The Barcelona Institute of Science and Technology, 08028 Barcelona, Spain
4 Department of Medicine, Universitat de Barcelona, 08007 Barcelona, Spain
5 Centro de Investigación Biomédica en Red de Enfermedades Infecciosas (CIBERINFEC), Instituto de Salud Carlos III, 28029 Madrid, Spain
* Correspondence: alexander.rombauts@gmail.com (A.R.); laranonell@gmail.com (L.N.); Tel.: +3493-291-90-00 (A.R.); +34-93-254-34-50 (L.N.)

Abstract: The clinical manifestations of SARS-CoV-2 infection vary widely, from asymptomatic infection to the development of acute respiratory distress syndrome (ARDS) and death. The host response elicited by SARS-CoV-2 plays a key role in determining the clinical outcome. We hypothesized that determining the dynamic whole blood transcriptomic profile of hospitalized adult COVID-19 patients and characterizing the subgroup that develops severe disease and ARDS would broaden our understanding of the heterogeneity in clinical outcomes. We recruited 60 hospitalized patients with RT-PCR-confirmed SARS-CoV-2 infection, among whom 19 developed ARDS. Peripheral blood was collected using PAXGene RNA tubes within 24 h of admission and on day 7. There were 2572 differently expressed genes in patients with ARDS at baseline and 1149 at day 7. We found a dysregulated inflammatory response in COVID-19 ARDS patients, with an increased expression of genes related to pro-inflammatory molecules and neutrophil and macrophage activation at admission, in addition to an immune regulation loss. This led, in turn, to a higher expression of genes related to reactive oxygen species, protein polyubiquitination, and metalloproteinases in the latter stages. Some of the most significant differences in gene expression found between patients with and without ARDS corresponded to long non-coding RNA involved in epigenetic control.

Keywords: COVID-19; SARS-CoV-2; transcriptomics; ARDS; gene expression; prognosis

Citation: Rombauts, A.; Bódalo Torruella, M.; Abelenda-Alonso, G.; Perera-Bel, J.; Ferrer-Salvador, A.; Acedo-Terrades, A.; Gabarrós-Subirà, M.; Oriol, I.; Gudiol, C.; Nonell, L.; et al. Dynamics of Gene Expression Profiling and Identification of High-Risk Patients for Severe COVID-19. *Biomedicines* **2023**, *11*, 1348. https://doi.org/10.3390/biomedicines11051348

Academic Editor: Christos K. Kontos

Received: 3 April 2023
Revised: 28 April 2023
Accepted: 1 May 2023
Published: 3 May 2023

1. Introduction

The coronavirus disease 2019 (COVID-19) pandemic, caused by the severe acute respiratory syndrome coronavirus 2 (SARS-CoV-2), the most recent zoonotic coronavirus to cause devastation in humans [1], is a public health problem of historic magnitude. As of March 2023, more than 676 million cases of COVID-19 have been reported globally, with more than 6.8 million deaths [2].

The clinical manifestations of SARS-CoV-2 infections vary broadly, ranging from an asymptomatic state to severe pneumonia, including acute respiratory distress syndrome (ARDS), multisystem organ failure, and eventually death [3,4]. Morbidity and mortality are almost exclusively driven by the development of ARDS.

An early adaptive immune response with a rapid production of bystander CD8 T cells and plasmablasts with almost no systemic inflammation appears to take place in

asymptomatic patients and in those with mild disease [5]. In contrast, progression to severe illness with ARDS has been associated with a proinflammatory immune dysregulation that includes a robust type 2 response [6,7]. Factors such as SARS-CoV-2 viral load [8], immunological imprinting due to previous infections with other coronaviruses [9], autoantibodies against interferon-ω [10], host genetic determinants [11], low levels of type I and III interferons (INF) together with elevated chemokines and high expression of IL-6 [12] may play a role in COVID-19 outcomes. Intriguingly, it remains unclear why some patients develop severe pneumonia with ARDS and others have zero or minimal symptoms.

A genome-wide association found that certain regions, such as 3p21.31, and blood group A, were related to severity [11–13]. In addition, several ACE2 polymorphisms [13] and inborn errors of type 1 INF [14] have been correlated with increased severity and susceptibility to COVID-19.

Regarding transcriptomics, most of the research has analyzed single-cell RNA extracted from peripheral mononuclear cells (PBMC) [15]; only a few studies have been performed on total RNA from whole blood. Some of these whole blood RNA studies focused on identifying a transcriptomic signature differentiating SARS-CoV-2 from influenza [16] and other viral respiratory pathogens [17], while others compared asymptomatic vs. symptomatic patients [6,18]. Investigations evaluating whole blood transcriptomic profiles according to clinical status found that more severe cases showed an upregulation of genes principally related to neutrophil activation [5,17,19–21], myeloid cells [20], Il2, Il6, IL8, protein autophagy, protein polyubiquitination [19], TNF-α, and glycolysis [5], while genes related to T-cell activation were under-expressed [16,19,20,22]. As for interferon gene expression, two studies found an enrichment [5,20], while one observed a down-regulation of IFN-γ related genes [19].

However, most of the transcriptomic studies of COVID-19 have analyzed a single time point per patient [16,17,19,20,22], thus disregarding the dynamic nature of the disease. In addition, several investigations observed heterogeneity in the transcriptomic profiles among the more severe groups of hospitalized COVID-19 patients [5,21,22].

The main goal of this study was to determine the dynamic transcriptomic profile of adult patients hospitalized for COVID-19 and to characterize the subgroup that developed severe disease and ARDS.

2. Materials and Methods

2.1. Study Design, Setting, Ethics and Patients

In this prospective study, 60 patients were enrolled at Bellvitge University Hospital. Transcriptomic analyses were performed at the Hospital del Mar Medical Research Institute (IMIM). Adult patients with a positive RT-PCR for SARS-CoV-2 in nasopharyngeal swabs and COVID-19 symptoms requiring hospitalization from 25 March 2020, to 31 July 2020 (during the first wave of the COVID-19 pandemic in Spain) were eligible for recruitment. Patients were enrolled within 24 h of admission. Blood samples were obtained at baseline and on day 7 of hospital admission. Patients were assigned a unique patient identifier (PID), which was applied to the clinical samples and the depersonalized data set. The list correlating the patient's identity with the PID is securely stored at Bellvitge University Hospital. Patients were prospectively followed-up and seen daily by the investigators. Data on demographic and clinical characteristics, biochemical analysis, treatments, and outcomes were collected in a pseudoanonymized database. The study was approved by the Bellvitge University Hospital Ethics Committee (PR148/20), and written informed consent was obtained for all cases.

We classified the patients according to their respiratory situation each day over the course of hospitalization (Figure 1). We hypothesized that patients with medium oxygen needs (oxygen mask with oxygen flow between 8 and 15 L/min) could express a transcriptomic profile overlapping ARDS and a more benign clinical evolution. Therefore, to increase the specificity of the transcriptomic profile associated with ARDS, patients who met the amplified definition of ARDS were compared with those with low flow oxygen

needs (oxygen masks up to 8 L/min). The transcriptomic profile of patients with low oxygen needs was compared to that of patients with ARDS at baseline. At day 7, the transcriptomic profile of all patients who had developed ARDS at any time was compared with those who had not.

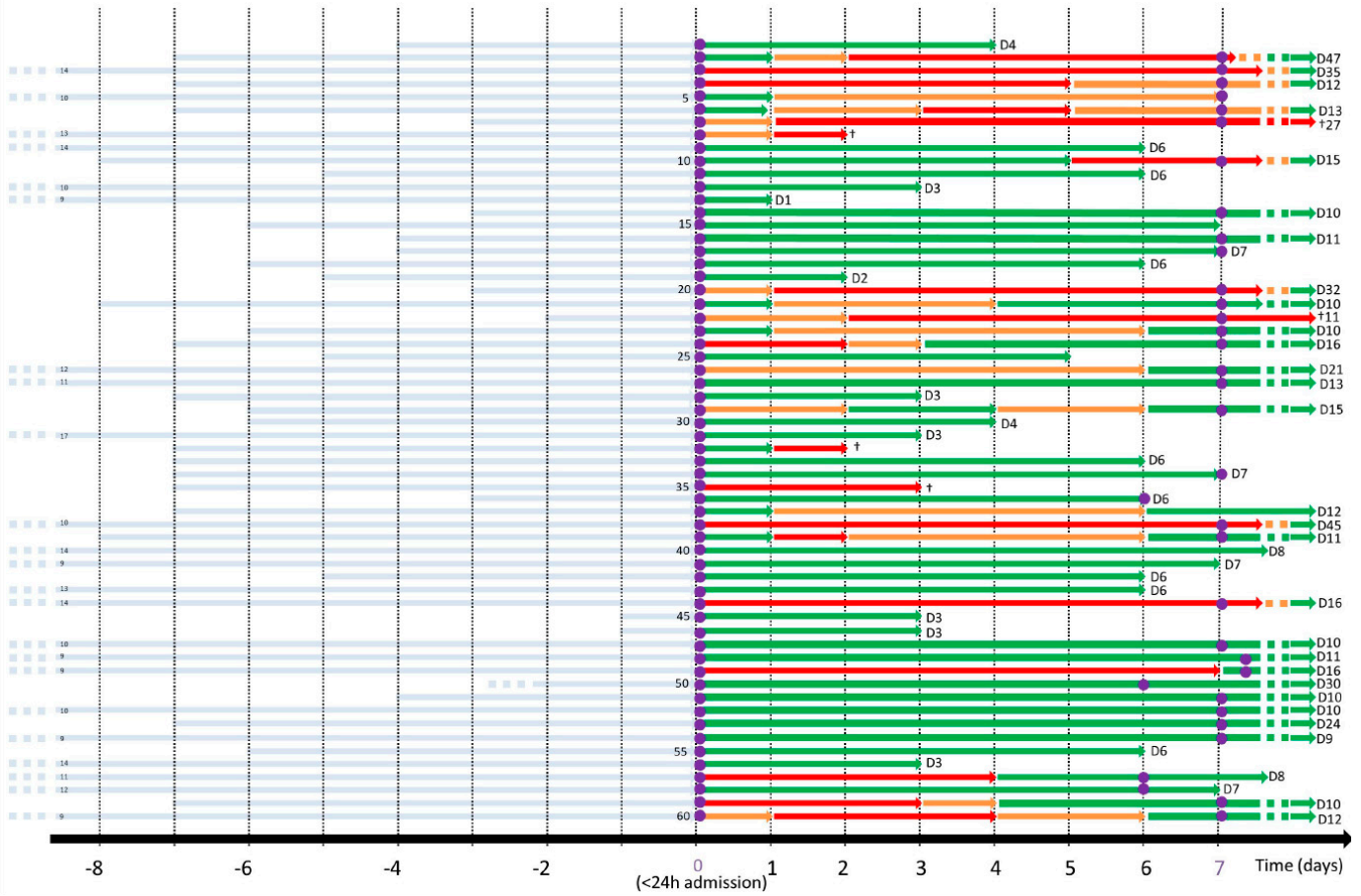

Figure 1. Clinical evolution of each individual patient according to oxygen need and day of sampling. The *x*-axis represents time expressed in days, and the light-blue rows represent symptoms duration prior to hospital admission (day 0). Green represents low oxygen need (oxygen mask up to 8 L/min), orange represents medium oxygen need (between 8 and 15 L/min), and red represents the amplified definition of ARDS (invasive or non-invasive mechanical ventilation, at least 24 h of FiO2 $\geq$ 70% and high-flow oxygen, $\geq$15 L/min, delivered by either non-rebreather masks or high-flow nasal oxygen). The purple circles represent peripheral blood sampling using PAXGene RNA tubes. The day of hospital discharge is detailed at the end of each row, and death is represented by the symbol †.

2.2. Definitions and Local Guidelines

COVID-19 pneumonia was defined as new or worsening pulmonary infiltrates on a chest x-ray or CT of the lungs with a confirmed positive RT-PCR for SARS-CoV-2. ARDS was defined as acute respiratory failure (PaO2/FiO2 < 300) with bilateral opacities and no acute heart failure. Due to the overburdening of the health-care system and the scarcity of critical care beds during the first COVID-19 wave, we decided to broaden the classical Berlin definition [23] to eliminate the requirement of a positive end-expiratory pressure of at least 5 cmH_2O. In addition to invasive (IV) or non-invasive mechanical ventilation (NIV), patients who required at least 24 h of FiO2 $\geq$ 70% and high-flow oxygen ($\geq$15 L/min) delivered by either non-rebreather masks or high-flow nasal oxygen (HFNO) were considered to have ARDS [24]. The case report form and other definitions can be found in the Supplementary Materials section. Corticosteroids and tocilizumab were administered at the attending physician's discretion.

2.3. RNA Extraction

Peripheral blood was collected using PAXGene RNA tubes from Qiagen. RNA was extracted using a CE-certified PAXGene blood RNA kit at the IMIM's COVID room with special biosecurity measures (see Supplementary Materials). The quantity and integrity of the samples were assessed with Nanodrop, Qubit, and Bioanalyzer instruments. Samples of sufficient quality were selected for further processing.

2.4. Library Preparation

PAXGene RNA samples were processed using NEBNext Globin rRNA Depletion and NEBNext UltraII DirecRNA LibPrep in order to obtain the libraries. Laboratory parameters (initial input, PCR cycles, and adaptor dilution) were adjusted considering the quantity and quality of the different types of samples. Library profiles were checked using the bioanalyzer instrument and Qubit dsDNA kit to quantify them. Libraries that passed quality control were transferred to the CRG Core Facility. At the CRG, qPCR of the libraries was performed prior to running the flow cell. Samples were sequenced by Illumina HiSeq 2500, resulting in paired 75-nt reads.

2.5. RNA-Seq Bioinformatic Processing

Initial quality control was carried out using FastQC (v0.11.5) and FastQ Screen (v0.14.0) and summarized with Multiqc (v1.7). All QC metrics were deemed correct, with a median of 49 million read-pairs per sample. No ribosomal contamination was detected (neither in humans nor in other species). Raw sequencing reads in the fastq files were mapped with STAR version 2.7.1a Gencode release v36 based on the GRCh38.p13 reference genome and the corresponding GTF file.

2.6. Statistical Analysis

SAMtools v1.8 was used to index bam files. The algorithm CollectRnaSeqMetrics from Picard v2.2.4 was used to retrieve alignment metrics. The table of counts was obtained with the featureCounts function in the package subread (v1.6.4). The differential gene expression (DEG) analysis was assessed with voom + limma in the limma package (v3.46.0) using R (v4.0.3). Linear models included the batch as a covariate. Significant mean positive log2-fold changes correspond to upregulation, while negative changes correspond to downregulation. Functional analysis was performed with the clusterProfiler R package (v4.2.2) and the Hallmark collection from the Molecular Signatures Database (MSigDB, v7.5.1). Deconvolution analyses were performed to track compositional alterations of cell types in gene expression data. To deconvolute cell types, the immunedeconv R package (v2.0.4) with method CIBERSORT absolute was used.

3. Results

The characteristics of the 60 enrolled patients hospitalized due to SARS-CoV-2 infection are shown in Table 1.

The mean age was 63 years (SD 14.8), 23 (38.3%) were women, 11 (18.3%) had diabetes mellitus, 14 (23.3%) had dyslipidemia, 5 (8.3%) had chronic heart disease, and 5 (8.3%) had chronic pulmonary diseases. The median time from symptom onset until hospital admission was 7.8 days (SD 3.6). Most patients presented with fever (88.3%), cough (71.7%), dyspnea (45%), and diarrhea (18.3%). Almost all patients (91.7%) had pneumonia at admission, most of them bilateral (76.6%). Since many of the patients were included during the first wave, treatments included hydroxychloroquine (66.7%), lopinavir-ritonavir (28.3%), corticosteroids (53.3%), remdesivir (25%), and tocilizumab (21.7%) during hospitalization. A total of 19 (31.6%) patients required the use of a non-rebreather mask $\geq$24 h, 12 (20%) required a high flow nasal cannula or non-invasive mechanical ventilation, 6 (10%) were admitted to the ICU, and 3 (5%) underwent invasive mechanical ventilation. The median length of hospital stay was 9.6 days (SD 2.1). In-hospital mortality was 8.3%. A total of 9 patients (15%) met the amplified definition of ARDS at admission and 19 (31.6%) at

any given time during hospitalization. Patients' respiratory status during each day of hospitalization is represented in Figure 1.

Table 1. Patients' characteristics.

Patients' Characteristics	***n* (%)**
Age (mean, SD)	63 (14.8)
Woman	23 (38.3%)
Active tobacco use	0 (0%)
Diabetes mellitus	11 (18.3%)
Dyslipidemia	14 (23.3%)
Preexisting pulmonary diseases	5 (8.3%)
Heart disease	5 (8.3%)
Stroke	3 (5%)
Renal failure	2 (3.3)
Dementia	2 (3.3%)
Solid organ transplant recipient	2 (3.3)
Obesity (BMI > 30)	31 (51.7%)
Morbid obesity (BMI > 40)	4 (6.7%)
Clinical presentation	
Duration of symptoms (mean days, SD)	7.8 (3.6)
Fever	53 (88.3%)
Cough	43 (71.7%)
Dyspnea	27 (45%)
Diarrhea	11 (18.3%)
Cephalea	8 (13.3%)
Altered consciousness	5 (8.3%)
Mean room air saturation (%, SD)	94.9% (4)
Room air pulsioximetry <94% (%)	26 (43.3%)
Mean respiratory rate (SD)	24.2 (6.9)
Respiratory rate >30	11 (18.3%)
Mean lymphocytes ($\times 10^6$, SD)	1083 (465)
Mean C reactive protein (mg/L, SD)	128 (107)
Pneumonia at presentation	55 (91.7%)
Bilateral pneumonia at presentation	46 (76.6%)
COVID-19 treatment	
Lopinavir-ritonavir	17 (28.3%)
Hydroxychloroquine	40 (66.7%)
Remdesivir	15 (25%)
Tocilizumab	13 (21.7%)
Steroids	32 (53.3%)
Outcomes	
Use of non-rebreather mask $\geq$24 h any given time	19 (31.6%)

Table 1. *Cont.*

Patients' Characteristics	***n* (%)**
Use of high flow nasal cannula or non-invasive mechanical ventilation any given time	12 (20%)
ICU admission	6 (10%)
Median APACHE II score at ICU admission (SD)	12.33 (2.7)
Mechanical ventilation	3 (5%)
Nosocomial infection	8 (13.3%)
Median length of hospitalization stay (days, SD)	9.6 (2.1)
In-hospital mortality	5 (8.3%)

Baseline comparison (within 24 h of admission) of patients with ARDS with those with low oxygen needs (maximum 6 L/min, n = 44) showed 2572 genes with log2-fold changes above 1. Several genes associated with T-cell activation (e.g., TRAV20, TRBV13, TRAV23DV6) and carbohydrate and galactose (e.g., CLEC4F) binding were found to be downregulated in ARDS. In contrast, many upregulated genes identified in ARDS are involved in immunoglobulin production (e.g., IGHV1-69-2, IGHV2-70D, TMIGD3, IGLV5-45), monocytes/macrophages (e.g., MAOA, MACIR), neutrophil activation (e.g., CD177, LCN2), and NF-Kappa B activation (e.g., upregulation of PCSK9 and downregulation of TIFAB). In agreement with these results, CIBERSORT deconvolution analysis showed a decrease in the population of naive $CD4^+$ T cells, resting memory $CD4^+$ T cells, $CD8^+$ T cells, resting NK cells, and monocytes in samples from patients with ARDS. The opposite pattern was observed in the neutrophil cell population. Various upregulated genes identified in ARDS control lipid metabolic functions (e.g., OLAH, PCSK9, ACBD7, LPL, FABP2), polyubiquitination (e.g., SCN5A, UBQLN4P1, GRB10), and metalloproteinases (e.g., ADAMTS3, TIMP4, MMP1, MMP8). Interestingly, a variety of long non-coding RNAs (e.g., KCNMA1-AS1, AL592158.1, AC012146.1, IRAIN, A2M-AS1, PVT1, etc.), many of them probably involved in epigenetic control, were differentially expressed in patients with ARDS. In addition, we found significant increased and decreased levels of several non-coding microRNAs (miRNAs). Pathway analysis showed significantly enriched IL-6 and JAK-STAT3 signaling in ARDS. On the other hand, two specific enriched pathways, related to Myc V2 targets and WNT/β-catenin signaling, were identified in patients with less severe pneumonia. Figure 2 shows the heatmap, and the comparison of the CIBERSORT distribution at baseline of patients with ARDS to those with low oxygen.

When comparing whole blood transcriptomics at day 7 in all patients who had developed ARDS at any time with those without, 1149 significant differentially expressed genes were found. Figure 3 shows the heatmap and CIBERSORT distribution at day 7.

We found an upregulation of genes related to lipid control (e.g., OLAH, LPL, ECHDC3, ALOX15B, PCSK9), oxidation (e.g., MAOA, MAOB), polyubiquitination, and metalloproteinases in patients with ARDS by day 7 of hospitalization. Conversely, TIFAB (which enhances NF-kappa B inhibition) and KLRC2 (involved in NK activation) were downregulated in patients with ARDS. Again, we found significant increased and decreased levels of several lncRNAs and miRNAs between patients with ARDS at any given time and those without at day 7. Pathway analysis found a significantly enhanced expression of IL-6 and JAK STAT3 signaling and genes related to androgen response in patients with ARDS compared to those with those with lower oxygen needs. A pathway analysis comparing baseline and day 7 is shown in Figure 4.

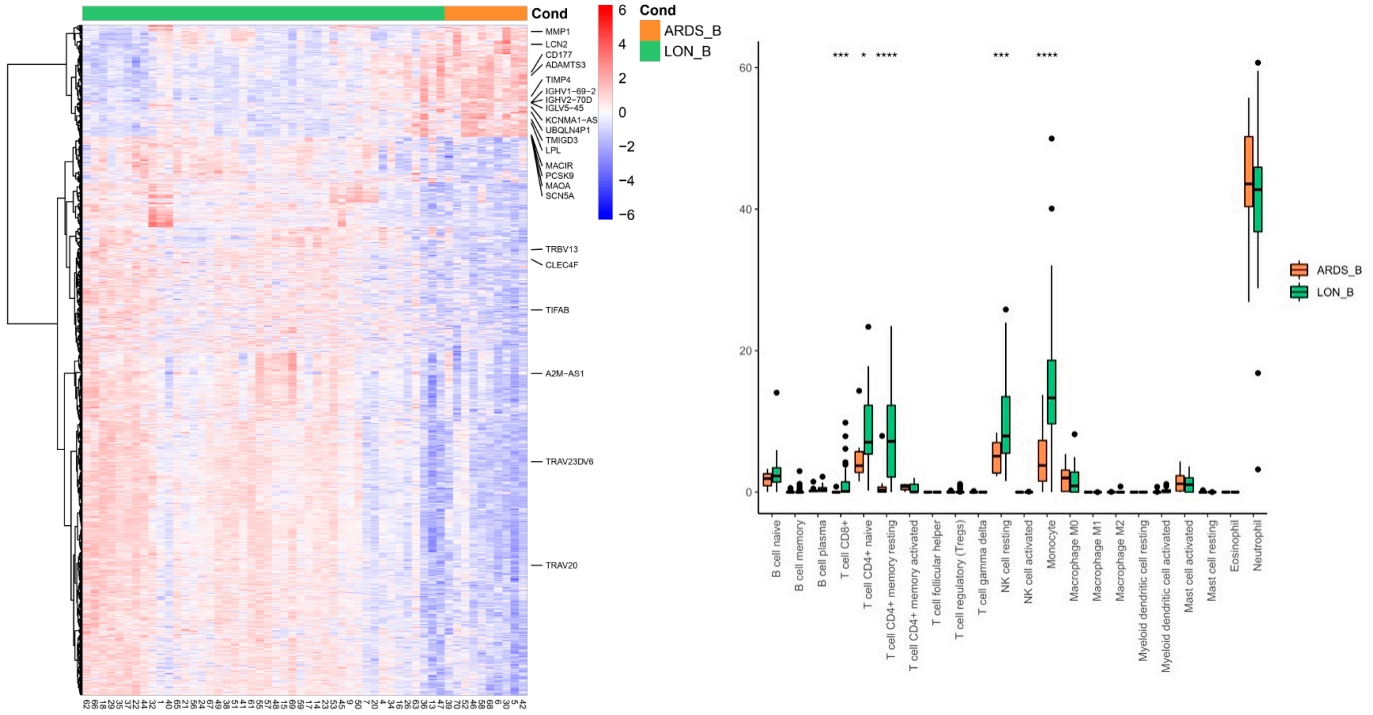

(**a**) (**b**)

Figure 2. (**a**) Heatmap depicting the gene expression of differentially expressed genes (DEGs) obtained from the baseline comparison between COVID-19 patients with ARDS (ARDS_B) and those with low oxygen needs (LON_B). Each column in the figure represents a sample, and each row represents a gene. The colors in the graph indicate the magnitude of gene expression in the sample. Red indicates that the gene is highly expressed in the sample, and blue indicates that the gene expression is low. Genes included have an absolute log2 fold change of more than 1 and an adjusted *p*-value of <0.05. Genes involved in immunoglobulin production (e.g., IGHV1-69-2, IGHV2-70D, TMIGD3, IGLV5-45), monocytes/macrophages (e.g., MAOA, MACIR), neutrophil activation (e.g., CD177, LCN2), and NF-Kappa B activation were upregulated in ARDS patients, while genes associated with T-cell activation were downregulated. (**b**) Baseline comparison between patients with ARDS (ARDS_B) and those with low oxygen needs (LON_B) using CIBERSORT deconvolution analysis and comparison. Significance is noted by: * for *p*-value < 0.05, *** for *p*-value < 0.001 and **** for *p*-value < 0.0001.

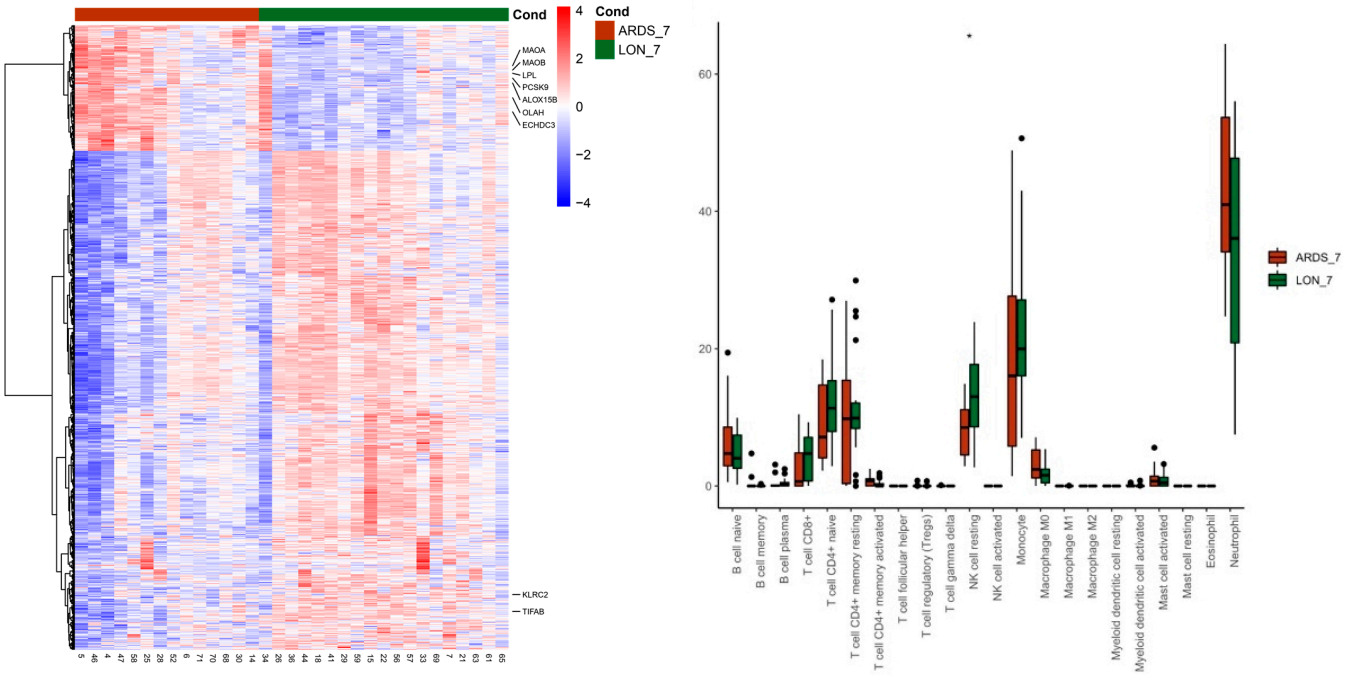

(**a**) (**b**)

Figure 3. (**a**) Heatmap depicting the gene expression of differentially expressed genes (DEGs) comparing COVID-19 patients with ARDS at any given time by day 7 of hospital admission (ARDS_7) and those who did not (LON_7). Each column in the figure represents a sample, and each row represents a gene. The colors in the graph indicate the magnitude of gene expression in the sample. Red indicates that the gene is highly expressed in the sample, and blue indicates that the gene expression is low. Genes included have an absolute log2 fold change of more than 1 and an adjusted *p* value of <0.05. Genes related to lipid control (e.g., OLAH, ECHDC3, PCSK9, LPL), oxidation (e.g., MAOA, MAOB), polyubiquitination, and metalloproteinases were upregulated in patients who had presented with ARDS by day 7. (**b**) COVID-19 patients with ARDS at any given time by day 7 of hospital admission (ARDS_7) and those who did not (LON_7) CIBERSORT deconvolution analysis and comparison. Significance is noted by: * for *p*-value < 0.05.

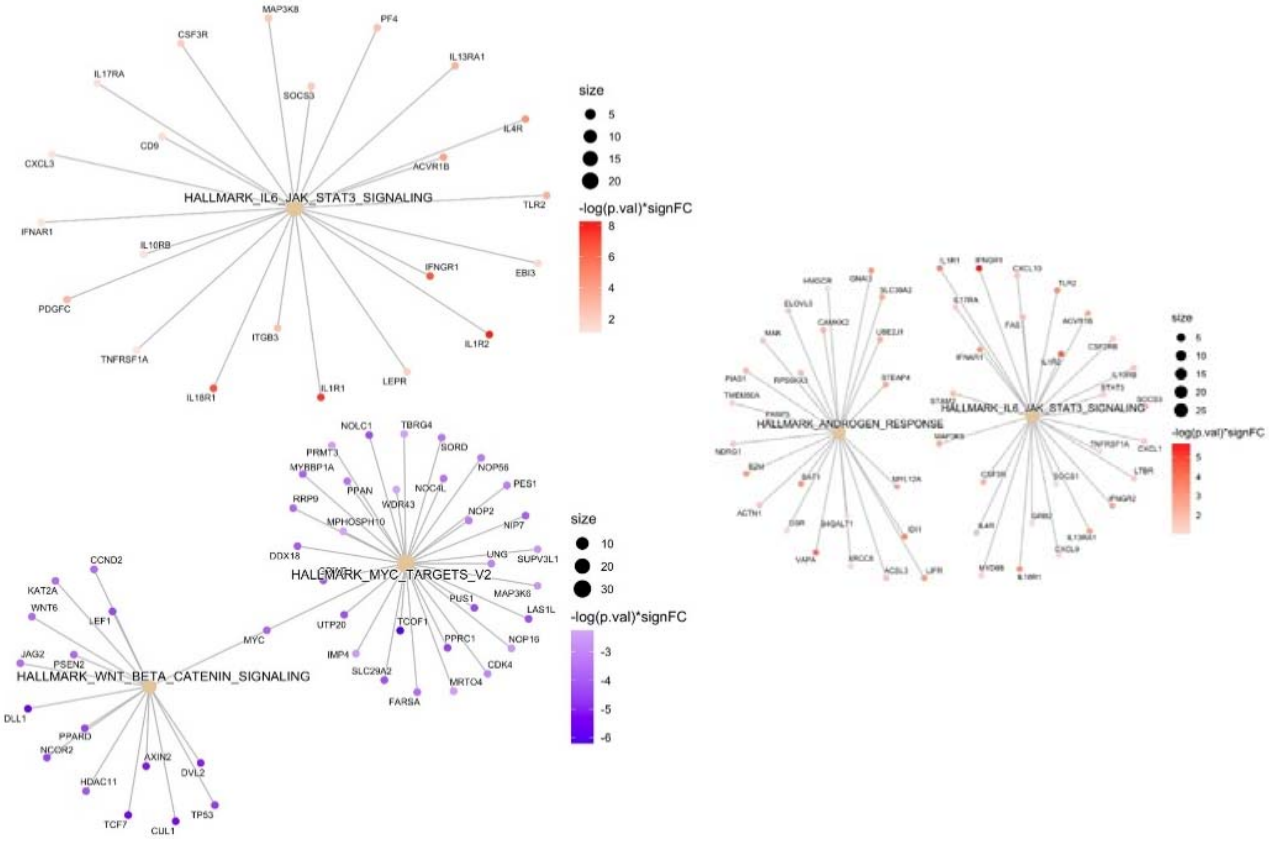

(**a**) (**b**)

Figure 4. (**a**) Network plot of enriched terms at baseline comparing COVID-19 patients with and without ARDS. Target genes of each of the pathways are shown in colored circles; enriched (upregulated) genes in ARDS patients are represented in red, while downregulated genes are represented in blue, with the color intensity corresponding to increasing statistical significance. Results showed enriched IL-6 and JAK STAT3 signaling in ARDS patients, while pathways related to Myc V2 targets and WNT/β-catenin signaling were downregulated. (**b**) A network plot of enriched terms comparing COVID-19 patients with ARDS at any given time by day 7 of hospital admission to those without showed enhanced expression of IL-6, JAK-STAT3 signaling, and genes related to androgen response in ARDS patients.

4. Discussion

The host-pathogen interaction in COVID-19 is complex and leads to heterogeneous clinical presentations. This means that there is a particular interest in understanding the underlying transcriptomic host response to SARS-CoV-2 infection. In this study, by stratifying patients according to oxygen requirement, we attempted to reduce the heterogeneity in the transcriptomic profiles observed in previous studies in hospitalized COVID-19 patients [5,21,22].

Our study adds to the evidence that a dysregulated inflammatory response [5,25,26] is the major driver behind severe pneumonia in SARS-CoV-2 infection. Patients with ARDS at baseline showed an upregulation of genes related to IL-6 and JAK-STAT3 signaling and neutrophil activation, as seen in other studies [5,17,19], a downregulation of T-cell activation, and a subsequent loss of $CD4^+$ T cells [5,20]. We also observed an increased expression of genes related to reactive oxygen species metabolism at baseline in ARDS, an increase that a previous study had reported at later stages of COVID-19 [5]. This discrepancy is likely explained by a delay in hospital admission in our cohort since many of the patients presented to the emergency department with already established ARDS. Our findings concur with other transcriptomic studies that have encountered an upregulation of genes related to protein polyubiquitination [19] and metalloproteinases [27] in later

stages of COVID-19 induced ARDS. On the other hand, in non-ARDS COVID-19 patients, we observed an increased expression of Wnt/β-catenin signaling and Myc V2 targets, a subgroup of genes regulated by Myc. Wnt/β-catenin pathway components modulate T-cell priming and infiltration [28] and negatively regulate NF-κB [29], thus enhancing viral tolerance and limiting inflammation. Myc, in addition to its well-known role in cancer, directly programs immune suppression by inhibiting macrophage activation [30] and preventing endothelial inflammation [31].

Our results further highlight the importance of long non-coding RNAs [32] and microRNAs [33] as emerging regulators in SARS-CoV-2 infection. Patients with ARDS at baseline presented higher levels of CLRN1-AS1, a lncRNA that inactivates the Wnt/β-catenin signaling pathway [34], and IRAIN, which enhances the formation of an intrachromosomal promoter loop of IGF1R [35]. Higher serum levels of IGF1R correlate with COVID-19 mortality [36]. On the other hand, the expression of the lncRNAs A2M-AS1, LEF-AS1, and RORA-AS-1 was significantly decreased in patients with ARDS. A2M-AS1 probably has an anti-proliferation and pro-apoptosis effect [37], and LEF1-AS1 and RORA-AS-1 have been found to be involved in T cell differentiation in COVID-19 patients [38]. The decreased levels of A2M-AS-1 in severe COVID-19 patients are in accordance with a previous study [39].

Our study has several limitations that should be acknowledged. Firstly, the majority of patients correspond to the first wave, in which lineage A predominated [40]. Subsequent SARS-CoV-2 variants and subvariants might have elicited different host responses. Secondly, the sample size was relatively small—only 60 patients, of whom only 19 developed ARDS. However, one of the strengths of the study is that the patients were followed up every day, which allowed an accurate assessment of their respiratory status. Additionally, our results are validated by the concordance of the cell composition of the samples studied with previous studies performed on single-cell RNA sequencing [41–44].

In conclusion, we found a dysregulated inflammatory response in COVID-19 ARDS patients with an increased expression of genes related to pro-inflammatory molecules and neutrophil and macrophage activation at admission, in addition to the loss of immune regulation. This led to a higher expression of genes related to reactive oxygen species, protein polyubiquitination, and metalloproteinases. These results should now be assessed in new studies with other variants (Omicron subvariants) and in populations with preexisting immunity.

Supplementary Materials: The following supporting information can be downloaded at: https://www.mdpi.com/article/10.3390/biomedicines11051348/s1, Case report form, IMIM's biosecurity measures.

Author Contributions: Conceptualization, A.R., C.G., L.N. and J.C.; Data curation, M.B.T., J.P.-B., A.F.-S., A.A.-T. and M.G.-S.; Formal analysis, M.B.T., J.P.-B., A.F.-S., A.A.-T., M.G.-S. and L.N.; Funding acquisition, J.C.; Investigation, A.R., G.A.-A., I.O. and C.G.; Methodology, A.R., A.F.-S., L.N. and J.C.; Project administration, J.C.; Resources, G.A.-A.; Software, M.B.T., J.P.-B. and L.N.; Supervision, L.N. and J.C.; Validation, M.B.T. and L.N.; Visualization, J.C.; Writing—original draft, A.R., L.N. and J.C.; Writing—review and editing, A.R., G.A.-A., J.P.-B., A.A.-T., I.O., C.G., L.N. and J.C. All authors have read and agreed to the published version of the manuscript.

Funding: A.R. received a predoctoral research grant from the Instituto de Salud Carlos III, the Spanish Ministry of Science, Innovation, and Universities, (PFIS grant FI18/00183). G.A.A. reports a predoctoral research grant from the 201808-10 project, funded by La Marató de TV3. This work was supported by the Instituto de Salud Carlos III, Subdirección General de Redes y Centros de Investigación Cooperativa, Ministerio de Economía, Industria y Competitividad, Centro de Investigación Biomédica en Red de Enfermedades Infecciosas (CIBERINFEC) [CB21/13/00009], Madrid, Spain. The project was funded through a grant from the Department de Salut of the Generalitat de Catalunya (20DPS005) and from the Instituto de Salud Carlos III (COV20_00121). We thank the CERCA Programme/Generalitat de Catalunya for their institutional support.

Institutional Review Board Statement: The study was approved by the Institutional Review Board at Bellvitge University Hospital (local reference number PR148/20).

Informed Consent Statement: Written informed consent has been obtained from the patients to publish this paper.

Data Availability Statement: The gene expression data set for this study will soon be made public in the Gene Expression Omnibus [36].

Acknowledgments: The authors would like to thank all the members of the Clinical Research Support Unit (HUB-IDIBELL), in particular Sebastià Videla Cés and the research nurses, for selflessly allowing the use of their facilities. We would also like to acknowledge the efforts of all healthcare workers who dedicated countless hours to provide care for COVID-19 patients during the successive waves of the COVID-19 pandemic.

Conflicts of Interest: The authors declare no conflict of interest. The funders had no role in the design of the study; in the collection, analyses, or interpretation of data; in the writing of the manuscript; or in the decision to publish the results.

References

1. Dos Santos Bezerra, R.; Valença, I.N.; de Cassia Ruy, P.; Ximenez, J.P.B.; da Silva Junior, W.A.; Covas, D.T.; da Silva Junior, W.A.; Covas, D.T.; Kashima, S.; Slavov, S.N. The novel coronavirus SARS-CoV-2: From a zoonotic infection to coronavirus disease 2019. *J. Med. Virol.* **2020**, *92*, 2607–2615. [CrossRef] [PubMed]
2. Johns Hopkins University Coronavirus Resource Center. COVID-19 Dashboard. Available online: https://coronavirus.jhu.edu/map.html (accessed on 10 March 2023).
3. Gandhi, R.T.; Lynch, J.B.; Del Rio, C. Mild or Moderate COVID-19. *N. Engl. J. Med.* **2020**, *383*, 1757–1766. [CrossRef] [PubMed]
4. Berlin, D.A.; Gulick, R.M.; Martinez, F.J. Severe COVID-19. *N. Engl. J. Med.* **2020**, *383*, 2451–2460. [CrossRef] [PubMed]
5. Bergamaschi, L.; Mescia, F.; Turner, L.; Hanson, A.L.; Kotagiri, P.; Dunmore, B.J.; Ruffieux, H.; De Sa, A.; Huhn, O.; Morgan, M.D.; et al. Longitudinal analysis reveals that delayed bystander CD8+ T cell activation and early immune pathology distinguish severe COVID-19 from mild disease. *Immunity* **2021**, *54*, 1257–1275.e8. [CrossRef]
6. Chan, Y.H.; Fong, S.W.; Poh, C.M.; Carissimo, G.; Yeo, N.K.; Amrun, S.N.; Goh, Y.S.; Lim, J.; Xu, W.; Chee, R.S.; et al. Asymptomatic COVID-19: Disease tolerance with efficient anti-viral immunity against SARS-CoV-2. *EMBO Mol. Med.* **2021**, *13*, e14045. [CrossRef]
7. Fang, F.C.; Benson, C.A.; Del Rio, C.; Edwards, K.M.; Fowler, V.G.; Fredricks, D.N.; Limaye, A.P.; Murray, B.E.; Naggie, S.; Pappas, P.G.; et al. COVID-19-Lessons Learned and Questions Remaining. *Clin. Infect Dis.* **2021**, *72*, 2225–2240. [CrossRef]
8. Fajnzylber, J.; Regan, J.; Coxen, K.; Corry, H.; Wong, C.; Rosenthal, A.; Worrall, D.; Giguel, F.; Piechocka-Trocha, A.; Atyeo, C.; et al. SARS-CoV-2 viral load is associated with increased disease severity and mortality. *Nat. Commun.* **2020**, *11*, 5493. [CrossRef]
9. Aydillo, T.; Rombauts, A.; Stadlbauer, D.; Aslam, S.; Abelenda-Alonso, G.; Escalera, A.; Amanat, F.; Jiang, K.; Krammer, F.; Carratala, J.; et al. Immunological imprinting of the antibody response in COVID-19 patients. *Nat. Commun.* **2021**, *12*, 3781. [CrossRef] [PubMed]
10. Bastard, P.; Rosen, L.B.; Zhang, Q.; Michailidis, E.; Hoffmann, H.; Zhang, Y.; Dorgham, K.; Philippot, Q.; Rosain, J.; Béziat, V.; et al. Autoantibodies against type I IFNs in patients with life-threatening COVID-19. *Science* **2020**, *370*, eabd4585. [CrossRef]
11. Severe COVID-19 GWAS Group; Ellinghaus, D.; Degenhardt, F.; Bujanda, L.; Buti, M.; Albillos, A.; Invernizzi, P.; Fernández, J.; Prati, D.; Baselli, G.; et al. Genomewide Association Study of Severe COVID-19 with Respiratory Failure. *N. Engl. J. Med.* **2020**, *383*, 1522–1534.
12. Blanco-Melo, D.; Nilsson-Payant, B.E.; Liu, W.C.; Uhl, S.; Hoagland, D.; Møller, R.; Jordan, T.X.; Oishi, K.; Panis, M.; Sachs, D.; et al. Imbalanced Host Response to SARS-CoV-2 Drives Development of COVID-19. *Cell.* **2020**, *181*, 1036–1045.e9. [CrossRef] [PubMed]
13. Suryamohan, K.; Diwanji, D.; Stawiski, E.W.; Gupta, R.; Miersch, S.; Lui, J.; Chen, C.; Jiang, Y.P.; Fellouse, F.A.; Sathirapongsasuti, J.F.; et al. Human ACE2 receptor polymorphisms and altered susceptibility to SARS-CoV-2. *Commun. Biol.* **2021**, *4*, 475. [CrossRef] [PubMed]
14. Zhang, Q.; Bastard, P.; Liu, Z.; Le Pen, J.; Moncada-Velez, M.; Chen, J.; Ogishi, M.; Sabli, I.K.D.; Hodeib, S.; Korol, C.; et al. Inborn errors of type I IFN immunity in patients with life-threatening COVID-19. *Science* **2020**, *370*, eabd4570. [CrossRef] [PubMed]
15. Ren, X.; Wen, W.; Fan, X.; Hou, W.; Su, B.; Cai, P.; Li, J.; Liu, Y.; Tang, F.; Zhang, F.; et al. COVID-19 immune features revealed by a large-scale single-cell transcriptome atlas. *Cell* **2021**, *184*, 1895–1913.e19. [CrossRef] [PubMed]
16. Bibert, S.; Guex, N.; Lourenco, J.; Brahier, T.; Papadimitriou-Olivgeris, M.; Damonti, L.; Manuel, O.; Liechti, R.; Götz, L.; Tschopp, J.; et al. Transcriptomic Signature Differences Between SARS-CoV-2 and Influenza Virus Infected Patients. *Front. Immunol.* **2021**, *12*, 666163. [CrossRef]
17. McClain, M.T.; Constantine, F.J.; Henao, R.; Liu, Y.; Tsalik, E.L.; Burke, T.W.; Steinbrink, J.M.; Petzold, E.; Nicholson, B.P.; Rolfe, R.; et al. Dysregulated transcriptional responses to SARS-CoV-2 in the periphery. *Nat. Commun.* **2021**, *12*, 1079. [CrossRef]
18. Kwan, P.K.W.; Cross, G.B.; Naftalin, C.M.; Ahidjo, B.A.; Mok, C.K.; Fanusi, F.; Permata Sari, I.; Chia, S.C.; Kumar, S.K.; Alagha, R.; et al. A blood RNA transcriptome signature for COVID-19. *BMC Med. Genomics.* **2021**, *14*, 155. [CrossRef]
19. Wu, P.; Chen, D.; Ding, W.; Wu, P.; Hou, H.; Bai, Y.; Zhou, Y.; Li, K.; Xiang, S.; Liu, P.; et al. The trans-omics landscape of COVID-19. *Nat. Commun.* **2021**, *12*, 4543. [CrossRef]

20. Russick, J.; Foy, P.E.; Josseaume, N.; Meylan, M.; Hamouda, N.B.; Kirilovsky, A.; Sissy, C.E.; Tartour, E.; Smadja, D.M.; Karras, A.; et al. Immune Signature Linked to COVID-19 Severity: A SARS-Score for Personalized Medicine. *Front. Immunol.* **2021**, *12*, 701273. [CrossRef]
21. Prokop, J.W.; Hartog, N.L.; Chesla, D.; Faber, W.; Love, C.P.; Karam, R.; Abualkheir, N.; Feldmann, B.; Teng, L.; McBride, T.; et al. High-Density Blood Transcriptomics Reveals Precision Immune Signatures of SARS-CoV-2 Infection in Hospitalized Individuals. *Front. Immunol.* **2021**, *12*, 694243. [CrossRef]
22. Aschenbrenner, A.C.; Mouktaroudi, M.; Krämer, B.; Oestreich, M.; Antonakos, N.; Nuesch-Germano, M.; Gkizeli, K.; Bonaguro, L.; Reusch, N.; Baßler, K.; et al. Disease severity-specific neutrophil signatures in blood transcriptomes stratify COVID-19 patients. *Genome Med.* **2021**, *13*, 7. [CrossRef]
23. ARDS Definition Task Force; Ranieri, V.M.; Rubenfeld, G.D.; Thompson, B.T.; Ferguson, N.D.; Caldwell, E.; Fan, E.; Camporota, L.; Slutsky, A.S. Acute respiratory distress syndrome: The Berlin Definition. *JAMA* **2012**, *307*, 2526–2533. [PubMed]
24. Matthay, M.A.; Thompson, B.T.; Ware, L.B. The Berlin definition of acute respiratory distress syndrome: Should patients receiving high-flow nasal oxygen be included? *Lancet Respir. Med* **2021**, *9*, 933–936. [CrossRef]
25. Arunachalam, P.S.; Wimmers, F.; Mok, C.K.P.; Perera, R.A.P.M.; Scott, M.; Hagan, T.; Sigal, N.; Feng, Y.; Bristow, L.; Tak-Yin Tsang, O.; et al. Systems biological assessment of immunity to mild versus severe COVID-19 infection in humans. *Science* **2020**, *369*, 1210–1220. [CrossRef]
26. Merad, M.; Martin, J.C. Pathological inflammation in patients with COVID-19: A key role for monocytes and macrophages. *Nat. Rev. Immunol.* **2020**, *20*, 355–362. [CrossRef]
27. Gelzo, M.; Cacciapuoti, S.; Pinchera, B.; De Rosa, A.; Cernera, G.; Scialò, F.; Comegna, M.; Mormile, M.; Fabbrocini, G.; Parrella, R.; et al. Matrix metalloproteinases (MMP) 3 and 9 as biomarkers of severity in COVID-19 patients. *Sci. Rep.* **2022**, *12*, 1212. [CrossRef]
28. Spranger, S.; Dai, D.; Horton, B.; Gajewski, T.F. Tumor-Residing Batf3 Dendritic Cells Are Required for Effector T Cell Trafficking and Adoptive T Cell Therapy. *Cancer Cell.* **2017**, *31*, 711–723.e4. [CrossRef] [PubMed]
29. Ma, B.; Hottiger, M.O. Crosstalk between Wnt/β-Catenin and NF-κB Signaling Pathway during Inflammation. *Front. Immunol.* **2016**, *7*, 378. [CrossRef] [PubMed]
30. Pello, O.M.; De Pizzol, M.; Mirolo, M.; Soucek, L.; Zammataro, L.; Amabile, A.; Doni, A.; Nebuloni, M.; Swigart, L.B.; Evan, G.I.; et al. Role of c-MYC in alternative activation of human macrophages and tumor-associated macrophage biology. *Blood* **2012**, *119*, 411–421. [CrossRef]
31. Florea, V.; Bhagavatula, N.; Simovic, G.; Macedo, F.Y.; Fock, R.A.; Rodrigues, C.O. c-Myc is essential to prevent endothelial pro-inflammatory senescent phenotype. *PLoS ONE* **2013**, *8*, e73146. [CrossRef]
32. Yang, Q.; Lin, F.; Wang, Y.; Zeng, M.; Luo, M. Long Noncoding RNAs as Emerging Regulators of COVID-19. *Front. Immunol.* **2021**, *12*, 700184. [CrossRef] [PubMed]
33. Jankovic, M.; Nikolic, D.; Novakovic, I.; Petrovic, B.; Lackovic, M.; Santric-Milicevic, M. miRNAs as a Potential Biomarker in the COVID-19 Infection and Complications Course, Severity, and Outcome. *Diagnostics* **2023**, *13*, 1091. [CrossRef] [PubMed]
34. Wang, C.; Tan, C.; Wen, Y.; Zhang, D.; Li, G.; Chang, L.; Su, J.; Wang, X. FOXP1-induced lncRNA CLRN1-AS1 acts as a tumor suppressor in pituitary prolactinoma by repressing the autophagy via inactivating Wnt/β-catenin signaling pathway. *Cell Death Dis.* **2019**, *10*, 499. [CrossRef] [PubMed]
35. Sun, J.; Li, W.; Sun, Y.; Yu, D.; Wen, X.; Wang, H.; Cui, J.; Wang, G.; Hoffman, A.R.; Hu, J.F. A novel antisense long noncoding RNA within the IGF1R gene locus is imprinted in hematopoietic malignancies. *Nucleic Acids Res.* **2014**, *42*, 9588–9601. [CrossRef]
36. Fraser, D.D.; Cepinskas, G.; Patterson, E.K.; Slessarev, M.; Martin, C.; Daley, M.; Patel, M.A.; Miller, M.R.; O'Gorman, D.B.; Gill, S.E.; et al. Novel Outcome Biomarkers Identified with Targeted Proteomic Analyses of Plasma from Critically Ill Coronavirus Disease 2019 Patients. *Crit. Care Explor.* **2020**, *2*, e0189. [CrossRef]
37. Song, X.L.; Zhang, F.F.; Wang, W.J.; Li, X.N.; Dang, Y.; Li, Y.X.; Yang, Q.; Shi, M.J.; Qi, X.Y. LncRNA A2M-AS1 lessens the injury of cardiomyocytes caused by hypoxia and reoxygenation via regulating IL1R2. *Genes Genom.* **2020**, *42*, 1431–1441. [CrossRef]
38. Zheng, H.Y.; Xu, M.; Yang, C.X.; Tian, R.R.; Zhang, M.; Li, J.J.; Wang, X.C.; Ding, Z.L.; Li, G.M.; Li, X.L.; et al. Longitudinal transcriptome analyses show robust T cell immunity during recovery from COVID-19. *Signal Transduct Target Ther.* **2020**, *5*, 294. [CrossRef]
39. Badr, E.A.E.; El Sayed, I.E.; Gabber, M.K.R.; Ghobashy, E.A.E.; Al-Sehemi, A.G.; Algarni, H.; Elghobashy, Y.A. Are Antisense Long Non-Coding RNA Related to COVID-19? *Biomedicines* **2022**, *10*, 2770. [CrossRef]
40. López, M.G.; Chiner-Oms, Á.; García de Viedma, D.; Rodriguez, P.; Bracho, M.A.; Cancino-Muñoz, I.; D'Auria, G.; de Marco, G.; García-González, N.; Goig, G.A.; et al. The first wave of the COVID-19 epidemic in Spain was associated with early introductions and fast spread of a dominating genetic variant. *Nat. Genet.* **2021**, *53*, 1405–1414. [CrossRef]
41. Bost, P.; De Sanctis, F.; Canè, S.; Ugel, S.; Donadello, K.; Castellucci, M.; Eyal, D.; Fiore, A.; Anselmi, C.; Barouni, R.M.; et al. Deciphering the state of immune silence in fatal COVID-19 patients. *Nat. Commun.* **2021**, *12*, 1428. [CrossRef]
42. Bernardes, J.P.; Mishra, N.; Tran, F.; Bahmer, T.; Best, L.; Blasé, J.I.; Bordoni, D.; Franzenburg, J.; Geisen, U.; Josephs-Spaulding, J.; et al. Longitudinal Multi-omics Analyses Identify Responses of Megakaryocytes, Erythroid Cells, and Plasmablasts as Hallmarks of Severe COVID-19. *Immunity* **2020**, *53*, 1296–1314.e9. [CrossRef] [PubMed]

43. Le Bert, N.; Clapham, H.E.; Tan, A.T.; Chia, W.N.; Tham, C.Y.L.; Lim, J.M.; Kunasegaran, K.; Tan, L.W.L.; Dutertre, C.A.; Shankar, N.; et al. Highly functional virus-specific cellular immune response in asymptomatic SARS-CoV-2 infection. *J. Exp. Med.* **2021**, *218*, e20202617. [CrossRef] [PubMed]
44. Edgar, R.; Domrachev, M.; Lash, A.E. Gene Expression Omnibus: NCBI gene expression and hybridization array data repository. *Nucleic Acids Res.* **2002**, *30*, 207–210. [CrossRef] [PubMed]

Study 4

Immunological imprinting of the antibody response in COVID-19 patients.

Aydillo, T., **Rombauts, A.**, Stadlbauer, D., Aslam, S., Abelenda-Alonso, G., Escalera, A., Amanat, F., Jiang, K., Krammer, F.✉, Carratala, J.✉, & García-Sastre, A.✉ (2021).

Nature communications, 2021, 12(1), 3781

Impact factor: 16.6 (1st decile)

nature COMMUNICATIONS

ARTICLE

https://doi.org/10.1038/s41467-021-23977-1 OPEN

Immunological imprinting of the antibody response in COVID-19 patients

Teresa Aydillo[1,2], Alexander Rombauts[3,4], Daniel Stadlbauer[1], Sadaf Aslam[1,2], Gabriela Abelenda-Alonso[3,4], Alba Escalera[1,2,5], Fatima Amanat[1,5], Kaijun Jiang[1], Florian Krammer[1,6✉], Jordi Carratala[3,4✉] & Adolfo García-Sastre[1,2,7,8✉]

In addition to severe acute respiratory syndrome coronavirus 2 (SARS-CoV-2), humans are also susceptible to six other coronaviruses, for which consecutive exposures to antigenically related and divergent seasonal coronaviruses are frequent. Despite the prevalence of COVID-19 pandemic and ongoing research, the nature of the antibody response against severe acute respiratory syndrome coronavirus 2 (SARS-CoV-2) is unclear. Here we longitudinally profile the early humoral immune response against SARS-CoV-2 in hospitalized coronavirus disease 2019 (COVID-19) patients and quantify levels of pre-existing immunity to OC43, HKU1 and 229E seasonal coronaviruses, and find a strong back-boosting effect to conserved but not variable regions of OC43 and HKU1 betacoronaviruses spike protein. However, such antibody memory boost to human coronaviruses negatively correlates with the induction of IgG and IgM against SARS-CoV-2 spike and nucleocapsid protein. Our findings thus provide evidence of immunological imprinting by previous seasonal coronavirus infections that can potentially modulate the antibody profile to SARS-CoV-2 infection.

[1] Department of Microbiology, Icahn School of Medicine at Mount Sinai, New York, NY, USA. [2] Global Health and Emerging Pathogens Institute, Icahn School of Medicine at Mount Sinai, New York, NY, USA. [3] Department of Infectious Diseases, Bellvitge University Hospital, Bellvitge Biomedical Research Institute (IDIBELL), University of Barcelona, L'Hospitalet de Llobregat, Barcelona, Spain. [4] Spanish Network for Research on Infectious Diseases (REIPI, RD16/0016, Carlos III Health Institute, Madrid, Spain. [5] Graduate School of Biomedical Sciences, Icahn School of Medicine at Mount Sinai, New York, NY, USA. [6] Department of Pathology, Icahn School of Medicine at Mount Sinai, New York, NY, USA. [7] Division of Infectious Disease, Department of Medicine, Icahn School of Medicine at Mount Sinai, New York, NY, USA. [8] The Tisch Cancer Institute, Icahn School of Medicine at Mount Sinai, New York, NY, USA. ✉email: florian.krammer@mssm.edu; jcarratala@bellvitgehospital.cat; adolfo.garcia-sastre@mssm.edu

Since January 2020, the Severe Acute Respiratory Syndrome Coronavirus 2 (SARS-CoV-2) virus has been spreading globally causing the first documented pandemic of coronavirus in history[1,2]. SARS-CoV-2 is a betacoronavirus that belongs to a large family of viruses capable to infect both mammals and birds. Humans are susceptible to at least other six viruses from the genus alpha and betacoronavirus[3]. All of them typically cause respiratory illness but to a different extent. While SARS-CoV-1 and Middle East Respiratory Syndrome Coronavirus, are highly pathogenic betacoronaviruses that have caused zoonotic outbreaks in humans in the last 20 years[4,5], the alphacoronaviruses 229E and NL63, and the betacoronaviruses OC43 and HKU1, frequently cause mild upper respiratory tract disease and have been circulating in humans as seasonal viruses[3,6]. The ongoing pandemic of coronavirus disease 2019 (COVID-19), the disease caused by SARS-CoV-2, is still challenging healthcare systems and the research community. SARS-CoV-2 can cause a different range of clinical manifestations, from asymptomatic to severe respiratory syndrome. However, a high percentage of severe cases have been reported and estimated numbers of patients that succumbed to COVID-19 disease are more than 3 million according to WHO as May 2021[2,7] (https://covid19.who.int/). Many vaccine candidates are being tested in clinical trials and several have already been authorized for use in the population[8–10]. However, we are still in an early phase and studies regarding vaccine effectiveness in special populations are needed. Similarly, longevity of the humoral immunity after infection and vaccination is still an ongoing debate.

One of the main targets of antibody responses to coronaviruses is the spike, the surface glycoprotein that mediates attachment to the host receptor and membrane fusion. Two subunits can be identified, the S1 subunit containing the receptor-binding domain (RBD), essential for binding to the entry receptor[11–13]; and the S2 subunit, responsible of virus cell fusion[14]. Different human coronaviruses use different domains to bind their human receptors and to mediate cell entry. While the human endemic betacoronaviruses OC43 and HKU1, bind to sialic acids, 229E alphacoronavirus uses human aminopeptidase N as a cellular determinant for susceptibility[15,16]. NL63, SARS-CoV, and SARS-CoV-2, in contrast, need direct interaction with the angiotensin-converting enzyme 2 to infect cells[13,17]. Therefore, antibodies directed against the RBD of human coronaviruses are capable to neutralize the virus[15,18,19] and no cross-reactive neutralizing antibodies among seasonal human coronavirus are expected due to the high specificity of this process and the sequence divergence between the RBD of these viruses[20–23]. In addition, the more cross-reactive viral nucleoprotein (N) has also shown to be immunogenic and induce antibodies in COVID-19 patients. However, in contrast to RBD antibodies, N antibodies are not able to neutralize the virus in tissue culture[11,23,24].

Several studies have demonstrated that T cells can recognize homologous epitopes shared between different endemic coronaviruses[25–30]. However, serum cross-reactivity between conserved epitopes from SARS-CoV-2 and seasonal human coronaviruses is still under investigation[23,31–33] and the role of pre-existing humoral immunity and immunodominance for B cell responses needs to be addressed. Immune imprinting (or original antigenic sin), refers to the preference of the immune system to recall existing memory cells, rather than stimulating de novo responses when encountering a novel but closely related antigen[34]. This has been shown for viruses like influenza virus, in which subsequent infections with antigenically related strains produce a recall response or 'back-boosting' that generates an increase in antibody titers toward epitopes shared between the current and the historic strains encountered earlier in life[35–38]. Boost of cross-reactive antibody responses can also occur for viruses like dengue virus (DENV) upon secondary infections with a different serotype[39,40]. In this case, specific titers to the original DENV were higher than those specific to the second infecting DENV upon secondary DENV infection[41,42].

Here, we profile the antibody responses of a longitudinal cohort of hospitalized patients with COVID-19. We characterize de novo antibody responses against SARS-CoV-2 and pre-existing immunity against selected endemic coronavirus being targeted by the humoral immune system to investigate the role of immunological imprinting on COVID-19 patients' antibody response. We show that the induction of antibodies against conserved epitopes of seasonal coronaviruses may hinder the induction of specific antibodies toward divergent SARS-CoV-2 antigens. This study provides a dynamic characterization of the co-evolving nature of antibody responses to human coronaviruses, both seasonal and pandemic, and contributes to a better understanding of cross-reactive antibody responses and B cells immunodominance against human coronaviruses.

Results

The BACO cohort. Thirty-seven COVID-19 patients were recruited at the University Hospital of Bellvitge during the first wave of SARS-CoV-2 in Barcelona (Spain) from March 26, 2020 to May 28, 2020. Mean age was 65 years and 67% were male. Chronic comorbidities were frequent among COVID-19 patients (25, 67.7%). In particular, 16 (43.2%) of patients were obese (body mass index >30) at the time of hospitalization. A high percentage of patients had respiratory symptoms, such as coughing (26, 70.3%) and dyspnea (14, 37.8%), whereas diarrhea was also present in seven (18.9%) of the patients. While no remdesivir was available, lopinavir/ritonavir was used for 17 (45.9%) patients. All patients, except one (36, 97.3%), developed SARS-CoV-2 viral pneumonia and four (10.8%) required intensive care unit admission. Five (13.5%) patients died. Demographics, clinical characteristics, interventions, such as drug therapy and outcomes are detailed in Table 1.

Acute blood samples were collected longitudinally in the BACO cohort at the recruitment upon hospital admission, and at days 3 and 7 in 33 (89.1%) and 22 (59.4%) patients, respectively. Mean time from symptom onset to inclusion in the study was 7 days (range 2–14). Most of the patients (25, 67.5%) were recruited within the first week of symptom onset, whereas 12 (32.4%) patients had longer periods until hospitalization. COVID-19 survivors were followed up in the convalescence period and 28 out of 32 survivors (87.5%) had another blood draw after hospital discharge with a mean time of 46 days post recruitment (range, 30–56 days).

COVID-19 patients developed anti-SARS-CoV-2 antibodies linked to back-boosting of antibodies against S2 domain of betacoronaviruses. To profile the early antibody response in COVID-19 patients, we investigated the levels of neutralizing antibodies against authentic SARS-CoV-2 virus and IgG/IgM ELISAs against multiple antigens including the full-length spike (S), the spike RBD S and the N of SARS-CoV-2. IgG and IgM levels were quantified as area under the curve (AUC) by plotting normalized optical density (OD) values against the reciprocal serum sample dilutions for ELISAs (Supplementary Fig. 1A). To improve visualization, the longitudinal antibody profile of each individual patient together with the geometric mean titer (GMT, CI 95%) at each time point is shown for AUC ELISA and neutralizing titers in Fig. 1A and Supplementary Table 1. All patients developed detectable levels of neutralizing antibodies at day 7 post recruitment while levels remained stable during the convalescent phase, except for two survivors. Similar responses were

Table 1 Demographics and clinical characteristics of the BACO cohort.

	Total ($n = 37$)
Demographics and comorbidities	
Age (mean, IQR)	67 (25)
Men (*n*, %)	25 (67.6)
Comorbidities (*n*, %)	25 (67.7)
Lung disease (*n*, %)	7 (18.9)
Diabetes mellitus	7 (18.9)
Heart disease (*n*, %)	5 (13.5)
Kidney disease (*n*, %)	3 (8.1)
Obesity (*n*, %)	16 (43.2)
SOTR (*n*, %)	1 (2.7)
Signs and symptoms	
Days from symptom onset to enrollment (mean, range)	7.19 (2–14)
Days of fever (mean, range)	4.68 (0–12)
Throat ache (*n*, %)	4 (10.8)
Cough (*n*, %)	26 (70.3)
Dyspnea (*n*, %)	14 (37.8)
Diarrhea (*n*, %)	7 (18.9)
Sp02 < 94% (*n*, %)	14 (37.8)
Drug therapy	
Hydroxychloroquine (*n*, %)	36 (97.3)
Lopinavir/Ritonavir (*n*, %)	17 (45.9)
Tocilizumab (*n*, %)	10 (27)
Antibiotics (*n*, %)	19 (51.4)
Corticosteroids (*n*, %)	18 (48.6)
Outcomes	
Pneumonia (*n*, %)	36 (97.3)
ICU (*n*, %)	4 (10.8)
Days from hospitalization to ICU (mean, range)	9.5 (5–12)
Days in ICU (mean, range)	15 (15–22)
Non-mechanical ventilation (*n*, %)	11 (29.7)
Mechanical ventilation (*n*, %)	2 (5.4)
Nosocomial co-infection (*n*, %)	2 (5.4)
Mortality (*n*, %)	5 (13.5)
Days of hospitalization (mean, range)	11.2 (2–47)

SOTR solid organ transplant recipient, *SpO2 < 94%* pulse oximetry below 94%, *ICU* intensive care unit.

found by ELISA, although higher levels of antibodies against IgG S compared to IgG RBD were present. When comparing to the induction of anti-spike antibodies, the IgG isotype reached higher titers than the IgM isotype, whereas anti-N protein IgG had similar induction than the anti-S IgG. We then determined fold increase of antibody titers from baseline levels. Overall, all patients had a high induction of SARS-CoV-2 S and RBD antibodies at day 7 post recruitment. IgG titers against the S and RBD of SARS-CoV-2 remained stable at the convalescent time point with similar levels compared to peak titers at day 7. By contrast, IgM against the S, IgG against N and neutralizing titers against authentic SARS-CoV-2 virus decreased to levels resembling those at day 3. Geometric mean fold rise (GMFR) and adjusted *p* values on pairwise comparisons after related samples Friedman's two-way ANOVA at each time points are shown Fig. 1B. We next tested the correlation between neutralization activity and levels of anti-SARS-CoV-2 antibodies. Scatterplot matrices shown in Supplementary Fig. 2 indicate that the antibodies detected against SARS-CoV-2 antigens correlated well with neutralizing activity, with Pearson R^2 ranging from 69 to 81% in the case of IgG against the RBD S of SARS-CoV-2.

The S gene of SARS-CoV-2 is highly divergent from human seasonal coronaviruses (hCoV). Infection with endemic hCoV in humans happens frequently[3,6,43], causing mild respiratory disease. Multiple sequence alignment (MSA) between the S of SARS-CoV-2 and selected seasonal coronaviruses showed amino acid identity ranging from 28% for alphacoronaviruses (229E) and 32.5% and 33% for betacoronaviruses (OC43 and HKU1, respectively). To identify conserved amino acid regions, we also estimated the relative conservation scores of the S protein of SARS-CoV-2 using the chain A of the SARS-CoV-2 spike protein in the closed state as a reference. MSA and relative amino acid conservation was determined by using the ConSurf server. Figure 2A shows the conservation score for each amino acid position and projected on the S protein structure. Evolutionary conservation analysis showed that the S2 subunit had the highest degree of identity among the sequences tested. Given the high probability of previous exposure to seasonal coronaviruses in the BACO cohort, we screened levels of antibodies against the spike of alphacoronavirus 229E and betacoronaviruses HKU1, OC43. Antigens tested included full-length S protein for all three endemic coronaviruses together with the less conserved HKU1 S1 subunit (Supplementary Fig. 3A). Remarkably, COVID-19 patients exhibited an outstanding back-boosting of antibodies to the beta- CoV spikes tested, with similar a longitudinal profile as the one observed for the SARS-CoV-2 spike and for SARS-CoV-2 neutralizing titers (Fig. 3A). The back-boost was higher at day 7, with a GMFR from baseline levels of 3.8 and 4 for HKU1 S and OC43 S, respectively (Fig. 3B, Supplementary Table 1). While IgG levels against 229E were already high at baseline, no increase was detected at any time point during the follow-up on patients with COVID-19. Interesting, no back-boosting was found when we tested antibody titers against the more divergent S1 subunit of HKU1, pointing to an increase of immune responses towards conserved epitopes of the S2 subunit of the spike protein of beta-human coronaviruses. Similar to influenza viruses, HKU1 and OC43 use sialic acids as canonical receptor to infect human cells[16]. This is mediated by an additional surface protein in these viruses with hemagglutination (HA) activity (hemagglutinin-esterase (HE) protein). No increase in OC43 HA inhibitory antibodies was found in COVID-19 patients, consistent with the lack of HE in SARS-CoV-2. Longitudinal profile and fold increase antibody titers to selected seasonal human coronaviruses antigens are shown in Fig. 3 and Supplementary Table 1.

To test whether the antibody response characterized in the BACO cohort correlated with disease trajectory, we grouped patients according to disease phenotype. Patients were assigned as mild/moderate ($N = 26$, 70.3%) or severe/severe end-of organ disease (EOD, $N = 11$, 29.7%) based on a previously described severity scale[44]. No statistically significant differences were found between humoral immune response in patients with mild and severe/severe EOD disease, but the latter tended to have a delay in the antibody response towards SARS-CoV-2 antigens compared to moderate cases (Fig. 4A). Patients with severe disease had lower Ct values, and therefore higher viral loads (Fig. 4B). Besides, a positive correlation was found between anti- SARS-CoV2 antibodies and mean Ct values in paired nasopharyngeal swabs of COVID-19 patients acknowledging an interplay between antibodies and virus control and disease severity in COVID-19 patients. However, no correlation was found between antibodies against seasonal coronaviruses and viral loads in the BACO Cohort (Fig. 4C).

Immunological imprinting results in a bias in the induction of antibodies to conserved vs. variable regions of the SARS-COV-2 spike. Given the strong back-boosting observed to the conserved epitopes of the S domains of human betacoronaviruses in patients with COVID-19, we next investigated whether a strong back-boosting might reduce the induction of de novo humoral immune responses against specific epitopes of the spike of SARS-CoV-2 defined as fold induction over baseline levels.

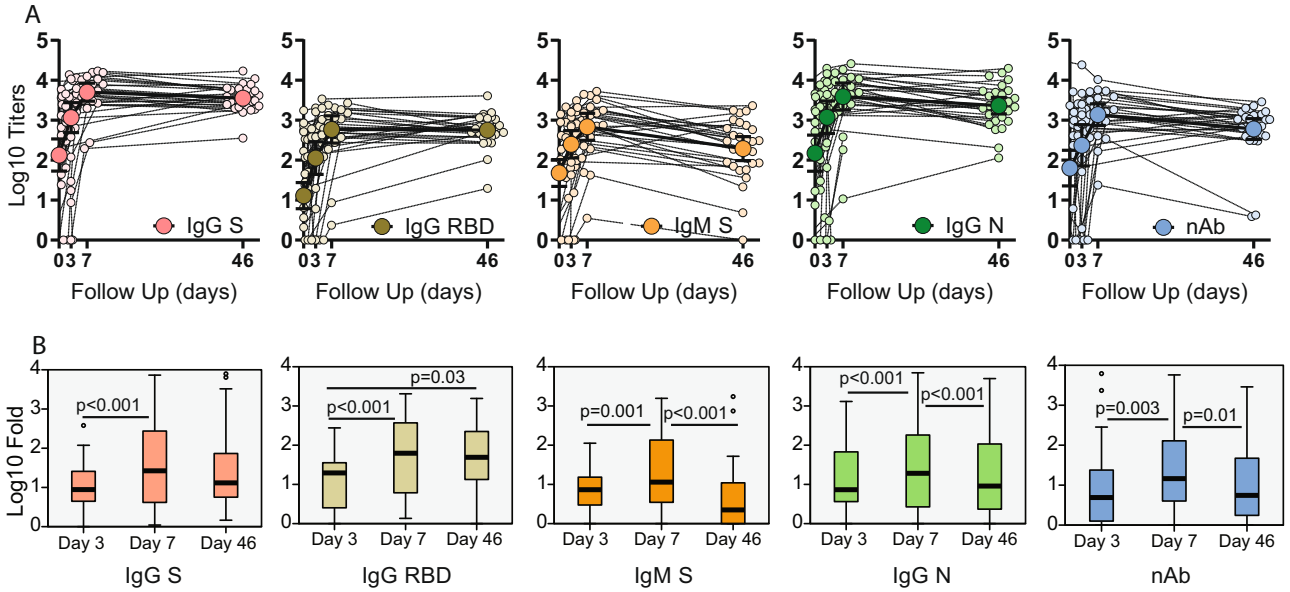

Fig. 1 Longitudinal antibody response to SARS-CoV-2 antigens. Serum from hospitalized COVID-19 patients was analyzed at baseline, at hospital recruitment and days 3 and 7. A subsequent sample was collected in the convalescence period in the COVID-19 survivors with mean time of 46 days. **A** Longitudinal profile of antibodies against SARS-CoV-2. Antibody titer was quantified as area under the curve (AUC) after serial serum dilution for each sample (Supplementary Fig. 1). Calculated AUC at each time is shown to quantify changes over time for each individual (small dots) against immunoglobulin G (IgG) spike, IgG receptor-binding domain (RBD), immunoglobulin M (IgM) spike and IgG nucleocapsid (N); and neutralizing activity (nAb) as inhibitory concentration 50% (IC50%). Geometric mean titer (GMT, big dots) and confidence interval (CI 95%) are also shown. **B** Boxplot diagram of geometric mean fold rise (GMFR) antibody titers against SARS-CoV-2 at the same time points: IgG spike, IgG RBD, IgM spike and IgG NP; and neutralizing activity (nAb). Related-samples Friedman's two-way ANOVA was performed. Significant adjusted *p* values after pairwise comparisons are shown for each comparison. Black bar indicates GMFR values, box indicates IQR (Q1–Q3), lines indicate minimum and maximum. Outliers from the observed distribution are shown. Total $n = 116$ biologically independent serum samples (day 0 = 37, day 3 = 29, day 7 = 22, day 46 = 28). $n = 116$ biological samples examined against four different SARS-CoV-2 substrates for ELISA assays; ELISAs for each substrate were run once each. $N = 116$ serum samples examined over two independent experiments for neutralization assays.

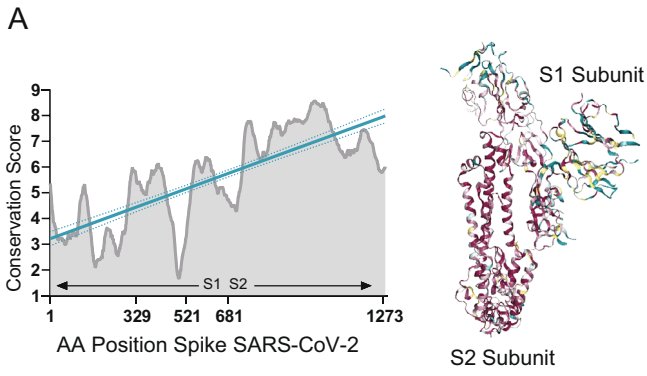

Fig. 2 Conservation of SARS-CoV-2 S protein. A Multiple sequence alignment was generated by the ConSurf algorithm (https://consurf.tau.ac.il) using the chain A of the SARS-CoV-2 spike protein in the closed state (PDB ID 6VXX) as a reference. Amino acid conservation scores were classified into nine levels. Structure of the SARS-CoV-2 S protein (chain A) with amino acid residues colored according to conservation on a scale from green (1, most variable) to dark purple (9, most conserved) is also shown.

To test this hypothesis, we examined the relationship between pre-exposure to HKU1, OC43, and 229E viruses and the induction of SARS-CoV-2 S, RBD, and N antibodies in our cohort, and determined Pearson correlation coefficients between IgG levels at baseline against seasonal human coronaviruses and the fold induction of SARS-CoV-2 antigens at days 3, 7 and convalescence. Pearson correlation matrices according to seasonal coronavirus subtype are shown in Fig. 5. Striking differences were found according to virus types. While pre-existing IgG levels against HKU1 and OC43 spike protein negatively impacted the induction of de novo IgG and IgM against SARS-CoV-2 antigens, including S and N protein (Fig. 5A, B), no influence was found when testing the relationship between pre-existing anti-229E spike IgG levels (Fig. 5D). Moreover, correlations became stronger over time, and while this correlation was lower at day 3, a stronger correlation was found at day 7, and convalescence time points in the surviving patients. Besides, a comparable performance was observed when testing the subsequent induction of the IgG antibodies against the variable RBD domain of SARS-CoV-2 spike. This result suggests that pre-existing immunity against seasonal betacoronaviruses biases the humoral response towards betacoronaviruses cross-reactive antibodies in detriment of antibodies against the more divergent and antigenically unique domains of the S of SARS-CoV-2, such as those of the RBD domain (Fig. 5A, B). This was also evidenced by the lack of impact of pre-existing HKU1 S1 IgG levels (S1 is divergent and harbors the RBD) on specific SARS-CoV-2 antibodies induction (Fig. 5C). Thus, only the levels of antibodies against cross-reactive epitopes of human betacoronaviruses had an effect on the subsequent antibody response to SARS-CoV-2 unique spike antigens. Because neutralization activity has been linked to in vivo protection after challenge with SARS-CoV-2[45], we also tested if immune imprinting could hinder the induction of neutralizing antibodies against SARS-CoV-2. No significant correlation was found. However, linear regression analysis determined a standardized beta coefficient of −0.32 (95% CI −0.35–0.05, $p = 0.13$) and −0.31 (95% CI −0.28–0.02, $p = 0.1$) at day 7 and convalescence time points, respectively, for pre-existing HKU1 spike antibody levels approximating a negative impact of

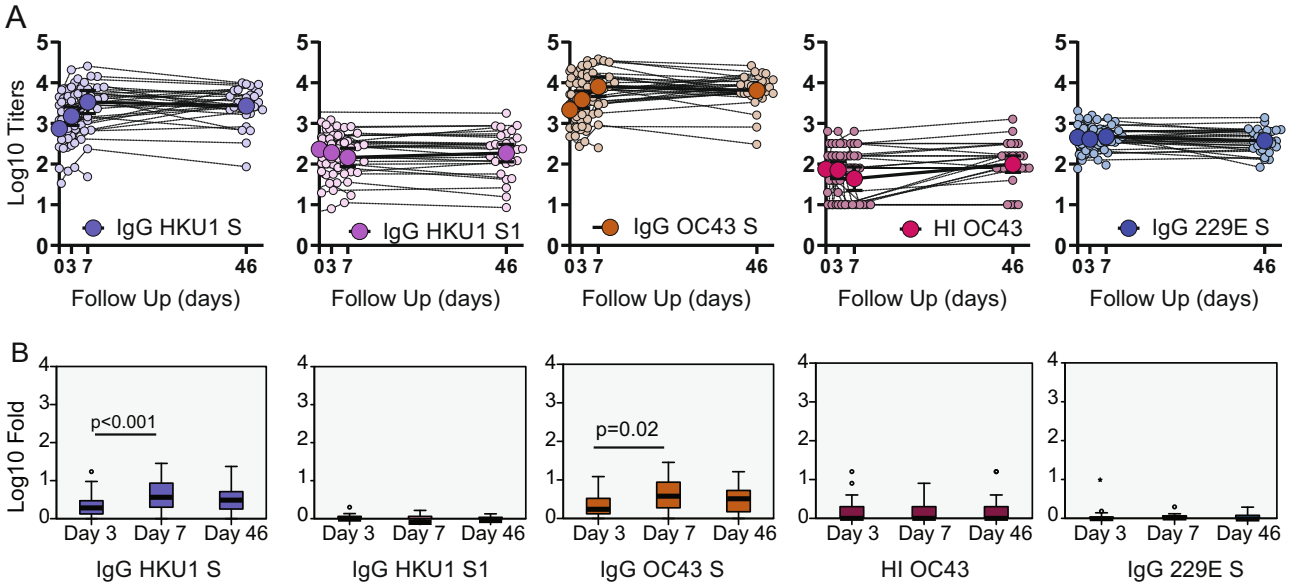

Fig. 3 Longitudinal antibody response to selected seasonal human coronaviruses antigens. Serum from hospitalized COVID-19 patients was analyzed at baseline, at hospital recruitment and days 3 and 7. A subsequent sample was collected in the convalescence period in the COVID-19 survivors with mean time of 46 days. **A** Longitudinal profile of antibodies against betacoronavirus (HKU1 and OC43) and alphacoronavirus (229E) antigens. Antibody titer was quantified as area under the curve (AUC) after serial serum dilution for each sample (Supplementary Fig. 1). Calculated AUC at each time is shown to quantify changes over time for each individual (small dots) against immunoglobulin G (IgG) HKU1 spike, IgG HKU1 S1, IgG OC43 spike and IgG 229E. Geometric mean titer (GMT, big dots) and confidence interval (CI 95%) are also shown. Hemagglutination inhibition (HI) assay were also performed for OC43 and GMT of end point titers are shown at each time point. **B** Boxplot diagram of geometric mean fold rise (GMFR) antibody titers against seasonal coronaviruses at the same time points: IgG HKU1 spike, IgG HKU1 S1, IgG OC43 spike and IgG 229E; and HI titer. Related-samples Friedman's two-way ANOVA was performed. Significant adjusted *p* values after pairwise comparisons are shown for each comparison. Black bar indicates GMFR values, box indicates IQR (Q1-Q3), lines indicate minimum and maximum. Outliers from the observed distribution are shown. Total $n = 116$ biologically independent serum samples (day 0 = 37, day 3 = 29, day 7 = 22, day 46 = 28). $n = 116$ biological samples examined against four different seasonal coronavirus substrates for ELISA assays; ELISAs for each substrate were run once each. $N = 116$ serum samples examined over two independent experiments for hemagglutination assays.

HKU1 pre-existing immunity on induction of neutralizing antibodies against SARS-CoV-2 in COVID-19 patients over time (Fig. 6A). A similar trend was found for the levels of pre-existing antibodies against the OC43 spike (Fig. 6B). Interestingly, the impact of back-boosting on IgM against the S protein was smaller when compared to IgG S or RBD. Scatterplots and the predicted regression lines for the relationship of induction of antibodies against SARS-CoV-2 and pre-exposure to betacoronaviruses are shown in Fig. 5A–D according to time points in the longitudinal follow-up. To assess neutralization potency according to the levels of pre-existing levels of seasonal coronaviruses, we normalized levels of IgG against seasonal human coronavirus antigens by the levels of anti- spike IgG from SARS-CoV-2 virus at the same time points. This analysis allows for comparison of high vs. low presence of pre-existing antibodies toward OC43, 229E, or HKU1 (antibodies at baseline) against the elicitation of SARS-CoV-2 antibodies over the observation course. We then tested whether those patients with higher hCoV/SARS-CoV-2 IgG ratio had lower induction of neutralizing antibodies. After linear regression analysis some disparities were found (Fig. 7). In general, the higher hCoV/SARS-CoV-2 IgG ratio for HKU1 and OC43 IgG S at baseline and day 3, the lower was the induction of antibodies with neutralizing activity to SARS-CoV-2, suggesting some limitations for the ability to elicit robust protective antibody responses against novel antigenic epitopes of SARS-CoV-2 in patients with high levels of cross-reactive antibodies against circulating betacoronaviruses.

Finally, and to test whether imprinting on B cell compartment could also influence antibody responses against more divergent mutated spike proteins from SARS-CoV-2 variants, we measured antibody responses against the spike protein of two SARS-CoV-2 variants. These variants, B.1.1.7 and B.1.351 emerged in late 2020 in United Kingdom and South Africa, respectively. Both B.1.1.7 and B.1.351 bear a N501Y mutation within the RBD while B.1.351 contains also K417N, E484K changes. In addition, further mutations can be found outside of the RBD domain. We performed ELISA against the B.1.1.7 and B.1.351 RBDs as well as neutralization assays against the authentic hCoV-19/England/204820464/2020 (B.1.1.7) and hCoV-19/South Africa/KRISP-K005325/2020 (B.1.351) variants. Interesting, when percentage of decrease compared to the reference was calculated, we found that responses targeting the RBD dropped from 50 to almost 100% for B.1.1.7 and B.1.351, respectively (Fig. 8A). In contrast, neutralizing titers against B.1.1.7 were similar to USA-WA1/2020, while percentage of decrease respect to B.1.351 was around 50%, indicating presence of neutralizing antibodies directed against epitopes different to those contained in the RBD, such as those directed against the N-terminal domain (Fig. 8B). Finally, we calculated Pearson correlation coefficients to examine the relationship between seasonal coronavirus HKU1 and OC43 pre-existing immunity and the ELISA antibody responses against the mutated RBDs. Pearson correlation matrices in Fig. 8C, D shows the relationship between pre-existing antibody levels against OC43 and HKU1 and fold induction against RBDs containing N501Y only, or N501Y, K417N, and E484K mutations. No significant correlation was found between pre-exposure to seasonal coronaviruses and responses against the mutated RBDs. The BACO cohort presented in here was enrolled in the first wave of SARS-CoV-2 in Spain, and the likelihood of being infected against a similar variant to Wuhan-Hu-1 is high. It is

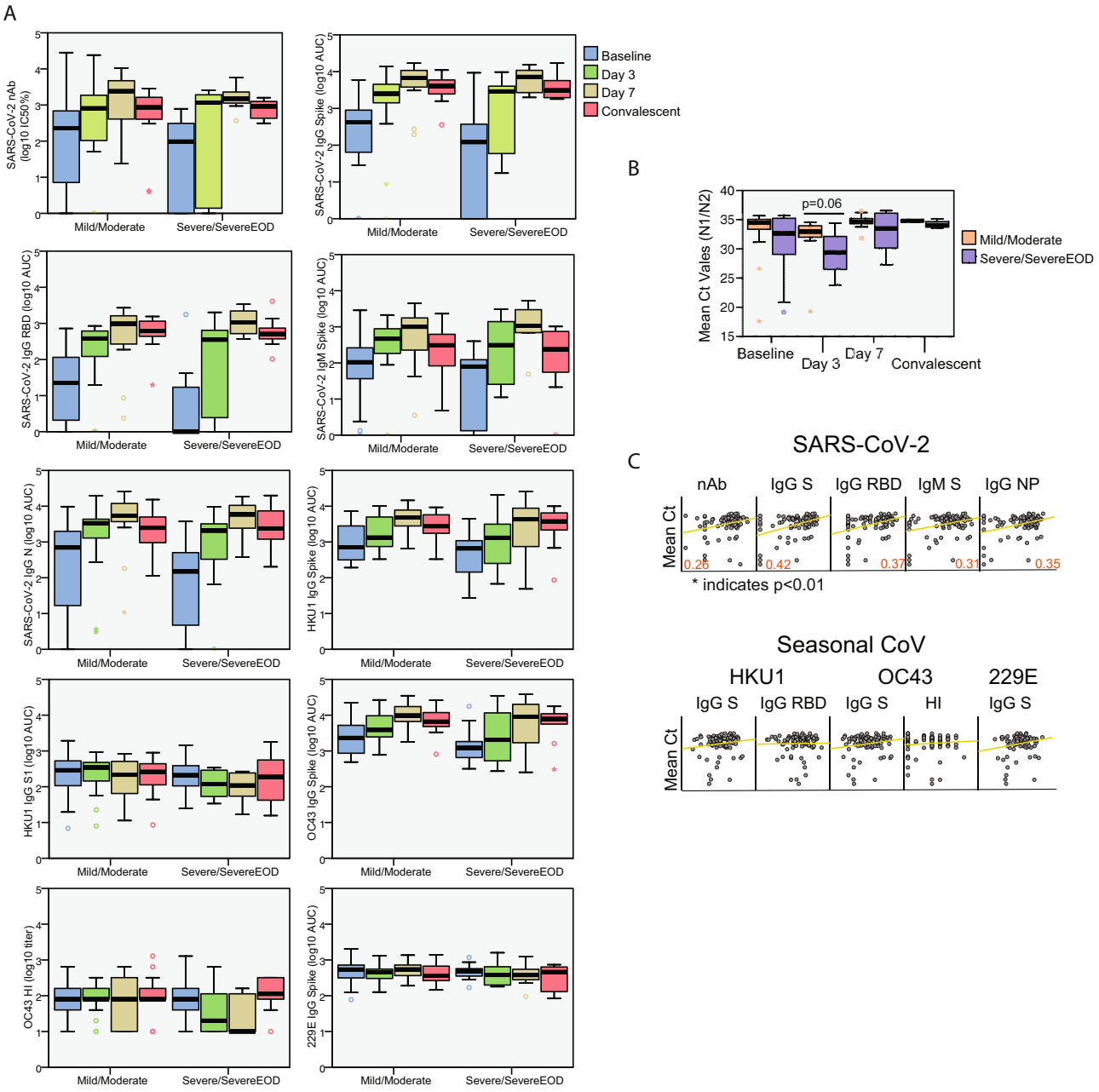

Fig. 4 Antibody response according to disease severity and viral loads in the BACO cohort. A Boxplot diagram of ELISA as area under the curve (AUC) titers against SARS-CoV-2 and endemic human coronaviruses at each time point in mild/moderate vs. severe COVID-19: IgG spike, IgG RBD, IgM spike and IgG NP; and neutralizing titer (IC50%); and HKU1 IgG spike, HKU1 IgG S1 subunit, OC43 IgG spike and 229E IgG spike; and OC43 hemagglutination titers. Black bar indicated median values, box indicates IQR (Q1–Q3), and lines indicate minimum and maximum. Outliers from the observed distribution are shown when present in each case. Total $n = 116$ biologically independent serum samples (day 0 = 37, day 3 = 29, day 7 = 22, day 46 = 28). $n = 116$ biological samples examined against eight different SARS-CoV-2 and seasonal coronavirus substrates for ELISA assays; ELISAs for each substrate were run once each. $N = 116$ serum samples examined over two independent experiments for neutralization and hemagglutination assays. **B** Boxplot diagram of mean threshold cycle (Ct) values in mild/moderate vs. severe COVID-19 during the follow-up. N protein was detected by RT-qPCR. Black bars indicate median values, the box indicates IQR (Q1–Q3), and lines indicate minimum and maximum. Outliers from the observed distribution are shown when present in each case. Total $n = 93$ biologically independent nasopharyngeal swab (day 0 = 37, day 3 = 28, day 7 = 22, day 46 = 6). $n = 93$ biological samples examined against two different SARS-CoV-2 primers over two independent experiments each. Mann–Whitney *U* test for independent samples was performed. Reported *p* values are based on two-tailed tests. **C** Scatterplot of the relationship between measured SARS-CoV-2 and seasonal coronaviruses antibody responses and Ct values in the COVID-19 patients. Pearson coefficient of statistically significant correlations is indicated in red. Matrix axis are log10 values scaled from 0 to 4. Total $n = 93$ biologically independent nasopharyngeal (NP) swab and 93 paired serum samples. Pearson correlation was calculated based on matched NP and serum samples. *P* values for statistically significant values are shown and based on two-tailed tests. Source data are provided as a Source Data File.

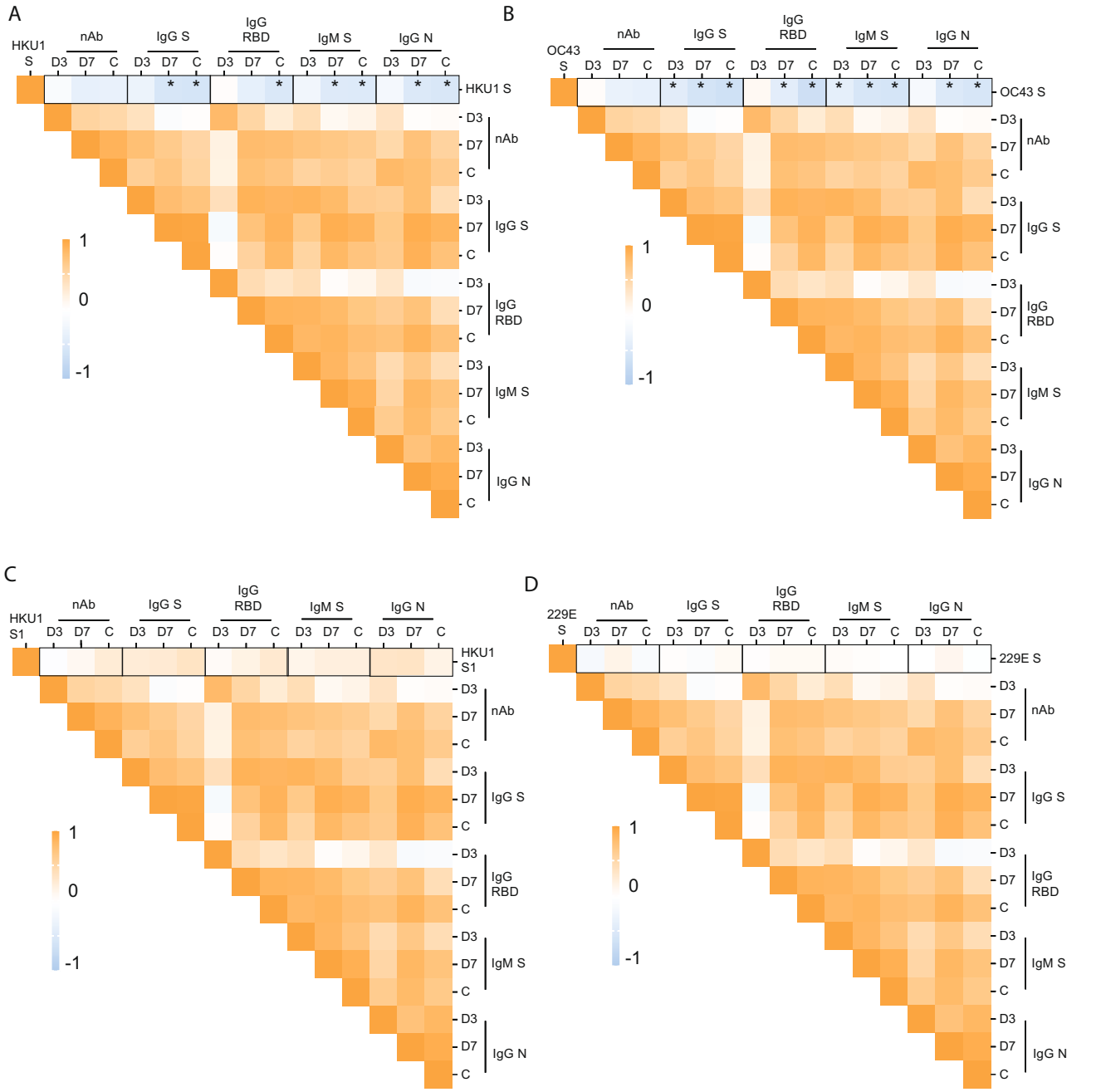

Fig. 5 Immunological imprinting on SARS-CoV-2 antibody response. A, **B** Heat map of Pearson correlation matrices between pre-existing levels of seasonal hCoV (A IgG HKU1 S; and B IgG OC43 S) and fold induction of SARS-CoV-2 antibodies at each time point: neutralizing (nAb), IgG spike, IgG RBD, IgM spike and IgG NP. Statistically significant correlations in the underlined intersections are indicated with asterisk (*); D3: day 3; D7: day 7; C: convalescence. **C**, **D** Scatterplot of baseline IgG levels for HKU1 and OC43 S protein and fold induction of SARS-CoV-2 antibodies: neutralizing (nAb), IgG spike, IgG RBD. Overlay shows relationship with induction of de novo antibodies against SARS-CoV-2 at each time point. Fitted linear regression and standardized beta coefficient (95% confidence interval, CI) for significant linear regressions are shown.

likely that the drop on RBD titers for the variants is responsible for the lack of detection of an imprinting effect with these variants.

Discussion

Our findings provide a dynamic characterization of the antibody response to SARS-CoV-2 in COVID-19 patients and provide evidence of immune imprinting in these patients. Our results demonstrate back-boosting in the BACO cohort against the conserved epitopes of the spike protein of OC43 and HKU1 betacoronaviruses. No induction was detected for the variable regions of these viruses, such as the S1 domain, or to more divergent seasonal alphacoronaviruses, such as 229E. Although antibody cross-reactivity has been reported in cross-sectional studies[22,23,25,32], our cohort has allowed for quantification and detailed representation of the longitudinal outcome of the immune response by taking into consideration past exposure to related antigens. Neutralization activity of antibodies might be used as a proxy for protection against SARS-CoV-2 infection[46,47]. IgG responses to the spike and RBD of SARS-CoV-2 showed persistence over the time period of our study with slight changes in antibody levels in convalescent sera as compared to the peak of

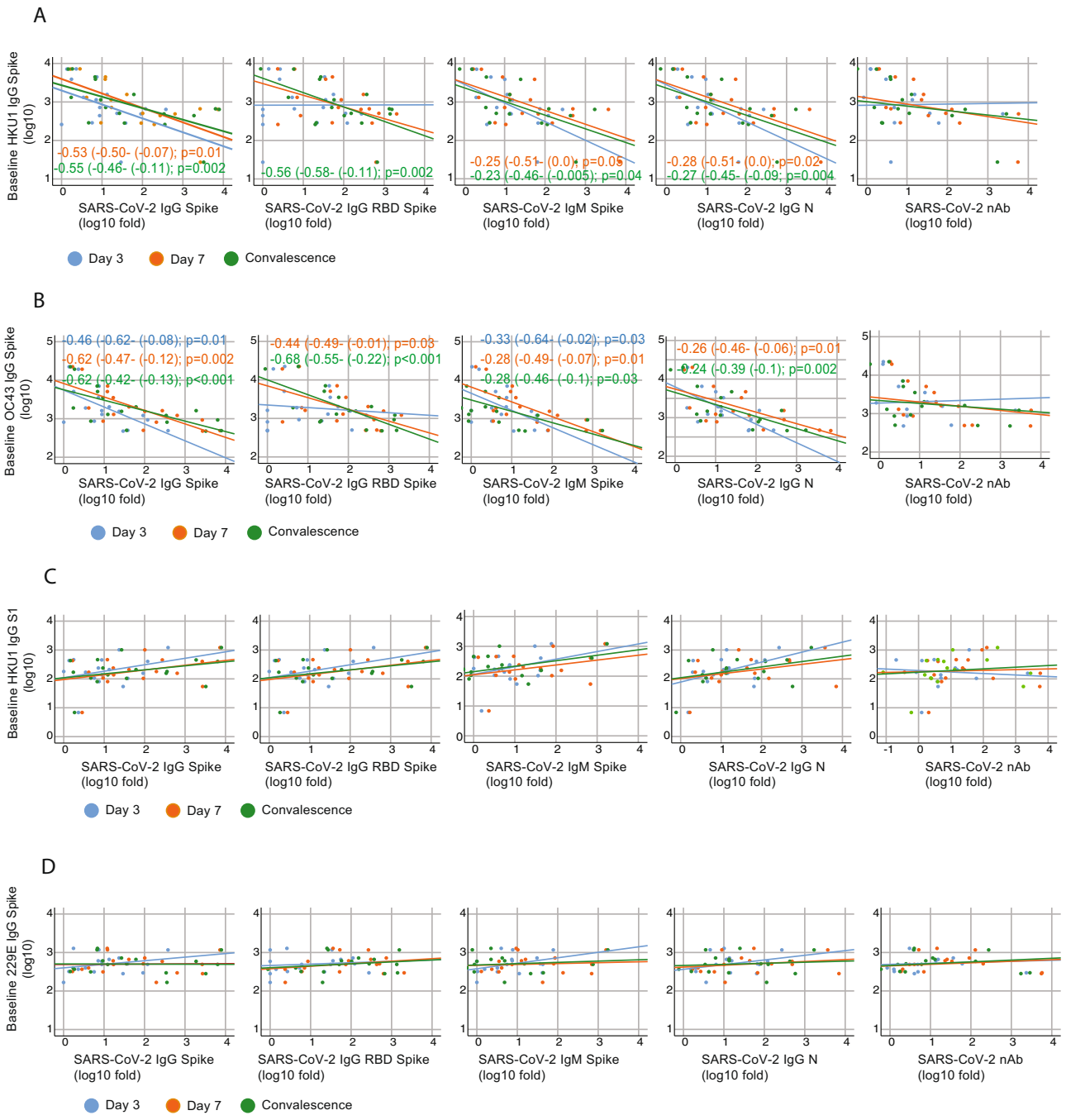

Fig. 6 Cross-reactivity with conserved epitopes against selected betacoronaviruses predicts negative influence on de novo anti-SARS-CoV-2 antibody responses. A–D Scatterplot of baseline IgG levels for HKU1, OC43 and 229E S protein; and HKU1 S1 and fold induction of SARS-CoV-2 antibodies: neutralizing (nAb), IgG spike, IgG RBD, IgM spike, and nucleoprotein. Overlay shows relationship with induction of de novo antibodies against SARS-CoV-2 at each time point. Fitted linear regression and standardized beta coefficient (95% Confidence Interval, CI) for significant linear regressions are shown. Reported *p* values are based on two-tailed tests.

antibody induction at day 7. Importantly, immunity to other betacoronavirus spikes, like HKU1 and OC43, limited the induction of de novo responses to all SARS-CoV-2 antigens tested. All patients also developed detectable levels of spike IgG/IgM and N IgG. Although no significant correlation was found between pre-exposure to seasonal coronaviruses and induction of protective antibodies with neutralizing activity, simple linear regression estimated a negative relationship, and the predicted line approximated a negative influence on development of de novo neutralizing antibodies over time. Similarly, baseline antibody levels to HKU1 or OC43 spike after SARS-CoV-2 IgG levels normalization limited the induction of neutralizing antibody levels after in the follow-up.

While we could not find statistically significant differences for antibody levels in patients with mild vs. severe disease, the latter showed a delay in antibody responses. Moreover, anti-SARS-CoV-2 antibodies inversely correlated with viral loads in respiratory samples, whereas virus clearance could not be linked to back-boosting of antibodies toward the S2 subunit of the seasonal human coronaviruses. Importantly, several reports have shown cross-reactivity between pre-existing memory T cells to seasonal coronaviruses and SARS-CoV-2[25,48] pointing to a

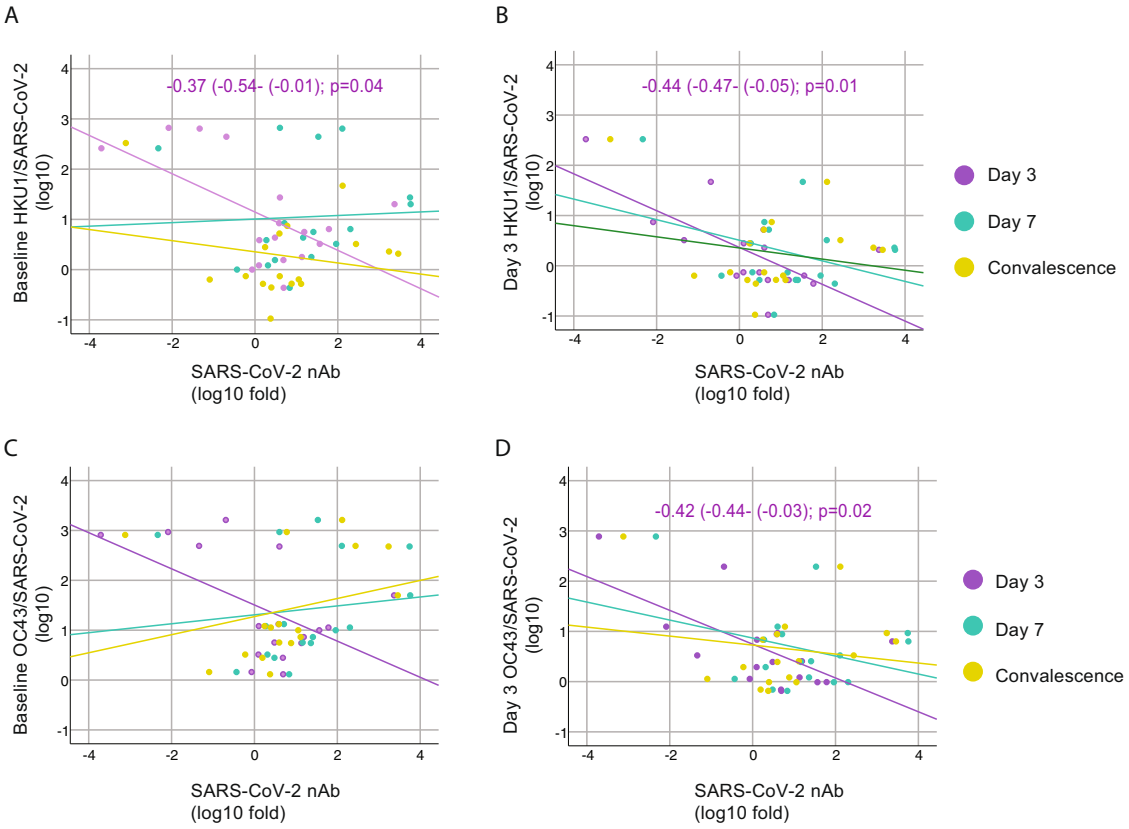

Fig. 7 Influence of levels of back-boosting to HKU1 and OC43 normalized by levels of anti- SARS-CoV-2 antibodies on neutralizing antibodies induction. A–D Scatterplot of baseline and day 3 IgG levels for HKU1 and OC43 S protein normalized by the levels of SARS-CoV-2 IgG and their relationships with fold induction of SARS-CoV-2 neutralizing antibodies (nAb) over time. Overlay shows linear regression at each time point. Fitted linear regression and standardized beta coefficient (95% confidence interval, CI) for significant regression are shown. Reported *p* values are based on two-tailed tests.

potential role of heterologous immunity as an additional mechanism of protection or even differences on COVID-19 outcomes. However, our results allow for a contrasting hypothesis in which early priming of the memory B cell compartment due to pre-exposure to seasonal coronaviruses could dampen secondary responses toward new epitopes of SARS-CoV-2. Nonetheless, all patients from the BACO cohort developed antibody responses against SARS-CoV-2 antigens and specific neutralizing antibodies. In addition, SARS-CoV-2 is evolving, and some variants including 501Y spike mutations have emerged and rapidly spread in countries, such as UK, South Africa, and Brazil (https://www.who.int/csr/don/31-december-2020-sars-cov2-variants/en/). These variants contain mutations that introduce amino acid changes in RBD residues targeted by neutralizing antibodies and therefore have functional significance. There is a general concern on whether new emerging variants (also known as variants of concern, VOC) could evade immunity generated not only by previous infections but also vaccination causing a drop on the effectiveness of COVID-19 vaccines. It is possible that first-generation COVID-19 vaccines will need to be updated according to the circulating variants in the future.

Our observation has important impact of on the development of COVID-19 vaccines and the potential interactions with pre-existing immunity should be taken into consideration in the path to optimal vaccines. COVID-19 vaccines in use aim at the induction of responses against the full-length S protein of SARS-CoV-2[49], which is known to contain cross-reactive non-neutralizing epitopes that are shared with seasonal human betacoronaviruses. A similar scenario to our studies in infected people could be proposed for the vaccines, with some differences due to the nature of the stimulus itself. Back-boost of cross-reactive antibody responses might lead to less protective antibodies directed against non-neutralizing conserved epitopes between the S antigen of the vaccine and the S proteins of seasonal human betacoronaviruses[50]. On the other hand, it is also possible that cross-reactive antibodies provide protection from severe disease outcomes by immune mechanisms of action different from those involved on in vitro virus neutralization, such as antibody-dependent cytotoxicity. That is the case for broadly cross-reactive and non-neutralizing anti-influenza antibodies targeting the conserved stalk domain of the hemagglutinin protein of influenza viruses. HA stalk antibodies can mediate antibody-dependent cell cytotoxicity, contributing to protection from disease severity independently of neutralizing activity[51]. Whether in vitro non-neutralizing anti-SARS-CoV-2 antibodies contribute to protection or disease or are neutral is still not clear.

Our study has several limitations. We comprehensively characterized antigen specificity, neutralization potency, and viral cross-reactivity against multiple coronaviruses over time. However, the number of subject enrolled remained relatively small due to the challenges and restrictions faced by the hospitals during the initial spread of SARS-CoV-2, underpowering the conclusions of this study. In addition, all the patients enrolled required hospitalization, and the pre-existing immunity of asymptomatic or mild cases of COVID-19 could not be characterized in this study. Still, our results demonstrate that the antibody response against SARS-CoV-2 infection and, potentially vaccination, is influenced by imprinting of the B cell compartment due to previous

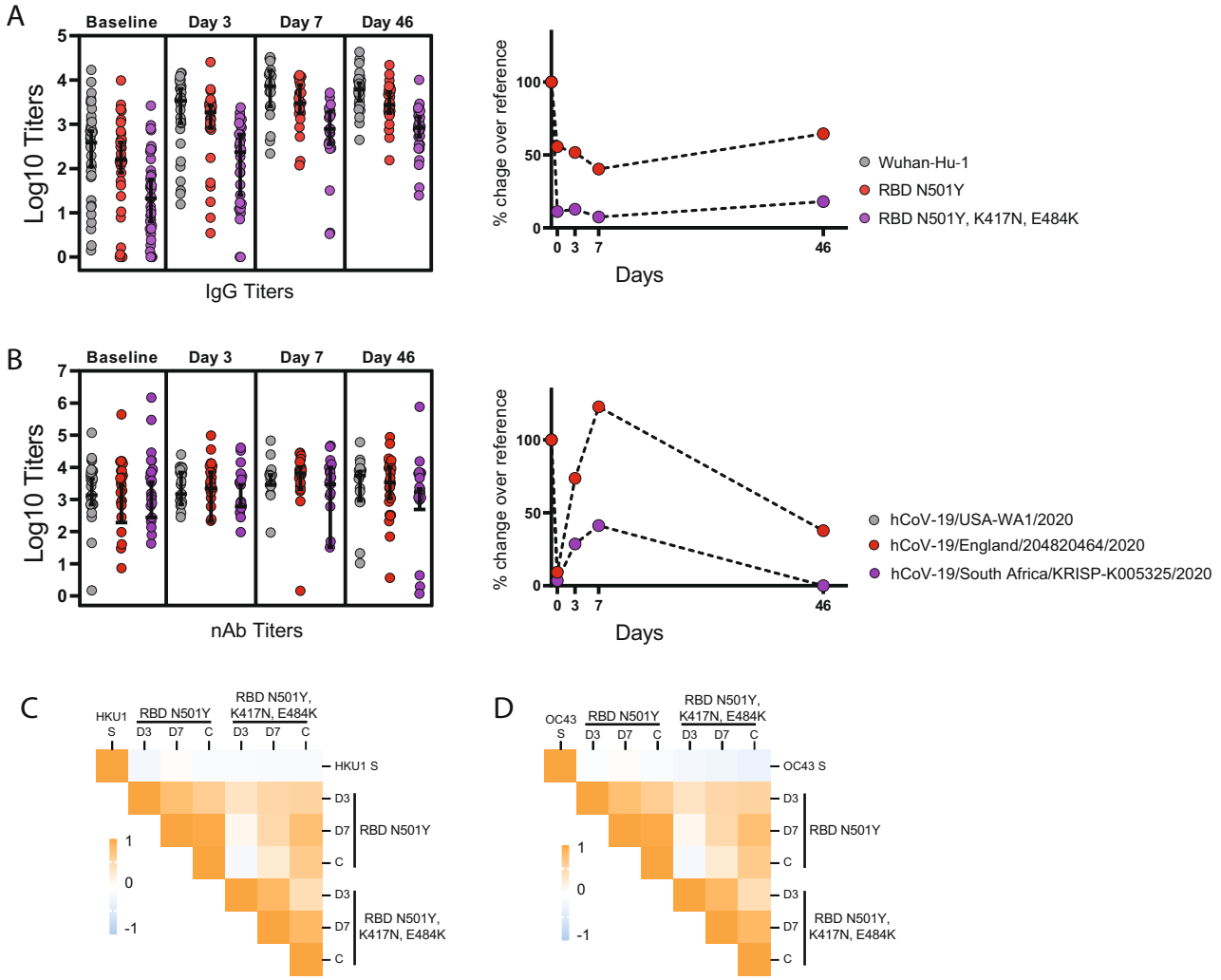

Fig. 8 Imprinting and antibody response against emerging variants of SARS-CoV-2. A ELISA against the receptor-binding domains (RBDs) of Wuhan-Hu-1 (reference), and mutated RBDs representative of UK (N501Y) and South African (K417N, E484K and N501Y) variants. **B** Neutralizing titers against the authentic hCoV-19/England/204820464/2020 (B.1.1.7) and hCoV-19/South Africa/KRISP-K005325/2020 (B.1.351). Errors indicate geometric mean titer (GMT) and confidence interval (CI 95%) at each time point for ELISA against each RBD or neutralizing titers against each variant. Percentage of decrease titers compared to reference has been calculated and data are shown in the right for ELISA and nAb titers. Total $n = 116$ biologically independent serum samples (day 0 = 37, day 3 = 29, day 7 = 22, day 46 = 28). $n = 116$ biological samples examined against three different SARS-CoV-2 RBDs; ELISAs for each substrate were run once each. $N = 116$ serum samples examined for three different SARS-CoV-2 variants over two independent experiments each. **C**–**D** Heat map of Pearson correlation matrices between pre-existing levels of seasonal CoVs: IgG HKU1 S; and B IgG OC43 S; and fold induction of antibodies against RBD N501Y and RBD N501Y, K417N, E484K RBD at each time point. D3 day 3, D7 day 7, C convalescence.

exposure to seasonal human betacoronaviruses. This is consistent with additional recent studies[33]. It will be important to investigate the potential functional consequences of this imprinting in the induction of protective immune responses after SARS-CoV-2 infection and vaccination in the long term, and in the very likely case that the current pandemic evolves into epidemic outbreaks.

Methods

Experimental model and subject details: The BACO cohort. An observational prospective human cohort study of COVID-19 was carried out during the first pandemic wave (March–May 2020) of SARS-CoV-2 in Barcelona (Spain) and was termed the BACO Cohort. A positive case was defined according to international guidelines when a nasopharyngeal (NP) swab tested positive for SARS-CoV-2 by reverse transcriptase quantitative polymerase chain reaction (RT-qPCR) upon hospital admission. All patients or their legally authorized representatives provided informed consent. Serum and samples were collected at the enrollment in the study (baseline), and at days 3 and 7 post enrollment. A convalescence sample was collected from survivors after recovery and hospital discharge with a mean time of 46 days (range, 30–56 days). The total number of serum samples was 116. Data on demographics, including age and sex, comorbidities, clinical signs and symptoms, interventions, and outcomes are described in Table 1. Severity of COVID-19 was assigned following a described severity scale based on oxygen saturation (SpO_2), presence of pneumonia/imaging, oxygen support defined as use of high-flow nasal cannula (HFNC), non-rebreather mask (NRB), bilevel positive airway pressure (BIPAP) or mechanical ventilation (MV); and kidney (creatinine clearance, CrCl) and liver (alanine aminotransferase, ALT) function[44]: mild (SpO2 > 94% AND no pneumonia), moderate (SpO2 < 94% AND/OR pneumonia), severe (use of HFNC, NRB, BIPAP or MV AND no vasopressor use AND CrCl >30 AND ALT < 5x upper limit of normal) and severe with end-of organ disease (Use of HFNC, NRB, BIPAP or MV AND vasopressor use OR CrCl >30 or new HD OR ALT < 5x upper limit of normal).

The study protocol was approved by the Institutional Review Board of University Hospital of Bellvitge, Barcelona, Spain; and by the Icahn School of Medicine at Mount Sinai, New York, US.

Cell lines. Vero E6 cells were originally purchased from the American Type Culture Collection (ATCC, Cat# CRL-1586). Cells were maintained in Dulbecco's modified Eagle's medium (DMEM) w/ L-glutamate, sodium pyruvate (Corning) supplemented with 10% fetal bovine serum (FBS), 10 U penicillin per ml, and 10 mg streptomycin per ml. HCT-8 human cells line was obtained from the ATCC (Cat#CCL-24) and maintained in Roswell Park Memorial Institute 1640 medium (Gibco) supplemented with 10% FBS, 10 U penicillin per ml, and 10 mg

streptomycin per ml. Cell lines were supplemented with Normocyn (Invivogen, Cat. ant-nr-1) to prevent Mycoplasma contamination.

Virus strains. SARS-CoV-2, isolate USA-WA1/2020, was initially obtained from BEI Resources (Cat#NR-52281) and further propagated in Vero E6 cells[52]. Human coronavirus OC43 was obtained from the ATCC (Cat#VR-1558) and propagated on HCT-8 cells following ATCC recommendations.

Microneutralization assays. Microneutralization (MN) assays for antibody characterization were performed as described[52]. Briefly, Vero E6 cells were seeded in a 96-well cell culture plate with complete Dulbecco's Modified Eagle Medium (cDMEM)(Corning) [Penicillin-streptomycin (Corning), non-essential amino acids (Corning), 10% FBS (Peak)]. The following day, heat-inactivated serum samples were serially diluted three-fold in 1x minimum essential medium with 2% FBS with a final volume of 200 µl. 80 µl of serum dilution was transferred to a new 96-well plate and 600 Tissue Culture Infectious Dose 50 percent per well of SARS-CoV-2 (80 µl/well) and mixed with serum dilution and incubated for 1 h at 37 °C. Then, cDMEM was removed from Vero e6 cells and 120 µl of virus-serum mixture was added to the cells. The cells were incubated at 37 °C for 1 h. Virus-serum mixture was removed from the cells and 100 µl of serum dilutions and 100 µl of 1xMEM with 2% FBS was added to the cells. The cells were incubated for 24 h and then fixed with 10% paraformaldehyde (Polysciences) for 24 h at 4 °C. Following fixation, the cells were washed with phosphate-buffered saline (Corning) with tween-20 (Fisher) (PBST) and permeabilized with 0.1% Triton X-100 (Fisher) for 15 min at room temperature. The cells were washed three times using PBST and blocked with 3% milk in PBST for 1 h at room temperature. Then, the cells were incubated with mouse antibody 1C7 (anti-SARS N antibody, kindly provided by Dr. Moran) at a dilution of 1:1000 in 1% milk in PBST and incubated for 1 h at room temperature. The cells were washed three times with PBST. Then, the cells were incubated with goat anti-mouse IgG-HRP (Abcam, Cat. ab6823) at a dilution of 1:10,000 in 1% milk in PBST and incubated for 1 h at room temperature. The cells were washed three times with PBST and TMBE Elisa peroxidase substrate (Rockland) was added. After 15 min incubation, sulfuric acid 4.0 N (Fisher) was added to stop the reaction and the readout was done using a Synergy H1 plate reader (BioTek) at an OD450.

Recombinant proteins. The recombinant spike protein and recombinant RBD of SARS-CoV-2 were generated and expressed as previously described in detail[52,53]. In brief, the mammalian cell codon-optimized nucleotide sequence for the soluble version of the spike protein (amino acids 1-1213) including a C-terminal thrombin cleavage site, signal peptide, hexahistidine tag and T4 foldon trimerization domain were cloned into pCAGGS mammalian expression vector. The sequence of the spike protein was additionally modified to remove the polybasic cleavage site and two proline residues introduced to increase protein stability. The nucleotide sequence for the RBD (amino acids 319-541) including a signal peptide was cloned into pCAGGS. RBD mutants were generated in the pCAGGS RBD construct by changing single residues using site-directed mutagenesis. The expression plasmids encoding for the spike of common human coronavirus 229E, OC43, and HKU1 were obtained from the NIH (kindly provided by Kizzmekia Corbett and Barney Graham) and the expression plasmid encoding for SARS-CoV-2 NP was constructed at Mount Sinai. The recombinant proteins were expressed in Expi293F cells (Thermo Fisher) using the ExpiFectamine 293 Transfection Kit (Thermo Fisher) according to the manufacturer's protocol. Cell supernatant was harvested, and the proteins purified using Ni-NTA Agarose (Qiagen). The proteins were concentrated in Amicon centrifugal units (EMD Milipore) and correct size confirmed by reducing sodium dodecyl sulfate-polyacrylamide gel electrophoreses. The recombinant S1 subunit of HKU1 was purchased from Sino Biological (Cat. 40021-V08H).

Enzyme-linked immunosorbent assay (ELISA). Ninety-six-well microtiter plates (Thermo Fisher) were coated with 50 µL recombinant protein (RBD, SARS-CoV-2 full-length spike, SARS-CoV-2 NP, OC43 spike, 229E spike, or HKU1 spike, respectively) at a concentration of 2 µg/mL overnight, 4 °C. The next day, the plates were washed three times with PBS (phosphate-buffered saline; Gibco) containing 0.1% Tween-20 (T-PBS, Fisher Scientific) using an automatic plate washer (BioTek). After washing, the plates were blocked for 1 h at room temperature with 200 µl blocking solution (PBS-T with 3% (w/v) milk powder (American Bio)) per well. The blocking solution was removed and serum samples diluted to a starting concentration of 1:80, serially diluted 1:3 in PBS-T supplemented with 1% (w/v) milk powder and incubated at room temperature for 2 h. The plates were washed three times with PBS-T and 50 µl anti-human IgG (Fab-specific) horseradish peroxidase antibody (HRP, Sigma, Cat. A0293) diluted 1:3,000 in PBS-T containing 1% milk powder was added to all wells and incubated for 1 h at room temperature. The plates were washed three times using the plate washer and 100 µL SigmaFast o-phenylenediamine dihydrochloride (Sigma) was added to all wells for 10 min. The enzymatic reaction was stopped with 50 µL 3 M hydrochloric acid (Thermo Fisher) per well and the plates read at a wavelength of 490 nm with a plate reader (BioTek). The results were recorded in Microsoft Excel and AUC values were computed by plotting normalized OD values against the reciprocal serum sample dilutions for ELISAs in GraphPad Prism.

Hemagglutination inhibition (HAI) assay. Serum samples were incubated overnight with receptor-destroying enzyme (RDE; Denka Seiken) for 16–18 h in a 37 °C water bath. Three volumes (relative to serum) of 2.5% sodium citrate solution were added and the resulting solution was heat inactivated at 56 °C in a water bath (30 min). Final serum dilutions were adjusted to 1:10 in PBS. OC43 virus was diluted to a final concentration of 8 HA units/50 µL in fluorescent treponemal antibody HA buffer (BD Biosciences). Twofold dilutions of RDE treated serum (25 µL) were incubated with equal amount of the virus at 8 HA units/50 µL (30 min, room temperature). Chicken red blood cells (RBCs) (Lampire Biological) at 0.5% in HA buffer (50 µL) were added and incubated 45 min at 4 °C. The HAI titer was determined by taking the reciprocal dilution of the last well in which serum inhibited the HA of RBCs.

Viral loads and qRT-PCR. To detect SARS-CoV-2 RNA in nasal swabs, a modified version of the CDC 2019-nCoV real-time RT-qPCR was used. Primers and probes were commercially available (Integrated DNA Technologies, cat. 10006713, RUO Kit). SARS-CoV-2 primer and probe sets consisted of two 2019-nCoV-specific sets (N1, N2). A third primer set was used to detect host cellular RNaseP. Reactions were run using the QuantiFast Pathogen RT-PCR + IC Kit (QIAGEN, cat. 211454). A list of all primers used, including the names and sequences, is shown in Supplementary Table 3. Assays were run using USA/WA-1/2020 SARS-CoV-2 RNA as a positive control (20,000 genome copies per reaction) and nuclease-free water as a non-template control in a 384-well format. Reactions were performed in duplicate using the following cycling conditions on the Roche LightCycler 480 Instrument II (Roche Molecular Systems, 05015243001): 50 °C for 20 min, 95 °C for 1 s, 95 °C for 5 min, followed by 45 cycles of 95 °C for 15 s and 60 °C for 45 s. Limit of detection for SARS-CoV-2 was determined by using a commercially available plasmid control (Integrated DNA Technologies, cat. 10006625).

Multiple sequences alignment and conservation scores. MSA to determine the spike protein sequence identity among SARS-CoV-2 (NC_045512.2), and the human endemic betacoronaviruses HKU1 (YP_173238) and OC43 (YP_009555241.1), and alphacoronavirus 229E (NP_073551.1) was performed with ClustalW. Conservation patterns and scores of the spike protein of SARS-CoV-2 were determined using the ConSurf server (https://consurf.tau.ac.il/). Briefly, a MSA of 150 homologous sequences was constructed using MAFFT. Position-specific conservation scores were computed using an empirical Bayesian algorithm and divided into a discrete scale of nine grades. The conservation scores were projected onto the SARS-CoV-2 spike protein in the closed state (PDB ID 6VXX) as a reference.

Quantification and statistical analysis. All immune assay values were log10-transformed to improve linearity. The GMT and 95% confidence intervals (CI 95%) were computed by taking the exponent (log10) of the mean and of the lower and upper limits of the 95% CI of the log10-transformed titers. Fold rise was calculated as the ratio between days 3, 7 or convalescent antibody value to baseline levels. GMFR was computed by taking the exponent (log10) of the mean fold rise and of the lower and upper limits of the CI 95% of the log10-transformed titers. Statistical significance was established at $p < 0.05$. All reported p values are based on two-tailed tests. Correlation (Pearson), linear regression, local regression fit-line and related-sample multiple comparison (Friedman's two-way analysis of variance by ranks, also known as Friedman's two-way ANOVA, and pairwise comparison adjusted by Bonferroni correction) were performed using IBM SPSS Statistics (version 26).

Reporting summary. Further information on research design is available in the Nature Research Reporting Summary linked to this article.

Data availability

All data are available in the manuscript or the supplementary materials. Source data are provided with this paper. The accession codes for the Structure of the SARS-CoV-2 spike glycoprotein (closed state) EMD: 21452 and PDB: 6VXX. Source data are provided with this paper.

Received: 5 January 2021; Accepted: 25 May 2021;
Published online: 18 June 2021

References

1. Zhu, N. et al. A novel coronavirus from patients with pneumonia in China, 2019. *N. Engl. J. Med.* **382**, 727–733 (2020).
2. Morens, D. M. & Fauci, A. S. Emerging pandemic diseases: how we got to COVID-19. *Cell* **182**, 1077–1092 (2020).
3. Ieven, M. et al. Aetiology of lower respiratory tract infection in adults in primary care: a prospective study in 11 European countries. *Clin. Microbiol Infect.* **24**, 1158–1163 (2018).

4. Zaki, A. M., van Boheemen, S., Bestebroer, T. M., Osterhaus, A. D. & Fouchier, R. A. Isolation of a novel coronavirus from a man with pneumonia in Saudi Arabia. *N. Engl. J. Med.* **367**, 1814–1820 (2012).
5. Peiris, J. S. et al. Coronavirus as a possible cause of severe acute respiratory syndrome. *Lancet* **361**, 1319–1325 (2003).
6. Forni, D., Cagliani, R., Clerici, M. & Sironi, M. Molecular evolution of human coronavirus genomes. *Trends Microbiol.* **25**, 35–48 (2017).
7. Bi, Q. et al. Epidemiology and transmission of COVID-19 in 391 cases and 1286 of their close contacts in Shenzhen, China: a retrospective cohort study. *Lancet Infect. Dis.* **20**, 911–919 (2020).
8. Jackson, L. A., et al. An mRNA vaccine against SARS-CoV-2 - preliminary report. *N. Engl. J. Med.* **383**, 1920–1931 (2020).
9. Mercado, N. B., et al. Single-shot Ad26 vaccine protects against SARS-CoV-2 in rhesus macaques. *Nature* **586**, 583–588 (2020).
10. van Doremalen, N. et al. ChAdOx1 nCoV-19 vaccine prevents SARS-CoV-2 pneumonia in rhesus macaques. *Nature* **586**, 578–582 (2020).
11. Piccoli, L. et al. Mapping neutralizing and immunodominant sites on the SARS-CoV-2 spike receptor-binding domain by structure-guided high-resolution serology. *Cell* **83**, 1024–1042 (2020).
12. Yuan, M. et al. A highly conserved cryptic epitope in the receptor binding domains of SARS-CoV-2 and SARS-CoV. *Science* **368**, 630–633 (2020).
13. Boni, M. F. et al. Evolutionary origins of the SARS-CoV-2 sarbecovirus lineage responsible for the COVID-19 pandemic. *Nat. Microbiol.* **5**, 1408–1417 (2020).
14. Walls, A. C. et al. Structure, function, and antigenicity of the SARS-CoV-2 spike glycoprotein. *Cell* **183**, 1735 (2020).
15. Lachance, C., Arbour, N., Cashman, N. R. & Talbot, P. J. Involvement of aminopeptidase N (CD13) in infection of human neural cells by human coronavirus 229E. *J. Virol.* **72**, 6511–6519 (1998).
16. Hulswit, R. J. G. et al. Human coronaviruses OC43 and HKU1 bind to 9-O-acetylated sialic acids via a conserved receptor-binding site in spike protein domain A. *Proc. Natl Acad. Sci. USA* **116**, 2681–2690 (2019).
17. Ge, X. Y. et al. Isolation and characterization of a bat SARS-like coronavirus that uses the ACE2 receptor. *Nature* **503**, 535–538 (2013).
18. Ju, B. et al. Human neutralizing antibodies elicited by SARS-CoV-2 infection. *Nature* **584**, 115–119 (2020).
19. Shi, R. et al. A human neutralizing antibody targets the receptor-binding site of SARS-CoV-2. *Nature* **584**, 120–124 (2020).
20. Wang, Q. et al. Structural and functional basis of SARS-CoV-2 entry by using human ACE2. *Cell* **181**, 894–904 (2020). e899.
21. Letko, M., Marzi, A. & Munster, V. Functional assessment of cell entry and receptor usage for SARS-CoV-2 and other lineage B betacoronaviruses. *Nat. Microbiol.* **5**, 562–569 (2020).
22. Lv, H. et al. Cross-reactive antibody response between SARS-CoV-2 and SARS-CoV infections. *Cell Rep.* **31**, 107725 (2020).
23. Shrock, E. et al. Viral epitope profiling of COVID-19 patients reveals cross-reactivity and correlates of severity. Science **370**, eabd4250 (2020).
24. Van Elslande, J. et al. Antibody response against SARS-CoV-2 spike protein and nucleoprotein evaluated by four automated immunoassays and three ELISAs. *Clin. Microbiol. Infect.* **26**, 1557.e1–1557.e7 (2020).
25. Mateus, J. et al. Selective and cross-reactive SARS-CoV-2 T cell epitopes in unexposed humans. *Science* **370**, 89–94 (2020).
26. de Vries, R. D. SARS-CoV-2-specific T-cells in unexposed humans: presence of cross-reactive memory cells does not equal protective immunity. *Signal Transduct. Target Ther.* **5**, 224 (2020).
27. Braun, J. et al. SARS-CoV-2-reactive T cells in healthy donors and patients with COVID-19. *Nature* **587**, 270–274 (2020).
28. Grifoni, A. et al. Targets of T cell responses to SARS-CoV-2 coronavirus in humans with COVID-19 disease and unexposed individuals. *Cell* **181**, 1489–1501 (2020). e1415.
29. Meckiff, B. J. et al. Single-cell transcriptomic analysis of SARS-CoV-2 reactive CD4 (+) T cells. https://doi.org/10.1101/2020.06.12.148916 (2020).
30. Weiskopf, D. et al. Phenotype and kinetics of SARS-CoV-2-specific T cells in COVID-19 patients with acute respiratory distress syndrome. *Sci. Immunol.* **5**, eabd2071 (2020).
31. Che, X. Y. et al. Antigenic cross-reactivity between severe acute respiratory syndrome-associated coronavirus and human coronaviruses 229E and OC43. *J. Infect. Dis.* **191**, 2033–2037 (2005).
32. Nguyen-Contant, P. et al. S protein-reactive IgG and memory B cell production after human SARS-CoV-2 infection includes broad reactivity to the S2 subunit. mBio **11**, e01991–20 (2020).
33. Ng, K. W. et al. Preexisting and de novo humoral immunity to SARS-CoV-2 in humans. *Science* **370**, 1339–1343 (2020).
34. Kelvin, A. A. & Zambon, M. Influenza imprinting in childhood and the influence on vaccine response later in life. *Euro Surveill.* **24**, 1900720 (2019).
35. Fonville, J. M. et al. Antibody landscapes after influenza virus infection or vaccination. *Science* **346**, 996–1000 (2014).
36. Dugan, H. L. et al. Preexisting immunity shapes distinct antibody landscapes after influenza virus infection and vaccination in humans. *Sci. Transl. Med.* **12**, eabd3601 (2020).
37. Erbelding, E. J. et al. A universal influenza vaccine: the strategic plan for the national institute of allergy and infectious diseases. *J. Infect. Dis.* **218**, 347–354 (2018).
38. Monto, A. S., Malosh, R. E., Petrie, J. G. & Martin, E. T. The doctrine of original antigenic sin: separating good from evil. *J. Infect. Dis.* **215**, 1782–1788 (2017).
39. Gostic, K. M. et al. Childhood immune imprinting to influenza A shapes birth year-specific risk during seasonal H1N1 and H3N2 epidemics. *PLoS Pathog.* **15**, e1008109 (2019).
40. Meade, P. et al. Influenza virus infection induces a narrow antibody response in children but a broad recall response in adults. *mBio* **11,** e03243–19 (2020).
41. Halstead, S. B., Rojanasuphot, S. & Sangkawibha, N. Original antigenic sin in dengue. *Am. J. Trop. Med. Hyg.* **32**, 154–156 (1983).
42. Midgley, C. M. et al. An in-depth analysis of original antigenic sin in dengue virus infection. *J. Virol.* **85**, 410–421 (2011).
43. Gorse, G. J., Patel, G. B., Vitale, J. N. & O'Connor, T. Z. Prevalence of antibodies to four human coronaviruses is lower in nasal secretions than in serum. *Clin. Vaccin. Immunol.* **17**, 1875–1880 (2010).
44. Del Valle, D. M. et al. An inflammatory cytokine signature predicts COVID-19 severity and survival. *Nat. Med.* **26**, 1636–1643 (2020).
45. Tortorici, M. A. et al. Ultrapotent human antibodies protect against SARS-CoV-2 challenge via multiple mechanisms. *Science* **370**, 950–957 (2020).
46. Addetia, A. et al. Neutralizing antibodies correlate with protection from SARS-CoV-2 in humans during a fishery vessel outbreak with high attack rate. *J. Clin. Microbiol.* **58**, e02107–20 (2020).
47. Hassan, A. O. et al. A SARS-CoV-2 infection model in mice demonstrates protection by neutralizing antibodies. *Cell* **182**, 744–753 (2020). e744.
48. Saletti, G. et al. Older adults lack SARS CoV-2 cross-reactive T lymphocytes directed to human coronaviruses OC43 and NL63. *Sci. Rep.* **10**, 21447 (2020).
49. Amanat, F. & Krammer, F. SARS-CoV-2 vaccines: status report. *Immunity* **52**, 583–589 (2020).
50. Amanat, F. et al. The plasmablast response to SARS-CoV-2 mRNA vaccination is dominated by non-neutralizing antibodies that target both the NTD and the RBD. https://doi.org/10.1101/2021.03.07.21253098 (2021).
51. Aydillo, T. et al. Pre-existing hemagglutinin stalk antibodies correlate with protection of lower respiratory symptoms in flu-infected transplant patients. *Cell Rep. Med.* **1**, 100130 (2020).
52. Amanat, F. et al. A serological assay to detect SARS-CoV-2 seroconversion in humans. *Nat. Med.* **26**, 1033–1036 (2020).
53. Stadlbauer, D. et al. SARS-CoV-2 seroconversion in humans: a detailed protocol for a serological assay, antigen production, and test setup. *Curr. Protoc. Microbiol.* **57**, e100 (2020).

Acknowledgements

We thank the BACO cohort patients and their families. We also thank Randy Albrecht for support with the BSL3 facility and procedures at the ISMMS and Richard Cadagan for excellent technical assistance. We also want to thank Kizzmekia Corbett and Barney Graham at the Vaccine Research Center at NIAID for sharing expression plasmids for hCoV spike proteins. This work was partly funded by CRIP (Center for Research on Influenza Pathogenesis), a NIAID funded Center of Excellence for Influenza Research and Surveillance (CEIRS, contract #HHSN272201400008C), by SEM-CIVIC, a NIAID funded Collaborative Influenza Vaccine Innovation Center (contract #75N93019C00051), by NCI SeroNet grant U54CA260560, and by the generous support of the JPB Foundation, the Open Philanthropy Project (research grant 2020-215611 (5384)) and anonymous donors to A.G.S. A.R. is a recipient of a predoctoral fellowship from the Instituto de Salud Carlos III, Spanish Ministry of Science, Innovation and Universities (PFIS contract FI18/00183).

Author contributions

T.A. performed experiments, analyzed data, and wrote the manuscript. A.R., G.A.A., and J.C. collected samples and data. D.S., S.A., A.E., K.J., and F.A. performed experiments. F.K. provided reagents, methods, and expertise. T.A. and A.G.S. conceived and designed the study. T.A., J.C., and A.G.S. supervised the study. All of the authors reviewed and edited the manuscript.

Competing interests

A.G.S. is inventor of patents owned by the Icahn School of Medicine at Mount Sinai in the field of influenza virus vaccines. The A.G.S. lab has received research funds from Avimex, GSK, and 7Hills to investigate novel influenza virus vaccines. The Icahn School of Medicine at Mount Sinai has filed patent applications relating to SARS-CoV-2 serological assays and NDV-based SARS-CoV-2 vaccines which list F.K. as co-inventor. D.S. and F.A. are also listed on the serological assay patent application as co-inventors. Mount Sinai has spun out a company, Kantaro, to market serological tests for SARS-CoV-2. F.K. has consulted for Merck and Pfizer (before 2020), and is currently consulting for Pfizer, Seqirus, and Avimex. The Krammer laboratory is also collaborating with Pfizer on animal models of SARS-CoV-2. The other authors declare no competing interests.

Additional information

Supplementary information The online version contains supplementary material available at https://doi.org/10.1038/s41467-021-23977-1.

Correspondence and requests for materials should be addressed to F.K., J.C. or A.G.-S.

Peer review information *Nature Communications* thanks Galit Alter and Anna Durbin for their contribution to the peer review of this work.

Reprints and permission information is available at http://www.nature.com/reprints

Publisher's note Springer Nature remains neutral with regard to jurisdictional claims in published maps and institutional affiliations.

Study 5

SARS-CoV-2 infection induces robust mucosal antibody responses in the upper respiratory tract

Escalera, A., Rojo-Fernandez, A., **Rombauts, A.**, Abelenda-Alonso, G., Carratalà, J., García-Sastre, A., & Aydillo, T✉.

. *iScience*, 2024, 27(3), 109210.

Impact factor: 5.8 (1st quartile)

iScience

CellPress
OPEN ACCESS

Article

SARS-CoV-2 infection induces robust mucosal antibody responses in the upper respiratory tract

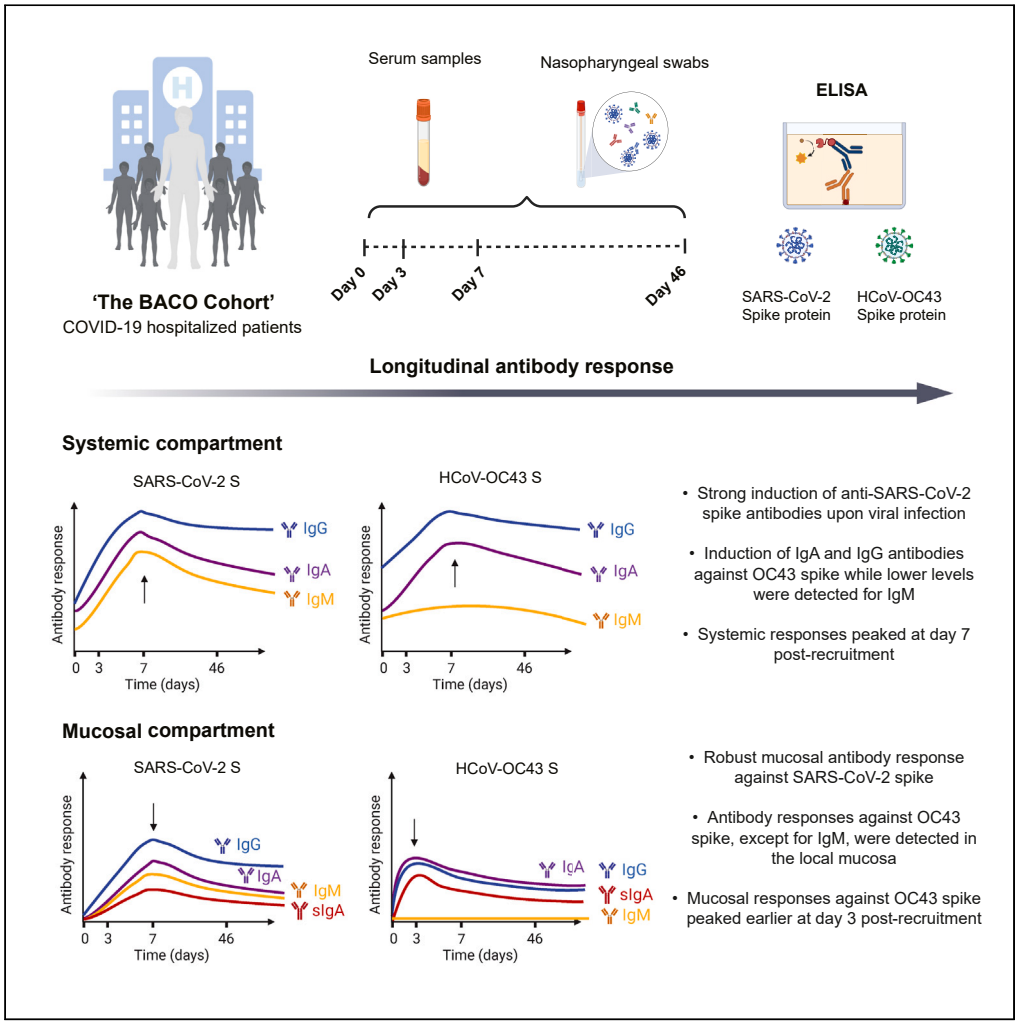

Alba Escalera, Amaya Rojo-Fernandez, Alexander Rombauts, Gabriela Abelenda-Alonso, Jordi Carratalà, Adolfo García-Sastre, Teresa Aydillo

adolfo.garcia-sastre@mssm.edu (A.G.-S.)
teresa.aydillo-gomez@mssm.edu (T.A.)

Highlights

COVID-19 patients mounted robust mucosal antibody responses against SARS-CoV-2 S

COVID-19 patients showed IgG, sIgA, and IgA, but not IgM, responses against HCoV-OC43 S

Mucosal antibody titers against SARS-CoV-2 and OC43 peaked at day 7 and 3, respectively

Our data suggest an immune memory recall toward conserved beta-HCoVs epitopes

Escalera et al., iScience 27, 109210
March 15, 2024
https://doi.org/10.1016/j.isci.2024.109210

iScience

CellPress
OPEN ACCESS

Article

SARS-CoV-2 infection induces robust mucosal antibody responses in the upper respiratory tract

Alba Escalera,[1,2,3] Amaya Rojo-Fernandez,[1,2] Alexander Rombauts,[4] Gabriela Abelenda-Alonso,[4,5] Jordi Carratalà,[4,5] Adolfo García-Sastre,[1,2,6,7,8,9,*] and Teresa Aydillo[1,2,10,*]

SUMMARY

Despite multiple research efforts to characterize coronavirus disease 2019 (COVID-19) in humans, there is no clear data on the specific role of mucosal immunity on COVID-19 disease. Here, we longitudinally profile the antibody response against severe acute respiratory syndrome coronavirus 2 (SARS-CoV-2) and seasonal HCoV-OC43 S proteins in serum and nasopharyngeal swabs from COVID-19 patients. Results showed that specific antibody responses against SARS-CoV-2 and HCoV-OC43 S proteins can be detected in the upper respiratory tract. We found that COVID-19 patients mounted a robust mucosal antibody response against SARS-CoV-2 S with specific secretory immunoglobulin A (sIgA), IgA, IgG, and IgM antibody subtypes detected in the nasal swabs. Additionally, COVID-19 patients showed IgG, IgA, and sIgA responses against HCoV-OC43 S in the local mucosa, whereas no specific IgM was detected. Interestingly, mucosal antibody titers against SARS-CoV-2 peaked at day 7, whereas HCoV-OC43 titers peaked earlier at day 3 post-recruitment, suggesting an immune memory recall to conserved epitopes of beta-HCoVs in the upper respiratory tract.

INTRODUCTION

Severe acute respiratory syndrome coronavirus 2 (SARS-CoV-2) is the causative agent of coronavirus disease 2019 (COVID-19), a respiratory illness that has affected more than 770 million people worldwide (https://covid19.who.int/, as September 2023). Since the emergence of this novel betacoronavirus in late 2019,[1] research efforts have been focused on understanding the nature and dynamics of the systemic immune responses against SARS-CoV-2 virus. Upon infection, COVID-19 patients rapidly produce immunoglobulin M (IgM), IgG, and IgA antibodies that predominantly target the spike (S) protein, the main surface glycoprotein that binds to the human angiotensin-converting enzyme 2 (ACE2) receptor and mediates viral entry into the host cell. Additionally, antibodies directed against the viral nucleocapsid protein have also been detected.[2–4] These antibodies are present in serum within the first week of symptom onset and have been shown to exert different properties such as binding, neutralizing, and Fc-mediated effector functions.[5,6] Although levels of these serum antibodies tend to decay, they can remain stable for months, especially in the case of IgG antibodies.[7–9] Additionally, local immune responses are also expected to be induced in the respiratory tract upon SARS-CoV-2 infection due to ACE2 receptor expression in the human airway epithelia and lung parenchyma.[10,11] Humoral responses in the mucosal compartment are mainly characterized by the production of secretory IgA (sIgA) antibodies.[12,13] These antibodies are generated through a complex multi-step process in which dimeric IgA antibodies secreted by local plasma cells are covalently linked by a protein component known as the joining (J) chain. Then, this complex migrates to the mucosal lumen where a proteolytic cleavage occurs, resulting in the attachment of dimeric IgA to the secretory component (SC). This SC is one of the main features of sIgA and protects the complex from proteolysis. Importantly, mucosal sIgA and IgA antibodies serve as the first line of defense[14,15] against respiratory pathogens such as influenza virus and can effectively block infection.[16,17] Similarly, some studies have reported the presence of virus-specific IgG and IgA in saliva and nasal secretions of patients with COVID-19 disease.[18–20] However, the specific role of local immune responses in mucosal surfaces upon SARS-CoV-2 infection is unclear. On the other hand, there is now evidence that pre-existing immunity against other seasonal human coronaviruses (HCoV) can modulate *de novo* immune responses against SARS-CoV-2 virus.[2,21–25] The authors[2]

[1]Department of Microbiology, Icahn School of Medicine at Mount Sinai, New York, NY 10029, USA
[2]Global Health and Emerging Pathogens Institute, Icahn School of Medicine at Mount Sinai, New York, NY 10029, USA
[3]Graduate School of Biomedical Sciences, Icahn School of Medicine at Mount Sinai, New York, NY 10029, USA
[4]Department of Infectious Diseases, Bellvitge University Hospital, Bellvitge Biomedical Research Institute (IDIBELL), University of Barcelona, L'Hospitalet de Llobregat, 08908 Barcelona, Spain
[5]Center for Biomedical Research in Infectious Diseases (CIBERINFEC), Carlos III Health Institute (ISCII), 28029 Madrid, Spain
[6]Department of Medicine, Division of Infectious Diseases, Icahn School of Medicine at Mount Sinai, New York, NY 10029, USA
[7]The Tisch Cancer Institute, Icahn School of Medicine at Mount Sinai, New York, NY 10029, USA
[8]Department of Pathology, Molecular and Cell-Based Medicine, Icahn School of Medicine at Mount Sinai, New York, NY 10029, USA
[9]The Icahn Genomics Institute, Icahn School of Medicine at Mount Sinai, New York, NY 10029, USA
[10]Lead contact
*Correspondence: adolfo.garcia-sastre@mssm.edu (A.G.-S.), teresa.aydillo-gomez@mssm.edu (T.A.)
https://doi.org/10.1016/j.isci.2024.109210

and others[24–26] have shown that antibody cross-reactivity between conserved epitopes from SARS-CoV-2 proteins and seasonal HCoVs may occur upon SARS-CoV-2 infection.[2] This effect led to an imprinted antibody response on the systemic responses to SARS-CoV-2 antigens. However, our knowledge about the consequences of pre-existing immunity and cross-reactivity to HCoVs on COVID-19 disease outcomes when considering mucosal immune memory is limited. Whether cross-reactive antibodies in respiratory secretions are protective or not against SARS-CoV-2 transmission or severe disease outcomes is not known.

Here, we expand on our previous study[2] and add data on the immune profile in the systemic and mucosal compartments by using our previously published clinical cohort study of SARS-CoV-2-infected individuals—the BACO cohort.[2] We longitudinally characterized the early antibody response and immunoglobulin repertoire against SARS-CoV-2 and seasonal HCoV-OC43 S proteins in the serum and nasopharyngeal (NP) swabs of COVID-19 patients. We found that specific antibody responses against SARS-CoV-2 S protein can be detected in nasal swabs early upon SARS-CoV-2 infection. Half of the patients showed detectable levels of IgG and IgM at baseline, whereas IgA and sIgA were found in 80% and 44% of infected patients, respectively. Moreover, COVID-19 patients showed an induction of IgG and IgA against HCoV-OC43, whereas no specific IgM levels were detected, suggesting a memory recall of pre-existing immune cells targeting conserved S epitopes shared between SARS-CoV-2 and HCoV-OC43 virus. Interestingly, mucosal antibody titers against SARS-CoV-2 peaked at day 7, similar to systemic responses, whereas specific antibodies against HCoV-OC43 showed a higher increase at day 3 post-recruitment. Despite intense efforts to monitor specific immune responses after SARS-CoV-2 infection, we still have limited knowledge about the role of mucosal immunity in COVID-19 disease. This study shows that SARS-CoV-2 infection induces robust mucosal immunity. Additionally, a back-boosting effect of human beta-HCoVs on the mucosal respiratory compartment was present upon SARS-CoV-2 infection.

RESULTS

Systemic antibody responses against SARS-CoV-2 and beta-HCoV-OC43

We used serum samples from a previously published longitudinal cohort of hospitalized COVID-19 patients from Barcelona, Spain—the BACO cohort—[2]to first expand on the systemic immunoglobulin profile against SARS-CoV-2 virus and HCoV-OC43 and second to characterize the immune responses to both SARS-CoV-2 virus and HCoV-OC43 in the local upper respiratory mucosa of COVID-19 patients. A detailed description of clinical characteristics and serum IgG responses against SARS-CoV-2 and other HCoVs antigens in the BACO cohort can be found in Aydillo et al.[2] and Table S1. Briefly, this clinical cohort was composed of a total of 37 COVID-19 patients who were hospitalized at the University Hospital of Bellvitge during the first pandemic wave of SARS-CoV-2 in Barcelona, Spain (March-May 2020). Study participants had a mean age of 67 years and 67% were male. Blood samples were collected longitudinally upon hospital admission (day 0, baseline) and at days 3 and 7 in 33 (89.1%) and 22 (59.4%) patients, respectively. An additional sample was collected at the convalescence period (mean time of 46 days, range 30–56 days) in 28 patients (75.7%). For the present study, we quantified the levels of IgA and IgM antibodies against SARS-CoV-2 and HCoV-OC43 full-length spike (S) protein in the serum samples using enzyme-linked immunosorbent assay (ELISA) and used these data to complement the IgG responses described in Aydillo et al.[2] In general, we observed a strong induction of anti- SARS-CoV-2 S IgA, IgG, and IgM antibodies upon viral infection (Figures 1A and S1A). Antibody titers significantly increased up to day 7 and started waning during the convalesce phase in the case of IgM and IgA. As expected, we found that SARS-CoV-2 infection strongly boosted long-lasting IgG responses as compared with other immunoglobulin isotypes. Consistently, we observed that fold-increase peaked at day 7 post-recruitment, and only IgA and IgM responses decreased at the convalescent time point reaching titers below those detected at day 3 (Figure 1B, and Tables S2 and S3).

We previously showed that the COVID-19 patients from The BACO cohort developed a strong IgG response against the conserved S2 domain of the beta-HCoVs S protein upon SARS-CoV-2 infection. This back-boosting effect related to residual effects from past virus exposures to the antigenically related beta-HCoV-OC43 and HCoV-HKU1.[2] Therefore, we next characterized IgA and IgM against the S protein of HCoVs-OC43 in serum. All patients mounted a strong IgA and IgG response against HCoV-OC43 S, whereas lower levels were detected for IgM antibodies (Figures 1C and S1B). Similar to SARS-CoV-2 responses, IgG titers against HCoV-OC43 S were strongly induced, and levels were higher compared with the other immunoglobulin subtypes. Besides, all immunoglobulins followed a similar induction pattern than antibodies directed against SARS-CoV-2, with peak titers at day 7 post-recruitment (Figure 1D, and Tables S2 and S3). Finally, and to understand whether differences on immunoglobulin levels could influence disease trajectory, we compared the serum antibody responses in patients according to disease severity. For this, COVID-19 patients were classified into mild/moderate (N = 26, 70.3%) or severe/severe end-of-organ disease (EOD, N = 11, 29.7%) based on a previously described severity scale.[27] Figure 2 shows the antibody responses against SARS-CoV-2 and HCoV-OC43 S antigens according to disease phenotype. Data showed no significant differences in the humoral immune response against SARS-CoV-2 nor HCoV-OC43 S protein in mild/moderate versus severe/severe EOD patients. However, severe patients seemed to have lower baseline antibody levels, suggesting a delay in mounting humoral responses against SARS-CoV-2 S as compared with moderate patients.

COVID-19 patients mount robust mucosal antibody responses against SARS-CoV-2 and HCoVs-OC43 in the upper respiratory tract

Immune responses in the mucosal compartment are largely mediated by IgA and secretory IgA (sIgA) antibodies, which have been shown to provide protection against some respiratory infections.[16,17] However, there are no clear data on the role of mucosal immunity on COVID-19 disease. Besides, it is not known whether pre-existing immunity against seasonal HCoVs in the upper respiratory tract could also mediate protection against SARS-CoV-2 infection. We used NP swabs from COVID-19 patients from the BACO cohort to investigate the nature

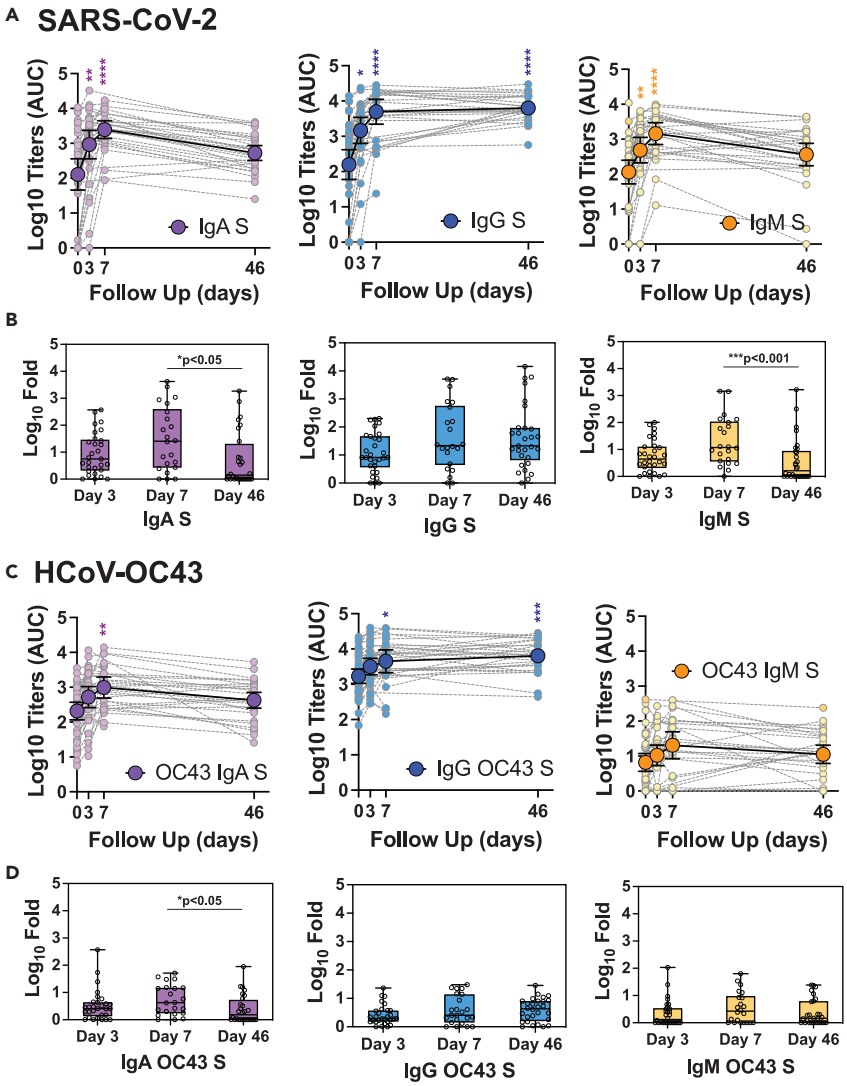

Figure 1. Longitudinal antibody profile against SARS-CoV-2 and seasonal beta-HCoV-OC43 spike proteins in serum

Serum samples from hospitalized COVID-19 patients were collected upon hospital admission (baseline, day 0) and days 3 and 7. A convalescence sample was collected from survivors after recovery with a mean time of 46 days (range, 30–56 days). IgA, IgG, and IgM antibody titers against SARS-CoV-2 full-length S protein (A) and OC43 full-length S protein (C). Antibody titers were calculated and represented as area under the curve (AUC). Small dots with dotted lines represent the antibody response of each individual over time. Geometric mean titer (GMT, big dots) and confidence interval (CI 95%) are also shown. Kruskal-Wallis test was performed to compare differences at each time point over baseline. Statistical significance was considered when $p \leq 0.05$ (*$p < 0.05$, **$p < 0.01$, ***$p < 0.001$, ****$p < 0.0001$, ns, not significant). Fold change antibody titers against SARS-CoV-2 full-length S protein (B) and HCoV-OC43 full-length S protein (D) represented as box-and-whisker diagrams. Box indicates interquartile range (IQR, Q1–Q3) with horizontal line showing the median and vertical lines indicating minimum and maximum. All individual values are represented as small dots. Kruskal-Wallis test was performed, and significant adjusted p values after pairwise comparisons are shown for each comparison. A total of 116 biologically independent serum samples (day 0 = 37, day 3 = 29, day 7 = 22, day 46 = 28) were run against SARS-CoV-2 and HCoV-OC43 S antigens to examine the three different immunoglobulin isotypes using ELISA. ELISAs for each antigen and isotype were performed once due to the limited amount of serum samples. A value of 1 was assigned to the samples with no detectable antibodies.

and dynamics of immune responses in the local immune compartment against both SARS-CoV-2 and HCoV-OC43 S antigens. For this, NP swabs were collected at the same time points than serum samples in 36 out of the 37 hospitalized COVID-19 patients. Acute NP specimens were taken longitudinally upon hospital admission (day 0, baseline) in 34 patients (94.4%) and at days 3 and 7 in 23 (63.9%) and 20 (55.6%) patients, respectively. A follow-up sample during the convalescence phase with a mean time of 46 days after hospital admission (range, 30–56 days) was also collected in four (11.1%) patients. To inactivate any potentially infectious SARS-CoV-2 virus in these samples, NP swabs were treated with Triton X-100 prior to performing any antibody quantification. Importantly, because it has been shown that total IgA antibodies in the saliva can vary between individuals and between samples from the same individual due to factors such as stress,[12,28] we first

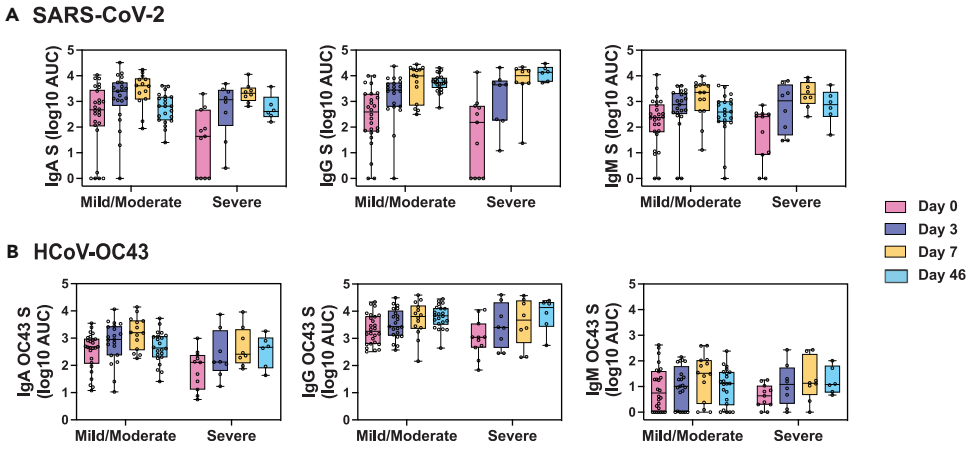

Figure 2. Systemic antibody response according to disease severity in the BACO cohort

Box-and-whisker diagrams of area under the curve (AUC) IgA, IgG, and IgM titers against SARS-CoV-2 S (A) and seasonal HCoV-OC43 S (B) in mild/moderate and severe COVID-19 patients from the BACO cohort. Severity of COVID-19 was assigned following a previously described severity scale.[27] Box indicates interquartile range (IQR, Q1–Q3), with horizontal line showing the median and vertical lines indicating minimum and maximum. All individual values are represented as small dots and each time point is shown in different colors. A total of 116 biologically independent serum samples (day 0 = 37, day 3 = 29, day 7 = 22, day 46 = 28) were run against SARS-CoV-2 and HCoV-OC43 S antigens to assess the antibody isotype profile of these patients using ELISA. A value of 1 was assigned to the samples with no detectable antibodies.

tested whether total IgA titers in the upper respiratory tract were different among the COVID-19 patients from the BACO cohort. Our results showed that COVID-19 patients had comparable concentrations of nasal IgA antibodies (Figure S2A), limiting any potential bias on the quantification of anti- SARS-CoV-2 sIgA antibodies in the nasal cavity. Next, we measured the levels of sIgA, IgA, IgG, and IgM against SARS-CoV-2 full-length S protein in these samples using ELISA assays. Results showed that COVID-19 patients from the BACO cohort developed detectable mucosal immune responses in the upper respiratory tract against SARS-CoV-2 S protein for all the immunoglobulin isotypes tested (Figures 3A and S3A). Additionally, antibody quantification showed higher antibody levels for IgA, IgG, and IgM subtypes compared with antigen-specific sIgA. Interestingly, antibody profiles showed similar kinetics than systemic responses, and peak titers were observed at day 7 post-hospitalization for all the immunoglobulin subtypes tested (Figure 3B and Tables S4 and S5). Next, we characterized and profiled the mucosal immune responses against seasonal HCoV-OC43 full-length S protein in the NP swabs (Figures 3C and S3B). Similar to our previous data on serum, a high percentage of COVID-19 patients showed induction of IgG (N = 15, 41.7%), IgA (N = 28, 77.8%), and sIgA (N = 15, 41.7%) antibodies against HCoV-OC43 S protein in the upper respiratory mucosa. These cross-reactive immune responses, probably directed against conserved epitopes of human beta-HCoVs, showed some degree of maturity as none of the patients showed detectable levels of IgM antibodies. Moreover, anti-OC43 S sIgA, IgA, and IgG titers peaked earlier at day 3 (Figure 3D; Tables S4 and S5), in contrast to the SARS-CoV-2 mucosal responses, suggesting a back-boosting effect upon SARS-CoV-2 infection. These data support our conclusion of this effect being a result of a recall of pre-existing immune memory cells toward conserved beta-HCoVs epitopes.

Next, and to investigate the relationship between systemic and mucosal immune compartments, we performed a correlation analysis of antibody titers in the paired serum samples and NP swabs. Interestingly, a strong correlation between serum and mucosal IgA, IgG, and IgM titers against SARS-CoV-2 S protein was found in the aggregate of samples (Spearman correlation coefficients: 0.54 (IgA), 0.64 (IgG), and 0.62 (IgM); p value <0.0001, respectively) (Figure 4A). On the contrary, serum and nasal anti-OC43 S protein IgA and IgG titers correlated poorly with Spearman correlation coefficients ranging from 0.17 for IgA and 0.34 for IgG levels (p value = 0.19 and 0.01, respectively) (Figure 4B). No correlation analysis was performed for IgM responses against OC43 S as no IgM titers were detected in the mucosal compartment. Additional correlation analysis according to time point of collection between serum and mucosal antibody titers against both SARS-CoV-2 and OC43 S was also performed (Figure S4). To understand whether a correlation was also found between different immunoglobulin isotypes, we performed additional correlation analysis between IgG and IgA serum and mucosal compartments. As expected, a significant positive correlation between both immunoglobulins was found (Figure S5).

Finally, we tested whether humoral immune responses against SARS-CoV-2 and HCoV-OC43 S antigens in the mucosal compartment correlated with disease outcomes. Similar to earlier discussion, we compared antibody responses in the mild/moderate (N = 25, 69.4%) versus severe/severe end-of-organ disease (EOD, N = 11, 30.6%) patients. Mann-Whitney test showed no significant differences in the antibody response against both SARS-CoV-2 and OC43 S antigens between mild/moderate and severe groups in the upper respiratory tract (Figures 5A and 5B). Nonetheless, severe patients tended to have lower early antibody levels similar to systemic responses.

DISCUSSION

The COVID-19 pandemic has highlighted the importance of understanding host immune responses against emerging pathogens. Many advances have been made in characterizing the immunopathogenesis of COVID-19. However, most of the effort has been focused on

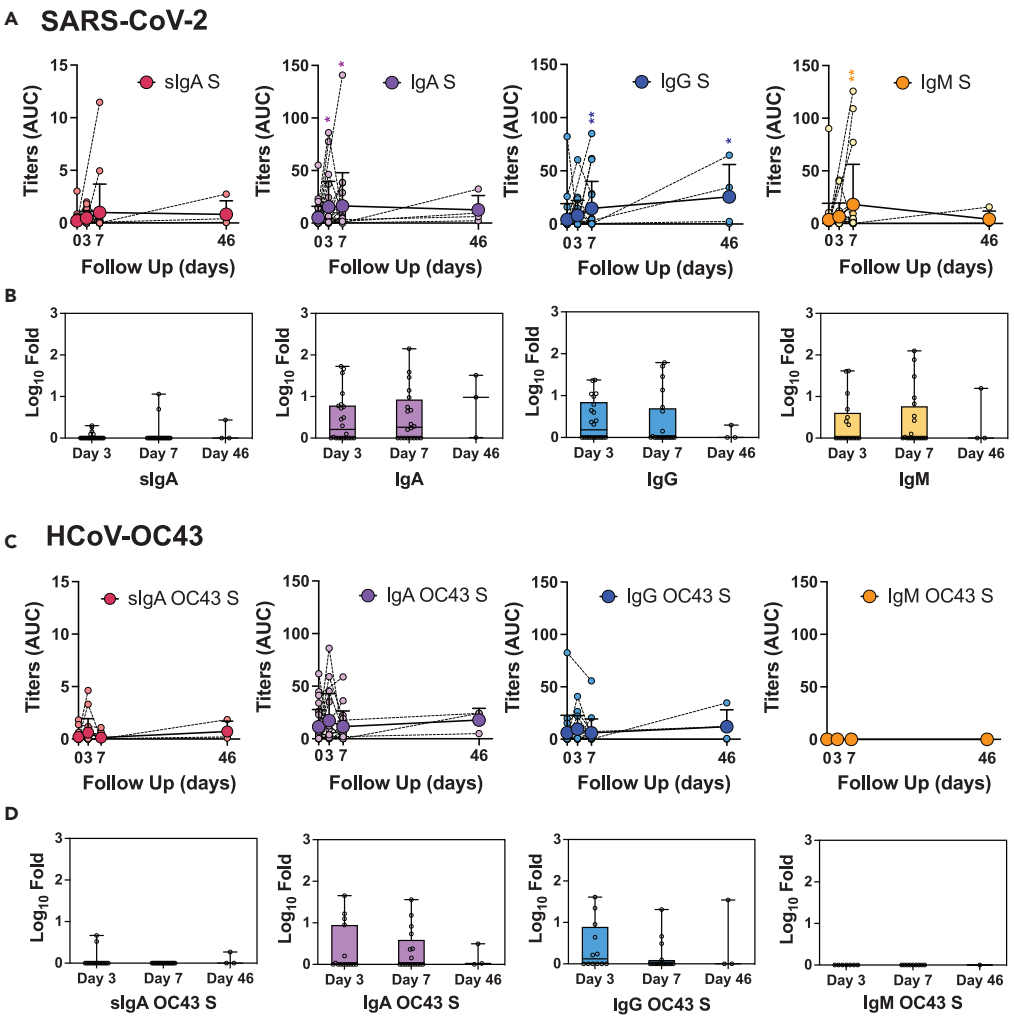

Figure 3. Longitudinal antibody profile against SARS-CoV-2 and seasonal beta-HCoV-OC43 spike proteins in upper respiratory tract

Nasopharyngeal (NP) swabs specimens from hospitalized COVID-19 patients were collected upon hospital admission (baseline, day 0), and days 3 and 7. A convalescence sample was collected from survivors after recovery with a mean time of 46 days (range, 30–56 days). Secretory IgA (sIgA), IgA, IgG, and IgM antibody titers against SARS-CoV-2 full-length S protein (A) and HCoV-OC43 full-length S protein (C). Antibody titers were calculated and represented as area under the curve (AUC). Small dots with dotted lines represent the longitudinal antibody profile of each individual. Mean titers (big dots) and standard deviation (SD) are also shown. Kruskal-Wallis test was performed to compare differences at each time point over baseline. Statistical significance was considered when $p \leq 0.05$ (*$p < 0.05$, **$p < 0.01$, ***$p < 0.001$, ****$p < 0.0001$; ns, not significant). Fold change antibody titers against SARS-CoV-2 full-length S protein (B) and HCoV-OC43 full-length S protein (D) represented as box-and-whisker diagrams. Box indicates interquartile range (IQR, Q1–Q3), with horizontal line showing the median and vertical lines indicating minimum and maximum. All individual values are represented as small dots. Kruskal-Wallis test was performed, and significant adjusted p values after pairwise comparisons are shown for each comparison. A total of 81 biologically independent NP swabs samples were collected. Number of NP samples run against each S antigen and immunoglobulin subtype and summarized in Table S6. A value of 0.001 was assigned to the samples with no detectable antibodies.

understanding systemic immune responses after COVID-19 infection and vaccination, and little attention has been given, so far, to the role of local immune responses in mucosal surfaces, like the upper respiratory tract. Although some studies have documented the presence of virus-specific IgG and IgA in saliva and NP samples of patients with COVID-19 infection or vaccination, these studies failed to address the role of adaptive immune mechanisms at mucosal sites in preventing transmission or severe outcomes. Here, we provide a dynamic and comprehensive characterization of the immunoglobulin repertoire elicited in the mucosal compartment upon SARS-CoV-2 infection. Additional studies should be conducted to analyze the impact of these responses in protection against SARS-CoV-2 infection.

sIgA and IgA antibodies are the predominant immunoglobulin isotypes at mucosal surfaces.[12,29] We found a strong induction of IgA antibodies against SARS-CoV-2 S protein in the upper respiratory tract. Moreover, our results showed robust mucosal sIgA production in the NP swabs from the BACO cohort by measuring the SC levels associated with SARS-CoV-2 S-specific antibodies (Figures 3A and 3B). Although some studies have found that IgA levels in the saliva can be very variable due to differences in the method of sample collection,[12,28] our results

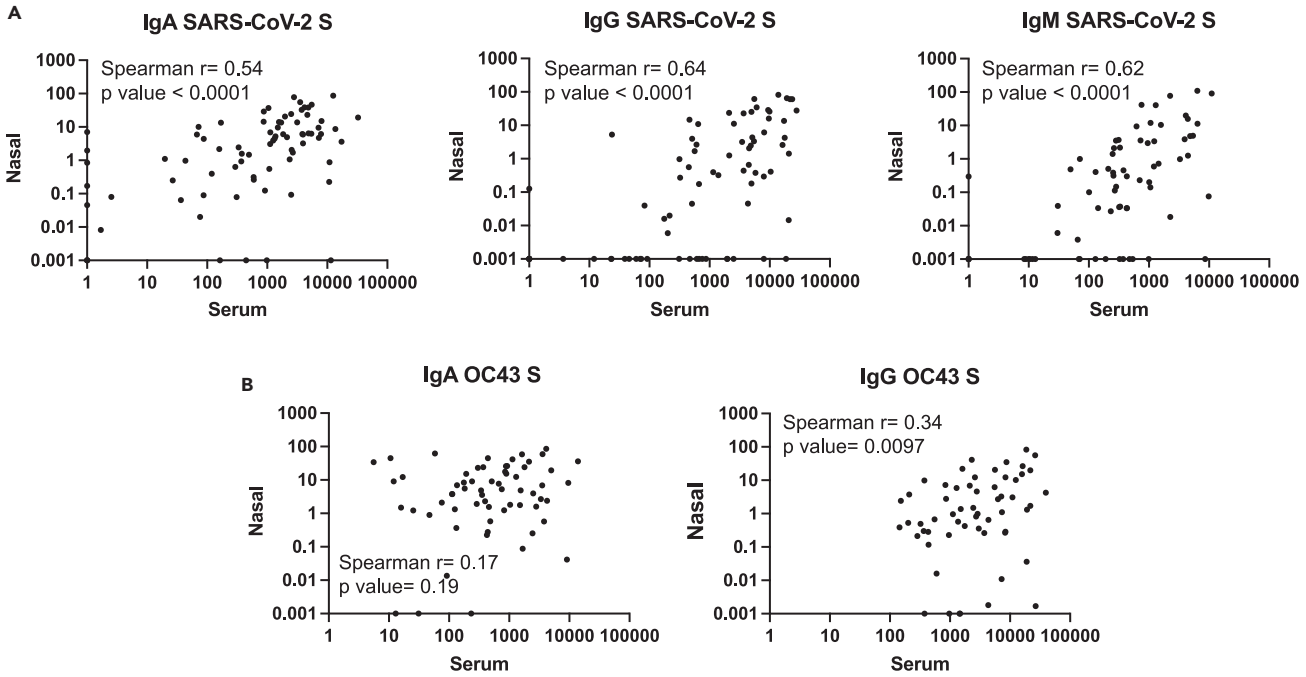

Figure 4. Correlation between antibody responses in serum and upper respiratory tract

(A) Correlation between anti-SARS-CoV-2 S IgA, IgG, and IgM antibody titers measured in serum and NP swabs.

(B) Correlation between anti-HCoV-OC43 S IgA and IgG antibody titers measured in serum and NP swabs. Number of NP swabs and paired serum samples for each correlation analysis is summarized in Table S7. Spearman correlation coefficient and p values (two-tailed) are shown above each graph. A value of 1 or 0.001 was assigned to serum or mucosal samples, respectively, when no antibodies were detected.

showed equivalent levels of non-specific IgA in the upper respiratory tract of these COVID-19 patients (Figure S2), and therefore, no normalization was required to assess antigen-specific sIgA responses. Importantly, our study shows that IgA and sIgA antibodies are robustly induced in the mucosal compartment upon SARS-CoV-2 infection. This is important because recent publications have also described the production of specific mucosal IgA responses during SARS-CoV-2 mRNA intramuscular vaccination.[28,30] Although it is still unclear the mechanism by which intramuscularly vaccines induced mucosal sIgA responses, there is a growing interest to develop next-generation COVID-19 vaccines that boost mucosal antibody responses in the nasal cavity to potentially reduce viral transmission and protect from severe disease.[31] In this scenario, mucosal vaccines delivered intranasally would be ideal.[32,33] However, many questions about the nature and durability of mucosal responses upon SARS-CoV-2 infection or vaccination remained opened. Some preliminary studies have suggested that mucosal immunity could last up to 7 months after SARS-CoV-2 infection,[34] whereas others have described low-level but durable (>6 months) sIgA response after COVID-19 mRNA vaccination.[35] Further research is needed to develop next-generation COVID-19 vaccine candidates that could provide broader and lasting immune protection against emerging SARS-CoV-2 variants in the systemic and mucosal compartments.

In this context, the potential effect of an imprinted immune response to human coronaviruses is of great importance. We have previously shown that systemic IgG responses against SARS-CoV-2 antigens are strongly induced in COVID-19 patients from the BACO cohort.[2] Additionally, when we quantified the levels of pre-existing immunity against seasonal HCoVs OC43, HKU1, and 229E in the serum samples from these patients, we found a strong back-boosting effect to conserved epitopes of the S protein from beta-HCoV OC43 and HKU1. Importantly, this memory recall to conserved S antigens of seasonal beta-HCoVs negatively correlated with *de novo* antibody responses to SARS-CoV-2 virus. Although our previous study provides evidence of immunological imprinting in the systemic compartment, it still remains unknown whether imprinting could also occur in the upper respiratory tract. In the present study, we detected IgG, sIgA, and IgA antibodies against HCoV-OC43 S protein in the local upper respiratory mucosa, whereas no IgM responses were observed (Figure 3C). Moreover, antibody responses against HCoV-OC43 S peaked earlier than SARS-CoV-2 S antibody titers in the local mucosa (Figure 3D, and Table S3), suggesting some maturity in the cross-reactive immune responses against conserved epitopes of beta-HCoVs in the upper respiratory tract. Further studies are needed to address the role of immune imprinting in the mucosal compartment during COVID-19 disease. However, our findings support the idea that upon SARS-CoV-2 infection, memory B cells generated from prior infections with antigenically related HCoVs will be rapidly activated, perhaps competing with the activation of naive B cells specific for SARS-CoV-2 novel epitopes.

Limitations of the study

There are some potential limitations in our study. The BACO cohort is composed of 37 hospitalized COVID-19 patients from Spain, a relatively small number of individuals in a study cohort. Still, this number of participants allowed us to perform a robust and unbiased descriptive

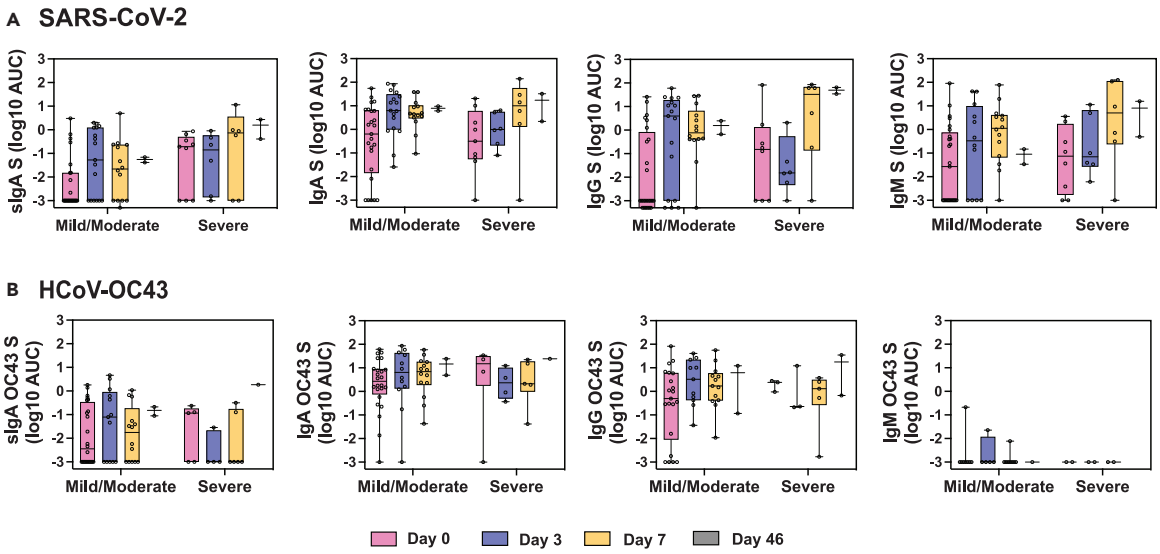

Figure 5. Antibody response in the upper respiratory tract according to disease severity in the BACO cohort

Box-and-whisker diagrams of area under the curve (AUC) ELISA IgA, IgG, and IgM titers against SARS-CoV-2 spike (A) and seasonal HCoV-OC43 spike (B) in mild/moderate and severe COVID-19 patients from the BACO cohort. Severity of COVID-19 was assigned following a previously described severity scale.[27] Box indicates interquartile range (IQR, Q1–Q3), with horizontal line showing the median and vertical lines indicating minimum and maximum. All individual values are represented as small dots, and each time point is shown in different color. A total of 81 biologically independent NP samples were collected. Number of NP samples run against each S antigen and immunoglobulin subtype and summarized in Table S6. A value of 0.001 was assigned to the samples with no detectable antibodies.

characterization of the immunoglobulin repertoire in the local mucosa. Although this number could limit some potential conclusions on the role of mucosal immune responses in disease outcome, our data allowed to detect specific trends, and severe patients showed a delay in antibody responses to SARS-CoV-2 antigens when compared with mild cases. Additionally, as found by the authors and others,[28] levels of mucosal sIgA were generally lower as compared with total specific IgA titers that could have also compromised the statistical power of the analysis. Moreover, no long-term samples were collected; therefore, we still do not know the durability of the immune response in the upper respiratory tract. In summary, our study provides a better understanding of the immune responses elicited in the upper respiratory tract upon SARS-CoV-2 infection as well as some evidence of pre-existing immunity and immune memory recall in the local respiratory mucosa in COVID-19 disease.

STAR★METHODS

Detailed methods are provided in the online version of this paper and include the following:

- KEY RESOURCES TABLE
- RESOURCE AVAILABILITY
  - Lead contact
  - Materials availability
  - Data and code availability
- EXPERIMENTAL MODEL AND STUDY PARTICIPANT DETAILS
  - The BACO cohort
  - Recombinant proteins
- METHOD DETAILS
  - Antigen-specific IgG, IgM and IgA ELISAs in serum
  - Antigen-specific sIgA, IgA, IgG and IgM ELISAs in nasopharyngeal swabs
  - Quantification of total IgA in nasopharyngeal swabs
- QUANTIFICATION AND STATISTICAL ANALYSIS

SUPPLEMENTAL INFORMATION

Supplemental information can be found online at https://doi.org/10.1016/j.isci.2024.109210.

ACKNOWLEDGMENTS

We thank the BACO cohort patients and their families. We also thank Richard Cadagan for excellent technical assistance. This work was partly funded by CRIPT (Center for Research on Influenza Pathogenesis and Transmission) and NIAID-funded Center of Excellence for Influenza Research and Response (CEIRR, contract # 75N93021C00014) to A.G.-S and T.A. and the Systems Biology Lens (SYBIL, # U19AI135972) and the Viral Immunity and Vaccination (VIVA) Human Immunology Project Consortium (HIPC) (# U19AI168631) to A.G.-S. T.A. was also funded by the American Lung Association: ALA grant # COVID-1034091.

AUTHOR CONTRIBUTIONS

T.A. and A.G.S. conceived and designed the study. T.A. supervised and provided training to A.E. and A.R.F. A.E. optimized and performed experiments. A.R.F. performed experiments. A.R., G.A.A., and J.C. collected samples and clinical data. T.A., A.G.S., and J.C. supervised the study. T.A. and A.E. analyzed data, prepared figures, and wrote the manuscript. All authors reviewed the manuscript.

DECLARATION OF INTERESTS

The A.G.-S. laboratory has received research support from GSK, Pfizer, Senhwa Biosciences, Kenall Manufacturing, Blade Therapeutics, Avimex, Johnson & Johnson, Dynavax, 7Hills Pharma, Pharmamar, ImmunityBio, Accurius, Nanocomposix, Hexamer, N-fold LLC, Model Medicines, Atea Pharma, Applied Biological Laboratories, and Merck, outside of the reported work. A.G.-S. has consulting agreements for the following companies involving cash and/or stock: Castlevax, Amovir, Vivaldi Biosciences, Contrafect, 7Hills Pharma, Avimex, Pagoda, Accurius, Esperovax, Farmak, Applied Biological Laboratories, Pharmamar, CureLab Oncology, CureLab Veterinary, Synairgen, Paratus, Pfizer, and Prosetta, outside of the reported work. A.G.-S. has been an invited speaker in meeting events organized by Seqirus, Janssen, Abbott, and AstraZeneca. A.G.-S. is inventor on patents and patent applications on the use of antivirals and vaccines for the treatment and prevention of virus infections and cancer, owned by the Icahn School of Medicine at Mount Sinai, New York, outside of the reported work.

Received: November 1, 2023
Revised: December 15, 2023
Accepted: February 7, 2024
Published: February 10, 2024

REFERENCES

1. Zhu, N., Zhang, D., Wang, W., Li, X., Yang, B., Song, J., Zhao, X., Huang, B., Shi, W., Lu, R., et al. (2020). A Novel Coronavirus from Patients with Pneumonia in China, 2019. N. Engl. J. Med. *382*, 727–733. https://doi.org/10.1056/NEJMoa2001017.
2. Aydillo, T., Rombauts, A., Stadlbauer, D., Aslam, S., Abelenda-Alonso, G., Escalera, A., Amanat, F., Jiang, K., Krammer, F., Carratala, J., and García-Sastre, A. (2021). Immunological imprinting of the antibody response in COVID-19 patients. Nat. Commun. *12*, 3781. https://doi.org/10.1038/s41467-021-23977-1.
3. Long, Q.-X., Liu, B.-Z., Deng, H.-J., Wu, G.-C., Deng, K., Chen, Y.-K., Liao, P., Qiu, J.-F., Lin, Y., Cai, X.-F., et al. (2020). Antibody responses to SARS-CoV-2 in patients with COVID-19. Nat. Med. *26*, 845–848. https://doi.org/10.1038/s41591-020-0897-1.
4. Suthar, M.S., Zimmerman, M.G., Kauffman, R.C., Mantus, G., Linderman, S.L., Hudson, W.H., Vanderheiden, A., Nyhoff, L., Davis, C.W., Adekunle, O., et al. (2020). Rapid Generation of Neutralizing Antibody Responses in COVID-19 Patients. Cell Rep. Med. *1*, 100040. https://doi.org/10.1016/j.xcrm.2020.100040.
5. Tso, F.Y., Lidenge, S.J., Poppe, L.K., Peña, P.B., Privatt, S.R., Bennett, S.J., Ngowi, J.R., Mwaiselage, J., Belshan, M., Siedlik, J.A., et al. (2021). Presence of antibody-dependent cellular cytotoxicity (ADCC) against SARS-CoV-2 in COVID-19 plasma. PLoS One *16*, e0247640. https://doi.org/10.1371/journal.pone.0247640.
6. Yu, Y., Wang, M., Zhang, X., Li, S., Lu, Q., Zeng, H., Hou, H., Li, H., Zhang, M., Jiang, F., et al. (2021). Antibody-dependent cellular cytotoxicity response to SARS-CoV-2 in COVID-19 patients. Signal Transduct. Target. Ther. *6*, 346. https://doi.org/10.1038/s41392-021-00759-1.
7. Wajnberg, A., Amanat, F., Firpo, A., Altman, D.R., Bailey, M.J., Mansour, M., McMahon, M., Meade, P., Mendu, D.R., Muellers, K., et al. (2020). Robust neutralizing antibodies to SARS-CoV-2 infection persist for months. Science *370*, 1227–1230. https://doi.org/10.1126/science.abd7728.
8. Seow, J., Graham, C., Merrick, B., Acors, S., Pickering, S., Steel, K.J.A., Hemmings, O., O'Byrne, A., Kouphou, N., Galao, R.P., et al. (2020). Longitudinal observation and decline of neutralizing antibody responses in the three months following SARS-CoV-2 infection in humans. Nat. Microbiol. *5*, 1598–1607. https://doi.org/10.1038/s41564-020-00813-8.
9. Anand, S.P., Prévost, J., Nayrac, M., Beaudoin-Bussières, G., Benlarbi, M., Gasser, R., Brassard, N., Laumaea, A., Gong, S.Y., Bourassa, C., et al. (2021). Longitudinal analysis of humoral immunity against SARS-CoV-2 Spike in convalescent individuals up to 8 months post-symptom onset. Cell Rep. Med. *2*, 100290. https://doi.org/10.1016/j.xcrm.2021.100290.
10. Hoffmann, M., Kleine-Weber, H., Schroeder, S., Krüger, N., Herrler, T., Erichsen, S., Schiergens, T.S., Herrler, G., Wu, N.H., Nitsche, A., et al. (2020). SARS-CoV-2 Cell Entry Depends on ACE2 and TMPRSS2 and Is Blocked by a Clinically Proven Protease Inhibitor. Cell *181*, 271–280.e8. https://doi.org/10.1016/j.cell.2020.02.052.
11. Jia, H.P., Look, D.C., Shi, L., Hickey, M., Pewe, L., Netland, J., Farzan, M., Wohlford-Lenane, C., Perlman, S., and McCray, P.B., Jr. (2005). ACE2 receptor expression and severe acute respiratory syndrome coronavirus infection depend on differentiation of human airway epithelia. J. Virol. *79*, 14614–14621. https://doi.org/10.1128/jvi.79.23.14614-14621.2005.
12. Brandtzaeg, P. (2007). Induction of secretory immunity and memory at mucosal surfaces. Vaccine *25*, 5467–5484. https://doi.org/10.1016/j.vaccine.2006.12.001.
13. Corthésy, B. (2013). Multi-Faceted Functions of Secretory IgA at Mucosal Surfaces. Front. Immunol. *4*, 185. https://doi.org/10.3389/fimmu.2013.00185.
14. Bakema, J.E., and van Egmond, M. (2011). The human immunoglobulin A Fc receptor FcαRI: a multifaceted regulator of mucosal immunity. Mucosal Immunol. *4*, 612–624. https://doi.org/10.1038/mi.2011.36.
15. Breedveld, A., and van Egmond, M. (2019). IgA and FcαRI: Pathological Roles and Therapeutic Opportunities. Front. Immunol. *10*, 553. https://doi.org/10.3389/fimmu.2019.00553.
16. Tamura, S.-I., Funato, H., Hirabayashi, Y., Kikuta, K., Suzuki, Y., Nagamine, T., Aizawa, C., Nakagawa, M., and Kurata, T. (1990). Functional role of respiratory tract haemagglutinin-specific IgA antibodies in protection against influenza. Vaccine *8*, 479–485. https://doi.org/10.1016/0264-410X(90)90250-P.

17. Terauchi, Y., Sano, K., Ainai, A., Saito, S., Taga, Y., Ogawa-Goto, K., Tamura, S.I., Odagiri, T., Tashiro, M., Fujieda, M., et al. (2018). IgA polymerization contributes to efficient virus neutralization on human upper respiratory mucosa after intranasal inactivated influenza vaccine administration. Hum. Vaccin. Immunother. *14*, 1351–1361. https://doi.org/10.1080/21645515.2018.1438791.

18. Wright, P.F., Prevost-Reilly, A.C., Natarajan, H., Brickley, E.B., Connor, R.I., Wieland-Alter, W.F., Miele, A.S., Weiner, J.A., Nerenz, R.D., and Ackerman, M.E. (2022). Longitudinal Systemic and Mucosal Immune Responses to SARS-CoV-2 Infection. J. Infect. Dis. *226*, 1204–1214. https://doi.org/10.1093/infdis/jiac065.

19. Sterlin, D., Mathian, A., Miyara, M., Mohr, A., Anna, F., Claër, L., Quentric, P., Fadlallah, J., Devilliers, H., Ghillani, P., et al. (2021). IgA dominates the early neutralizing antibody response to SARS-CoV-2. Sci. Transl. Med. *13*, eabd2223. https://doi.org/10.1126/scitranslmed.abd2223.

20. Isho, B., Abe, K.T., Zuo, M., Jamal, A.J., Rathod, B., Wang, J.H., Li, Z., Chao, G., Rojas, O.L., Bang, Y.M., et al. (2020). Persistence of serum and saliva antibody responses to SARS-CoV-2 spike antigens in COVID-19 patients. Sci. Immunol. *5*, eabe5511. https://doi.org/10.1126/sciimmunol.abe5511.

21. Ng, K.W., Faulkner, N., Cornish, G.H., Rosa, A., Harvey, R., Hussain, S., Ulferts, R., Earl, C., Wrobel, A.G., Benton, D.J., et al. (2020). Preexisting and *de novo* humoral immunity to SARS-CoV-2 in humans. Science *370*, 1339–1343. https://doi.org/10.1126/science.abe1107.

22. Nguyen-Contant, P., Embong, A.K., Kanagaiah, P., Chaves, F.A., Yang, H., Branche, A.R., Topham, D.J., and Sangster, M.Y. (2020). S Protein-Reactive IgG and Memory B Cell Production after Human SARS-CoV-2 Infection Includes Broad Reactivity to the S2 Subunit. mBio *11*, e01991-20. https://doi.org/10.1128/mBio.01991-20.

23. Miyara, M., Saichi, M., Sterlin, D., Anna, F., Marot, S., Mathian, A., Atif, M., Quentric, P., Mohr, A., Claër, L., et al. (2022). Pre-COVID-19 Immunity to Common Cold Human Coronaviruses Induces a Recall-Type IgG Response to SARS-CoV-2 Antigens Without Cross-Neutralisation. Front. Immunol. *13*, 790334. https://doi.org/10.3389/fimmu.2022.790334.

24. Grifoni, A., Weiskopf, D., Ramirez, S.I., Mateus, J., Dan, J.M., Moderbacher, C.R., Rawlings, S.A., Sutherland, A., Premkumar, L., Jadi, R.S., et al. (2020). Targets of T Cell Responses to SARS-CoV-2 Coronavirus in Humans with COVID-19 Disease and Unexposed Individuals. Cell *181*, 1489–1501.e15. https://doi.org/10.1016/j.cell.2020.05.015.

25. Mateus, J., Grifoni, A., Tarke, A., Sidney, J., Ramirez, S.I., Dan, J.M., Burger, Z.C., Rawlings, S.A., Smith, D.M., Phillips, E., et al. (2020). Selective and cross-reactive SARS-CoV-2 T cell epitopes in unexposed humans. Science *370*, 89–94. https://doi.org/10.1126/science.abd3871.

26. Braun, J., Loyal, L., Frentsch, M., Wendisch, D., Georg, P., Kurth, F., Hippenstiel, S., Dingeldey, M., Kruse, B., Fauchere, F., et al. (2020). SARS-CoV-2-reactive T cells in healthy donors and patients with COVID-19. Nature *587*, 270–274. https://doi.org/10.1038/s41586-020-2598-9.

27. Del Valle, D.M., Kim-Schulze, S., Huang, H.H., Beckmann, N.D., Nirenberg, S., Wang, B., Lavin, Y., Swartz, T.H., Madduri, D., Stock, A., et al. (2020). An inflammatory cytokine signature predicts COVID-19 severity and survival. Nat. Med. *26*, 1636–1643. https://doi.org/10.1038/s41591-020-1051-9.

28. Sano, K., Bhavsar, D., Singh, G., Floda, D., Srivastava, K., Gleason, C., PARIS Study Group, Carreño, J.M., Simon, V., and Krammer, F. (2022). SARS-CoV-2 vaccination induces mucosal antibody responses in previously infected individuals. Nat. Commun. *13*, 5135. https://doi.org/10.1038/s41467-022-32389-8.

29. Russell, M.W. (2007). Biological Functions of IgA. In Mucosal Immune Defense: Immunoglobulin A, C.S. Kaetzel, ed. (Springer US), pp. 144–172. https://doi.org/10.1007/978-0-387-72232-0_6.

30. Sheikh-Mohamed, S., Isho, B., Chao, G.Y.C., Zuo, M., Cohen, C., Lustig, Y., Nahass, G.R., Salomon-Shulman, R.E., Blacker, G., Fazel-Zarandi, M., et al. (2022). Systemic and mucosal IgA responses are variably induced in response to SARS-CoV-2 mRNA vaccination and are associated with protection against subsequent infection. Mucosal Immunol. *15*, 799–808. https://doi.org/10.1038/s41385-022-00511-0.

31. Russell, M.W., Moldoveanu, Z., Ogra, P.L., and Mestecky, J. (2020). Mucosal immunity in COVID-19: a neglected but critical aspect of SARS-CoV-2 infection. Front. Immunol. *11*, 611337.

32. Sun, W., Liu, Y., Amanat, F., González-Domínguez, I., McCroskery, S., Slamanig, S., Coughlan, L., Rosado, V., Lemus, N., Jangra, S., et al. (2021). A Newcastle disease virus expressing a stabilized spike protein of SARS-CoV-2 induces protective immune responses. Nat. Commun. *12*, 6197. https://doi.org/10.1038/s41467-021-26499-y.

33. Zhang, L., Jiang, Y., He, J., Chen, J., Qi, R., Yuan, L., Shao, T., Zhao, H., Chen, C., Chen, Y., et al. (2023). Intranasal influenza-vectored COVID-19 vaccine restrains the SARS-CoV-2 inflammatory response in hamsters. Nat. Commun. *14*, 4117. https://doi.org/10.1038/s41467-023-39560-9.

34. Marking, U., Bladh, O., Havervall, S., Svensson, J., Greilert-Norin, N., Aguilera, K., Kihlgren, M., Salomonsson, A.C., Månsson, M., Gallini, R., et al. (2023). 7-month duration of SARS-CoV-2 mucosal immunoglobulin-A responses and protection. Lancet Infect. Dis. *23*, 150–152. https://doi.org/10.1016/s1473-3099(22)00834-9.

35. Zuo, F., Marcotte, H., Hammarström, L., and Pan-Hammarström, Q. (2022). Mucosal IgA against SARS-CoV-2 Omicron Infection. N. Engl. J. Med. *387*, e55. https://doi.org/10.1056/NEJMc2213153.

STAR★METHODS

KEY RESOURCES TABLE

REAGENT or RESOURCE	SOURCE	IDENTIFIER
Antibodies		
Anti-human IgG-HRP antibody (Fc-specific)	Sigma-Aldrich	Cat. #A0170; RRID: AB_257868
Anti-human IgM-HRP antibody	Sigma-Aldrich	Cat. #A6907; RRID: AB_258318
Anti-human IgA-HRP antibody (α-chain)	Sigma-Aldrich	Cat. #A0295; RRID: AB_257876
Anti-human sIgA antibody	Millipore	Cat. #411423; RRID: AB_10681347
Anti-mouse IgG-HRP antibody	Abcam	Cat. #ab6823; RRID: AB_955395
Anti-human IgA antibody	Bethyl Laboratories	Cat. #A80-102A
Biological samples		
Human serum samples from COVID-19 infected individuals from 'The BACO Cohort'	University Hospital of Bellvitge, Barcelona (Spain)	*Aydillo* et al., *2021*[2]
Human nasopharyngeal swabs from COVID-19 infected individuals from 'The BACO Cohort'	University Hospital of Bellvitge, Barcelona	
Chemicals, peptides, and recombinant proteins		
SARS-CoV-2 full-length spike protein	Sino Biological	Cat. #40589-V08H4
OC43 full-length spike protein	Sino Biological	Cat. #40607-V08B
3,3′ ,5,5′ -Tetra- methylbenzidine (TMBE)	Rockland	Cat. #TMBE-1000
Sulfuric Acid 2M	Fisher Scientific	Cat. #S25898
Software and algorithms		
GraphPad Prism 9	GraphPad	https://www.graphpad.com/scientific-software/prism/
Other		
Phosphate-buffered saline (PBS)	Corning	Cat. #21-040-CV
Tween-20	Fisher Scientific	Cat. #BP337-100
Non-fat milk powder	RPI	Cat. #M17200-500
Triton X-100	Fisher Scientific	Cat. #BP151-500
4 HBX 96-well microtiter plates	Thermo Fisher Scientific	Cat. #3855
405 TS microplate washer	BioTek	
Synergy 4 plate reader	BioTek	

RESOURCE AVAILABILITY

Lead contact

Further information and requests for resources and reagents should be directed to and will be fulfilled by the lead contact, Teresa Aydillo (teresa.aydillo-gomez@mssm.edu).

Materials availability

This study did not generate new unique reagents.

Data and code availability

- All data reported in this paper will be shared by the lead contact upon request.
- This paper does not report original code.
- Any additional information required to reanalyze the data reported in this paper is available from the lead contact upon request.

EXPERIMENTAL MODEL AND STUDY PARTICIPANT DETAILS

The BACO cohort

The BACO cohort is a prospective human cohort study of COVID-19 disease carried out during the first pandemic wave (March–May 2020) of SARS-CoV-2 in Barcelona (Spain). A positive COVID-19 case was defined according to international guidelines when a nasopharyngeal (NP) swab tested positive for SARS-CoV-2 by reverse transcriptase quantitative polymerase chain reaction (RT-qPCR) upon hospital admission. All patients or their legally authorized representatives provided informed consent prior to sample and data collection. Samples from patients including serum and NP swabs, were collected at the enrollment in the study (baseline), and at days 3 and 7 post enrollment. A convalescence sample was collected from survivors after recovery and hospital discharge with a mean time of 46 days (range, 30–56 days). The total number of serum samples and NP swabs was 116 and 81, respectively. All samples were stored at -80°C. Data on demographics, including age and sex, comorbidities, clinical signs and symptoms, interventions, and outcomes are described in Table S1. Severity of COVID-19 was assigned following a described severity scale based on oxygen saturation (SpO2), presence of pneumonia/imaging, oxygen support defined as use of high-flow nasal cannula (HFNC), non-rebreather mask (NRB), bilevel positive airway pressure (BIPAP) or mechanical ventilation (MV); and kidney (creatinine clearance, CrCl) and liver (alanine aminotransferase, ALT) function:[27] mild (SpO2 > 94% AND no pneumonia), moderate (SpO2 < 94% AND/OR pneumonia), severe (use of HFNC, NRB, BIPAP or MV AND no vasopressor use AND CrCl >30 AND ALT < 5x upper limit of normal) and severe with end-of organ disease (Use of HFNC, NRB, BIPAP or MV AND vasopressor use OR CrCl >30 or new HD OR ALT < 5x upper limit of normal). The study protocol was approved by the Institutional Review Board of University Hospital of Bellvitge, Barcelona, Spain, and by the Icahn School of Medicine at Mount Sinai, New York, US.

Recombinant proteins

The recombinant spike proteins from SARS-CoV-2 and beta-coronavirus OC43 were purchased from Sino Biological (Cat. #40589-V08H4 and #40607-V08B). Proteins were stored at -80°C until use.

METHOD DETAILS

Antigen-specific IgG, IgM and IgA ELISAs in serum

Serum ELISAs against SARS-CoV-2 and OC43 spike proteins were performed as previously described.[2] Briefly, Immulon 4 HBX 96-well microtiter plates (Thermo Fisher Scientific) were coated overnight at 4°C with 50 μL recombinant protein (SARS-CoV-2 or OC43 full-length spike, respectively) at a concentration of 2 μg/mL. The next day, the plates were washed three times with phosphate-buffered saline (PBS; Corning) containing 0.1% Tween-20 (PBS-T, Fisher Scientific) using an automatic plate washer (BioTek). After washing, the plates were blocked for 1 h at room temperature (RT) with 200 μl/well of 3% (w/v) non-fat milk powder diluted in PBS-T. The blocking solution was removed, and 100 μL of serum samples diluted (starting concentration of 1:80 and serially diluted three-fold) in PBS-T containing 1% (w/v) non-fat milk was added to the wells and incubated for 1 h at RT. The plates were washed three times with PBS-T and 100 μl of anti-human IgG-HRP antibody (Fc-specific) (Sigma, Cat. A0170) at a dilution of 1:20,000; or anti-human IgM-HRP antibody at a dilution 1:3000 (Sigma, Cat. A6907); or anti-human IgA-HRP antibody (α-chain) at a dilution 1:3000 (Sigma, Cat. A0295) was added to the wells. All secondary antibodies were diluted in PBS-T containing 1% (w/v) non-fat milk and incubated for 1h at RT. The plates were washed four times with PBS-T with shaking using the plate washer and 100 μL of TMBE (Rockland) was added to all wells for 10 min. The reaction was stopped by the addition of 100 μL of sulfuric acid per well. Optical density (OD) at a wavelength of 450 nm was read using Synergy 4 (BioTek) plate reader. OD values of samples were adjusted by subtracting the average of the blank plus three times the standard deviation of the blank. Area under the curve (AUC) values were computed by plotting normalized OD values against the reciprocal serum sample dilutions in GraphPad Prism. The assay was done one per sample due to the limited amount of sample.

Antigen-specific sIgA, IgA, IgG and IgM ELISAs in nasopharyngeal swabs

All nasopharyngeal swabs were treated with 0.5% Triton X-100 (v/v) to inactivate SARS-CoV-2 virus prior performing any experiments. Sample inactivation was performed in an enhanced biosafety level 2 (BSL-2+) facility following Icahn School of Medicine biosafety guidelines. Immulon 4 HBX 96-well microtiter plates (Thermo Fisher Scientific) were coated overnight at 4°C with 50 μL recombinant protein (SARS-CoV-2 or OC43 full-length spike, respectively) at a concentration of 2 μg/mL. The next day, the plates were washed three times with PBS-T using an automatic plate washer (BioTek). After washing, the plates were blocked for 1 h at RT with 200 μl/well of 5% (w/v) non-fat milk powder diluted in PBS-T. The blocking solution was removed, and 50 μL of inactivated nasopharyngeal swab (starting undiluted and serially diluted two-fold with PBS-T containing 2.5% (w/v) non-fat milk) was added to the wells and incubated at 4°C overnight. The next day, plates were washed three times with PBS-T using the plate washer. For sIgA detection, 100 μl of anti-human sIgA antibody (Millipore, Cat. 411423) diluted to 5 μg/mL in PBS-T containing 2.5% (w/v) non-fat milk were added to the wells and incubated for 2 h at RT. Plates were washed again three times with PBS-T using the plate washer and secondary anti-mouse IgG-HRP antibody (Abcam, Cat. ab6823) diluted 1:5000 in 2.5% (w/v) non-fat milk PBS-T was added to the wells. For IgA, IgG and IgM measurement, incubation of samples with antigen was also performed overnight at 4°C. After washing with PBS-T three times, 100 μl of anti-human IgA-HRP antibody (α-chain) (Sigma, Cat. A0295) at a dilution of 1:3000; or anti-human IgG-HRP antibody (Fc-specific) (Sigma, Cat. A0170) at a dilution of 1:20,000; or anti-human IgM-HRP antibody at a dilution 1:3000 (Sigma, Cat. A6907) was added to the wells. All secondary antibodies were diluted in PBS-T containing 2.5% (w/v) non-fat milk and incubated for 1 h at RT. After incubation with the corresponding secondary HRP-conjugated antibodies, plates were washed four times with PBS-T with shaking using

the plate washer and 100 μL of TMBE (Rockland) was added to all wells for 10 min. The reaction was stopped by the addition of 100 μL of sulfuric acid per well. Optical density (OD) at a wavelength of 450 nm was read using Synergy 4 (BioTek) plate reader. OD values of samples were adjusted by subtracting the average of the blank plus three times the standard deviation of the blank. Area under the curve (AUC) values were computed by plotting normalized OD values against the reciprocal serum sample dilutions in GraphPad Prism. The assay was done one per sample due to the limited amount of sample.

Quantification of total IgA in nasopharyngeal swabs

Immulon 4 HBX 96-well microtiter plates (Thermo Fisher Scientific) were coated overnight at 4°C with 50 μL of goat anti-human IgA (Bethyl Laboratories #A80-102A) at a concentration of 250 ng/well. The next day, the plates were washed three times with PBS-T using an automatic plate washer (BioTek). After washing, the plates were blocked for 1 h at RT with 200 μl/well of 5% (w/v) non-fat milk powder diluted in PBS-T. The blocking solution was discarded, and 75 μL of inactivated nasopharyngeal swab (starting 1:40 and serially diluted three-fold) with 2.5% (w/v) non-fat milk PBS-T was added to the wells and incubated at 4°C for 2 h. The next day, plates were washed three times with PBS-T using the plate washer and anti-human IgA-HRP antibody (α-chain) (Sigma, Cat. A0295) diluted 1:1500 was added to the wells. After 1h incubation at RT, plates were washed four times with PBS-T with shaking using the plate washer and 100 μL of TMBE (Rockland) was added to all wells for 10 min. The reaction was stopped by the addition of 100 μL of sulfuric acid per well. Optical density (OD) at a wavelength of 450 nm was read using Synergy 4 (BioTek) plate reader. OD values of samples were adjusted by subtracting the average of the blank plus three times the standard deviation of the blank. Area under the curve (AUC) values were computed by plotting normalized OD values against the reciprocal serum sample dilutions in GraphPad Prism. The assay was done one per sample due to the limited amount of sample.

QUANTIFICATION AND STATISTICAL ANALYSIS

All statistical analyses and AUC calculation were performed using Graphpad Prism 9. Geometric mean titers (GMT) and 95% confidence intervals (CI 95%) were computed by taking the exponent (log10) of the mean and of the lower and upper limits of the 95% CI of the serum log10-transformed titers. Mean and standard deviation (SD) were calculated for mucosal antibody titers. Kruskal-Wallis test with Dunn's multiple comparison test, Mann-Whitney t test and non-parametric Spearman correlation were performed. Statistical significance was considered when $p \leq 0.05$ (*$p < 0.05$, **$p < 0.01$, ***$p < 0.001$, ****$p < 0.0001$, ns, not significant).

Study 6

Metabolomic profile associated with COVID-19 severity and a signature that predicts progression towards severe disease status, a prospective cohort study (METCOVID)

Mallol, R.*, **Alexander Rombauts, A**.*✉, Abelenda-Alonso, G., Gudiol, C., Balsalobre, M., Carratalà, J.
*Both authors contributed equally to the study.

Submitted

Metabolomic profile associated with COVID-19 severity and a signature that predicts progression towards severe disease status, a prospective cohort study (METCOVID)

Roger Mallol[1,2ǂ], Alexander Rombauts[3*ǂ], Gabriela Abelenda-Alonso[3], Carlota Gudiol[3,4,5], Marc Balsalobre[1], Jordi Carratalà[3,4,5]

1. Human Environment Research, La Salle-Universitat Ramon Llull, 08022, Barcelona, Spain
2. Fundació Institut Universitari per a la recerca a l'Atenció Primària de Salut Jordi Gol i Gurina (IDIAPJGol), 08007, Barcelona, Spain
3. Department of Infectious Diseases, Hospital Universitari de Bellvitge-IDIBELL, 08908, Barcelona, Spain
4. Universitat de Barcelona, Department of Medicine, 08007, Barcelona, Spain
5. Centro de Investigación Biomédica en Red de Enfermedades Infecciosas (CIBERINFEC), Instituto de Salud Carlos III, 28029, Madrid, Spain

ǂBoth authors contributed equally to the study.

Roger Mallol; rmallol@idiapjgol.info
Alexander Rombauts; alexander.rombauts@gmail.com
Gabriela Abelenda-Alonso; gabi.abelenda.alonso@gmail.com
Marc Balsalobre; marc.balsalobre@students.salle.url.edu
Carlota Gudiol; cgudiol_ext@iconcologia.net
Jordi Carratalà; jcarratala@bellvitgehospital.cat

*Correspondence (Alexander Rombauts) alexander.rombauts@gmail.com

Keywords: SARS-CoV-2, COVID-19, prognosis, severity, metabolomics, NMR-spectroscopy.

Abstract:

Background: Profound metabolomic alterations occur during COVID-19. Early identification of the subset of hospitalised COVID-19 patients at risk of developing severe disease is critical for optimal resource utilization and timely treatment initiation. We aimed to delineate the metabolomic profile of hospitalized adult COVID-19 patients who progressed to severe disease and to establish a predictive signature for assessing the risk of disease progression.

Methods: Metabolite profiling was conducted using nuclear magnetic resonance (NMR) spectroscopy in 148 hospitalized COVID-19 patients within 48 hours of admission. Lipoprotein profiling was performed using the ^{1}H-NMR-based Liposcale® test, while low molecular weight metabolites were analyzed using one-dimensional Carr-Purcell-Meiboom-Gill pulse spectroscopy and an adaptation of the Dolphin method for lipophilic extracts. Patients were closely monitored daily until discharge or death.

Findings: Severe COVID-19, as per the WHO Clinical Progression Scale, was characterized by altered lipoprotein distribution indicative of increased atherogenic risk, elevated signals of glyc-A and glyc-B, a shift towards a catabolic state with elevated levels of branched-chain amino acids, and accumulation of ketone bodies. Furthermore, COVID-19 patients initially presenting with moderate disease but progressing to severe stages exhibited a distinct metabolic signature, distinct from those who did not progress to severe disease. Our multivariate model demonstrated a cross-validated AUC of 0·82 and predictive accuracy of 72% for progression towards severity.

Interpretation: Metabolomic profiling via NMR spectroscopy enables the identification of moderate COVID-19 patients at risk of disease progression, offering a valuable tool for adequate resource allocation and early treatment.

Research in context:

Evidence before this study: We conducted a comprehensive search on PubMed utilizing the terms "COVID-19" and/or "SARS-CoV-2", "metabolomic" and/or "metabolism", and "NMR" and/or "magnetic resonance". Our objective was to identify metabolomic studies focusing on COVID-19. Several metabolomic studies were identified, primarily aimed to establish a discriminative COVID-19 metabolomic profile for effective identification and differentiation of COVID-19 clinical statuses. Additionally, a handful of studies explored dynamic metabolomic changes in long-COVID. Our search, however, revealed only one NMR-based study, involving 36 patients, which evaluated a prognostic metabolomic profile for mortality.

Added value of this study: Our study, including 148 patients, employed an NMR-based platform to identify metabolomic alterations in COVID-19. We developed a predictive model to anticipate progression to severe disease. Serum samples were collected within 48 hours of admission, and patients were monitored daily to accurately ascertain their clinical disease status. Through this method, we identified several metabolomic alterations associated with severe COVID-19. Furthermore, we observed that COVID-19 patients initially presenting with moderate disease, who later progressed to severe disease, exhibited a distinct metabolomic signature. This profile contrasted with that found in those patients with moderate COVID-19 who did not escalate to severe disease.

Implications of all the available evidence: COVID-19 patients with severe disease and those initially presenting with moderate disease at a high risk of deterioration display characteristic metabolomic profiles. These profiles can be swiftly determined using NMR-based platforms. Such findings carry significant clinical implications, facilitating early identification and treatment of hospitalized patients at a high risk of progressing to severe disease. Moreover, our findings pave the way for further research into identifying metabolomic profiles through NMR to offer a more personalized approach in managing various infectious diseases.

1. INTRODUCTION

The clinical manifestations of SARS-CoV-2 infections vary broadly, ranging from an asymptomatic state to severe pneumonia, including acute respiratory distress syndrome (ARDS), multisystem organ failure, and eventually death[1,2]. Morbidity and mortality are almost exclusively driven by the development of ARDS. Certain genomic regions[3], ACE2 polymorphism[4], immunological imprinting due to prior infections with other coronavirus[5] and an excessive proinflammatory immune dysregulation play a role in coronavirus diseases 2019 (COVID-19) outcomes[6–8].
Patients hospitalized with COVID-19 remain at a high risk for mortality, ranging from 15% to 5% during delta and late omicron periods[9]. Early identification of the subset of hospitalized COVID-19 patients who will develop severe disease is critical for adequate resource allocation and prompt treatment initiation. Clinical predictors of severity such as male sex, older age, hypertension and a higher number of comorbidities were quickly identified[10,11]. Nevertheless, it remains unclear why some hospitalized, a priori low-risk patients develop severe pneumonia with ARDS and others with several risk factors present a favourable evolution.
Several studies have investigated the underlying metabolic alterations associated with COVID-19 [12-27], most with an emphasis on discriminating between SARS-CoV-2 infected patients from non-infected individuals. Among SARS-CoV-2 infected patients notable alterations have been observed, including glycerophospholipid metabolism remodeling[12–14], enriched purine metabolism[12,16], lipoprotein distribution changes marked by elevated of VLDL and triglycerides[17–19], and dysregulation in glycolysis[19]. Moreover, increased COVID-19 severity was associated with disruptions in mitochondrial activity[17,20,21], altered fatty acid oxidation[20], reduced amino-acids reflecting a catabolic state[17,21–23], impaired cholesterol homeostasis [12,14,17,24] and a decline in tryptophan reflecting immune dysregulation[25–27]. Additionally, low levels of circulating lysoPCs and PCs have been directly associated with COVID-19 severity[12,20,23,26]. Few studies have aimed to identify a metabolomic signature capable of predicting COVID-19 progression[13,25,26]. However, most of the included patients in these studies had already progressed to critical states when their blood samples were collected, with the metabolomic profile correlating COVID-19 severity rather than disease progression risk. Importantly, nuclear magnetic resonance (NMR) spectroscopy stands out among among the possible metabolomics analytical platforms due to its rapid, highly accurate, non-destructive, and quantitative features[28,29]. Of note, to our knowledge, only one NMR-based study, involving a cohort of merely 36 patients, has explored a prognostic metabolomic profile for mortality[30].

In this study, we aimed to delineate the metabolomic profile of hospitalized adult COVID-19 patients who progressed to severe disease and to establish a predictive signature for assessing the risk of disease progression.

2. MATERIALS AND METHODS

2.1. Study subjects

In this prospective study, 148 patients were recruited at Bellvitge University Hospital. Metabolomic analyses were performed at Biosfer Teslab (Reus, Spain). Adult patients with a positive RT-PCR SARS-CoV-2 nasopharyngeal swab and COVID-19 hospitalized from January 2021 to May 2021 were eligible. Recruitment and blood sampling was performed within 48h of hospital admission. We

assigned patients a unique patient identifier (PID), which was then applied to the clinical samples and the de-identified data set. We securely stored the list correlating the PID with the patient's identity at Bellvitge University Hospital. The investigators prospectively followed-up and daily visited the patients until hospital discharge. We collected data on demographic and clinical characteristics, blood analysis, treatments, and outcomes. We compared the metabolomic profile of patients with severe COVID-19 versus moderate COVID-19 at the moment of sampling and with the subgroup of patients who remained moderate over the course of hospitalization. For the development of a signature predictive of progression towards severe disease status, we compared the metabolomic profiles of moderate patients at the moment of sampling who did not progress with those who progressed to severity.

2.2. Definitions and Local Guidelines

We defined COVID-19 pneumonia as new or worsening pulmonary infiltrates on a chest x-ray or CT of the lungs with a confirmed positive RT-PCR for SARS-CoV-2. Severity was defined according to the patient's respiratory situation following the WHO Clinical Progression Scale [34]. In brief, moderate disease comprehend categories 4 (hospitalized with no oxygen therapy) and 5 (hospitalized with oxygen by mask of nasal prongs) while severe disease includes categories 6 to 9 (referring to patients requiring high-flow oxygen, non-invasive or invasive mechanical ventilation with varying degree of organ failure). Institutional guidelines at the study moment recommended corticosteroids, preferable dexamethasone at a daily dose of 6mg, for all patients >7 days from symptoms onset and requiring oxygen supplementation. Tocilizumab was recommended for patients with C - reactive protein >75 mg/dl and severe disease status and/or progression towards severity. Remdesivir was recommended for patients with low-flow oxygen requirement (oxygen mask or nasal prongs) and <7 days from symptoms onset.

2.3. Metabolomics analyses

Lipoprotein profile. The lipoprotein profile was measured in serum samples (250 μL) using the ^{1}H-NMR-based Liposcale® test, a new generation nuclear magnetic resonance test by Biosfer Teslab (Reus, Spain). The lipid concentrations (i.e., triglycerides and cholesterol) of the four main classes of lipoproteins (very low-density lipoprotein (VLDL); intermediate-density lipoprotein (IDL), low-density lipoprotein (LDL), and high-density lipoprotein (HDL)), and the particle numbers of nine subclasses (large, medium, and small particle numbers of each of the following: VLDL, LDL, and HDL) were determined as previously reported [35]. The different lipoprotein subclasses corresponded to the following diameter size ranges: large VLDL, 68.5 to 95.9 nm; medium VLDL, 47 to 68.5 nm; small VLDL, 32.5 to 47 nm; large LDL, 24 to 32.5 nm; medium LDL, 20.5 to 24 nm; small LDL, 17.5 to 20.5 nm; large HDL, 10.5 to 13.5 nm; medium HDL, 8.5 to 10.5 nm; and small HDL, 7.5 to 8.5 nm.

Glycoprotein profile. The glycoprotein profile was determined by analysing the specific ^{1}H-NMR spectral region where these protein–sugar bonds resonate (2.15–1.90 ppm) by deconvoluting the spectra by using three Lorentzian functions, as previously reported [36]. For each function, we determined the total area (proportional to concentration), height, position, and bandwidth. The area of glycoprotein A (Glyc-A) provided the concentration of acetyl groups of protein-bond N-acetylglucosamine and N-acetylgalactosamine, and the area of glycoprotein B (Glyc-B) provided the concentration of N-acetylneuraminic acid. The glycoprotein F (Glyc-F) area arises from the concentration in the acetyl groups of N-acetylglucosamine, N-acetylgalactosamine, and N-acetylneuraminic acid unbound to proteins (free fraction). H/W ratios, which reflect the aggregation state of the sugar-protein bonds, were

also reported for Glyc-A and Glyc-B[37]. Height was calculated as the difference from the baseline to maximum of the corresponding NMR peaks, and the width value corresponded to the peak width at half height.

Low molecular weight metabolites (LMWMs) profile. Intact serum was analysed by ^{1}H-NMR using a one-dimensional Carr-Purcell-Meiboom-Gill (CPMG) pulse. LMWMs were identified using an adaptation of Dolphin [38]. Each metabolite was identified by checking for all its resonances along the spectra and then quantified using line–shape fitting methods on one of its signals.

Lipidomic profile. Lipophilic extracts were obtained from two 100 µL aliquots of freshly thawed plasma using the BUME method [38] with slight modifications. Specifically, BUME was optimized for batch extractions with di-isopropyl ether (DIPE) replacing heptane as the organic solvent. This procedure was performed with a BRAVO liquid handling robot, which has the capacity to extract 96 samples at once. The upper lipophilic phase was completely dried in Speedvac until evaporation of organic solvents and frozen at -80°C until NMR analysis. Lipid extracts were reconstituted in a solution of CDCl3:CD3OD: D2O (16:7:1, v/v/v) containing tetramethylsilane (TMS) at 1.18 mM as a chemical shift reference and transferred into 5-mm NMR glass tubes. ^{1}H-NMR spectra were measured at 600.20 MHz using an Avance III 600 Bruker spectrometer. A 90° pulse with water pre-saturation sequence (zgpr) was used. Quantification of lipid signals in ^{1}H-NMR spectra was carried out with LipSpin [39]. Resonance assignments were made based on values in the literature [40].

2.4. Statistical analysis

General data analysis procedures. Except when otherwise stated, all data are presented as the mean and interquartile range (IQR) for continuous variables. Differences in the mean values of clinical variables across groups were assessed using the Kruskal Wallis test for continuous variables and the Chi-square test for categorical variables. Negative and zero values in the metabolomics data set were set to "not a number". Association between disease status (exposure) and log-transformed metabolomics profiles (outcome) was assessed using linear regression models adjusted by body mass index (BMI), sex, smoking status, statins use, and presence of diabetes treatment. Finally, the diagnostic performance of the metabolomics profiles was assessed by means of the MetaboAnalyst platform [41]. First, the metabolomics data set was normalized by median and scaled using the autoscale scaling method. Then, a partial least squares – discriminant analysis (PLS-DA) multivariate model with two latent variables provided in this platform was used to build a predictive model, where features were ranked according to its individual diagnostic performance based on area under the curve (AUC) score. Also, our multivariate analysis included metabolite ratios (top 20 metabolite ratios based on individual performance). Finally, ROC curves were generated by Monte-Carlo cross validation (MCCV) using balanced sub-sampling. In brief, in each MCCV, two thirds (2/3) of the samples were used to evaluate the feature importance. The top 3, 5, 10, 20, 50, and 100 important features were then used to build classification models which were validated on the 1/3 the samples that were left out. The procedure was repeated multiple times to calculate the performance and confidence interval of each model.

2.5. Ethics

The study was approved by the Bellvitge University Hospital Ethics Committee in accordance with Spanish legislation, and the procedures followed complied with the ethical standards of the Helsinki Declaration (PR037/21), and written informed consent was obtained for all cases.

2.6 Data deposition and materials sharing

The raw data of this study will be made available in a public metabolomic repository on publication.

2.6. Role of funding source

The funding source had no role in data collection, analysis, interpretation, writing or decision to submit the manuscript. No authors were paid to write this article by any pharmaceutical company or other entity.

3. RESULTS

3.1. Cohort characteristics

The clinical characteristics, blood test results at the time of sampling, COVID-19 treatment and outcomes of the 148 included hospitalized COVID-19 patients are summarized in Table 1 and 2. Patients were classified according the WHO Clinical Progression Scale at baseline and over the course of their hospitalization. A total of 126 (85·1%) patients had moderate disease status (categories 4 and 5) at baseline of whom 19 (12·8%) progressed to severity and 108 (72·3%) did not, while 22 (14·8%) were severe (categories 6 to 9) at the time of sampling. The mean age was 64.4 years, 65 (43·9%) were assigned female at birth, 38 (25·7%) had diabetes, 27 pre-existing lung disease (18·2%), 23 (15·5%) heart disease and 19 (12·8%) chronic renal failure. Patients' characteristics and comorbidities between moderate without progression, moderate with progression and severe disease status were similar except for severe subjects being older (64 vs 73 years). The mean time from symptoms onset to hospital admission was 7 days and most patients presented with cough (70.9%), dyspnoea (48%), diarrhoea (33·8%), and cephalea (17·6%). Routine blood test results at the time of sampling showed significant differences between moderate patients without progression and moderate with progression to severity. Higher glucose, C-reactive protein levels, and reduced lymphocyte count were noted in those patients who later progressed to severity. Patients who were already severe at baseline had even higher levels of glucose, C-reactive protein and presented an increased neutrophils count. Treatments included corticosteroids (87·2%), remdesivir (37·8%) and tocilizumab (30·4%). The median length of hospitalization stay was 8 days, which was significantly longer for severe patients (seven vs 21·8). A total of 26 patients (17·6%) required a non-rebreather mask (NRB), 40 (27%) high flow nasal cannula (HFNC), 2 (1·4%) non-invasive (NIV) and 8 (5·4%) invasive mechanical ventilation at any given time during hospitalization for at least 24h. Eleven (7·4%) patients were admitted to the intensive care unit (ICU) and in-hospital mortality was 6·8%.

3.2. Metabolomic profile of severe COVID-19.

In order to develop a metabolomics profile of severe COVID-19, the serum metabolites of patients with severe disease status (WHO Clinical Progression Scale categories 6 to 9) at the moment of sampling (n=22) were compared to patients with moderate disease status (WHO Clinical Progression Scale categories 4 or 5). Regarding the lipoprotein and glycoprotein analysis (Table 3), all lipid-related parameters (cholesterol and triglycerides) were significantly increased in severe disease status, except for HDL-C, which was reduced, and LDL-C, for which no differences were detected. Different lipoprotein particle concentrations, with an increase in total VLDL in severe patients driven by an increase of small VLDL particles, were found. This, however, did not lead to significant differences in the average size of VLDL particles. In contrast, severe disease status was associated with lower levels of small HDL particles and enlarged HDL particles. While no statistically significant differences in the particle concentration of LDL subclasses were found, average LDL particle size was higher in severe patients. In addition, four out of five analysed glycoproteins (Glyc-B, Glyc-A, H/W glyc-B, H/W Glyc-A) showed increased concentrations severe patients. As for the analysis of low-molecular weight metabolites (Table 4), 3-hydroxibutyrate, glucose, glycerol, lactate, threonine, valine, isoleucine, and leucine were significantly increased in severe patients. In addition, several lipid-related parameters (Table 5) showed higher concentrations in the severe group.

When the moderate group was restricted to patients without progression towards severity (n = 108), all the previous parameters were still significant except for VLDL-TG, PL and PUFA4, which, although showing a trend, lost their statistical significance.

3.2. Prediction of progression towards severity

With a view to develop a model predictive of progression towards severity, moderate patients at baseline (WHO Clinical Progression Scale categories 4 or 5) at baseline who did not progress towards severity (WHO Clinical Progression Scale categories 6 to 9) over the course of hospitalization (n=108) were compared to those with those who did (n=19). The univariate analysis showed nine parameters with significant differences (small LDL-P, medium HDL-P, Glyc-B, alanine, glutamine, isoleucine, SFA, w6+w7, and ARA+EPA), see Tables 3, 4 and 5.

We developed a multivariate statistical model to create a metabolomic signature of progression towards severity. Metabolite ratios were incorporated into the model in order to increase the statistical power. The 20 most important ratios based on their individual performance to distinguish progression towards severity and on the p-values resulting from a t-test, were included in the data set to build and validate the multivariate model. Our multivariate model showed a cross-validated AUC of 0.82 and a predictive accuracy of 72% (Figure 1) for progression towards severity (WHO Clinical Progression Scale categories 6 to 9) for hospitalized COVID-19 patients with moderate disease status (WHO Clinical Progression Scale categories 4 or 5). The two most important variables of our multivariate model were the small LDL-P/medium HDL-P and LDL-C/medium HDL-P ratios (Figures 2 and 3). While in the first case the two constituents (i.e. small LDL-P and medium HDL-P) were significant in our univariate analysis, in the second case only medium HDL-P had been found significant as an individual marker, while LDL-C had been found suggestively significant. Overall, 6 out of 9 suggestive parameters were involved in the ratios found to be important for our multivariate model. In addition to LDL-C, the other suggestive parameters were LDL-P, HDL-Z, Glyc-A, PUFA2, and EC. On the other hand, 7 important ratios had one of the two constituents that, individually, were not discriminant of disease progression

(univariate P-value > 0,1). These constituents were HDL-TG, large HDL-P, LDL-Z, leucine, glycerol, creatine, and SM.

The 25 most important variables of our multivariate predictive model are shown in Figure 2, eighteen of which were metabolite ratios (and half of them had medium HDL-P as constituent). The two most important variables of our multivariate model were the small LDL-P/medium HDL-P and LDL-C/medium HDL-P ratios (Figures 2 and 3).

4. Discussion:

Our prospective study, employing an NMR-based analytical platform, unveiled a metabolomic profile indicative of severe COVID-19. Furthermore, we identified a metabolomic signature capable of predicting progression towards severity at the time of hospital admission, preceding the onset of severe disease status.

The metabolic profile associated with severe COVID-19 is largely consistent with previous studies on metabolomics. We found profound changes in lipoprotein distribution in severe COVID-19, showing an increased atherogenic risk with increased severity, small VLDL particles were increased while small HDL particles were diminished. Small HDL particles, the HDL subspecies most decreased in this study as well as another study[42], is also the HDL subspecies most strongly associated with cholesterol efflux capacity function[43]. Severe disease status (WHO Clinical Progression Scale categories 6 to 9) was associated with an intense lipoprotein dysregulation towards increased TG, free cholesterol and anomalous lipoprotein distribution with elevated IDL-C, LDL-C and VLDL subclasses while HDL-C was decreased.

Our results are in line with previous studies who found a correlation between COVID-19 severity with high triglyceride concentrations, no-HDL-C and low plasma HDL-cholesterol[14,44], an increased mean size of VLCL particles[17] and higher levels of free cholesterol[14]. We also found, unsurprisingly, an elevated glyc-A and glyc-B signal in more severe patients. Glyc-A and glyc-B represent different glycosylated amino sugar residues on acute phase reactants [45], with α-1-acid glycoprotein having the strongest correlation with Glyc-A [46]. Previous studies have related glyc-A with chronic inflammation [47], metabolic syndrome[48], increased severity [49,50] and higher levels of CPR and IL-6 in COVID-19 [50]. Furthermore, severe COVID-19 patients had elevated levels of branched-chained amino acids (BCAAs: leucine, isoleucine and valine) compared to moderate COVID-19 patients, results which are concordant with prior studies [16,21,51,52]. BCAAs are essential amino acids which act as substrates and regulator of protein and glycogen metabolism [53,54], and modulate glucose metabolism. Elevated circulating levels of BCAAs are associated with catabolic states[55], and, through mTOR activation, linked to reactive oxygen species production and mitochondrial dysfunction [56] in addition to promoting endothelial dysfunction [57]. In addition, concordant with prior studies, we found elevated glucose[14] and accumulation of ketone bodies in severe COVID-19 patients [21,58], reflecting dysregulation of hepatic carbon metabolism[17].

When comparing moderate COVID-19 patients who did not progress with those who did, several of the alterations in serum metabolites associated with severe disease status lost their significance. Most notably, no differences in free cholesterol, phospholipids, IDL, VLDL, HDL were found, suggesting that most of the intense lipoprotein dysregulation occurs in later disease stages. Higher levels of small LDL particles with a decrease in medium HDL particles, not present in the metabolomic comparison of moderate versus severe patients, was found to be predictive. A reduction of HDL has been previously associated with worse outcomes[18,44] and a predominance of small LDL particles compared to larger LDL particles has been identified in COVID-19 patients [42]. Increased levels of isoleucine, saturated

fatty acids, and glyc-B, both associated with severe disease status, were also found to be predictive for progression to severity. Furthermore, our results showed increased risk for progression in patients with increased alanine and glutamine levels. These particular findings are surprising as glutamine is essential for lymphocyte proliferation, cytokine production and macrophage activation, with increased demand in catabolic/hypercatabolic circumstances[59]. In addition, prior studies comparing uninfected controls versus COVID-19 patients found both decreased levels of alanine[51,60] and glutamine[17,49,61] in COVID-19 patients and severe COVID-19[21]. These diverging results may stem from differences in the compared cohorts. SARS-CoV-2 infection correlates with reduced glutamine levels compared to uninfected individuals. However, we compared moderate COVID-19 patients without progression with those who did progress at later stages. We also found higher levels of Arachidonic Acid in patients with progression.

Several strengths of our study should be noted. Firstly, we utilized NMR based spectroscopy, which allows for a rapid, highly accurate, non-destructive, and quantitative analysis. Unlike many studies that employ heterogeneous definitions of COVID-19 severity, potentially leading to misclassification amid healthcare resource strain during surges, we defined severity according to the WHO Clinical Progression Scale categories. In contrast to several prior predictive metabolomics models, which often compare patients who have already reached severe disease with mild to moderate COVID-19 patients[13,25,26,64], our approach involved comparing patients with equivalent clinical status at baseline status. Furthermore, our multivariate model, incorporating metabolite ratios, showed a cross-validated AUC of 0·82 and a predictive accuracy of 72% for progression towards severity upon admission for hospitalized COVID-19 patients with moderate disease status and similar oxygen saturation.

In conclusion, severe COVID-19 was associated with a distinct metabolomic signature associated with an increased atherogenic risk and a pro-inflammatory catabolic state with dysregulated carbon metabolism. Notably, patients presenting with moderate disease but at a high risk of deterioration exhibit a characteristic metabolomic signature, which can be swiftly, determined using NMR-based platforms, thereby providing a better metric for resource allocation and early treatment. These results should be assessed in larger prospective cohorts with other variants and populations with pre-existing immunity. Moreover, our findings opens avenues for further research.

5. Limitations of the study:

Our study has some limitations that should be acknowledged. Firstly, due to the nascent stage of vaccine within the general population in Spain at the study period, only unvaccinated patients without prior known COVID-19 were included. Secondly, the study period coincided with the predominance of the Alpha (B.1.1.7) variant of SARS-CoV-2. Subsequent variants and subvariants might have elicited different host responses. Lastly, the sample size was moderately small, 148 patients of whom 19 progressed following baseline sampling. However, the patients included in our study were followed up daily, which allowed an accurate assessment of their clinical disease trajectory.

6. Acknowledgments:

A.R. received a predoctoral research grant from the Instituto de Salud Carlos III, the Spanish Ministry of Science, Innovation, and Universities, (PFIS grant FI18/00183). G.A.A. reports a predoctoral research grant from the 201808-10 project, funded by La Marató de TV3. The project was supported through a grant from the Department de Salut of the Generalitat de Catalunya (20DPS005) and from the Instituto de Salud Carlos III, Mardid, Spain (COV20_00121). We thank the CERCA

Programme/Generalitat de Catalunya for their institutional support. The authors would like to thank all the members of the Clinical Research Support Unit (HUB-IDIBELL) for selflessly allowing the use of their facilities.

7. Author contributions:

Conceptualization, A.R., C.G., and J.C.; Sample acquisition and patient follow-up: A.R., G.A.; Data curation and formal analysis, R.M.; Funding acquisition, J.C.; Methodology, A.R., J.C., C.G., and R.M.; Project administration, J.C.; Supervision, C.G. and J.C.; Visualization, J.C.; Writing—original draft, A.R., R.M., and J.C.; Writing—review and editing, A.R., G.A., R.M., C.G., and J.C. All authors have read and agreed to the published version of the manuscript.

8. Declaration of interests:

The authors declare no competing interests.

9. References:

1. Gandhi RT, Lynch JB, del Rio C. Mild or Moderate Covid-19. *N Engl J Med*. 2020;383(18):1757-1766. doi:10.1056/NEJMCP2009249
2. Berlin DA, Gulick RM, Martinez FJ. Severe Covid-19. *N Engl J Med*. 2020;383(25):2451-2460. doi:10.1056/NEJMCP2009575
3. Genomewide Association Study of Severe Covid-19 with Respiratory Failure. *N Engl J Med*. 2020;383(16):1522-1534. doi:10.1056/nejmoa2020283
4. Suryamohan K, Diwanji D, Stawiski EW, et al. Human ACE2 receptor polymorphisms and altered susceptibility to SARS-CoV-2. *Commun Biol*. 2021;4(1). doi:10.1038/s42003-021-02030-3
5. Aydillo T, Rombauts A, Stadlbauer D, et al. Immunological imprinting of the antibody response in COVID-19 patients. *Nat Commun*. 2021;12(1). doi:10.1038/S41467-021-23977-1
6. Chan Y, Fong S, Poh C, et al. Asymptomatic COVID-19: disease tolerance with efficient anti-viral immunity against SARS-CoV-2. *EMBO Mol Med*. 2021;13(6):1-15. doi:10.15252/emmm.202114045
7. Fang FC, Benson CA, Del Rio C, et al. COVID-19-Lessons Learned and Questions Remaining. *Clin Infect Dis*. 2021;72(12):2225-2240. doi:10.1093/CID/CIAA1654
8. Rombauts A, Bódalo Torruella M, Abelenda-Alonso G, et al. Dynamics of Gene Expression Profiling and Identification of High-Risk Patients for Severe COVID-19. *Biomedicines*. 2023;11(5). doi:10.3390/BIOMEDICINES11051348
9. https://www.cdc.gov/mmwr/volumes/71/wr/mm7137a4.htm.
10. Berenguer J, Ryan P, Rodríguez-Baño J, et al. Characteristics and predictors of death among 4035 consecutively hospitalized patients with COVID-19 in Spain. *Clin Microbiol Infect*. 2020. doi:10.1016/j.cmi.2020.07.024
11. Guan W, Ni Z, Hu Y, et al. Clinical Characteristics of Coronavirus Disease 2019 in China. *N Engl J Med*. 2020;382(18):1708-1720. doi:10.1056/NEJMOA2002032
12. Delafiori J, Navarro LC, Siciliano RF, et al. Covid-19 Automated Diagnosis and Risk Assessment through Metabolomics and Machine Learning. *Anal Chem*. 2021;93(4):2471-2479. doi:10.1021/ACS.ANALCHEM.0C04497/SUPPL_FILE/AC0C04497_SI_001.PDF
13. López-Hernández Y, Monárrez-Espino J, Oostdam ASH van, et al. Targeted metabolomics identifies high performing diagnostic and prognostic biomarkers for COVID-19. *Sci Rep*. 2021;11(1):14732. doi:10.1038/S41598-021-94171-Y

14. Song JW, Lam SM, Fan X, et al. Omics-Driven Systems Interrogation of Metabolic Dysregulation in COVID-19 Pathogenesis. *Cell Metab*. 2020;32(2):188. doi:10.1016/J.CMET.2020.06.016
15. Wu D, Shu T, Yang X, et al. Plasma metabolomic and lipidomic alterations associated with COVID-19. *Natl Sci Rev*. 2020;7(7):1157. doi:10.1093/NSR/NWAA086
16. Sameh M, Khalaf HM, Anwar AM, et al. Integrated multiomics analysis to infer COVID-19 biological insights. *Sci Reports* |. 123AD;13:1802. doi:10.1038/s41598-023-28816-5
17. Bruzzone C, Bizkarguenaga M, Gil-Redondo R, et al. SARS-CoV-2 Infection Dysregulates the Metabolomic and Lipidomic Profiles of Serum. *iScience*. 2020;23(10). doi:10.1016/J.ISCI.2020.101645
18. Overmyer KA, Shishkova E, Miller IJ, et al. Large-Scale Multi-omic Analysis of COVID-19 Severity. *Cell Syst*. 2021;12(1):23. doi:10.1016/J.CELS.2020.10.003
19. Chen Y, Zheng Y, Yu Y, et al. Blood molecular markers associated with COVID-19 immunopathology and multi-organ damage. *EMBO J*. 2020;39(24). doi:10.15252/EMBJ.2020105896
20. Gardinassi LG, Servian C do P, Lima G da S, et al. Integrated Metabolic and Inflammatory Signatures Associated with Severity of, Fatality of, and Recovery from COVID-19. *Microbiol Spectr*. 2023;11(2). doi:10.1128/SPECTRUM.02194-22
21. Páez-Franco JC, Torres-Ruiz J, Sosa-Hernández VA, et al. Metabolomics analysis reveals a modified amino acid metabolism that correlates with altered oxygen homeostasis in COVID-19 patients. *Sci Rep*. 2021;11(1). doi:10.1038/S41598-021-85788-0
22. Soares NC, Hussein A, Muhammad JS, Semreen MH, ElGhazali G, Hamad M. Plasma metabolomics profiling identifies new predictive biomarkers for disease severity in COVID-19 patients. *PLoS One*. 2023;18(8):e0289738. doi:10.1371/JOURNAL.PONE.0289738
23. Oostdam ASH Van, Castañeda-Delgado JE, Oropeza-Valdez JJ, et al. Immunometabolic signatures predict risk of progression to sepsis in COVID-19. *PLoS One*. 2021;16(8). doi:10.1371/JOURNAL.PONE.0256784
24. Caterino M, Gelzo M, Sol S, et al. Dysregulation of lipid metabolism and pathological inflammation in patients with COVID-19. *Sci Rep*. 2021;11(1). doi:10.1038/S41598-021-82426-7
25. D'Amora P, Silva IDCG, Budib MA, et al. Towards risk stratification and prediction of disease severity and mortality in COVID-19: Next generation metabolomics for the measurement of host response to COVID-19 infection. *PLoS One*. 2021;16(12). doi:10.1371/JOURNAL.PONE.0259909
26. Sindelar M, Stancliffe E, Schwaiger-Haber M, et al. Longitudinal metabolomics of human plasma reveals prognostic markers of COVID-19 disease severity. *Cell Reports Med*. 2021;2(8):100369. doi:10.1016/J.XCRM.2021.100369
27. Ansone L, Briviba M, Silamikelis I, et al. Amino Acid Metabolism is Significantly Altered at the Time of Admission in Hospital for Severe COVID-19 Patients: Findings from Longitudinal Targeted Metabolomics Analysis. *Microbiol Spectr*. 2021;9(3). doi:10.1128/SPECTRUM.00338-21/SUPPL_FILE/SPECTRUM00338-21_SUPP_2_SEQ5.XLSX
28. Beckonert O, Keun HC, Ebbels TMD, et al. Metabolic profiling, metabolomic and metabonomic procedures for NMR spectroscopy of urine, plasma, serum and tissue extracts. *Nat Protoc*. 2007;2(11):2692-2703. doi:10.1038/nprot.2007.376
29. Nicholson JK, Lindon JC, Holmes E. "Metabonomics": Understanding the metabolic responses of living systems to pathophysiological stimuli via multivariate statistical analysis of biological NMR spectroscopic data. *Xenobiotica*. 1999;29(11):1181-1189. doi:10.1080/004982599238047
30. Costantini S, Madonna G, Di Gennaro E, et al. New Insights into the Identification of Metabolites and Cytokines Predictive of Outcome for Patients with Severe SARS-CoV-2 Infection Showed Similarity with Cancer. *Int J Mol Sci*. 2023;24(5). doi:10.3390/ijms24054922
31. Kazenwadel J, Berezhnoy G, Cannet C, et al. Stratification of hypertension and SARS-CoV-2 infection by quantitative NMR spectroscopy of human blood serum. *Commun Med*. 2023;3(1).

doi:10.1038/s43856-023-00365-y
32. Ansone L, Rovite V, Brīvība M, et al. Longitudinal NMR-Based Metabolomics Study Reveals How Hospitalized COVID-19 Patients Recover: Evidence of Dyslipidemia and Energy Metabolism Dysregulation. *Int J Mol Sci*. 2024;25(3). doi:10.3390/ijms25031523
33. Paris D, Palomba L, Albertini MC, et al. The biomarkers' landscape of post-COVID-19 patients can suggest selective clinical interventions. *Sci Rep*. 2023;13(1):1-15. doi:10.1038/s41598-023-49601-4
34. Marshall JC, Murthy S, Diaz J, et al. A minimal common outcome measure set for COVID-19 clinical research. *Lancet Infect Dis*. 2020;20(8):e192-e197. doi:10.1016/S1473-3099(20)30483-7
35. Mallol R, Amigó N, Rodríguez MA, et al. Liposcale: A novel advanced lipoprotein test based on 2D diffusion-ordered 1H NMR spectroscopy. *J Lipid Res*. 2015;56(3):737-746. doi:10.1194/jlr.D050120
36. Fuertes-Martín R, Taverner D, Vallvé JC, et al. Characterization of 1H NMR Plasma Glycoproteins as a New Strategy to Identify Inflammatory Patterns in Rheumatoid Arthritis. *J Proteome Res*. 2018;17(11):3730-3739. doi:10.1021/acs.jproteome.8b00411
37. Fuertes-Martín R, Moncayo S, Insenser M, et al. Glycoprotein A and B Height-to-Width Ratios as Obesity-Independent Novel Biomarkers of Low-Grade Chronic Inflammation in Women with Polycystic Ovary Syndrome (PCOS). *J Proteome Res*. 2019;18(11):4038-4045. doi:10.1021/acs.jproteome.9b00528
38. Gómez J, Brezmes J, Mallol R, et al. Dolphin: A tool for automatic targeted metabolite profiling using 1D and 2D 1 H-NMR data. *Anal Bioanal Chem*. 2014;406(30):7967-7976. doi:10.1007/s00216-014-8225-6
39. Barrilero R, Gil M, Amigó N, et al. LipSpin: A New Bioinformatics Tool for Quantitative 1H NMR Lipid Profiling. *Anal Chem*. 2018;90(3):2031-2040. doi:10.1021/acs.analchem.7b04148
40. Löfgren L, Ståhlman M, Forsberg GB, Saarinen S, Nilsson R, Hansson GI. The BUME method: A novel automated chloroform-free 96-well total lipid extraction method for blood plasma. *J Lipid Res*. 2012;53(8):1690-1700. doi:10.1194/jlr.D023036
41. https://www.metaboanalyst.ca/.
42. Ballout RA, Kong H, Sampson M, et al. The NIH lipo-COVID study: A pilot NMR investigation of lipoprotein subfractions and other metabolites in patients with severe COVID-19. *Biomedicines*. 2021;9(9). doi:10.3390/BIOMEDICINES9091090/S1
43. Heinecke JW. Small HDL promotes cholesterol efflux by the ABCA1 pathway in macrophages: Implications for therapies targeted to HDL. *Circ Res*. 2015;116(7):1101-1103. doi:10.1161/CIRCRESAHA.115.306052
44. Masana L, Correig E, Ibarretxe D, et al. Low HDL and high triglycerides predict COVID-19 severity. *Sci Rep*. 2021;11(1):7217. doi:10.1038/S41598-021-86747-5
45. Holmes E, Nicholson JK, Lodge S, et al. Diffusion and relaxation edited proton NMR spectroscopy of plasma reveals a high-fidelity supramolecular biomarker signature of SARS-CoV-2 infection. *Anal Chem*. 2021;93(8):3976-3986. doi:10.1021/ACS.ANALCHEM.0C04952/ASSET/IMAGES/LARGE/AC0C04952_0006.JPEG
46. Otvos JD, Shalaurova I, Wolak-Dinsmore J, et al. GlycA: A composite nuclear magnetic resonance biomarker of systemic inflammation. *Clin Chem*. 2015;61(5):714-723. doi:10.1373/clinchem.2014.232918
47. Ritchie SC, Würtz P, Nath AP, et al. The Biomarker GlycA is Associated with Chronic Inflammation and Predicts Long-Term Risk of Severe Infection. *Cell Syst*. 2015;1(4):293-301. doi:10.1016/j.cels.2015.09.007
48. Gruppen EG, Connelly MA, Otvos JD, Bakker SJ, Dullaart RP. A novel protein glycan biomarker and LCAT activity in metabolic syndrome. Eur J Clin Invest. 2015;45(8):850-859. doi:10.1111/eci.12481.
49. Ghini V, Meoni G, Pelagatti L, et al. Profiling metabolites and lipoproteins in COMETA, an Italian cohort of COVID-19 patients. *PLoS Pathog*. 2022;18(4). doi:10.1371/JOURNAL.PPAT.1010443
50. Rössler T, Berezhnoy G, Singh Y, et al. Quantitative Serum NMR Spectroscopy Stratifies

COVID-19 Patients and Sheds Light on Interfaces of Host Metabolism and the Immune Response with Cytokines and Clinical Parameters. *Metabolites*. 2022;12(12). doi:10.3390/metabo12121277
51. Banach M, Maltais-Payette I, Lajeunesse-Trempe F, Pibarot P, Biertho L, Tchernof A. Association between Circulating Amino Acids and COVID-19 Severity. 2023. doi:10.3390/metabo13020201
52. Danlos FX, Grajeda-Iglesias C, Durand S, et al. Metabolomic analyses of COVID-19 patients unravel stage-dependent and prognostic biomarkers. *Cell Death Dis*. 2021;12(3). doi:10.1038/s41419-021-03540-y
53. Holeček M. The BCAA-BCKA cycle: Its relation to alanine and glutamine synthesis and protein balance. *Nutrition*. 2001;17(1):70. doi:10.1016/S0899-9007(00)00483-4
54. Monirujjaman M, Ferdouse A. Metabolic and Physiological Roles of Branched-Chain Amino Acids. *Adv Mol Biol*. 2014;2014:1-6. doi:10.1155/2014/364976
55. Holeček M. Why are branched-chain amino acids increased in starvation and diabetes? *Nutrients*. 2020;12(10):1-15. doi:10.3390/nu12103087
56. Zhenyukh O, Civantos E, Ruiz-Ortega M, et al. High concentration of branched-chain amino acids promotes oxidative stress, inflammation and migration of human peripheral blood mononuclear cells via mTORC1 activation. *Free Radic Biol Med*. 2017;104(July 2016):165-177. doi:10.1016/j.freeradbiomed.2017.01.009
57. Zhenyukh O, González-Amor M, Rodrigues-Diez RR, et al. Branched-chain amino acids promote endothelial dysfunction through increased reactive oxygen species generation and inflammation. *J Cell Mol Med*. 2018;22(10):4948-4962. doi:10.1111/jcmm.13759
58. Ding Shi, Ren Yan, Longxian Lv, Huiyong Jiang, Yingfeng Lu, Jifang Sheng, Jiaojiao Xie, Wenrui Wu, Jiafeng Xia, Kaijin Xu, Silan Gu, Yanfei Chen, Chenjie Huang, Jing Guo, Yiling Du, Lanjuan LiaDing Shi, Ren Yan, Longxian Lv, Huiyong Jiang, Yingfeng Lu, Ji LL. The serum metabolome of COVID-19 patients is distinctive and predictive. *Metabolism*. 2021;118.
59. Cruzat V, Rogero MM, Keane KN, Curi R, Newsholme P. Glutamine: Metabolism and immune function, supplementation and clinical translation. *Nutrients*. 2018;10(11):1-31. doi:10.3390/nu10111564
60. Caterino M, Costanzo M, Fedele R, et al. The serum metabolome of moderate and severe covid-19 patients reflects possible liver alterations involving carbon and nitrogen metabolism. *Int J Mol Sci*. 2021;22(17):1-18. doi:10.3390/ijms22179548
61. Masuda R, Lodge S, Nitschke P, et al. Integrative Modeling of Plasma Metabolic and Lipoprotein Biomarkers of SARS-CoV-2 Infection in Spanish and Australian COVID-19 Patient Cohorts. *J Proteome Res*. 2021;20(8):4139-4152. doi:10.1021/ACS.JPROTEOME.1C00458/ASSET/IMAGES/LARGE/PR1C00458_0007.JPEG
62. Snider JM, You JK, Wang X, et al. Group IIA secreted phospholipase A2 is associated with the pathobiology leading to COVID-19 mortality. *J Clin Invest*. 2021;131(19):1-11. doi:10.1172/JCI149236
63. Steer SA, Corbett JA. The Role and Regulation of COX-2 during Viral Infection. *Viral Immunol*. 2003;16(4):447–460.
64. Soares NC, Hussein A, Muhammad JS, Semreen MH, El Ghazali G, Hamad M. Plasma metabolomics profiling identifies new predictive biomarkers for disease severity in COVID-19 patients. *PLoS One*. 2023;18(8 August):1-20. doi:10.1371/journal.pone.0289738

10. Figures

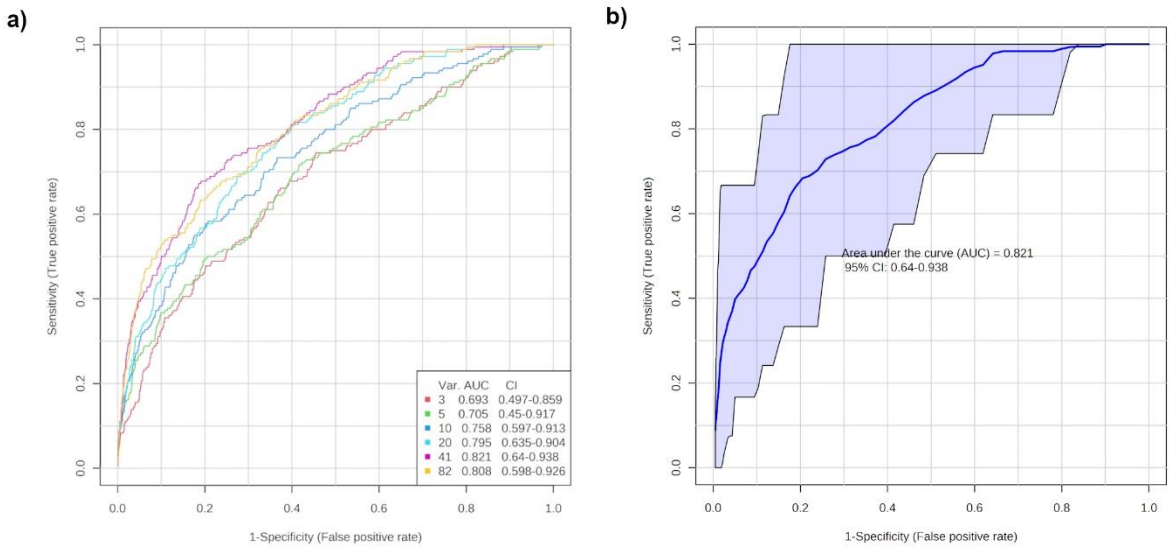

Figure 1. Area under the curve (AUC) of the sensitivity (a) and specificity (b) of the multivariate model for progression towards severity (WHO Clinical Progression Scale categories 6 to 9) for hospitalized COVID-19 patients with moderate disease status (WHO Clinical Progression Scale categories 4 or 5). The models shows a predictive accuracy of 72% with a cross-validated AUC of 0·82.

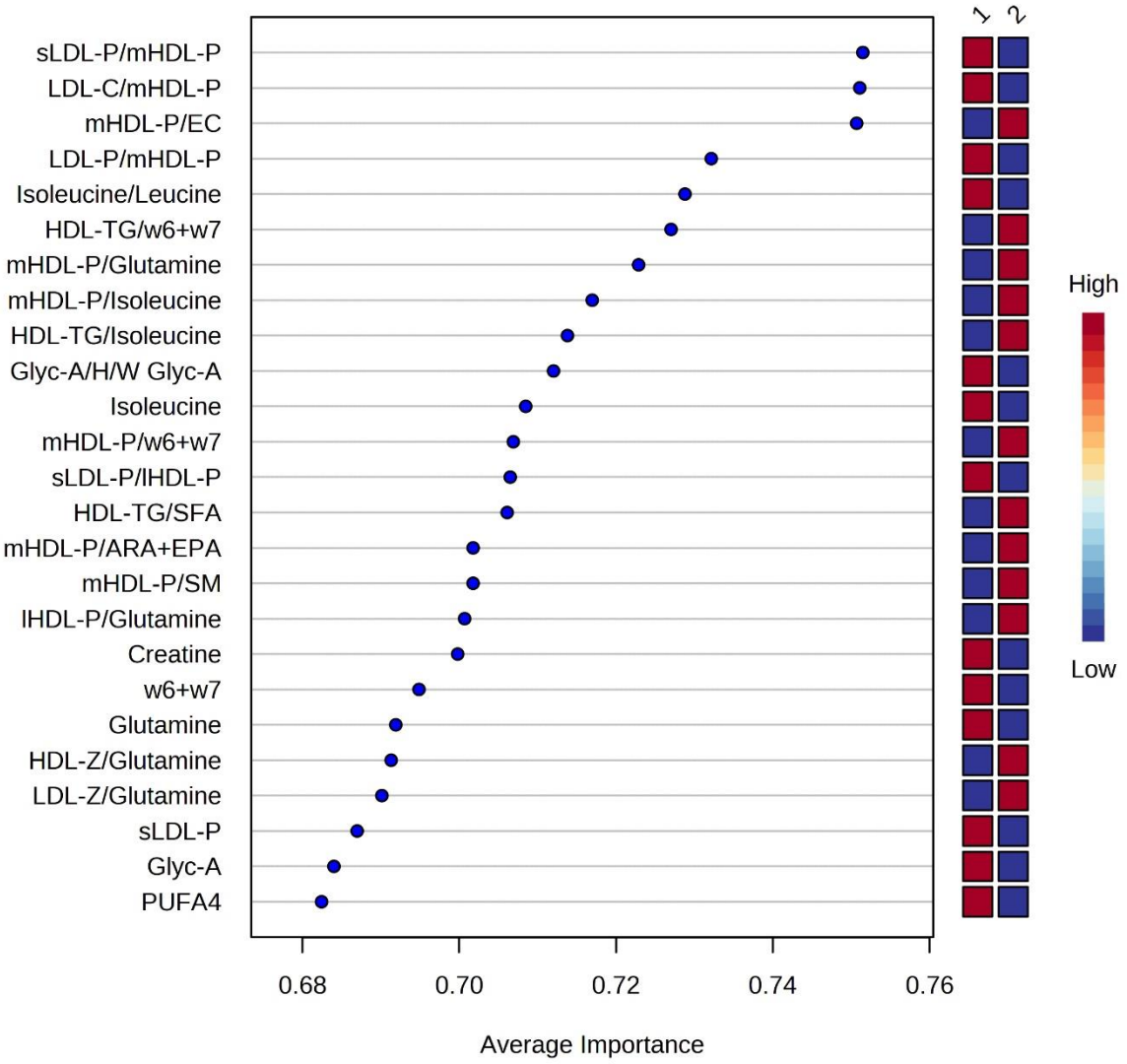

Figure 2. The 25 most important variables to predict progression towards severity (WHO Clinical Progression Scale categories 6 to 9) for hospitalized COVID-19 patients with moderate disease status (WHO Clinical Progression Scale categories 4 or 5), of which eighteen are metabolite ratios included in the data set to build and validate the multivariate predictive model. Class 1: Moderate disease status with progression; Class 2: Moderate disease status without progression.

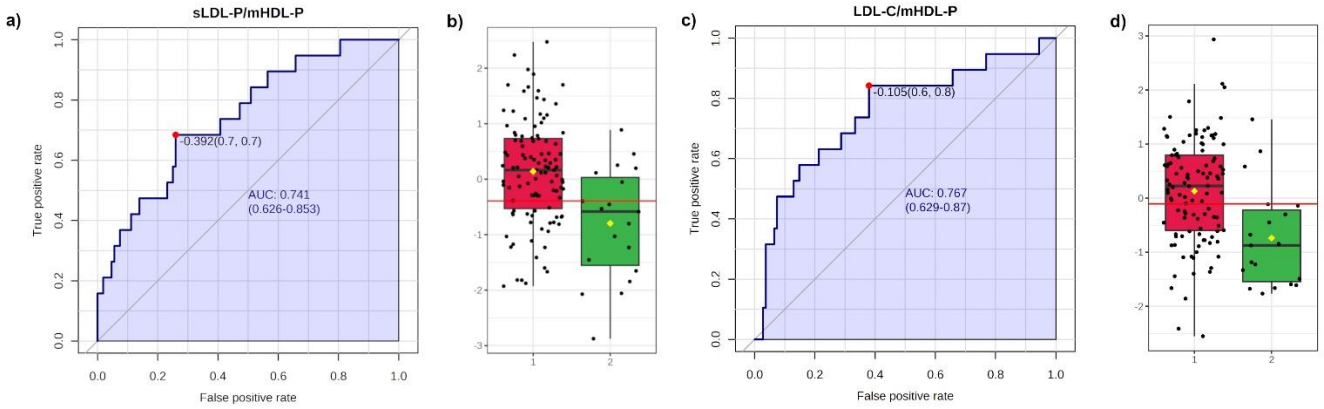

Figure 3 shows the individual performance to distinguish progression towards severity (WHO Clinical Progression Scale categories 6 to 9) for hospitalized COVID-19 patients with moderate disease status (WHO Clinical Progression Scale categories 4 or 5) of the two most important variables of our multivariate model, small LDL-P/medium HDL-P (a and b) and LDL-C/medium HDL-P ratios (c and d). Class 1: Moderate disease status with progression; Class 2: Moderate disease status without progression.

11. Tables

Table 1. Demographic data, clinical characteristics, blood test results, symptoms of the cohort of COVID-19 patients at the time of sampling (<48 hours of hospital admission).

	Total (n = 148)	**Moderate at baseline without progression (n = 107)**	**Moderate at baseline with progression (n = 19)**	**Severe at baseline (n = 22)**	***P*-value**
Demographic and clinical characteristics					
Age (mean), years	67·5 (22·0)	64·0 (23·8)	73·0 (15·0)	73·0 (22·0)	0·0264
Sex assigned at birth, n (%) women	65 (43·9)	48 (44·9)	8 (42·1)	9 (40·9)	0·9302
Body mass index (BMI), kg · m^{-2}	30·0 (6·8)	30·5 (6·7)	27·0 (4·7)	31·4 (7·8)	0·0184
Obesity ≥ class II (BMI>35), n (%) yes	45 (30·4)	30 (28·0)	3 (15·8)	12 (54·6)	0·0161
Influenza vaccine, n (%) yes	72 (48·7)	50 (46·7)	13 (68·4)	9 (40·9)	0.1605
Risk factors, n (%) yes*	100 (67·6)	69 (64·5)	12 (63·2)	19 (86·4)	0·1237
Diabetes, n (%) yes	38 (25·7)	27 (25·2)	5 (26·3)	6 (27·3)	0.9780
Pre-existing lung disease, n (%) yes	27 (18·2)	20 (18·7)	4 (21·1)	3 (13·6)	0.8073
Heart disease, n (%) yes	23 (15·5)	16 (15·0)	2 (10·5)	5 (22·7)	0.5332
Chronic renal failure, n (%) yes	19 (12·8)	12 (11·2)	2 (10·5)	5 (22·7)	0.3222
Stroke, n (%) yes	5 (3·4)	4 (3·7)	0 (0·0)	1 (4·6)	0.6708
Hepatopathy, n (%) yes	5 (3·4)	4 (3·7)	0 (0·0)	1 (4·6)	0·6708
Blood test results					
Glucose· mg/dL	117·0 (38·8)	114·0 (32·0)	123·0 (39·8)	137·0 (110·0)	0·0262
Leucocytes/µL	6800 (3350)	6700 (3350)	5600 (3175)	8650 (8200)	0·0054
Neutrophils/µL	4870 (3210)	4690 (2917)	4270 (3015)	7050 (6630)	0·0009
Lymphocytes/µL	1000 (720)	1060 (635)	780 (1192)	845 (670)	0·0358
Platelets/µL	206000 (92000)	201000 (99250)	196000 (101250)	231500 (77000)	0·1035
Creatinine· µmol/L	73·5 (37·0)	73·0 (28·8)	91·0 (35·0)	82·0 (60·0)	0·1932
Uric acid· mg/L	32·0 (33·0)	29·5 (25·0)	39·0 (18·0)	54·5 (46·0)	0·1000
C-reactive protein· mg/L	82·7 (94·2)	69·2 (75·2)	104·6 (81·6)	141·5 (121·3)	<0·0001
Symptoms and vital constants					
Cough, n (%) yes	105 (70·9)	77 (72·0)	12 (63·2)	16 (72·7)	0·7238
Dyspnoea, n (%) yes	71 (48·0)	43 (40·2)	9 (47·4)	19 (86·4)	0·0004
Diarrhoea, n (%) yes	50 (33·8)	38 (35·5)	6 (31·6)	6 (27·3)	0·7403
Cephalea, n (%) yes	26 (17·6)	18 (16·8)	5 (26·3)	3 (13·6)	0·5273
Odynophagia, n (%) yes	10 (6·8)	6 (5·6)	1 (5·3)	3 (13·6)	0·3783

Days from symptoms onset to hospital admission	7·0 (5·5)	7·0 (5·0)	6·0 (3·8)	6·5 (6·0)	0·2572
Oxygen saturation (SO_2)· %	95·0 (3·0)	95·0 (2·8)	95·0 (3·5)	88·0 (7·0)	<0·0001
Systolic blood pressure (SBP)· mmHg	131·5 (26·0)	134·0 (28·0)	124·0 (29·8)	127·0 (15·0)	0·1944
Diastolic blood pressure (DBP)· mmHg	77·0 (18·0)	77·5 (20·0)	76·0 (18·3)	72·5 (22·0)	0·5928
Temperature· ºC	36·6 (0·8)	36·6 (0·7)	36·5 (1·0)	36·6 (1·3)	0·5400
Cardiac frequency· bpm	88·0 (24·0)	86 (21·5)	90·0 (26·8)	89·5 (32·0)	0·8899

*Risk factors refers to any patients with diabetes· heart disease· pre-existing lung disease· stroke or chronic renal failure. Moderate disease status is defined as category 4 or 5· and severe disease status as categories 6 to 9 following the WHO Clinical Progression Scale. The P-value corresponds to the result of the Chi-square test for the qualitative variables and the Kruskal Wallis test for the quantitative ones.

Table 2 COVID-19 treatment and outcomes.

	Total (n = 148)	**Moderate without progression (n = 107)**	**Moderate with progression (n = 19)**	**Severe (n = 22)**	***P*-value**
COVID-19 treatments					
Corticosteroid,· n (%) yes	129 (87·2)	88 (82·2)	19 (100·0)	22 (100·0)	0·0154
Remdesivir, n (%) yes	56 (37·8)	39 (36·4)	13 (68·4)	4 (18·2)	0.0036
Tocilizumab, n (%) yes	45 (30·4)	21 (19·6)	11 (57·9)	13 (59·1)	<0·0001
Outcomes					
Median length of hospitalization stay (days· SD)	8·0 (7·0)	7·0 (4·0)	15·0 (10·8)	17·5 (16·0)	<0·0001
NRB >24 h at any given time, n (%) yes	26 (17·6)	0 (0·0)	12 (63·2)	14 (63·6)	<0·0001
HFNC >24h at any given time, n (%) yes	40 (27·0)	0 (0·0)	19 (100·0)	21 (95·5)	<0·0001
NIV >24h at any given time, n (%) yes	2 (1·4)	0 (0·0)	1 (5·3)	1 (4·6)	0·0696
Invasive mechanical ventilation, n (%) yes	8 (5·4)	0 (0·0)	1 (5·3)	7 (31·8)	<0·0001
Intensive care Unit admission, n (%) yes	11 (7·4)	1 (0·9)	2 (10·5)	8 (36·4)	<0·0001
In-hospital mortality, n (%) yes	10 (6·8)	0 (0·0)	3 (15·8)	7 (31·8)	<0·0001

NRB: non-rebreather mask; HFNC: High flow nasal cannula; NIV: Non-invasive mechanical ventilation. Moderate disease status is defined as category 4 or 5· and severe disease status as categories 6 to 9 following the WHO Clinical Progression Scale. The P-value corresponds to the result of the Chi-square test.

Table 3. Lipoproteins and glycoproteins comparison between groups.

	Moderate at baseline (n = 22) vs Severe at baseline (n = 127)			**Moderate at baseline without progression (n = 108) vs Severe at baseline (n = 22)**			**Moderate at baseline without progression (n = 19) vs Moderate at baseline with progression (n = 108)**		
Lipoproteins	***β***	**SE**	***P*-value**	***β***	**SE**	***P*-value**	***β***	**SE**	***P*-va**
VLDL-C	0·1037	0·0372	**0·0061**	0·1047	0·0387	**0·0078**	0·0315	0·1105	0·7
IDL-C	0·1728	0·0349	**0·0000**	0·1721	0·0366	**0·0000**	0·0072	0·1075	0·9
LDL-C	-0·0066	0·0177	0·7107	-0·0126	0·0182	0·4893	0·0982	0·0525	0·0
HDL-C	-0·0417	0·0187	**0·0273**	-0·0394	0·0176	**0·0272**	-0·0536	0·0535	0·3
VLDL-TG	0·0729	0·0349	**0·0386**	0·0698	0·0360	0·0551	0·1044	0·1018	0·3
IDL-TG	0·1361	0·0266	**0·0000**	0·1378	0·0279	**0·0000**	-0·0031	0·0807	0·9
LDL-TG	0·1233	0·0304	**0·0001**	0·1226	0·0317	**0·0002**	0·0433	0·0927	0·6
HDL-TG	0·0710	0·0175	**0·0001**	0·0735	0·0183	**0·0001**	-0·0593	0·0544	0·2
VLDL-P	0·0809	0·0344	**0·0203**	0·0792	0·0358	**0·0289**	0·0867	0·1005	0·3
Large VLDL-P	0·0469	0·0263	0·0771	0·0450	0·0273	0·1029	0·0815	0·0758	0·2
Medium VLDL-P	0·0664	0·0545	0·2253	0·0612	0·0554	0·2711	0·1310	0·1610	0·4
Small VLDL-P	0·0823	0·0346	**0·0190**	0·0810	0·0361	**0·0266**	0·0864	0·1007	0·3
LDL-P	0·0097	0·0172	0·5735	0·0042	0·0176	0·8138	0·0959	0·0506	0·0
Large LDL-P	0·0147	0·0146	0·3140	0·0114	0·0151	0·4527	0·0467	0·0435	0·2
Medium LDL-P	0·0517	0·0304	0·0916	0·0441	0·0314	0·1625	0·1394	0·0917	0·1
Small LDL-P	-0·0119	0·0148	0·4237	-0·0169	0·0150	0·2630	0·0904	0·0432	**0·0**
HDL-P	-0·0275	0·0163	0·0944	-0·0252	0·0155	0·1059	-0·0249	0·0469	0·5
Large HDL-P	0·0129	0·0117	0·2721	0·0102	0·0114	0·3730	-0·0162	0·0347	0·6
Medium HDL-P	0·0141	0·0124	0·2575	0·0169	0·0115	0·1452	-0·0863	0·0362	**0·0**
Small HDL-P	-0·0573	0·0277	**0·0406**	-0·0586	0·0256	**0·0241**	0·0036	0·0822	0·9
VLDL-Z	-0·0005	0·0006	0·3416	-0·0006	0·0006	0·2700	0·0001	0·0016	0·9
LDL-Z	0·0023	0·0009	**0·0083**	0·0023	0·0009	**0·0083**	-0·0014	0·0025	0·5
HDL-Z	0·0040	0·0013	**0·0030**	0·0040	0·0012	**0·0012**	-0·0061	0·0035	0·0
Glycoproteins									
Glyc-B	0·0359	0·0127	**0·0054**	0·0353	0·0117	**0·0031**	0·0844	0·0375	**0·0**
Glyc-F	0·0204	0·0147	0·1663	0·0198	0·0147	0·1788	0·0145	0·0458	0·7
Glyc-A	0·0461	0·0146	**0·0020**	0·0452	0·0142	**0·0018**	0·0824	0·0438	0·0
H/W Glyc-B	0·0351	0·0122	**0·0046**	0·0353	0·0119	**0·0037**	0·0473	0·0364	0·1
H/W Glyc-A	0·0448	0·0133	**0·0010**	0·0452	0·0131	**0·0008**	0·0434	0·0405	0·2

Analysis of lipoprotein and glycoprotein in patients with severe versus moderate disease status at baseline, severe disease status at baseline versus moderate without progression to severity and moderate patients with progression versus moderate without progression. Significant p values are highlighted in bold. Moderate disease status is defined as category 4 or 5, and severe disease status as categories 6 to 9 following the WHO Clinical Progression Scale.

Abbreviations: β (regression coefficient), SE (standard error), VLDL-C (very-low-density lipoprotein cholesterol), IDL-C (intermediate-density lipoprotein cholesterol), HDL-C (high-density lipoprotein cholesterol), VLDL-TG (very-low-density lipoprotein triglycerides), IDL-TG (intermediate-density lipoprotein triglycerides), LDL-TG (low-density lipoprotein triglycerides), HDL-TG (high-density lipoprotein triglycerides), VLDL-P (very-low-density lipoprotein particle), LDL-P (low-density lipoprotein particle), HDL-P (high-density lipoprotein particle), VLDL-Z (very-low-density lipoprotein diameter), LDL-Z (low-density lipoprotein diameter), HDL-Z (high-density lipoprotein diameter).

Table 4. Low-molecular-weight metabolites comparison between groups.

	Severe at baseline (n = 22) vs Moderate at baseline (n = 127)	**Severe at baseline (n = 22) vs Moderate at baseline without progression (n = 108)**	**Moderate at baseline with progression (n = 19) vs Moderate at baseline withou**

							progression (n = 108)		
	β	**SE**	***P*-value**	***β***	**SE**	***P*-value**	***β***	**SE**	***P*-va**
3-Hydroxybutyrate	0·3587	0·0939	**0·0002**	0·3739	0·0960	**0·0002**	-0·4490	0·2899	0·12
Acetone	0·1119	0·0620	0·0733	0·1179	0·0632	0·0645	-0·1882	0·1845	0·31
Alanine	-0·0294	0·0235	0·2136	-0·0367	0·0241	0·1297	0·1475	0·0729	**0·04**
Creatinine	0·0071	0·0353	0·8406	0·0128	0·0362	0·7244	-0·0698	0·1056	0·50
Creatine	0·0411	0·0332	0·2180	0·0394	0·0345	0·2559	0·1207	0·1016	0·23
Glucose	0·1360	0·0324	**0·0001**	0·1403	0·0347	**0·0001**	0·0180	0·0998	0·85
Glutamate	0·0658	0·0345	0·0589	0·0613	0·0344	0·0776	0·0465	0·1066	0·66
Glutamine	-0·0195	0·0197	0·3257	-0·0274	0·0195	0·1620	0·1800	0·0591	**0·00**
Glycerol	0·1357	0·0249	**0·0000**	0·1424	0·0260	**0·0000**	-0·0244	0·0761	0·74
Glycine	0·0088	0·0240	0·7152	0·0072	0·0247	0·7702	0·0438	0·0676	0·51
Histidine	-0·0010	0·0180	0·9569	-0·0010	0·0172	0·9554	0·0564	0·0545	0·30
Lactate	0·1473	0·0294	**0·0000**	0·1505	0·0312	**0·0000**	-0·0865	0·0891	0·33
Threonine	0·0582	0·0190	**0·0027**	0·0578	0·0202	**0·0050**	-0·0189	0·0546	0·72
Tyrosine	-0·0086	0·0229	0·7090	-0·0098	0·0230	0·6696	0·0003	0·0721	0·99
Valine	0·0568	0·0177	**0·0017**	0·0528	0·0188	**0·0059**	0·0439	0·0510	0·39
Isoleucine	0·0842	0·0308	**0·0071**	0·0698	0·0315	**0·0288**	0·2134	0·0895	**0·01**
Leucine	0·0912	0·0232	**0·0001**	0·0909	0·0244	**0·0003**	-0·0164	0·0684	0·81

Analysis of low-molecular-weight metabolites (LMWM) in patients with severe versus moderate disease status at baseline, severe disease status at baseline versus moderate without progression to severity and moderate patients with progression versus moderate without progression. Significant p values are highlighted in bold. Moderate disease status is defined as category 4 or 5, and severe disease status as categories 6 to 9 following the WHO Clinical Progression Scale.

Abbreviations: β (regression coefficient), SE (standard error).

Table 5. Lipids comparison between groups.

	Severe at baseline (n = 22) vs Moderate at baseline (n = 127)			**Severe at baseline (n = 22) vs Moderate at baseline without progression (n = 108)**			**Moderate at baseline with progression (n = 19) vs Moderate at baseline withou progression (n = 108)**		
	β	**SE**	***P*-value**	***β***	**SE**	***P*-value**	***β***	**SE**	***P*-va**
EC	0·0160	0·0155	0·3027	0·0116	0·0156	0·4600	0·0771	0·0462	0·09
FC	0·0376	0·0142	**0·0089**	0·0366	0·0148	**0·0145**	0·0178	0·0429	0·67
TG	0·0893	0·0364	**0·0154**	0·0833	0·0378	**0·0296**	0·1307	0·1063	0·22
PL	0·0341	0·0159	**0·0334**	0·0311	0·0167	0·0652	0·0525	0·0472	0·26
PC	0·0401	0·0160	**0·0135**	0·0359	0·0167	**0·0337**	0·0666	0·0479	0·16
SM	0·0032	0·0134	0·8104	0·0016	0·0137	0·9094	0·0331	0·0398	0·40
LPC	0·0094	0·0242	0·6981	-0·0003	0·0244	0·9892	0·1296	0·0719	0·07
PUFA1	-0·0155	0·0293	0·5982	-0·0188	0·0294	0·5246	0·0754	0·0896	0·40
PUFA2	0·0323	0·0352	0·3604	0·0225	0·0322	0·4873	0·2185	0·1110	0·05
PUFA3	-0·0062	0·0226	0·7852	-0·0085	0·0232	0·7155	0·0596	0·0664	0·37
PUFA4	0·0539	0·0270	**0·0480**	0·0482	0·0282	0·0905	0·1433	0·0814	0·08
Linoleic	0·0476	0·0281	0·0922	0·0397	0·0265	0·1371	0·1665	0·0868	0·05
SFA	0·0503	0·0187	**0·0080**	0·0396	0·0184	**0·0331**	0·1322	0·0560	**0·02**
w6+w7	0·0476	0·0184	**0·0108**	0·0407	0·0186	**0·0306**	0·1168	0·0550	**0·03**
w9	0·0890	0·0353	**0·0129**	0·0933	0·0369	**0·0128**	-0·0187	0·1069	0·86
w3	0·0266	0·0237	0·2639	0·0282	0·0250	0·2623	0·0436	0·0704	0·53
DHA	0·0405	0·0310	0·1939	0·0332	0·0324	0·3081	0·1370	0·0951	0·15
ARA+EPA	-0·0134	0·0204	0·5109	-0·0184	0·0201	0·3615	0·1181	0·0593	**0·04**

Analysis of lipids in patients with severe versus moderate disease status at baseline, severe disease status at baseline versus moderate without progression to severity and moderate patients with progression versus moderate without progression. Significant p values are highlighted in bold. Moderate disease status is defined as category 4 or 5, and severe disease status as categories 6 to 9 following the WHO Clinical Progression Scale. Abbreviations: β (regression coefficient), SE (standard error)· EC (esterified cholesterol), FC (free cholesterol), TG (triglycerides), PL (phospholipids), PC (phosphatidylcholine), SM (sphingomyelin), LPC (Lysophosphatidylcholine), PUFA (polyunsaturated fatty acids), SFA (saturated fatty acids), DHA (Docosahexaenoic acid)· ARA (Arachidonic Acid), EPA (eicosapentaenoic acid)

5. Discussion

Discussion

Our investigations focused on the host-pathogen interaction in CAP and COVID-19.

First, we focused on the genome-wide expression of all genes in the peripheral blood, examining the **whole-blood transcriptomic of hospitalised patients with CAP**. We compared the whole blood transcriptomic of those **who died with those who survived** in order to identify pathways that not only inform about pathophysiology but may also be suitable as prognostic biomarkers. Previous studies evaluating transcriptomic profiles associated with severity or mortality in CAP are scarce. For instance, Hopp et al (280) observed dysregulation in immune pathways, such as T-cell immune suppression, chemokine receptor deactivation, and macrophage polarization, in septic patients within the ICU. Similarly, Severino et al (281) noted differences in oxidative phosphorylation in mononuclear cells at hospitalisation seemed to be associated with prognosis. Moreover, comparisons between admission and follow-up samples highlighted distinct gene expression profiles between survivors and non-survivors, with a notable decrease in genes associated with immune functions. Our study distinguishes itself in terms of objectives, inclusion criteria, and methods for assessing gene expressions, employing whole blood instead of mononuclear cells.

Among the identified pathways, certain findings reveal a dual role—a "double-edged sword"—whereby they contribute both to pathogen defence and organ damage. Notably, gene sets positively enriched in deceased CAP patients were associated with apoptosis, interferon alpha response, and sex hormones. Dysregulated apoptosis, linked with stress-induced transcription factor p53 activation, may contribute to immune dysfunction, impaired perfusion, and tissue hypoxia, potentially leading to multiple organ failure in sepsis (282). Evidence suggests that prevention of cell apoptosis can improve prognosis in animal models of sepsis. A study documented that that the lungs of naive p53(-/-) mice display proinflammatory genes and clear pathogens more successfully than controls after intrapulmonary infection (283).

Furthermore, our data highlighted a significant enrichment in genes associated with spermatogenesis. Sex hormones have been described to have regulatory influences on immune responses. Oestradiol can stimulate the production of proinflammatory cytokines and macrophage activation, and testosterone has a suppressive impact on immune responses and enhances vulnerability to infection (284). High oestrogen levels, such as oestradiol, have been observed in male and female patients with sepsis and septic shock, and has been related

with a significant higher risk of in-hospital mortality (284,285). Moreover, in males with CAP, sex and mineralocorticoid hormone metabolites have been related with inflammation, disease severity and long-term survival (286).

Other key feature of the gene expression profile in CAP patients who died that we found was upregulation of the interferon-alpha response pathway. Beyond its antiviral properties, the type 1 interferon-alpha also has a role in bacterial replication and lung inflammation control. Improved outcomes were noted in animal models of bacterial pneumonia through interferon-alpha mediated neutrophil and macrophage activation (287). However, unchecked interferon-alpha activity may lead to pathogenic damage and an uncontrolled inflammatory response (288) and is associated with CAP severity (289).

Conversely, surviving CAP patients exhibited positively enriched gene sets related to oxidative stress, angiogenesis, and endoplasmic reticulum stress pathways. Regarding oxidative stress, organisms that live under aerobic conditions are exposed to several oxidizing agents, including reactive oxygen species and reactive nitrogen species. These reactive species have essential biological functions for normal cell development. However, the imbalance between the generation of reactive species and antioxidant defence, known as oxidative stress, can result in impaired homeostasis and lead to various pathologies (290). Oxidative stress is part of the pathogenic mechanism for CAP and is closely linked to inflammation (291).

Numerous biomarkers have been associated with angiogenesis, including angiopoietins, the members of the vascular endothelial growth factor family, transforming growth factors, interleukins, platelet-derived growth factor, and fibroblast growth factor family. During infection, factors related with angiogenesis and endothelial barrier are essential for the migration of the cells of the immune system into infected tissues, but they can also participate in the pathogenesis of septic shock and acute multiple organ dysfunction (292). Moreover, under conditions that causes stress and inflammation, endoplasmic reticulum loses the homeostasis in its function, which is termed as endoplasmic reticulum stress. During endoplasmic reticulum stress, unfolded protein response (UPR) is activated to restore the normal endoplasmic reticulum function. UPR preserves a homeostatic environment and regulates a wide variety of cellular processes, such as cellular proliferation and differentiation, inflammation, apoptosis, and angiogenesis. However, excessive and prolonged activation of UPR can lead to cell dysfunction, death, and disease (293). Finally,

transcription factor MYC may be an important regulatory gene in the underlying dysfunction of sepsis-induced ARDS (294).

Our study has several limitations that should be acknowledged. The small sample size of deceased patients warrants validation in larger cohorts, and confounding variables such as age and underlying diseases were not adjusted. Additionally, our study captured gene expression profiles at a single time point, thus, potentially overlooking dynamic changes throughout the disease course. Future research should address these limitations and confirm our findings using real-time quantitative polymerase chain reaction of target genes.

Following our investigation of the gene expression profile of hospitalised CAP patients, our research focus shifted towards describing host-pathogen factors contributing to one of the most significant complications of CAP—acute cardiac events. Although limited, previous studies have aimed to identify clinical risk factors for these events, and animal research has highlighted the strain-dependency of cardiac lesions induced by *S. pneumoniae*, the most frequent bacterial cause of CAP. Given this context, we sought to investigate both **the host factors and association between pneumococcal serotypes or clonal complexes and the risk of developing acute cardiac events**.

Among the host factors independently linked with acute cardiac events in pneumococcal pneumonia, we identified older age, pre-existing heart conditions, pneumococcal bacteraemia, septic shock at admission, and high risk-pneumonia. Notably, pre-hospitalisation antibiotic treatment for the acute episode of pneumococcal pneumonia showed a trend towards a protective effect against acute cardiac events, although statistical significance was not reached in multivariate analysis. Experimental animal studies have shown a significant positive correlation between pneumococcal blood load and cardiac damage (106,109) and pneumococcal bacteraemia has been shown to be an important trigger for the development of acute cardiac events in CAP patients. As we found a lower incidence of bacteraemia with a less severe clinical presentation in patients with pre-hospitalisation antibiotic treatment, a lower incidence of cardiac complications seems logical.

Existing data on pneumococcal strains and cardiac complications are primarily derived from limited studies (109,254). One experimental study involving a small sample size of mice revealed that only serotypes capable of causing high-grade bacteraemia, such as serotypes 2, 3, 4, and 6A, induced cardiac damage (109). Moreover, for the serotypes that could invade the heart, the type of cardiac damage was strain specific. Another study of patients with invasive pneumococcal disease found an association between serotypes 3 and

9N and acute cardiac events, although clonal complexes were not analysed (254). Contrary to these findings, our study, encompassing a larger patient cohort, did not find a significant association of serotypes 3 and 9N with acute cardiac events. Our study, analysing serotypes isolated from 872 patients and clonal complexes from 742, observed a negative trend linking acute cardiac events with certain highly clonal serotypes, notably 5 (CC289) or 1 (CC306), and a tendency for clonal complex CC230 to be associated with a higher incidence of acute cardiac events. This finding, though not statistically significant, holds potential clinical relevance. Especially considering that clonal complex CC230 is mainly related to serotypes 19A and 24F, with serotype 24F not being covered by existing vaccines. Additionally, our findings suggest that genetic background, and not serotype, could play a major role in these serious complications.

Our discovery regarding the potential association of CC230 with a higher incidence of acute cardiac events warrants further investigation through multicentre studies involving diverse geographical regions and a larger array of pneumococcal strains. Moreover, our study paves the way for future research exploring the long-term risk of serious cardiac events associated with specific pneumococcal serotypes and genotypes.

Despite a number of strengths, our study has some limitations that should be acknowledged. Firstly, the study involved a cohort of adults with pneumococcal pneumonia recorded over more than twenty years at a single centre. This may limit the extrapolation of our results to other geographical areas where other serotypes and clonal complexes may be more prevalent (295). Secondly, while serotyping and genotyping were not conducted for all isolates, they were determined for the majority of the 983 isolates, with serotypes identified in 89% and genotypes in 76% of cases, respectively. Thirdly, the small number of some serotypes and clonal complexes limited the analysis of their potential relationship with acute cardiac complications. Finally, the exacerbation of pre-existing heart conditions was considered as an acute cardiac event, which could potentially confound the results. However, when analysing only new-onset arrhythmias, new-onset heart failures, and myocardial infarctions, similar findings were observed.

With the emergence of SARS-CoV-2, a novel human betacoronavirus, and its wide spectrum of clinical presentations, there arose an urgent need for insights into its pathogenesis. However, many transcriptomic studies of COVID-19 focused on single time points per patient, overlooking the dynamic nature of the disease. Therefore, our objective

was to enhance comprehension of the underlying **transcriptomic host response to SARS-CoV-2 infection by examining the dynamic gene-expression profiles of whole peripheral blood from both severe and moderate hospitalised COVID-19 patients**.

Our study found a dysregulated inflammatory response behind severe pneumonia in SARS-CoV-2 infection. Consistent with findings in existing literature, we found that patients with ARDS at baseline showed an upregulation of genes related to IL-6 and JAK-STAT3 signalling and neutrophil activation (205,208,209), a downregulation of T-cell activation, and a subsequent loss of CD4+ T cells (208,210). Additionally, we identified an increase in gene expression related to reactive oxygen species metabolism in ARDS patients at baseline, a finding previously reported in later stages of COVID-19 (208). This discrepancy likely stems from delayed hospital admission in our cohort, with many patients presenting to the emergency department already in established ARDS. Our findings concur with other transcriptomic studies that have encountered an upregulation of genes related to protein polyubiquitination (209) and metalloproteinases (296) in later stages of COVID-19 induced ARDS. In contrast, non-ARDS COVID-19 patients exhibited increased expression of Wnt/β-catenin signalling and Myc V2 targets, a sub-group of genes regulated by Myc. Wnt/β-catenin pathway components modulate T-cell priming and infiltration (297) and negatively regulate NF-$\varkappa$B (298), thereby promoting viral tolerance and mitigating inflammation. Myc, known for its role in cancer, also directly contribute to immune suppression by inhibiting macrophage activation (299) and endothelial inflammation (300).

Furthermore, our results underscore the significance of long non-coding RNAs and microRNAs as emerging regulators in SARS-CoV-2 infection. Patients with ARDS at baseline presented higher levels of CLRN1-AS1, a lncRNA that deactivates the Wnt/β-catenin signalling pathway (301), and IRAIN, which enhances the formation of an intrachromosomal promoter loop of IGF1R (302). Increased serum levels of IGF1R correlate with COVID-19 mortality (303). On the other hand, the expression of the lncRNAs A2M-AS1, LEF-AS1, and RORA-AS-1 was significantly decreased in patients with ARDS. A2M-AS1 likely exerts anti-proliferation and pro-apoptosis effect [37], while LEF1-AS1 and RORA-AS-1 have been found to be involved in T cell differentiation in COVID-19 patients (304).

Our study has several limitations that should be acknowledged. Primarily, the majority of patients were from the first COVID-19 wave, dominated by lineage A. Subsequent SARS-CoV-2 variants and subvariants may elicit different host responses.

Secondly, the sample size was relatively small, with only 60 patients, of whom 19 developed ARDS. However, the strength of our study lies in daily follow-up assessments of patients, ensuring accurate respiratory status evaluation. Furthermore, the validation of our results is bolstered by the concordance of cell composition in the studied samples with previous studies conducted using single-cell RNA sequencing (305,306).

As previously mentioned, considerable gaps in our understanding or the pathogenesis of SARS-CoV-2 infection exist. Specifically, the intricate development of the humoral immune response was initially poorly understood, particularly, no data on the specific role of mucosal immunity was available. Moreover, it remained uncertain whether this immune response could be shaped by prior exposure to related viruses, a phenomenon well documented with influenza and other viruses. Therefore, our study aimed to **delineate the dynamic antibody responses involved in the generation of de novo antibodies against SARS-CoV-2 in** both **peripheral blood and respiratory mucosa**. Additionally, we sought to assess the influence of pre-existing immunity against select endemic coronaviruses, thereby exploring the concept of **immunological imprinting**.

Our findings present a dynamic characterization of the antibody response to SARS-CoV-2 and provide the first evidence of immune imprinting in this infection. Our cohort allowed for quantification and detailed representation of the longitudinal outcome of the immune response by taking into consideration past exposure to related antigens. Furthermore, in vitro neutralisation activity of antibodies might be used as a proxy for protection against SARS-CoV-2 infection (307,308). We observed back-boosting against the conserved epitopes of the spike protein of OC43 and HKU1 betacoronaviruses. No induction was detected for the variable regions of these viruses, such as the S1 domain, or to more divergent seasonal alphacoronaviruses, such as 229E. IgG responses to the spike and RBD of SARS-CoV-2 showed persistence over the time period of our study with slight changes in antibody levels in convalescent sera as compared to the peak of antibody induction at day 7. Importantly, immunity to other betacoronavirus spikes, like HKU1 and OC43, limited the induction of de novo responses to all tested SARS-CoV-2 antigens. All patients also developed detectable levels of spike IgG/IgM and N IgG. Although no significant correlation was found between pre-exposure to seasonal coronaviruses and the induction of protective antibodies with neutralizing activity, our data suggested a negative relationship. Baseline antibody levels to HKU1 or OC43 spike after SARS-CoV-2 IgG levels normalised limited the induction of neutralizing antibody levels during follow-up.

While statistically significant differences in antibody levels between patients with mild vs. severe disease were not found, severe cases exhibited a delay in antibody responses. Additionally, anti-SARS-CoV-2 antibodies inversely correlated with viral loads in respiratory samples, suggesting a potential role in viral clearance. We could not find a link between virus clearance and back-boosting of antibodies toward the S2 subunit of the seasonal human coronaviruses. Although, it has to be noted that cross-reactivity between pre-existing memory T cells to seasonal coronaviruses and SARS-CoV-22 has been described, (35,309) pointing to a potential role of heterologous immunity as an additional mechanism of protection. However, our results allow for a contrasting hypothesis in which early priming of the memory B cell compartment due to pre-exposure to seasonal coronaviruses could dampen secondary responses toward new epitopes of SARS-CoV-2. Nonetheless, all our patients developed antibody responses against SARS-CoV-2 antigens and specific neutralizing antibodies.

We found a strong induction of IgA antibodies against SARS-CoV-2 S protein in the upper respiratory tract, accompanied by robust mucosal sIgA production. Recent publications have similarly highlighted the emergence of specific mucosal IgA responses during SARS-CoV-2 mRNA intramuscular vaccination (310), albeit the duration of this response remains uncertain. Boosting mucosal antibody response to potentially mitigate viral transmission and bolster protection is of great interest. Additionally, we detected IgG, sIgA, and IgA antibodies against HCoV-OC43 S protein in the local upper respiratory mucosa, whereas no IgM responses were observed. Moreover, antibody responses against HCoV-OC43 S peaked earlier than SARS-CoV-2 S antibody titers in the local mucosa suggesting some maturity in the cross-reactive immune responses against conserved epitopes of beta-HCoVs in the upper respiratory tract. This observation underscores the phenomenon of immune imprinting within the mucosal compartment during COVID-19.

Our findings have significant implications for the development of COVID-19 vaccines. The potential interactions with pre-existing immunity should be carefully considered to optimize vaccine efficacy. Current COVID-19 vaccines aim to induce responses against the full-length S protein of SARS-CoV-2, which contains cross-reactive non-neutralizing epitopes shared with seasonal human betacoronaviruses. Back-boost of cross-reactive antibody responses might lead to less protective antibodies directed against non-neutralizing conserved epitopes between the S antigen of the vaccine and the S proteins of seasonal human betacoronaviruses. Therefore, cross-reactive antibody responses may affect the protective efficacy of these vaccines. However, whether in vitro non-neutralizing

anti-SARS-CoV-2 antibodies contribute to protection or disease or are neutral is still not clear. Additionally, our findings support the idea that upon SARS-CoV-2 infection, the immune imprinting in the mucosal compartment will activate memory B cells generated from prior infections with antigenically related HCoVs, perhaps competing with the activation of naive B cells specific for SARS-CoV-2 novel epitopes.

Despite the valuable insights provided by our study, there are limitations that should be acknowledged. The relatively small number of enrolled subjects and the requirement for hospitalisation may limit the generalizability of our findings. Additionally, the study did not include asymptomatic or mild cases of COVID-19, thus precluding characterization of pre-existing immunity in these populations.

Nevertheless, our results underscore the influence of immune imprinting due to previous exposure to seasonal human betacoronavirus on the antibody response to SARS-CoV-2 infection, which may have implications for vaccine development and efficacy. The importance of our findings are further highlighted by the fact that it has now be demonstrated that immune imprinting impairs neutralizing antibody titers for bivalent mRNA vaccination against SARS-CoV-2 Omicron subvariants (311).

Several metabolomic studies on COVID-19 have been conducted, primarily focused on establishing a discriminative COVID-19 metabolomic profile for effective identification and differentiation of COVID-19 clinical statuses. The majority of these studies utilized mass spectrometry techniques with a minority aiming to describe a prognostic metabolomic signature, despite the critical importance of early identification of hospitalised COVID-19 patients at risk of developing severe disease. This early identification is vital for optimizing resource allocation and initiating treatment promptly. In our last study, we aimed to **delineate the metabolomic profile of moderate and severe hospitalised adult COVID-19 patients**. Our objective was to **establish a metabolomics predictive signature** that could assess the risk of **disease progression**. Unlike many studies that employ heterogeneous definitions of COVID-19 severity, potentially leading to misclassification amid healthcare resource strain during surges, we defined severity according to the WHO Clinical Progression Scale categories. Furthermore, in contrast to several prior predictive metabolomics models, which often compare patients who have already reached severe disease with mild to moderate COVID-19 patients (225,226,231,235), our approach involved comparing patients with equivalent clinical status at baseline status.

We found profound changes in lipoprotein distribution in severe COVID-19, showing an increased atherogenic risk with increased severity, small VLDL particles were increased while small HDL particles were diminished. Small HDL particles, the HDL subspecies most decreased in our study as well as another study (312), is also the HDL subspecies most strongly associated with cholesterol efflux capacity function (313). Severe disease status (WHO Clinical Progression Scale categories 6 to 9) was associated with an intense lipoprotein dysregulation towards increased triglycerides, free cholesterol and anomalous lipoprotein distribution with elevated intermediate-density lipoprotein-cholesterol (IDL-C), LDL-cholesterol and VLDL subclasses while HDL-cholesterol was decreased.

Our results are in line with previous studies who found a correlation between COVID-19 severity with high triglyceride concentrations, no-HDL-cholesterol and low plasma HDL-cholesterol (114,115), an increased mean size of VLDL particles (238) and higher levels of free cholesterol (115). We also found, unsurprisingly, an elevated glyc-A and glyc-B signal in more severe patients. Glyc-A and glyc-B represent different glycosylated amino sugar residues on acute phase reactants (314), with α-1-acid glycoprotein having the strongest correlation with Glyc-A (315). Previous studies have related glyc-A with chronic inflammation (316), metabolic syndrome(317), increased severity (318,319) and higher levels of C-reactive protein and IL-6 in COVID-19 (319). Furthermore, severe COVID-19 patients had elevated levels of branched-chained amino acids (BCAAs: leucine, isoleucine and valine) compared to moderate COVID-19 patients, results which are concordant with prior studies (230,237,320,321). BCAAs are essential amino acids which act as substrates and regulator of protein and glycogen metabolism (322,323), and modulate glucose metabolism. Elevated circulating levels of BCAAs are associated with catabolic states (324), and, through mTOR activation, linked to reactive oxygen species production and mitochondrial dysfunction (325) in addition to promoting endothelial dysfunction (326). In addition, concordant with prior studies, we found elevated glucose (115) and accumulation of ketone bodies in severe COVID-19 patients (230,327), reflecting dysregulation of hepatic carbon metabolism (238).

When comparing moderate COVID-19 patients who did not progress with those who did, several of the alterations in serum metabolites associated with severe disease status lost their significance. Most notably, no differences in free cholesterol, phospholipids, IDL, VLDL, HDL were found, suggesting that most of the intense lipoprotein dysregulation occurs in later disease stages. Higher levels of small LDL particles with a decrease in medium

HDL particles, not present in the metabolomic comparison of moderate versus severe patients, was found to be predictive. A reduction of HDL has been previously associated with worse outcomes (114,239) and a predominance of small LDL particles compared to larger LDL particles has been identified in COVID-19 patients (312). Increased levels of isoleucine, saturated fatty acids, and glyc-B, both associated with severe disease status, were also found to be predictive for progression to severity. Furthermore, our results showed increased risk for progression in patients with increased alanine and glutamine levels. These particular findings are surprising as glutamine is essential for lymphocyte proliferation, cytokine production and macrophage activation, with increased demand in catabolic/hypercatabolic circumstances (328). In addition, prior studies comparing uninfected controls versus COVID-19 patients found both decreased levels of alanine (320,329) and glutamine (238,318,330) in COVID-19 patients and severe COVID-19 (230). These diverging results may stem from differences in the compared cohorts. SARS-CoV-2 infection correlates with reduced glutamine levels compared to uninfected individuals. However, we compared moderate COVID-19 patients without progression with those who did progress at later stages. With these results, and incorporating metabolite ratios, we were able to construct a multivariate model for progression towards severity upon admission for hospitalised COVID-19 patients with moderate disease status and similar oxygen saturation. Our predictive model showed a cross-validated AUC of 0.82 and a predictive accuracy of 72%.

This study has some limitations that should be acknowledged. Firstly, due to the nascent stage of vaccination within the general population in Spain at the study period, only unvaccinated patients without prior known COVID-19 were included. Secondly, the study period coincided with the predominance of the Alpha (B.1.1.7) variant of SARS-CoV-2. Subsequent variants and subvariants might have elicited different host responses. Lastly, the sample size was moderately small, 148 patients of whom 19 progressed following baseline sampling. However, the patients included in our study were followed up daily, which allowed an accurate assessment of their clinical disease trajectory.

6. Conclusions

Conclusions

1. The whole blood transcriptomic profiles of community-acquired pneumonia survivors and non-survivors presented differences, mainly related to interferon-alpha response, apoptosis, sex hormones, oxidative stress, unfolded protein response, and angiogenesis pathways. The differentially expressed genes could potentially be useful as risk-stratification biomarkers.

2. Host factors appear to be more important than pathogen-related factors for developing these acute cardiac events in pneumococcal community-acquired pneumonia. Clonal complex 230 appears to be associated with a higher incidence of acute cardiac events that could have relevant clinical implications as some serotypes associated with CC230, such as 24F, are not included in the current available vaccines.

3. Acute respiratory distress syndrome in COVID-19 is caused by a dysregulated inflammatory response an increased expression of genes related to pro-inflammatory molecules and neutrophil and macrophage activation at admission, in addition to the loss of immune regulation. This leads to a higher expression of genes related to reactive oxygen species, protein polyubiquitination, and metalloproteinases at latter stages.

4. Immunological imprinting by previous seasonal coronavirus infections modulates the antibody profile to SARS-CoV-2 infection. This antibody memory boost to human coronaviruses negatively correlates with the induction of IgG and IgM against SARS-CoV-2 spike and nucleocapsid protein. This finding has significant implications on the development of COVID-19 vaccines, as the potential interactions with pre-existing immunity should be taken into consideration in the path to optimal vaccines.

5. COVID-19 patients mount a robust mucosal antibody response against SARS-CoV-2 spike protein with specific secretory immunoglobulin A (sIgA), IgA, IgG, and IgM antibody subtypes. An immune memory recall to conserved epitopes of beta-coronaviruses is present in the upper respiratory tract during SARS-CoV-2 infection.

6. Severe COVID-19 is associated with a distinct metabolomic signature associated with an increased atherogenic risk and a pro-inflammatory catabolic state with dysregulated carbon metabolism. Patients presenting with moderate disease but at a high risk of deterioration exhibit a characteristic metabolomic signature, which can be determined using NMR-based platforms to predict disease progression.

7. References

References

1. Kyu HH, Vongpradith A, Sirota SB, Novotney A, Troeger CE, Doxey MC, et al. Age–sex differences in the global burden of lower respiratory infections and risk factors, 1990–2019: results from the Global Burden of Disease Study 2019. Lancet Infect Dis. 2022;22(11):1626–47.

2. Safiri S, Mahmoodpoor A, Kolahi AA, Nejadghaderi SA, Sullman MJM, Mansournia MA, et al. Global burden of lower respiratory infections during the last three decades. Front Public Heal. 2023;10.

3. Ramirez JA, Wiemken TL, Peyrani P, Arnold FW, Kelley R, Mattingly WA, et al. Adults Hospitalized with Pneumonia in the United States: Incidence, Epidemiology, and Mortality. Clin Infect Dis. 2017;65(11):1806–12.

4. de Miguel-Díez J, Jiménez-García R, Hernández-Barrera V, Jiménez-Trujillo I, de Miguel-Yanes JM, Méndez-Bailón M, et al. Trends in hospitalizations for community-acquired pneumonia in Spain: 2004 to 2013. Eur J Intern Med

5. Mandell G, Bennet J, Dolin R, Blaser M. Mandell, Douglas, and Bennett's Principles and Practice of Infectious Diseases. Elsevier Health Science, editor; 2014.

6. Molina J, González-Gamarra A, Ginel L, Peláez ME, Juez JL, Artuñedo A, et al. CAPPRIC Study-Characterization of Community-Acquired Pneumonia in Spanish Adults Managed in Primary Care Settings. Microorganisms. 2021 Feb;9(3).

7. Viasus D, Núñez-Ramos JA, Viloria SA, Carratalà J. Pharmacotherapy for community-acquired pneumonia in the elderly. Expert Opin Pharmacother. 2017 Jul;18(10):957–64.

8. Welte T, Torres A, Nathwani D. Clinical and economic burden of community-acquired pneumonia among adults in Europe. Thorax [Internet]. 2012 Jan [cited 2019 Jun 5];67(1):71–9.

9. Broulette J, Yu H, Pyenson B, Iwasaki K, Sato R. The incidence rate and economic burden of community-acquired pneumonia in a working-age population. Am Heal drug benefits. 2013 Sep;6(8):494–503.

10. Weycker D, Moynahan A, Silvia A, Sato R. Attributable Cost of Adult Hospitalized Pneumonia Beyond the Acute Phase. PharmacoEconomics - open. 2021 Jun;5(2):275–84.

11. Jain S, Self WH, Wunderink RG, Fakhran S, Balk R, Bramley AM, et al. Community-acquired pneumonia requiring hospitalization among U.S. adults. N Engl J Med. 2015 Jul 30;373(5):415–27.

12. Cilloniz C, Ewig S, Gabarrus A, Ferrer M, Puig de la Bella Casa J, Mensa J, et al. Seasonality of pathogens causing community-acquired pneumonia. Respirology. 2017 May;22(4):778–85.

13. Yildirim I, Shea KM, Pelton SI. Pneumococcal Disease in the Era of Pneumococcal Conjugate Vaccine. Infect Dis Clin North Am. 2015 Dec;29(4):679–97.

14. Waight PA, Andrews NJ, Ladhani SN, Sheppard CL, Slack MPE, Miller E. Effect of the 13-valent pneumococcal conjugate vaccine on invasive pneumococcal disease in England and Wales 4 years after its introduction: an observational cohort study. Lancet Infect Dis. 2015 May;15(5):535–43.

15. Moore MR, Link-Gelles R, Schaffner W, Lynfield R, Lexau C, Bennett NM, et al. Effect of use of 13-valent pneumococcal conjugate vaccine in children on invasive pneumococcal disease in children and adults in the USA: analysis of multisite, population-based surveillance. Lancet Infect Dis. 2015 Mar;15(3):301–9.

16. Torres A, Cillóniz C, Blasi F, Chalmers JD, Gaillat J, Dartois N, et al. Burden of pneumococcal community-acquired pneumonia in adults across Europe: A literature review. Respir Med. 2018 Apr;137:6–13.

17. Bonten MJM, Huijts SM, Bolkenbaas M, Webber C, Patterson S, Gault S, et al. Polysaccharide conjugate vaccine against pneumococcal pneumonia in adults. N Engl J Med. 2015 Mar;372(12):1114–25.

18. Løchen A, Croucher NJ, Anderson RM. Divergent serotype replacement trends and increasing diversity in pneumococcal disease in high income settings reduce the benefit of expanding vaccine valency. Sci Rep. 2020 Nov;10(1):18977.

19. de Miguel S, Domenech M, González-Camacho F, Sempere J, Vicioso D, Sanz JC, et al. Nationwide Trends of Invasive Pneumococcal Disease in Spain From 2009 Through 2019 in Children and Adults During the Pneumococcal Conjugate Vaccine Era. Clin Infect Dis an Off Publ Infect Dis Soc Am. 2021 Dec;73(11):e3778–87.

20. Ardanuy C, Broner S, Cabezas C, Ciruela P, Izquierdo C, Martínez M, et al. Epidemiologia de la malaltia pneumocòccica invasiva a Catalunya: informe 2021-2022; sistema de notificació microbiològica de Catalunya. Barcelona: Agència de Salut Pública de Catalunya.

21. Self WH, Wunderink RG, Williams DJ, Zhu Y, Anderson EJ, Balk RA, et al. Staphylococcus aureus Community-acquired Pneumonia: Prevalence, Clinical Characteristics, and Outcomes. Clin Infect Dis an Off Publ Infect Dis Soc Am. 2016 Aug;63(3):300–9.

22. Musher DM, Roig IL, Cazares G, Stager CE, Logan N, Safar H. Can an etiologic agent be identified in adults who are hospitalized for community-acquired pneumonia: results of a one-year study. J Infect. 2013 Jul;67(1):11–8.

23. Shoar S, Musher DM. Etiology of community-acquired pneumonia in adults: a systematic review. Pneumonia (Nathan Qld). 2020;12:11.

24. Gadsby NJ, Musher DM. The Microbial Etiology of Community-Acquired Pneumonia in Adults: from Classical Bacteriology to Host Transcriptional Signatures. Clin Microbiol Rev. 2022 Dec;35(4):e0001522.

25. Burk M, El-Kersh K, Saad M, Wiemken T, Ramirez J, Cavallazzi R. Viral infection in community-acquired pneumonia: A systematic review and meta-analysis [Internet]. Vol. 25, European Respiratory Review. European Respiratory Society; 2016. p. 178–88.

26. Tsalik EL, Henao R, Montgomery JL, Nawrocki JW, Aydin M, Lydon EC, et al. Discriminating Bacterial and Viral Infection Using a Rapid Host Gene Expression Test. Crit Care Med. 2021 Oct;49(10):1651–63.

27. Huang C, Wang Y, Li X, Ren L, Zhao J, Hu Y, et al. Clinical features of patients infected with 2019 novel coronavirus in Wuhan, China. Lancet (London, England). 2020 Feb;395(10223):497–506.

28. Lu R, Zhao X, Li J, Niu P, Yang B, Wu H, et al. Genomic characterisation and epidemiology of 2019 novel coronavirus: implications for virus origins and receptor binding. Lancet (London, England). 2020 Feb;395(10224):565–74.

29. Yao H, Song Y, Chen Y, Wu N, Xu J, Sun C, et al. Molecular Architecture of the SARS-CoV-2 Virus. Cell. 2020 Oct;183(3):730-738.e13.

30. Jamison DAJ, Anand Narayanan S, Trovão NS, Guarnieri JW, Topper MJ, Moraes-Vieira PM, et al. A comprehensive SARS-CoV-2 and COVID-19 review, Part 1: Intracellular overdrive for SARS-CoV-2 infection. Eur J Hum Genet. 2022 Aug;30(8):889–98.

31. Gordon DE, Jang GM, Bouhaddou M, Xu J, Obernier K, White KM, et al. A SARS-CoV-2 protein interaction map reveals targets for drug repurposing. Nature. 2020 Jul;583(7816):459–68.

32. Boni MF, Lemey P, Jiang X, Lam TT-Y, Perry BW, Castoe TA, et al. Evolutionary origins of the SARS-CoV-2 sarbecovirus lineage responsible for the COVID-19 pandemic. Nat Microbiol. 2020 Nov;5(11):1408–17.

33. Ieven M, Coenen S, Loens K, Lammens C, Coenjaerts F, Vanderstraeten A, et al. Aetiology of lower respiratory tract infection in adults in primary care: a prospective study in 11 European countries. Clin Microbiol Infect Off Publ Eur Soc Clin Microbiol Infect Dis. 2018 Nov;24(11):1158–63.

34. Zaki AM, van Boheemen S, Bestebroer TM, Osterhaus ADME, Fouchier RAM. Isolation of a novel coronavirus from a man with pneumonia in Saudi Arabia. N Engl J Med. 2012 Nov;367(19):1814–20.

35. Peiris JSM, Lai ST, Poon LLM, Guan Y, Yam LYC, Lim W, et al. Coronavirus as a possible cause of severe acute respiratory syndrome. Lancet (London, England). 2003 Apr;361(9366):1319–25.

36. Forni D, Cagliani R, Clerici M, Sironi M. Molecular Evolution of Human Coronavirus Genomes. Trends Microbiol. 2017 Jan;25(1):35–48.

37. Morens DM, Fauci AS. Emerging Pandemic Diseases: How We Got to COVID-19. Cell. 2020 Sep;182(5):1077–92.

38. Guan W, Ni Z, Hu Y, Liang W, Ou C, He J, et al. Clinical Characteristics of Coronavirus Disease 2019 in China. N Engl J Med [Internet]. 2020 Apr 30 [cited 2021 Dec 3];382(18):1708–20.

39. Brüssow H, Brüssow L. Clinical evidence that the pandemic from 1889 to 1891 commonly called the Russian flu might have been an earlier coronavirus pandemic. Microb Biotechnol. 2021 Sep;14(5):1860–70.

40. https://www.who.int/emergencies/diseases/novel-coronavirus-2019.

41. World Health Organization. Statement on the fifteenth meeting of the IHR (2005) Emergency Committee on the COVID-19 pandemic . Available from: https://www.who.int/news/item/05-05-2023-statement-on-the-fifteenth-meeting-of-the-international-health-regulations-(2005)-emergency-committee-regarding-the-coronavirus-disease-(covid-19)-pandemic

42. https://covid19.who.int/.

43. Markov P V., Ghafari M, Beer M, Lythgoe K, Simmonds P, Stilianakis NI, et al. The evolution of SARS-CoV-2. Nat Rev Microbiol 2023 216 . 2023 Apr 5 ;21(6):361–79.

44. https://covid.cdc.gov/covid-data-tracker/#trends_weeklydeaths_currenthospitaladmissions_00.

45. Tan CY, Chiew CJ, Pang D, Lee VJ, Ong B, Lye DC, et al. Protective immunity of SARS-CoV-2 infection and vaccines against medically attended symptomatic omicron BA.4, BA.5, and XBB reinfections in Singapore: a national cohort study. Lancet Infect Dis. 2023 Jul 1;23(7):799–805.

46. Osler W, McCrae T. The principles and practice of medicine. New York, London D Applet Co. 1920;

47. https://www.who.int/data/gho/data/themes/mortality-and-global-health-estimates/ghe-leading-causes-of-death.

48. Wuerth BA, Bonnewell JP, Wiemken TL, Arnold FW. Trends in Pneumonia Mortality Rates and Hospitalizations by Organism, United States, 2002–20111. Emerg Infect Dis . 2016 Sep;22(9):1624–7.

49. Marshall DC, Goodson RJ, Xu Y, Komorowski M, Shalhoub J, Maruthappu M, et al. Trends in mortality from pneumonia in the Europe union: A temporal analysis of the European detailed mortality database between 2001 and 2014. Respir Res. 2018;19(1):1–9.

50. Walden AP, Clarke GM, McKechnie S, Hutton P, Gordon AC, Rello J, et al. Patients with community acquired pneumonia admitted to European intensive care units: An epidemiological survey of the GenOSept cohort. Crit Care. 2014;18(2):1–9.

51. Ewig S, Torres A. Community-acquired pneumonia as an emergency: time for an aggressive intervention to lower mortality. Eur Respir J. 2011 Aug;38(2):253–60.

52. Eurich DT, Marrie TJ, Minhas-Sandhu JK, Majumdar SR. Ten-Year Mortality after Community-acquired Pneumonia. A Prospective Cohort. Am J Respir Crit Care Med . 2015 Sep 1 ;192(5):597–604.

53. Garcia-Vidal C, Ardanuy C, Tubau F, Viasus D, Dorca J, Liñares J, et al. Pneumococcal pneumonia presenting with septic shock: Host- and pathogen-related factors and outcomes. Thorax. 2010;65(1):77–81.

54. Prina E, Ranzani OT, Polverino E, Cillóniz C, Ferrer M, Fernandez L, et al. Risk factors associated with potentially antibiotic-resistant pathogens in community-acquired pneumonia. Ann Am Thorac Soc. 2015 Feb;12(2):153–60.

55. Liapikou A, Ferrer M, Polverino E, Balasso V, Esperatti M, Piñer R, et al. Severe Community-Acquired Pneumonia: Validation of the Infectious Diseases Society of America/American Thoracic Society Guidelines to Predict an Intensive Care Unit Admission. Clin Infect Dis. 2009;48(4):377–85.

56. Cillóniz C, Polverino E, Ewig S, Aliberti S, Gabarrús A, Menéndez R, et al. Impact of age and comorbidity on cause and outcome in community-acquired pneumonia. Chest. 2013;144(3):999–1007.

57. Cillóniz C, Dominedò C, Ielpo A, Ferrer M, Gabarrús A, Battaglini D, et al. Risk and Prognostic Factors in Very Old Patients with Sepsis Secondary to Community-

Acquired Pneumonia. J Clin Med. 2019 Jul;8(7).

58. Eurostat;https://ec.europa.eu/eurostat/statistics-explained/index.php?title=Causes_of_death_statistics.

59. Estimating excess mortality due to the COVID-19 pandemic: a systematic analysis of COVID-19-related mortality, 2020-21. Lancet (London, England). 2022 Apr;399(10334):1513–36.

60. https://www.cdc.gov/mmwr/volumes/71/wr/mm7137a4.htm.

61. Corrales-Medina VF, Alvarez KN, Weissfeld LA, Angus DC, Chirinos JA, Chang CCH, et al. Association between hospitalization for pneumonia and subsequent risk of cardiovascular disease. JAMA - J Am Med Assoc. 2015 Jan 20;313(3):264–74.

62. Restrepo MI, Reyes LF, Anzueto A. Complication of Community-Acquired Pneumonia (Including Cardiac Complications). Semin Respir Crit Care Med. 2016 Dec;37(6):897–904.

63. Cillóniz C, Ewig S, Polverino E, Muñoz-Almagro C, Marco F, Gabarrús A, et al. Pulmonary complications of pneumococcal community-acquired pneumonia: incidence, predictors, and outcomes. Clin Microbiol Infect Off Publ Eur Soc Clin Microbiol Infect Dis. 2012 Nov;18(11):1134–42.

64. Giacomelli A, Pezzati L, Conti F, Bernacchia D, Siano M, Oreni L, et al. Self-reported Olfactory and Taste Disorders in Patients With Severe Acute Respiratory Coronavirus 2 Infection: A Cross-sectional Study. Vol. 71, Clinical infectious diseases : an official publication of the Infectious Diseases Society of America. United States; 2020. p. 889–90.

65. Li Y, Li M, Wang M, Zhou Y, Chang J, Xian Y, et al. Acute cerebrovascular disease following COVID-19: a single center, retrospective, observational study. Stroke Vasc Neurol. 2020 Sep;5(3):279–84.

66. Mohamed MMB, Lukitsch I, Torres-Ortiz AE, Walker JB, Varghese V, Hernandez-Arroyo CF, et al. Acute Kidney Injury Associated with Coronavirus Disease 2019 in Urban New Orleans. Kidney360. 2020 Jul;1(7):614–22.

67. Rosón B, Carratalà J, Fernández-Sabé N, Tubau F, Manresa F, Gudiol F. Causes and factors associated with early failure in hospitalized patients with community-acquired pneumonia. Arch Intern Med. 2004 Mar;164(5):502–8.

68. Abelenda-Alonso G, Rombauts A, Gudiol C, García-Lerma E, Pallarés N, Ardanuy C, et al. Effect of positive microbiological testing on antibiotic de-escalation and outcomes in community-acquired pneumonia: a propensity score analysis. Clin Microbiol Infect Off Publ Eur Soc Clin Microbiol Infect Dis. 2022 Dec;28(12):1602–8.

69. Mummadi SR, Stoller JK, Lopez R, Kailasam K, Gillespie CT, Hahn PY. Epidemiology of Adult Pleural Disease in the United States. Chest. 2021 Oct;160(4):1534–51.

70. Hassan M, Patel S, Sadaka AS, Bedawi EO, Corcoran JP, Porcel JM. Recent Insights into the Management of Pleural Infection. Int J Gen Med. 2021;14:3415–29.

71. Wiese AD, Grijalva CG. Burden of all-cause and organism-specific parapneumonic empyema hospitalization rates prior to the SARS-CoV-2 pandemic in the United

States. Respir Med. 2023 Feb;207:107111.

72. Hassan M, Cargill T, Harriss E, Asciak R, Mercer RM, Bedawi EO, et al. The microbiology of pleural infection in adults: a systematic review. Eur Respir J. 2019 Sep;54(3).

73. Chatha N, Fortin D, Bosma KJ. Management of necrotizing pneumonia and pulmonary gangrene: a case series and review of the literature. Can Respir J. 2014;21(4):239–45.

74. Maharaj S, Isache C, Seegobin K, Chang S, Nelson G. Necrotizing Pseudomonas aeruginosa Community-Acquired Pneumonia: A Case Report and Review of the Literature. Vol. 2017, Case reports in infectious diseases. Egypt; 2017. p. 1717492.

75. Gillet Y, Issartel B, Vanhems P, Fournet J-C, Lina G, Bes M, et al. Association between Staphylococcus aureus strains carrying gene for Panton-Valentine leukocidin and highly lethal necrotising pneumonia in young immunocompetent patients. Lancet (London, England). 2002 Mar;359(9308):753–9.

76. Li Z, Stevens DL, Hamilton SM, Parimon T, Ma Y, Kearns AM, et al. Fatal S. aureus hemorrhagic pneumonia: genetic analysis of a unique clinical isolate producing both PVL and TSST-1. PLoS One. 2011;6(11):e27246.

77. Potere N, Valeriani E, Candeloro M, Tana M, Porreca E, Abbate A, et al. Acute complications and mortality in hospitalized patients with coronavirus disease 2019: a systematic review and meta-analysis. Crit Care. 2020 Jul;24(1):389.

78. Gattinoni L, Marini JJ, Pesenti A, Quintel M, Mancebo J, Brochard L. The "baby lung" became an adult. Intensive Care Med. 2016 May;42(5):663–73.

79. Gattinoni L, Coppola S, Cressoni M, Busana M, Rossi S, Chiumello D. COVID-19 Does Not Lead to a "Typical" Acute Respiratory Distress Syndrome. Vol. 201, American journal of respiratory and critical care medicine. United States; 2020. p. 1299–300.

80. Ackermann M, Verleden SE, Kuehnel M, Haverich A, Welte T, Laenger F, et al. Pulmonary Vascular Endothelialitis, Thrombosis, and Angiogenesis in Covid-19. N Engl J Med. 2020 Jul;383(2):120–8.

81. Grasselli G, Tonetti T, Protti A, Langer T, Girardis M, Bellani G, et al. Pathophysiology of COVID-19-associated acute respiratory distress syndrome: a multicentre prospective observational study. Lancet Respir Med. 2020 Dec;8(12):1201–8.

82. Beloncle FM. Is COVID-19 different from other causes of acute respiratory distress syndrome? J intensive Med. 2023 Apr;3(3):212–9.

83. Reddy MP, Subramaniam A, Chua C, Ling RR, Anstey C, Ramanathan K, et al. Respiratory system mechanics, gas exchange, and outcomes in mechanically ventilated patients with COVID-19-related acute respiratory distress syndrome: a systematic review and meta-analysis. Lancet Respir Med. 2022 Dec;10(12):1178–88.

84. Saha BK, Chong WH, Austin A, Kathuria R, Datar P, Shkolnik B, et al. Pleural abnormalities in COVID-19: a narrative review. J Thorac Dis. 2021 Jul;13(7):4484–99.

85. Singer M, Deutschman CS, Seymour CW, Shankar-Hari M, Annane D, Bauer M, et

al. The Third International Consensus Definitions for Sepsis and Septic Shock (Sepsis-3). JAMA. 2016 Feb;315(8):801–10.

86. Shah FA, Pike F, Alvarez K, Angus D, Newman AB, Lopez O, et al. Bidirectional relationship between cognitive function and pneumonia. Am J Respir Crit Care Med. 2013 Sep;188(5):586–92.

87. Uginet M, Breville G, Assal F, Lövblad K-O, Vargas MI, Pugin J, et al. COVID-19 encephalopathy: Clinical and neurobiological features. J Med Virol. 2021 Jul;93(7):4374–81.

88. Romero-Sánchez CM, Díaz-Maroto I, Fernández-Díaz E, Sánchez-Larsen Á, Layos-Romero A, García-García J, et al. Neurologic manifestations in hospitalized patients with COVID-19: The ALBACOVID registry. Neurology. 2020 Aug;95(8):e1060–70.

89. Nersesjan V, Amiri M, Nilsson AC, Wamberg C, Jensen VVS, Petersen CB, et al. SARS-CoV-2 and autoantibodies in the cerebrospinal fluid of COVID-19 patients: prospective multicentre cohort study. Brain Commun. 2023;5(5):fcad274.

90. Hirsch JS, Ng JH, Ross DW, Sharma P, Shah HH, Barnett RL, et al. Acute kidney injury in patients hospitalized with COVID-19. Kidney Int. 2020 Jul;98(1):209–18.

91. Drake TM, Riad AM, Fairfield CJ, Egan C, Knight SR, Pius R, et al. Characterisation of in-hospital complications associated with COVID-19 using the ISARIC WHO Clinical Characterisation Protocol UK: a prospective, multicentre cohort study. Lancet (London, England). 2021 Jul;398(10296):223–37.

92. Bhayana R, Som A, Li MD, Carey DE, Anderson MA, Blake MA, et al. Abdominal Imaging Findings in COVID-19: Preliminary Observations. Radiology. 2020 Oct;297(1):E207–15.

93. Corrales-Medina VF, Musher DM, Shachkina S, Chirinos JA. Acute pneumonia and the cardiovascular system. Lancet . 2013;381(9865):496–505.

94. Feldman C, Anderson R. Prevalence, pathogenesis, therapy, and prevention of cardiovascular events in patients with community-acquired pneumonia. Pneumonia. 2016;8(1):1–10.

95. Musher DM, Abers MS, Corrales-Medina VF. Acute Infection and Myocardial Infarction. N Engl J Med. 2019;380(2):171–6.

96. Viasus D, Garcia-Vidal C, Manresa F, Dorca J, Gudiol F, Carratalà J. Risk stratification and prognosis of acute cardiac events in hospitalized adults with community-acquired pneumonia. J Infect. 2013;66(1):27–33.

97. Violi F, Cangemi R, Falcone M, Taliani G, Pieralli F, Vannucchi V, et al. Cardiovascular complications and short-term mortality risk in community-acquired pneumonia. Clin Infect Dis. 2017;64(11):1486–93.

98. Griffin AT, Wiemken TL, Arnold FW. Risk factors for cardiovascular events in hospitalized patients with community-acquired pneumonia. Int J Infect Dis. 2013;17(12):e1125–9.

99. Corrales-Medina VF, Musher DM, Wells GA, Chirinos JA, Chen L, Fine MJ. Cardiac Complications in Patients With Community-Acquired Pneumonia. Circulation. 2012;125(6):773–81.

100. Eurich DT, Marrie TJ, Minhas-Sandhu JK, Majumdar SR. Risk of heart failure after community acquired pneumonia: prospective controlled study with 10 years of follow-up. BMJ . 2017;356:j413.

101. Corrales-medina VF, Taljaard M, Yende S, Kronmal R, Dwivedi G, Newman AB, et al. Intermediate and Long-term Risks of New-onset Heart Failure after Hospitalization for Pneumonia in Elderly Adults. Am Heart J. 2015;170(2):306–12.

102. Perry TW, Pugh MJ V, Waterer GW, Nakashima B, Orihuela CJ, Copeland LA, et al. Incidence of Cardiovascular Events Following Hospital Admission for Pneumonia. 2012;124(3):244–51.

103. Cangemi R, Calvieri C, Falcone M, Bucci T, Bertazzoni G, Scarpellini MG, et al. Relation of cardiac complications in the early phase of community-acquired pneumonia to long-term mortality and cardiovascular events. Am J Cardiol. 2015;116(4):647–51.

104. Warren-Gash C, Blackburn R, Whitaker H, McMenamin J, Hayward AC. Laboratory-confirmed respiratory infections as triggers for acute myocardial infarction and stroke: a self-controlled case series analysis of national linked datasets from Scotland. Eur Respir J. 2018 ;51(3).

105. Reyes LF, Restrepo MI, Hinojosa CA, Soni NJ, Anzueto A, Babu BL, et al. Severe pneumococcal pneumonia causes acute cardiac toxicity and subsequent cardiac remodeling. Am J Respir Crit Care Med. 2017;196(5):609–20.

106. Brown AO, Mann B, Gao G, Hankins JS, Humann J, Giardina J, et al. Streptococcus pneumoniae Translocates into the Myocardium and Forms Unique Microlesions That Disrupt Cardiac Function. PLoS Pathog. 2014;10(9).

107. Brissac T, Shenoy AT, Patterson LA, Orihuela CJ. Cell Invasion and Pyruvate Oxidase-Derived H2O2 Are Critical for Streptococcus pneumoniae-Mediated Cardiomyocyte Killing. Pirofski L, editor. Infect Immun. 2017;86(1).

108. Alhamdi Y, Neill DR, Abrams ST, Malak HA, Yahya R, Barrett-Jolley R, et al. Circulating Pneumolysin Is a Potent Inducer of Cardiac Injury during Pneumococcal Infection. PLoS Pathog. 2015;11(5):1–29.

109. Shenoy AT, Beno SM, Brissac T, Bell JW, Novak L, Orihuela CJ. Severity and properties of cardiac damage caused by Streptococcus pneumoniae are strain dependent. PLoS One. 2018;13(9):1–15.

110. Anderson R, Nel JG, Feldman C. Multifaceted role of pneumolysin in the pathogenesis of myocardial injury in community-acquired pneumonia. Int J Mol Sci. 2018;19(4):1–22.

111. Woodruff RC, Garg S, George MG, Patel K, Jackson SL, Loustalot F, et al. Acute Cardiac Events During COVID-19-Associated Hospitalizations. J Am Coll Cardiol. 2023 Feb;81(6):557–69.

112. Xie Y, Xu E, Bowe B, Al-Aly Z. Long-term cardiovascular outcomes of COVID-19. Nat Med. 2022 Mar;28(3):583–90.

113. Lala A, Johnson KW, Russak AJ, Paranjpe I, Zhao S, Solani S, et al. Prevalence and Impact of Myocardial Injury in Patients Hospitalized with COVID-19 Infection. medRxiv : the preprint server for health sciences. United States; 2020.

114. Masana L, Correig E, Ibarretxe D, Anoro E, Arroyo JA, Jericó C, et al. Low HDL and high triglycerides predict COVID-19 severity. Sci Rep. 2021;11(1):7217.

115. Song JW, Lam SM, Fan X, Cao WJ, Wang SY, Tian H, et al. Omics-Driven Systems Interrogation of Metabolic Dysregulation in COVID-19 Pathogenesis. Cell Metab. 2020 Aug 8;32(2):188.

116. Barda N, Dagan N, Ben-Shlomo Y, Kepten E, Waxman J, Ohana R, et al. Safety of the BNT162b2 mRNA Covid-19 Vaccine in a Nationwide Setting. N Engl J Med. 2021 Sep;385(12):1078–90.

117. Ciabatti M, Zocchi C, Olivotto I, Bolognese L, Pieroni M. Myocarditis and COVID-19 related issues. Glob Cardiol Sci Pract. 2023 Sep;2023(4):e202328.

118. Edmond K, Scott S, Korczak V, Ward C, Sanderson C, Theodoratou E, et al. Long term sequelae from childhood pneumonia; systematic review and meta-analysis. PLoS One. 2012;7(2):e31239.

119. Pizzutto SJ, Hare KM, Upham JW. Bronchiectasis in Children: Current Concepts in Immunology and Microbiology. Front Pediatr. 2017;5:123.

120. Zheng H-Q, Ma Y-C, Chen Y-Q, Xu Y-Y, Pang Y-L, Liu L. Clinical Analysis and Risk Factors of Bronchiolitis Obliterans After Mycoplasma Pneumoniae Pneumonia. Infect Drug Resist. 2022;15:4101–8.

121. Martinez-Pitre PJ, Sabbula BR, Cascella M. Restrictive Lung Disease. In Treasure Island (FL); StatPearls Publishing, 2024.

122. Grimwood K, Chang AB. Long-term effects of pneumonia in young children. Pneumonia (Nathan Qld). 2015;6:101–14.

123. Han X, Fan Y, Alwalid O, Zhang X, Jia X, Zheng Y, et al. Fibrotic Interstitial Lung Abnormalities at 1-year Follow-up CT after Severe COVID-19. Radiology. 2021 Dec;301(3):E438–40.

124. Pan F, Yang L, Liang B, Ye T, Li L, Li L, et al. Chest CT Patterns from Diagnosis to 1 Year of Follow-up in Patients with COVID-19. Radiology. 2022 Mar;302(3):709–19.

125. Luger AK, Sonnweber T, Gruber L, Schwabl C, Cima K, Tymoszuk P, et al. Chest CT of Lung Injury 1 Year after COVID-19 Pneumonia: The CovILD Study. Radiology. 2022 Aug;304(2):462–70.

126. Kanne JP, Little BP, Schulte JJ, Haramati A, Haramati LB. Long-term Lung Abnormalities Associated with COVID-19 Pneumonia. Radiology. 2023 Feb;306(2):e221806.

127. Guri A, Groner L, Escalon J, Saleh A. Algorithmic approach in the management of COVID-19 patients with residual pulmonary symptoms. Ann Thorac Med. 2023;18(4):167–72.

128. Righi E, Mirandola M, Mazzaferri F, Dossi G, Razzaboni E, Zaffagnini A, et al. Determinants of persistence of symptoms and impact on physical and mental wellbeing in Long COVID: A prospective cohort study. J Infect. 2022 Apr;84(4):566–72.

129. Premraj L, Kannapadi N V, Briggs J, Seal SM, Battaglini D, Fanning J, et al. Mid and

long-term neurological and neuropsychiatric manifestations of post-COVID-19 syndrome: A meta-analysis. J Neurol Sci. 2022 Mar;434:120162.

130. Lopez-Leon S, Wegman-Ostrosky T, Perelman C, Sepulveda R, Rebolledo PA, Cuapio A, et al. More than 50 long-term effects of COVID-19: a systematic review and meta-analysis. Sci Rep. 2021 Aug;11(1):16144.

131. Sudre CH, Murray B, Varsavsky T, Graham MS, Penfold RS, Bowyer RC, et al. Attributes and predictors of long COVID. Nat Med. 2021 Apr;27(4):626–31.

132. Rombauts A, Infante C, de Lagos MDÁM, Alba J, Valiente A, Donado-Mazarrón C, et al. Impact of SARS-CoV-2 RNAemia and other risk factors on long-COVID: A prospective observational multicentre cohort study. Vol. 86, The Journal of infection. England; 2023. p. 154–225.

133. Sandler CX, Wyller VBB, Moss-Morris R, Buchwald D, Crawley E, Hautvast J, et al. Long COVID and Post-infective Fatigue Syndrome: A Review. Open forum Infect Dis. 2021 Oct;8(10):ofab440.

134. SeyedAlinaghi S, Bagheri A, Razi A, Mojdeganlou P, Mojdeganlou H, Afsahi AM, et al. Late Complications of COVID-19; An Umbrella Review on Current Systematic Reviews. Arch Acad Emerg Med. 2023;11(1):e28.

135. Quinton LJ, Walkey AJ, Mizgerd JP. Integrative physiology of pneumonia. Physiol Rev. 2018;98(3):1417–64.

136. Mizgerd JP. Inflammation and Pneumonia: Why Are Some More Susceptible than Others? Clin Chest Med. 2018;39(4):669–76.

137. Tian C, Hromatka BS, Kiefer AK, Eriksson N, Noble SM, Tung JY, et al. Genome-wide association and HLA region fine-mapping studies identify susceptibility loci for multiple common infections. Nat Commun. 2017 Sep;8(1):599.

138. Reay WR, Geaghan MP, Cairns MJ. The genetic architecture of pneumonia susceptibility implicates mucin biology and a relationship with psychiatric illness. Nat Commun. 2022 Jun;13(1):3756.

139. Van de Bovenkamp JHB, Mahdavi J, Korteland-Van Male AM, Büller HA, Einerhand AWC, Borén T, et al. The MUC5AC glycoprotein is the primary receptor for Helicobacter pylori in the human stomach. Helicobacter. 2003;8(5):521–32.

140. Perez-Vilar J, Randell SH, Boucher RC. C-Mannosylation of MUC5AC and MUC5B Cys subdomains. Glycobiology. 2004 Apr;14(4):325–37.

141. Campos AI, Kho P, Vazquez-Prada KX, García-Marín LM, Martin NG, Cuéllar-Partida G, et al. Genetic Susceptibility to Pneumonia: A GWAS Meta-Analysis Between the UK Biobank and FinnGen. Twin Res Hum Genet Off J Int Soc Twin Stud. 2021 Jun;24(3):145–54.

142. Cappadona C, Rimoldi V, Paraboschi EM, Asselta R. Genetic susceptibility to severe COVID-19. Infect Genet Evol J Mol Epidemiol Evol Genet Infect Dis. 2023 Jun;110:105426.

143. D E, F D, L B, M BBB, A AA, P I, et al. Genomewide Association Study of Severe Covid-19 with Respiratory Failure. N Engl J Med. 2020;383(16):1522–34.

144. Blanco-Melo D, Nilsson-Payant BE, Liu WC, Uhl S, Hoagland D, Møller R, et al.

Imbalanced Host Response to SARS-CoV-2 Drives Development of COVID-19. Cell. 2020 181(5):1036-1045.e9.

145. Suryamohan K, Diwanji D, Stawiski EW, Gupta R, Miersch S, Liu J, et al. Human ACE2 receptor polymorphisms and altered susceptibility to SARS-CoV-2. Commun Biol. 2021;4(1).

146. Vuille-dit-Bille RN, Camargo SM, Emmenegger L, Sasse T, Kummer E, Jando J, et al. Human intestine luminal ACE2 and amino acid transporter expression increased by ACE-inhibitors. Amino Acids. 2015 Apr;47(4):693–705.

147. Downes DJ, Cross AR, Hua P, Roberts N, Schwessinger R, Cutler AJ, et al. Identification of LZTFL1 as a candidate effector gene at a COVID-19 risk locus. Nat Genet. 2021 Nov;53(11):1606–15.

148. Pereira E, Felipe S, de Freitas R, Araújo V, Soares P, Ribeiro J, et al. ABO blood group and link to COVID-19: A comprehensive review of the reported associations and their possible underlying mechanisms. Microb Pathog. 2022 Aug;169:105658.

149. Silva-Filho JC, Melo CGF de, Oliveira JL de. The influence of ABO blood groups on COVID-19 susceptibility and severity: A molecular hypothesis based on carbohydrate-carbohydrate interactions. Med Hypotheses. 2020 Nov;144:110155.

150. Stowell SR, Stowell CP. Biologic roles of the ABH and Lewis histo-blood group antigens part II: thrombosis, cardiovascular disease and metabolism. Vox Sang. 2019 Aug;114(6):535–52.

151. Zhang Q, Liu Z, Moncada-Velez M, Chen J, Ogishi M, Bigio B, et al. Inborn errors of type I IFN immunity in patients with life-threatening COVID-19. Science (80-). 2020;370(6515).

152. Huffnagle GB, Dickson RP, Lukacs NW. The respiratory tract microbiome and lung inflammation: a two-way street. Mucosal Immunol. 2017;10(2):299–306.

153. Wu BG, Segal LN. The Lung Microbiome and Its Role in Pneumonia [Internet]. Vol. 39, Clinics in Chest Medicine. W.B. Saunders; 2018 p. 677–89.

154. Yang D, Xing Y, Song X, Qian Y. The impact of lung microbiota dysbiosis on inflammation. Vol. 159, Immunology. Blackwell Publishing Ltd; 2020 . p. 156–66.

155. Dickson RP, Erb-Downward JR, Huffnagle GB. Towards an ecology of the lung: New conceptual models of pulmonary microbiology and pneumonia pathogenesis. Vol. 2, The Lancet Respiratory Medicine. Lancet Publishing Group; 2014. p. 238–46.

156. Zemans RL, Colgan SP, Downey GP. Transepithelial migration of neutrophils: Mechanisms and implications for acute lung injury. Vol. 40, American Journal of Respiratory Cell and Molecular Biology. American Thoracic Society; 2009. p. 519–35.

157. Brinkmann V, Zychlinsky A. Beneficial suicide: Why neutrophils die to make NETs. Nat Rev Microbiol. 2007 Aug;5(8):577–82.

158. Ebrahimi F, Giaglis S, Hahn S, Blum CA, Baumgartner C, Kutz A, et al. Markers of neutrophil extracellular traps predict adverse outcome in communityacquired pneumonia: Secondary analysis of a randomised controlled trial. Eur Respir J. 2018;51(4).

159. Kellum JA, Kong L, Fink MP, Weissfeld LA, Yealy DM, Pinsky MR, et al. Understanding the inflammatory cytokine response in pneumonia and sepsis: Results of the genetic and inflammatory markers of sepsis (GenIMS) study. Arch Intern Med. 2007 Aug;167(15):1655–63.

160. Paats MSM, Bergen IMI, Hanselaar WEJJ, Groeninx van Zoelen E, Hoogsteden HCH, Hendriks RWR, et al. Local and systemic cytokine profiles in nonsevere and severe community-acquired pneumonia. Eur Respir J. 2013;41(6):1378–85.

161. Antunes G, Evans SA, Lordan JL, Frew AJ. Systemic cytokine levels in community-acquired pneumonia and their association with disease severity. Eur Respir J. 2002;20(4):990–5.

162. Salluh JIF, Verdeal JC, Mello GW, Araújo L V., Martins GAR, De Sousa Santino M, et al. Cortisol levels in patients with severe community-acquired pneumonia. Intensive Care Med. 2006;32(4):595–8.

163. Cangemi R, Casciaro M, Rossi E, Calvieri C, Bucci T, Calabrese CM, et al. Platelet activation is associated with myocardial infarction in patients with pneumonia. J Am Coll Cardiol. 2014;64(18):1917–25.

164. Cangemi R, Pignatelli P, Carnevale R, Bartimoccia S, Nocella C, Falcone M, et al. Low-grade endotoxemia, gut permeability and platelet activation in community-acquired pneumonia. J Infect. 2016;73(2):107–14.

165. Pignatelli P, Pastori D, Carnevale R, Farcomeni A, Cangemi R, Nocella C, et al. Serum NOX2 and urinary isoprostanes predict vascular events in patients with atrial fibrillation. Thromb Haemost. 2015;113(3):617–24.

166. Siljan WW, Holter JC, Nymo SH, Husebye E, Ueland T, Aukrust P, et al. Cytokine responses, microbial aetiology and short-term outcome in community-acquired pneumonia. Eur J Clin Invest. 2018 Jan;48(1).

167. Karki R, Lee S, Mall R, Pandian N, Wang Y, Sharma BR, et al. ZBP1-dependent inflammatory cell death, PANoptosis, and cytokine storm disrupt IFN therapeutic efficacy during coronavirus infection. Sci Immunol. 2022 Aug;7(74):eabo6294.

168. Bryce C, Grimes Z, Pujadas E, Ahuja S, Beasley MB, Albrecht R, et al. Pathophysiology of SARS-CoV-2: the Mount Sinai COVID-19 autopsy experience. Mod Pathol an Off J United States Can Acad Pathol Inc. 2021 Aug;34(8):1456–67.

169. Hadjadj J, Yatim N, Barnabei L, Corneau A, Boussier J, Smith N, et al. Impaired type I interferon activity and inflammatory responses in severe COVID-19 patients. Science. 2020 Aug;369(6504):718–24.

170. Bermejo-Martin JF, Cilloniz C, Mendez R, Almansa R, Gabarrus A, Ceccato A, et al. Lymphopenic Community Acquired Pneumonia (L-CAP), an Immunological Phenotype Associated with Higher Risk of Mortality. EBioMedicine. 2017 Oct;24:231–6.

171. Almansa R, Socias L, Ramirez P, Martin-Loeches I, Vallés J, Loza A, et al. Imbalanced pro- and anti-Th17 responses (IL-17/granulocyte colony-stimulating factor) predict fatal outcome in 2009 pandemic influenza. Vol. 15, Critical Care. BioMed Central; 201. p. 448.

172. Schauwvlieghe AFAD, Rijnders BJA, Philips N, Verwijs R, Vanderbeke L, Van Tienen C, et al. Invasive aspergillosis in patients admitted to the intensive care unit

with severe influenza: a retrospective cohort study. 2018;6(10):782–92.

173. Bartoletti M, Pascale R, Cricca M, Rinaldi M, Maccaro A, Bussini L, et al. Epidemiology of Invasive Pulmonary Aspergillosis Among Intubated Patients With COVID-19: A Prospective Study. Clin Infect Dis. 2021;73(11).

174. Prattes J, Wauters J, Giacobbe DR, Salmanton-García J, Maertens J, Bourgeois M, et al. Risk factors and outcome of pulmonary aspergillosis in critically ill coronavirus disease 2019 patients-a multinational observational study by the European Confederation of Medical Mycology. Clin Microbiol Infect. 2022 Apr 1

175. Hoffmann M, Kleine-Weber H, Schroeder S, Krüger N, Herrler T, Erichsen S, et al. SARS-CoV-2 Cell Entry Depends on ACE2 and TMPRSS2 and Is Blocked by a Clinically Proven Protease Inhibitor. Cell. 2020 Apr;181(2):271-280.e8.

176. Brandtzaeg P. Induction of secretory immunity and memory at mucosal surfaces. Vaccine. 2007 Jul;25(30):5467–84.

177. Corthésy B. Multi-faceted functions of secretory IgA at mucosal surfaces. Front Immunol. 2013;4:185.

178. Bakema JE, van Egmond M. The human immunoglobulin A Fc receptor FcαRI: a multifaceted regulator of mucosal immunity. Mucosal Immunol. 2011 Nov;4(6):612–24.

179. Breedveld A, van Egmond M. IgA and FcαRI: Pathological Roles and Therapeutic Opportunities. Front Immunol. 2019;10:553.

180. Tamura S, Funato H, Hirabayashi Y, Kikuta K, Suzuki Y, Nagamine T, et al. Functional role of respiratory tract haemagglutinin-specific IgA antibodies in protection against influenza. Vaccine. 1990 Oct;8(5):479–85.

181. Terauchi Y, Sano K, Ainai A, Saito S, Taga Y, Ogawa-Goto K, et al. IgA polymerization contributes to efficient virus neutralization on human upper respiratory mucosa after intranasal inactivated influenza vaccine administration. Hum Vaccin Immunother. 2018 Jun;14(6):1351–61.

182. Wright PF, Prevost-Reilly AC, Natarajan H, Brickley EB, Connor RI, Wieland-Alter WF, et al. Longitudinal Systemic and Mucosal Immune Responses to SARS-CoV-2 Infection. J Infect Dis. 2022 Sep;226(7):1204–14.

183. Sterlin D, Mathian A, Miyara M, Mohr A, Anna F, Claër L, et al. IgA dominates the early neutralizing antibody response to SARS-CoV-2. Sci Transl Med. 2021 Jan;13(577).

184. Dörner T, Radbruch A. Antibodies and B cell memory in viral immunity. Immunity. 2007 Sep;27(3):384–92.

185. Palm A-KE, Henry C. Remembrance of Things Past: Long-Term B Cell Memory After Infection and Vaccination. Front Immunol. 2019;10:1787.

186. Kelvin AA, Zambon M. Influenza imprinting in childhood and the influence on vaccine response later in life. Euro Surveill Bull Eur sur les Mal Transm. Eur Commun Dis Bull. 2019 Nov;24(48).

187. Fonville JM, Wilks SH, James SL, Fox A, Ventresca M, Aban M, et al. Antibody landscapes after influenza virus infection or vaccination. Science. 2014

Nov;346(6212):996–1000.

188. Dugan HL, Guthmiller JJ, Arevalo P, Huang M, Chen Y-Q, Neu KE, et al. Preexisting immunity shapes distinct antibody landscapes after influenza virus infection and vaccination in humans. Sci Transl Med. 2020 Dec;12(573).

189. Monto AS, Malosh RE, Petrie JG, Martin ET. The Doctrine of Original Antigenic Sin: Separating Good From Evil. J Infect Dis. 2017 Jun;215(12):1782–8.

190. Halstead SB, Rojanasuphot S, Sangkawibha N. Original antigenic sin in dengue. Am J Trop Med Hyg. 1983 Jan;32(1):154–6.

191. Midgley CM, Bajwa-Joseph M, Vasanawathana S, Limpitikul W, Wills B, Flanagan A, et al. An in-depth analysis of original antigenic sin in dengue virus infection. J Virol. 2011 Jan;85(1):410–21.

192. Gostic KM, Bridge R, Brady S, Viboud C, Worobey M, Lloyd-Smith JO. Childhood immune imprinting to influenza A shapes birth year-specific risk during seasonal H1N1 and H3N2 epidemics. PLoS Pathog. 2019 Dec;15(12):e1008109.

193. Wang Q, Guo Y, Tam AR, Valdez R, Gordon A, Liu L, et al. Deep immunological imprinting due to the ancestral spike in the current bivalent COVID-19 vaccine. Cell reports Med. 2023 Nov;4(11):101258.

194. Erbelding EJ, Post DJ, Stemmy EJ, Roberts PC, Augustine AD, Ferguson S, et al. A Universal Influenza Vaccine: The Strategic Plan for the National Institute of Allergy and Infectious Diseases. J Infect Dis. 2018 Jul;218(3):347–54.

195. Yisimayi A, Song W, Wang J, Jian F, Yu Y, Chen X, et al. Repeated Omicron exposures override ancestral SARS-CoV-2 immune imprinting. Nature. 2024 Jan;625(7993):148–56.

196. Lowe R, Shirley N, Bleackley M, Dolan S, Shafee T. Transcriptomics technologies. PLoS Comput Biol. 2017 May;13(5):e1005457.

197. Nagano T, Fraser P. No-nonsense functions for long noncoding RNAs. Cell. 2011 Apr;145(2):178–81.

198. Cech TR. The RNA worlds in context. Cold Spring Harb Perspect Biol. 2012 Jul;4(7):a006742.

199. Nucci LA, Santos SS, Brunialti MKC, Sharma NK, Machado FR, Assunção M, et al. Expression of genes belonging to the interacting TLR cascades, NADPH-oxidase and mitochondrial oxidative phosphorylation in septic patients. PLoS One. 2017;12(2):e0172024.

200. Zhao J, He X, Min J, Yao RSY, Chen Y, Chen Z, et al. A multicenter prospective study of comprehensive metagenomic and transcriptomic signatures for predicting outcomes of patients with severe community-acquired pneumonia. EBioMedicine. 2023 Oct;96:104790.

201. Davenport EE, Burnham KL, Radhakrishnan J, Humburg P, Hutton P, Mills TC, et al. Genomic landscape of the individual host response and outcomes in sepsis: A prospective cohort study. Lancet Respir Med. 2016;4(4):259–71.

202. Bermejo-Martin JF, Martin-Loeches I, Rello J, Antón A, Almansa R, Xu L, et al. Host adaptive immunity deficiency in severe pandemic influenza. Crit Care. 2010

;14(5):R167.

203. Ren X, Wen W, Fan X, Hou W, Su B, Cai P, et al. COVID-19 immune features revealed by a large-scale single-cell transcriptome atlas. Cell. 2021;184(7):1895-1913.e19.

204. Bibert S, Guex N, Lourenco J, Brahier T, Papadimitriou-Olivgeris M, Damonti L, et al. Transcriptomic Signature Differences Between SARS-CoV-2 and Influenza Virus Infected Patients. Front Immunol. 2021;12(May):1–25.

205. McClain MT, Constantine FJ, Henao R, Liu Y, Tsalik EL, Burke TW, et al. Dysregulated transcriptional responses to SARS-CoV-2 in the periphery. Nat Commun. 2021;12(1):1–8.

206. Kwan PKW, Cross GB, Naftalin CM, Ahidjo BA, Mok CK, Fanusi F, et al. A blood RNA transcriptome signature for COVID-19. BMC Med Genomics. 2021;14(1):1–8.

207. Chan Y, Fong S, Poh C, Carissimo G, Yeo NK, Amrun SN, et al. Asymptomatic COVID-19: disease tolerance with efficient anti-viral immunity against SARS-CoV-2. EMBO Mol Med. 2021;13(6):1–15.

208. Bergamaschi Mescia, Federica, Turner, Lorinda, Hanson, Aimee L. L, Kotagiri Dunmore, Benjamin J. P, Ruffieux De Sa, Aloka, Huhn, Oisín, Morgan, Michael D. H, Gerber Wills, Mark R. PP, Baker Calero-Nieto, Fernando J. S, Doffinger Dougan, Gordon, Elmer, Anne, Goodfellow, Ian G. R, et al. Longitudinal analysis reveals that delayed bystander CD8+ T cell activation and early immune pathology distinguish severe COVID-19 from mild disease. Immunity. 2021.

209. Wu P, Chen D, Ding W, Wu P, Hou H, Bai Y, et al. The trans-omics landscape of COVID-19. Nat Commun. 2021;12(1):1–16.

210. Russick J, Foy PE, Josseaume N, Meylan M, Hamouda N Ben, Kirilovsky A, et al. Immune Signature Linked to COVID-19 Severity: A SARS-Score for Personalized Medicine. Front Immunol. 2021;12(July):1–14.

211. Prokop JW, Hartog NL, Chesla D, Faber W, Love CP, Karam R, et al. High-Density Blood Transcriptomics Reveals Precision Immune Signatures of SARS-CoV-2 Infection in Hospitalized Individuals. Front Immunol. 2021;12(July):1–15.

212. Aschenbrenner AC, Mouktaroudi M, Krämer B, Oestreich M, Antonakos N, Nuesch-Germano M, et al. Disease severity-specific neutrophil signatures in blood transcriptomes stratify COVID-19 patients. Genome Med. 2021;13(1):7.

213. Fiehn O. Metabolomics--the link between genotypes and phenotypes. Plant Mol Biol. 2002 Jan;48(1–2):155–71.

214. Chakraborty N. Metabolites: a converging node of host and microbe to explain meta-organism. Front Microbiol. 2024;15:1337368.

215. Chen Y, Li E-M, Xu L-Y. Guide to Metabolomics Analysis: A Bioinformatics Workflow. Metabolites. 2022 Apr;12(4).

216. Beckonert O, Keun HC, Ebbels TMD, Bundy J, Holmes E, Lindon JC, et al. Metabolic profiling, metabolomic and metabonomic procedures for NMR spectroscopy of urine, plasma, serum and tissue extracts. Nat Protoc. 2007;2(11):2692–703.

217. Nicholson JK, Lindon JC, Holmes E. "Metabonomics": Understanding the metabolic responses of living systems to pathophysiological stimuli via multivariate statistical analysis of biological NMR spectroscopic data. Xenobiotica. 1999;29(11):1181–9.

218. Veenstra TD. Metabolomics: the final frontier? Genome Med. 2012 Apr;4(4):40.

219. Gesell Salazar M, Neugebauer S, Kacprowski T, Michalik S, Ahnert P, Creutz P, et al. Association of proteome and metabolome signatures with severity in patients with community-acquired pneumonia. J Proteomics. 2020 Mar 1;214.

220. Zheng Y, Ning P, Luo Q, He Y, Yu X, Liu X, et al. Inflammatory responses relate to distinct bronchoalveolar lavage lipidome in community-acquired pneumonia patients: A pilot study. Respir Res . 2019;20(1):82.

221. Ning P, Zheng Y, Luo Q, Liu X, Kang Y, Zhang Y, et al. Metabolic profiles in community-acquired pneumonia: Developing assessment tools for disease severity. Crit Care. 2018;22(1):1–14.

222. Seymour CW, Yende S, Scott MJ, Pribis J, Mohney RP, Bell LN, et al. Metabolomics in pneumonia and sepsis: An analysis of the GenIMS cohort study. Intensive Care Med. 2013;39(8):1423–34.

223. Sharma NK, Tashima AK, Brunialti MKC, Ferreira ER, Torquato RJS, Mortara RA, et al. Proteomic study revealed cellular assembly and lipid metabolism dysregulation in sepsis secondary to community-acquired pneumonia. Sci Rep. 2017;7(1):1–13.

224. Ansell BJ, Watson KE, Fogelman AM, Navab M, Fonarow GC. High-density lipoprotein function recent advances. J Am Coll Cardiol. 2005 Nov;46(10):1792–8.

225. D'Amora P, Silva IDCG, Budib MA, Ayache R, Silva RMS, Silva FC, et al. Towards risk stratification and prediction of disease severity and mortality in COVID-19: Next generation metabolomics for the measurement of host response to COVID-19 infection. PLoS One [Internet]. 2021;16(12).

226. Sindelar M, Stancliffe E, Schwaiger-Haber M, Anbukumar DS, Adkins-Travis K, Goss CW, et al. Longitudinal metabolomics of human plasma reveals prognostic markers of COVID-19 disease severity. Cell Reports Med. 2021;2(8):100369.

227. Ansone L, Briviba M, Silamikelis I, Terentjeva A, Perkons I, Birzniece L, et al. Amino Acid Metabolism is Significantly Altered at the Time of Admission in Hospital for Severe COVID-19 Patients: Findings from Longitudinal Targeted Metabolomics Analysis. Microbiol Spectr. 2021;9(3).

228. Chen Y, Zheng Y, Yu Y, Wang Y, Huang Q, Qian F, et al. Blood molecular markers associated with COVID-19 immunopathology and multi-organ damage. EMBO J. 2020;39(24).

229. Gardinassi LG, Servian C do P, Lima G da S, Anjos DCC dos, Junior ARG, Guilarde AO, et al. Integrated Metabolic and Inflammatory Signatures Associated with Severity of, Fatality of, and Recovery from COVID-19. Microbiol Spectr. 2023;11(2).

230. Páez-Franco JC, Torres-Ruiz J, Sosa-Hernández VA, Cervantes-Díaz R, Romero-Ramírez S, Pérez-Fragoso A, et al. Metabolomics analysis reveals a modified amino acid metabolism that correlates with altered oxygen homeostasis in COVID-19 patients. Sci Rep. 2021;11(1).

231. Soares NC, Hussein A, Muhammad JS, Semreen MH, ElGhazali G, Hamad M, et al. Plasma metabolomics profiling identifies new predictive biomarkers for disease severity in COVID-19 patients. PLoS One. 2023;18(8 August):1–20.

232. Oostdam ASH Van, Castañeda-Delgado JE, Oropeza-Valdez JJ, Borrego JC, Monárrez-Espino J, Zheng J, et al. Immunometabolic signatures predict risk of progression to sepsis in COVID-19. PLoS One. 2021;16(8).

233. Caterino M, Gelzo M, Sol S, Fedele R, Annunziata A, Calabrese C, et al. Dysregulation of lipid metabolism and pathological inflammation in patients with COVID-19. Sci Rep. 2021 ;11(1).

234. Delafiori J, Navarro LC, Siciliano RF, De Melo GC, Busanello ENB, Nicolau JC, et al. Covid-19 Automated Diagnosis and Risk Assessment through Metabolomics and Machine Learning. Anal Chem. 2021;93(4):2471–9.

235. López-Hernández Y, Monárrez-Espino J, Oostdam ASH van, Delgado JEC, Zhang L, Zheng J, et al. Targeted metabolomics identifies high performing diagnostic and prognostic biomarkers for COVID-19. Sci Rep. 2021;11(1):14732.

236. Wu D, Shu T, Yang X, Song JX, Zhang M, Yao C, et al. Plasma metabolomic and lipidomic alterations associated with COVID-19. 2020];7(7).

237. Sameh M, Khalaf HM, Anwar AM, Osama A, Ahmed EA, Mahgoub S, et al. Integrated multiomics analysis to infer COVID-19 biological insights. Sci Reports |. 123AD;13:1802.

238. Bruzzone C, Bizkarguenaga M, Gil-Redondo R, Diercks T, Arana E, García de Vicuña A, et al. SARS-CoV-2 Infection Dysregulates the Metabolomic and Lipidomic Profiles of Serum. iScience. 2020 Oct 10;23(10).

239. Overmyer KA, Shishkova E, Miller IJ, Balnis J, Bernstein MN, Peters-Clarke TM, et al. Large-Scale Multi-omic Analysis of COVID-19 Severity. Cell Syst. 2021;12(1):23.

240. Costantini S, Madonna G, Di Gennaro E, Capone F, Bagnara P, Capone M, et al. New Insights into the Identification of Metabolites and Cytokines Predictive of Outcome for Patients with Severe SARS-CoV-2 Infection Showed Similarity with Cancer. Int J Mol Sci. 2023;24(5).

241. Centers for Disease Control Prevention. Pneumococcal Disease. (2015). Available from: https://www.cdc.gov/pneumococcal/index.html.

242. Marks LR, Reddinger RM, Hakansson AP. Biofilm formation enhances fomite survival of Streptococcus pneumoniae and Streptococcus pyogenes. Infect Immun. 2014 Mar;82(3):1141–6.

243. Khan MN, Xu Q, Pichichero ME. Protection against Streptococcus pneumoniae Invasive Pathogenesis by a Protein-Based Vaccine Is Achieved by Suppression of Nasopharyngeal Bacterial Density during Influenza A Virus Coinfection. Infect Immun. 2017 Feb;85(2).

244. Vu HTT, Yoshida LM, Suzuki M, Nguyen HAT, Nguyen CDL, Nguyen ATT, et al. Association between nasopharyngeal load of Streptococcus pneumoniae, viral coinfection, and radiologically confirmed pneumonia in Vietnamese children. Pediatr Infect Dis J. 2011 Jan;30(1):11–8.

245. Kadioglu A, Weiser JN, Paton JC, Andrew PW. The role of Streptococcus

pneumoniae virulence factors in host respiratory colonization and disease. Nat Rev Microbiol. 2008 Apr;6(4):288–301.

246. Alexander JE, Lock RA, Peeters CC, Poolman JT, Andrew PW, Mitchell TJ, et al. Immunization of mice with pneumolysin toxoid confers a significant degree of protection against at least nine serotypes of Streptococcus pneumoniae. Infect Immun. 1994 Dec;62(12):5683–8.

247. Zafar MA, Wang Y, Hamaguchi S, Weiser JN. Host-to-Host Transmission of Streptococcus pneumoniae Is Driven by Its Inflammatory Toxin, Pneumolysin. Cell Host Microbe. 2017 Jan;21(1):73–83.

248. Harvey RM, Hughes CE, Paton AW, Trappetti C, Tweten RK, Paton JC. The impact of pneumolysin on the macrophage response to Streptococcus pneumoniae is strain-dependent. PLoS One. 2014;9(8):e103625.

249. Shak JR, Ludewick HP, Howery KE, Sakai F, Yi H, Harvey RM, et al. Novel role for the Streptococcus pneumoniae toxin pneumolysin in the assembly of biofilms. MBio. 2013 Sep;4(5):e00655-13.

250. Jedrzejas MJ, Lamani E, Becker RS. Characterization of selected strains of pneumococcal surface protein A. J Biol Chem. 2001 Aug;276(35):33121–8.

251. Hammerschmidt S, Tillig MP, Wolff S, Vaerman JP, Chhatwal GS. Species-specific binding of human secretory component to SpsA protein of Streptococcus pneumoniae via a hexapeptide motif. Mol Microbiol. 2000 May;36(3):726–36.

252. Wartha F, Beiter K, Albiger B, Fernebro J, Zychlinsky A, Normark S, et al. Capsule and D-alanylated lipoteichoic acids protect Streptococcus pneumoniae against neutrophil extracellular traps. Cell Microbiol. 2007 May;9(5):1162–71.

253. MacLEOD CM, KRAUS MR. Relation of virulence of pneumococcal strains for mice to the quantity of capsular polysaccharide formed in vitro. J Exp Med. 1950 Jul;92(1):1–9.

254. Africano H, Serrano-Mayorga C, Ramirez-Valbuena P, Bustos I, Bastidas A, Vargas H, et al. Major adverse cardiovascular events during invasive pneumococcal disease are serotype dependent. Clin Infect Dis . 2020 Jan;213(2):314–23

255. Hallström T, Singh B, Resman F, Blom AM, Mörgelin M, Riesbeck K. Haemophilus influenzae protein E binds to the extracellular matrix by concurrently interacting with laminin and vitronectin. J Infect Dis. 2011 Oct;204(7):1065–74.

256. Su Y-C, Mukherjee O, Singh B, Hallgren O, Westergren-Thorsson G, Hood D, et al. Haemophilus influenzae P4 Interacts With Extracellular Matrix Proteins Promoting Adhesion and Serum Resistance. J Infect Dis. 2016 Jan;213(2):314–23.

257. Langereis JD, Hermans PWM. Novel concepts in nontypeable Haemophilus influenzae biofilm formation. FEMS Microbiol Lett. 2013 Sep;346(2):81–9.

258. Devaraj A, Buzzo JR, Mashburn-Warren L, Gloag ES, Novotny LA, Stoodley P, et al. The extracellular DNA lattice of bacterial biofilms is structurally related to Holliday junction recombination intermediates. Proc Natl Acad Sci U S A. 2019 Dec;116(50):25068–77.

259. Fleury C, Su Y-C, Hallström T, Sandblad L, Zipfel PF, Riesbeck K. Identification of a Haemophilus influenzae factor H-Binding lipoprotein involved in serum

resistance. J Immunol. 2014 Jun;192(12):5913–23.

260. Jiang Z, Li S, Zhu C, Zhou R, Leung PHM. Mycoplasma pneumoniae Infections: Pathogenesis and Vaccine Development. Pathog (Basel, Switzerland). 2021 Jan;10(2).

261. Nakane D, Kenri T, Matsuo L, Miyata M. Systematic Structural Analyses of Attachment Organelle in Mycoplasma pneumoniae. PLoS Pathog. 2015 Dec;11(12):e1005299.

262. Becker A, Kannan TR, Taylor AB, Pakhomova ON, Zhang Y, Somarajan SR, et al. Structure of CARDS toxin, a unique ADP-ribosylating and vacuolating cytotoxin from Mycoplasma pneumoniae. Proc Natl Acad Sci U S A. 2015 Apr;112(16):5165–70.

263. Bose S, Segovia JA, Somarajan SR, Chang T-H, Kannan TR, Baseman JB. ADP-ribosylation of NLRP3 by Mycoplasma pneumoniae CARDS toxin regulates inflammasome activity. MBio. 2014 Dec;5(6).

264. Yamamoto T, Kida Y, Sakamoto Y, Kuwano K. Mpn491, a secreted nuclease of Mycoplasma pneumoniae, plays a critical role in evading killing by neutrophil extracellular traps. Cell Microbiol. 2017 Mar;19(3).

265. Liu X, Shin S. Viewing Legionella pneumophila Pathogenesis through an Immunological Lens. J Mol Biol. 2019 Oct;431(21):4321–44.

266. Lozach P-Y. Cell Biology of Viral Infections. Vol. 9, Cells. Switzerland; 2020.

267. Fischer K, Groschup MH, Diederich S. Importance of Endocytosis for the Biological Activity of Cedar Virus Fusion Protein. Cells. 2020 Sep;9(9).

268. Liang Y. Pathogenicity and virulence of influenza. Virulence. 2023 Dec;14(1):2223057.

269. Chen J, Lee KH, Steinhauer DA, Stevens DJ, Skehel JJ, Wiley DC. Structure of the hemagglutinin precursor cleavage site, a determinant of influenza pathogenicity and the origin of the labile conformation. Cell. 1998 Oct;95(3):409–17.

270. de Bruin ACM, Funk M, Spronken MI, Gultyaev AP, Fouchier RAM, Richard M. Hemagglutinin Subtype Specificity and Mechanisms of Highly Pathogenic Avian Influenza Virus Genesis. Viruses. 2022 Jul;14(7).

271. Gabriel G, Dauber B, Wolff T, Planz O, Klenk H-D, Stech J. The viral polymerase mediates adaptation of an avian influenza virus to a mammalian host. Proc Natl Acad Sci U S A. 2005 Dec;102(51):18590–5.

272. Ayllon J, García-Sastre A. The NS1 protein: a multitasking virulence factor. Curr Top Microbiol Immunol. 2015;386:73–107.

273. Johnson SM, McNally BA, Ioannidis I, Flano E, Teng MN, Oomens AG, et al. Respiratory Syncytial Virus Uses CX3CR1 as a Receptor on Primary Human Airway Epithelial Cultures. PLoS Pathog. 2015 Dec;11(12):e1005318.

274. Merritt TN, Pei J, Leung DW. Pathogenicity and virulence of human respiratory syncytial virus: Multifunctional nonstructural proteins NS1 and NS2. Virulence. 2023 Nov;2283897.

275. Meng B, Kemp SA, Papa G, Datir R, Ferreira IATM, Marelli S, et al. Recurrent

emergence of SARS-CoV-2 spike deletion H69/V70 and its role in the Alpha variant B.1.1.7. Cell Rep. 2021 Jun;35(13):109292.

276. Liu H, Zhang Q, Wei P, Chen Z, Aviszus K, Yang J, et al. The basis of a more contagious 501Y.V1 variant of SARS-CoV-2. Vol. 31, Cell research. England; 2021. p. 720–2.

277. Zhu Y, Feng F, Hu G, Wang Y, Yu Y, Zhu Y, et al. A genome-wide CRISPR screen identifies host factors that regulate SARS-CoV-2 entry. Nat Commun. 2021 Feb;12(1):961.

278. Mlcochova P, Kemp SA, Dhar MS, Papa G, Meng B, Ferreira IATM, et al. SARS-CoV-2 B.1.617.2 Delta variant replication and immune evasion. Nature. 2021 Nov;599(7883):114–9.

279. Lyngse FP, Mortensen LH, Denwood MJ, Christiansen LE, Møller CH, Skov RL, et al. Household transmission of the SARS-CoV-2 Omicron variant in Denmark. Nat Commun. 2022 Sep;13(1):5573.

280. Hopp L, Loeffler-Wirth H, Nersisyan L, Arakelyan A, Binder H. Footprints of Sepsis Framed Within Community Acquired Pneumonia in the Blood Transcriptome. Front Immunol. 2018;9:1620.

281. Severino P, Silva E, Baggio-Zappia GL, Brunialti MKC, Nucci LA, Rigato OJ, et al. Patterns of gene expression in peripheral blood mononuclear cells and outcomes from patients with sepsis secondary to community acquired pneumonia. PLoS One. 2014;9(3):e91886.

282. Harjai M, Bogra J, Kohli M, Pant AB. Is suppression of apoptosis a new therapeutic target in sepsis? Anaesth Intensive Care. 2013 Mar;41(2):175–83.

283. Madenspacher JH, Azzam KM, Gowdy KM, Malcolm KC, Nick JA, Dixon D, et al. p53 Integrates host defense and cell fate during bacterial pneumonia. J Exp Med. 2013 May;210(5):891–904.

284. Feng J-Y, Liu K-T, Abraham E, Chen C-Y, Tsai P-Y, Chen Y-C, et al. Serum estradiol levels predict survival and acute kidney injury in patients with septic shock--a prospective study. PLoS One. 2014;9(6):e97967.

285. Tsang G, Insel MB, Weis JM, Morgan MAM, Gough MS, Frasier LM, et al. Bioavailable estradiol concentrations are elevated and predict mortality in septic patients: a prospective cohort study. Crit Care. 2016 Oct;20(1):335.

286. Zurfluh S, Nickler M, Ottiger M, Steuer C, Kutz A, Christ-Crain M, et al. Dihydrotestosterone is a predictor for mortality in males with community-acquired pneumonia: results of a 6-year follow-up study. Respir Res. 2018 Dec;19(1):240.

287. Damjanovic D, Khera A, Medina MF, Ennis J, Turner JD, Gauldie J, et al. Type 1 interferon gene transfer enhances host defense against pulmonary Streptococcus pneumoniae infection via activating innate leukocytes. Mol Ther Methods Clin Dev. 2014;1:5.

288. Goritzka M, Makris S, Kausar F, Durant LR, Pereira C, Kumagai Y, et al. Alveolar macrophage-derived type I interferons orchestrate innate immunity to RSV through recruitment of antiviral monocytes. J Exp Med. 2015 May;212(5):699–714.

289. Wang X, Guo J, Wang Y, Xiao Y, Wang L, Hua S. Expression Levels of Interferon

Regulatory Factor 5 (IRF5) and Related Inflammatory Cytokines Associated with Severity, Prognosis, and Causative Pathogen in Patients with Community-Acquired Pneumonia. Med Sci Monit Int Med J Exp Clin Res. 2018 May;24:3620–30.

290. Moreno G, Rodríguez A, Reyes LF, Gomez J, Sole-Violan J, Díaz E, et al. Corticosteroid treatment in critically ill patients with severe influenza pneumonia: a propensity score matching study. Intensive Care Med. 2018;44(9):1470–82.

291. Trefler S, Rodríguez A, Martín-Loeches I, Sanchez V, Marín J, Llauradó M, et al. Oxidative stress in immunocompetent patients with severe community-acquired pneumonia. A pilot study. Med intensiva. 2014 Mar;38(2):73–82.

292. Faiotto VB, Franci D, Enz Hubert RM, de Souza GR, Fiusa MML, Hounkpe BW, et al. Circulating levels of the angiogenesis mediators endoglin, HB-EGF, BMP-9 and FGF-2 in patients with severe sepsis and septic shock. J Crit Care. 2017 Dec;42:162–7.

293. Khan MM, Yang W-L, Wang P. Endoplasmic reticulum stress in sepsis. Shock. 2015 Oct;44(4):294–304.

294. Zhang J, Luo Y, Wang X, Zhu J, Li Q, Feng J, et al. Global transcriptional regulation of STAT3- and MYC-mediated sepsis-induced ARDS. Ther Adv Respir Dis. 2019;13:1753466619879840.

295. Lewnard JA, Hanage WP. Making sense of differences in pneumococcal serotype replacement. Lancet Infect Dis. 2019;19(6):e213–20.

296. Gelzo M, Cacciapuoti S, Pinchera B, De Rosa A, Cernera G, Scialò F, et al. Matrix metalloproteinases (MMP) 3 and 9 as biomarkers of severity in COVID-19 patients. Sci Rep. 2022 Jan;12(1):1212.

297. Spranger S, Dai D, Horton B, Gajewski TF. Tumor-Residing Batf3 Dendritic Cells Are Required for Effector T Cell Trafficking and Adoptive T Cell Therapy. Cancer Cell. 2017 May;31(5):711-723.e4.

298. Ma B, Hottiger MO. Crosstalk between Wnt/β-Catenin and NF-κB Signaling Pathway during Inflammation. Front Immunol. 2016;7:378.

299. Pello OM, De Pizzol M, Mirolo M, Soucek L, Zammataro L, Amabile A, et al. Role of c-MYC in alternative activation of human macrophages and tumor-associated macrophage biology. Blood. 2012 Jan;119(2):411–21.

300. Florea V, Bhagavatula N, Simovic G, Macedo FY, Fock RA, Rodrigues CO. c-Myc is essential to prevent endothelial pro-inflammatory senescent phenotype. PLoS One. 2013;8(9):e73146.

301. Wang C, Tan C, Wen Y, Zhang D, Li G, Chang L, et al. FOXP1-induced lncRNA CLRN1-AS1 acts as a tumor suppressor in pituitary prolactinoma by repressing the autophagy via inactivating Wnt/β-catenin signaling pathway. Cell Death Dis. 2019 Jun;10(7):499.

302. Sun J, Li W, Sun Y, Yu D, Wen X, Wang H, et al. A novel antisense long noncoding RNA within the IGF1R gene locus is imprinted in hematopoietic malignancies. Nucleic Acids Res. 2014 Sep;42(15):9588–601.

303. Fraser DD, Cepinskas G, Patterson EK, Slessarev M, Martin C, Daley M, et al. Novel Outcome Biomarkers Identified With Targeted Proteomic Analyses of

Plasma From Critically Ill Coronavirus Disease 2019 Patients. Crit care Explor. 2020 Sep;2(9):e0189.

304. Zheng H-Y, Xu M, Yang C-X, Tian R-R, Zhang M, Li J-J, et al. Longitudinal transcriptome analyses show robust T cell immunity during recovery from COVID-19. Signal Transduct Target Ther. 2020 Dec;5(1):294.

305. Bernardes JP, Mishra N, Tran F, Bahmer T, Best L, Blase JI, et al. Longitudinal Multi-omics Analyses Identify Responses of Megakaryocytes, Erythroid Cells, and Plasmablasts as Hallmarks of Severe COVID-19. Immunity. 2020;53(6):1296-1314.e9.

306. Bost P, De Sanctis F, Canè S, Ugel S, Donadello K, Castellucci M, et al. Deciphering the state of immune silence in fatal COVID-19 patients. Nat Commun. 2021 Mar;12(1):1428.

307. Addetia A, Crawford KHD, Dingens A, Zhu H, Roychoudhury P, Huang M-L, et al. Neutralizing Antibodies Correlate with Protection from SARS-CoV-2 in Humans during a Fishery Vessel Outbreak with a High Attack Rate. J Clin Microbiol. 2020 Oct;58(11).

308. Hassan AO, Case JB, Winkler ES, Thackray LB, Kafai NM, Bailey AL, et al. A SARS-CoV-2 Infection Model in Mice Demonstrates Protection by Neutralizing Antibodies. Cell. 2020 Aug;182(3):744-753.e4.

309. Saletti G, Gerlach T, Jansen JM, Molle A, Elbahesh H, Ludlow M, et al. Older adults lack SARS CoV-2 cross-reactive T lymphocytes directed to human coronaviruses OC43 and NL63. Sci Rep. 2020 Dec;10(1):21447.

310. Sano K, Bhavsar D, Singh G, Floda D, Srivastava K, Gleason C, et al. SARS-CoV-2 vaccination induces mucosal antibody responses in previously infected individuals. Nat Commun. 2022 Sep;13(1):5135.

311. Faraone JN, Liu S-L. Immune imprinting as a barrier to effective COVID-19 vaccines. Cell reports Med. 2023 Nov;4(11):101291.

312. Ballout RA, Kong H, Sampson M, Otvos JD, Cox AL, Agbor-Enoh S, et al. The NIH lipo-COVID study: A pilot NMR investigation of lipoprotein subfractions and other metabolites in patients with severe COVID-19. Biomedicines. 2021;9(9).

313. Heinecke JW. Small HDL promotes cholesterol efflux by the ABCA1 pathway in macrophages: Implications for therapies targeted to HDL. Circ Res. 2015;116(7):1101–3.

314. Holmes E, Nicholson JK, Lodge S, Nitschke P, Kimhofer T, Wist J, et al. Diffusion and relaxation edited proton NMR spectroscopy of plasma reveals a high-fidelity supramolecular biomarker signature of SARS-CoV-2 infection. Anal Chem. 2021;93(8):3976–86.

315. Otvos JD, Shalaurova I, Wolak-Dinsmore J, Connelly MA, Mackey RH, Stein JH, et al. GlycA: A composite nuclear magnetic resonance biomarker of systemic inflammation. Clin Chem. 2015;61(5):714–23.

316. Ritchie SC, Würtz P, Nath AP, Abraham G, Havulinna AS, Fearnley LG, et al. The Biomarker GlycA is Associated with Chronic Inflammation and Predicts Long-Term Risk of Severe Infection. Cell Syst. 2015;1(4):293–301.

317. Gruppen EG, Connelly MA, Otvos JD, Bakker SJ, Dullaart RP. A novel protein glycan biomarker and LCAT activity in metabolic syndrome. Eur J Clin Invest. 2015;45(8):850-859. doi:10.1111/eci.12481.

318. Ghini V, Meoni G, Pelagatti L, Celli T, Veneziani F, Petrucci F, et al. Profiling metabolites and lipoproteins in COMETA, an Italian cohort of COVID-19 patients. PLoS Pathog . 2022 ;18(4).

319. Rössler T, Berezhnoy G, Singh Y, Cannet C, Reinsperger T, Schäfer H, et al. Quantitative Serum NMR Spectroscopy Stratifies COVID-19 Patients and Sheds Light on Interfaces of Host Metabolism and the Immune Response with Cytokines and Clinical Parameters. Metabolites. 2022;12(12).

320. Banach M, Maltais-Payette I, Lajeunesse-Trempe F, Pibarot P, Biertho L, Tchernof A. Association between Circulating Amino Acids and COVID-19 Severity. 2023; 12(3)

321. Danlos FX, Grajeda-Iglesias C, Durand S, Sauvat A, Roumier M, Cantin D, et al. Metabolomic analyses of COVID-19 patients unravel stage-dependent and prognostic biomarkers. Cell Death Dis. 2021;12(3).

322. Holeček M. The BCAA-BCKA cycle: Its relation to alanine and glutamine synthesis and protein balance. Nutrition. 2001;17(1):70.

323. Monirujjaman M, Ferdouse A. Metabolic and Physiological Roles of Branched-Chain Amino Acids. Adv Mol Biol. 2014;2014:1–6.

324. Holeček M. Why are branched-chain amino acids increased in starvation and diabetes? Nutrients. 2020;12(10):1–15.

325. Zhenyukh O, Civantos E, Ruiz-Ortega M, Sánchez MS, Vázquez C, Peiró C, et al. High concentration of branched-chain amino acids promotes oxidative stress, inflammation and migration of human peripheral blood mononuclear cells via mTORC1 activation. Free Radic Biol Med]. 2017;104:165–77.

326. Zhenyukh O, González-Amor M, Rodrigues-Diez RR, Esteban V, Ruiz-Ortega M, Salaices M, et al. Branched-chain amino acids promote endothelial dysfunction through increased reactive oxygen species generation and inflammation. J Cell Mol Med. 2018;22(10):4948–62.

327. Ding Shi, Ren Yan, Longxian Lv, Huiyong Jiang, Yingfeng Lu, Jifang Sheng, Jiaojiao Xie, Wenrui Wu, Jiafeng Xia, Kaijin Xu, Silan Gu, Yanfei Chen, Chenjie Huang, Jing Guo, Yiling Du, Lanjuan LiaDing Shi, Ren Yan, Longxian Lv, Huiyong Jiang, Yingfeng Lu, Ji LL. The serum metabolome of COVID-19 patients is distinctive and predictive. Metabolism. 2021;118.

328. Cruzat V, Rogero MM, Keane KN, Curi R, Newsholme P. Glutamine: Metabolism and immune function, supplementation and clinical translation. Nutrients. 2018;10(11):1–31.

329. Caterino M, Costanzo M, Fedele R, Cevenini A, Gelzo M, Di Minno A, et al. The serum metabolome of moderate and severe covid-19 patients reflects possible liver alterations involving carbon and nitrogen metabolism. Int J Mol Sci. 2021;22(17):1–18.

330. Masuda R, Lodge S, Nitschke P, Spraul M, Schaefer H, Bong SH, et al. Integrative Modeling of Plasma Metabolic and Lipoprotein Biomarkers of SARS-CoV-2

Infection in Spanish and Australian COVID-19 Patient Cohorts. J Proteome Res. 2021;20(8):4139–52.